The membrane bound phosphatidic add phosphatase from avocado

Pearce, Matthew L.

The Membrane Bound Phosphatidic Acid Phosphatase from Avocado

By

Matthew L. Pearce B.Sc. (Hons.)

A thesis submitted for the degree of Doctor of Philosophy

at the University of Durham

Department of Biological Sciences

University of Durham

July, 1997.

The Membrane Bound Phosphatidic acid Phosphatase from Avocado

Submitted for the degree of Doctor of Philosophy

by Matthew L. Pearce B.Sc. (Hons.),

July, 1997.

Phosphatidate Phosphatase (EC 3.1.3.4) is an important enzyme in plant lipid metabolism as it lies at a theoretical branchpoint between phospholipid and triacylglycerol biosyntheses. Since it's identification in 1955, it has received very little attention in plant lipid research. Previous studies reported in the literature have been limited to the use of crude plant cell extracts, making an accurate evaluation of the data difficult.

The enzyme was characterised and purified to homogeneity from the microsomes of maturing avocado fruit, for the first time from any plant source. The novel procedure utilised detergent solubilisation in CHAPS, followed by anion exchange and Affi-Gel Blue chromatography, ammonium sulphate precipitation and Phenyl Superose chromatography. The enzyme had a subunit molecular mass, as determined by SDS-PAGE of 49kDa. Gel filtration studies revealed it was monomeric. Enzyme activity had a pH optimum of 6.0, was insensitive to *N*-ethylmaleimide and was stimulated by Mg^{2+}.

The homogenous enzyme was examined for the ability to hydrolyse *sn*-1,2-dioleoylglycerol-3-phosphate(PA), *sn*-1-oleoylglycerol-3-phosphate(LPA), *sn*-2-oleoylglycerol-3-phosphate, ceramide-1-phosphate and *p*-nitrophenylphosphate. All substrates were used, but the apparent V_{max} values for PA and LPA were considerably higher than the other substrates tested.

The Michaelis-Menten kinetic model of enzyme catalysis was found to be inappropriate as the surface active enzyme was shown to be dependent on the bulk and surface concentration of the substrate in Triton X-100 mixed micelles. The surface dilution kinetic model was used to study PA and LPA hydrolysis. LPA was a better substrate and was also a potent competitive inhibitor of PA hydrolysis. Considering the specificities of the other enzymes in triacylglycerol biosynthesis, this premature dephosphorylation of LPA would prevent triacylglycerol formation. These findings possibly indicate that strict metabolic channelling is in operation with very low steady state concentrations of LPA with respect to PA, thus preventing any interaction with LPA *in vivo*.

Table of Contents

List of Figures

List of Tables

Declaration

No part of this thesis has been previously submitted for a degree in this or any other University. I declare that, unless otherwise indicated, this thesis is entirely the result of my own work.

Matthew Pearce

July, 1997.

Acknowledgements

I would like to express my gratitude to Professor A.R. Slabas for his supervision and guidance throughout this work. I would also like to thank the Gatsby Charitable Foundation, and in particular Miss Janet Morgan, for the studentship and their constant support.

I thank Professor Ken Bowler for the use of the departmental facilities, and Dr. Ron Croy for his help on all matters concerning centrifugation. I am particularly indebted to Dr. Tony Fawcett, Dr. Kieran Elborough and Bill Simon for their advice, assistance and encouragement. A mention must go to Dr. Adrian Brown for his help before, and during, the course of this project; and to Russell Swinhoe for his invaluable technical assistance. Thank-you also to Johan Kroon for the very kind donation of *sn*-1-acyltransferase, and to Randall Weselake for the useful discussions in Toronto.

I am grateful for all of the advice/encouragement that I have received throughout my Ph.D. For example, having 'lost' all of the enzyme activity during a protein purification, my brother asked: "Have you looked under the chloroplast?"

Thanks also to (in no particular order): Neil, Siân, Duncan, Simon, Lee, Jonathan, Andy, Hayley, Clare, Bethan, Mark, Sipo, Fraser, Ted, Liz, Annette and Nishida for the chats, drinks, cheese scones, football, advice and, upon reflection, for an enjoyable time at Durham. Thanks also to Chris, Medic, Diarmuid, Beth, Jon, Paul, Sylvie and Gloucester RFC.

On a personal note, I would like to take this opportunity to thank my parents, Andrew and Mary, for the relentless love and support that they have shown me, especially throughout my education. I assure them that this is finally it. A big thank-you must also go to James and Kate for their support and many opinions. And finally, to Emma, without whom this thesis would not have been at all possible. Your love, support and friendship pulled me through the many tough times, 'thank-you' doesn't seem enough.

Matt

List of Abbreviations

ACP	Acyl carrier protein
ADP	Adenosine diphosphate
ATP	Adenosine triphosphate
BSA	Bovine serum albumin
CAPS	(3-[cyclohexylamino]-1-propanesulphonic acid
cDNA	complementary DNA
CDP	Cytidine diphosphate
CHAPS	3-[(3-cholamidopropyl)dimethylammonio]-1-propanesulphonic acid
CoA	Coenzyme A
CPM	Counts per minute
CMC	Critical micelle concentration
DAG	Diacylglycerol
DAGAT	Diacylglycerol acyltransferase
ddH_2O	Double-distilled water
DPM	Decays per minute
DPTA	dietylenetriaminepentaacetic acid
DTT	Dithiothreitol
EDTA	Ethylenediaminetetraacetic acid
EGTA	[Ethylenebis(oxyethylenenitrilo)]tetraacetic acid
FAS	Fatty acid synthase
g	Acceleration due to gravity
G-3-P	Glycerol-3-phosphate
GPAT	Glycerol-3-phosphate acyltransferase
kDa	Kilo Dalton
K_{cat}	Catalytic constant/Turnover number
K_m	Michaelis constant
K_m^B	Interfacial Michaelis constant

K_S^A	Dissociation constant
LPA	Lysophosphatidate
sn-1-LPA	*sn*-1-acylglycerol-3-phosphate
sn-2-LPA	*sn*-2-acylglycerol-3-phosphate
LPAAT	Lysophosphatidate acyltransferase
LPAP	Lysophosphatidate phosphatase activity
MAG	Monoacylglycerol
MES	2-[*N*-Morpholino]ethanesulfonic acid
NEM	*N*-ethylmaleimide
*p*NPP	*p*-Nitrophenylphosphate
PAGE	Polyacrylamide gel electrophoresis
PA	Phosphatidate, *sn*-1,2-diacylglycerol-3-phosphate
PAP	Phosphatidate phosphatase
PC	Phosphatidylcholine
Pi	Inorganic phosphate
PI	Phosphatidylinositol
PG	Phosphatidylglycerol
PGP	Phosphatidylglycerophosphate
PL	Phospholipid
PS	Phosphatidylserine
RPM	Revolutions per minute
SDS	Sodium dodecyl sulphate
TAG	Triacylglycerol
TEMED	N,N,N'N'-tetramethylethylene diamine
Tris	Tris (hydroxymethyl) aminoethane
U	Unit of enzyme activity
	(unless otherwise stated: μmol product/min)
UV	Ultra-violet
V_{max}	Maximum velocity
v/v	Volume for volume
w/v	Weight for volume

Chapter 1

Introduction

1.1 The Importance of Lipids in Plants.

All plant cells synthesise lipids autonomously (Somerville and Browse, 1991). The biological importance of lipids is manifested by their many diverse roles in all organisms. Principally, in the form of phospholipids, they provide the structural components of membranes. In plants, lipids are also associated with: protein-membrane anchorage (Low and Saltiel, 1988; Low, 1989); root nodule organogenesis (Lerouge *et al.*, 1991); the formation of cuticular waxes (Post-Beittenmiller, 1996); cold acclimation; chilling resistance (Steponkus *et al.*, 1988; Murata, 1983); and signal transduction (Mazliac, 1997). They also play an important role in energy storage (Slabas and Fawcett, 1992; Frentzen 1993).

Membrane integrity is critical for the survival of all plant cells. Successful germination of seeds from many plant species is dependent on the food reserves within the seed. The components of membranes and the seed energy stores are therefore fundamental to the survival and success of the plant. Membranes from all plants, and the energy stores in many plant species are composed of glycerolipid. Glycerolipids form the largest group of plant lipids (Frentzen, 1993) and thus play a major role in the life of a plant.

The glycerolipid composition of membranes and storage oils differ. Membranes predominantly consist of heterogeneous amphiphilic phospholipids with their properties governed by the two non-polar acyl groups and the polar head group attached to the glycerol backbone (Frentzen, 1993). The diversity of phospholipids exists not only with respect to the composition of the polar head groups, but also with

respect to the acyl groups (Hjelmestad and Bell, 1991). Plant seeds store triacylglycerols as food reserves for germination and post-germinative growth of the seedling. Triacylglycerols have different properties that depend on the individual fatty acids esterified with each of the three hydroxyl groups of glycerol.

1.2 Phospholipid biosynthesis in plants

Due to the evolutionary pressure to maintain functionality, the phospholipids within membranes are generally conserved in respect to acyl composition and the degree of unsaturation (Vogel and Browse, 1996). *De novo* fatty acid biosynthesis occurs almost exclusively within the plastid, where acetyl-CoA and malonyl-CoA are sequentially condensed onto the growing acyl chain by the discrete fatty acid synthase activities (Weaire and Kekwick, 1975; Roughan, 1987). Acyl-ACP moieties with 16 and 18 carbon atoms (C16 and C18) are produced within plastids and used either in the synthesis of plastid glycerolipids or exported as acyl-CoA (Figure 1.1).

In plants, the acyl composition of glycerolipids of the plastid membranes differs substantially to that of other membranes. This led to the observation that there are two separate pathways for glycerolipid biosynthesis (Roughan and Slack, 1982; Browse and Somerville, 1991; Frentzen 1993) as shown in figure 1.1. The glycerolipids from these two pathways can be distinguished by the characteristic pattern of C16 and C18 acyl groups at positions *sn*-1 and *sn*-2 of the glycerol backbone. The plastid lipids exclusively carry C16 fatty acids at the *sn*-2 position, with predominantly C18 fatty acids at the *sn*-1. This pattern is characteristic of lipids produced in cyanobacteria, and is termed the Prokaryotic pathway. Extra-plastidial glycerolipids exclusively contain C18 at position *sn*-2, with either C16 or C18 at position *sn*-1 (Roughan and Slack, 1982), and result from the Eukaryotic pathway within the endoplasmic reticulum. In 16:3 plants (such as spinach and *Arabidopsis*), much of the diacylglycerol synthesised in the plastid membranes contributes to the

synthesis of plastid lipids such as galactolipids and sulpholipids (Browse and Somerville, 1991). In 18:3 plants, only phosphatidylglycerol is synthesised in the chloroplast, with the remainder of plastid lipids originating from the eukaryotic pathway.

As depicted in Figure 1.2, phosphatidate (PA) is the key intermediate in the biosynthesis of various eukaryotic glycerolipids. It can serve as a precursor for phoshatidylinositol (PI), phosphatidylglycerol (PG) and phosphatidylserine (PS), or it can be converted to diacylglycerol (DAG) by the action of phosphatidate phosphatase (EC 3.1.3.4). DAG is the intermediate for phosphatidylcholine (PC) and phosphatidylethanolamine (PE) synthesis and is also utilised by diacylglycerol acyltransferase in the synthesis of triacylglycerol (TAG). Thus within the endoplasmic reticulum, the TAG and phospholipids are synthesised from common intermediates.

1.3 Triacylglycerol in plants.

The biosynthesis of TAG in oilseeds involves at least three cellular compartments (Figure 1.1). The primary acyl-groups are synthesised by the fatty acid synthetase complex which is localised in the plastid. *sn*-Glycerol-3-phosphate is produced in the cytosol from dihydroxyacetone-phosphate by the action of NAD^+:glycerol-3-phosphate oxidoreductase (Gee *et al.*, 1988) and from glycerol by the action of glycerol kinase (Frentzen, 1993). TAG assembly proceeds via the Kennedy Pathway (Figure 1.2) in the endoplasmic reticulum, where the sequential acylation of *sn*-glycerol-3-phosphate occurs in four enzymatic steps (Stymne and Stobart, 1987; Frentzen, 1993).

Figure 1.1

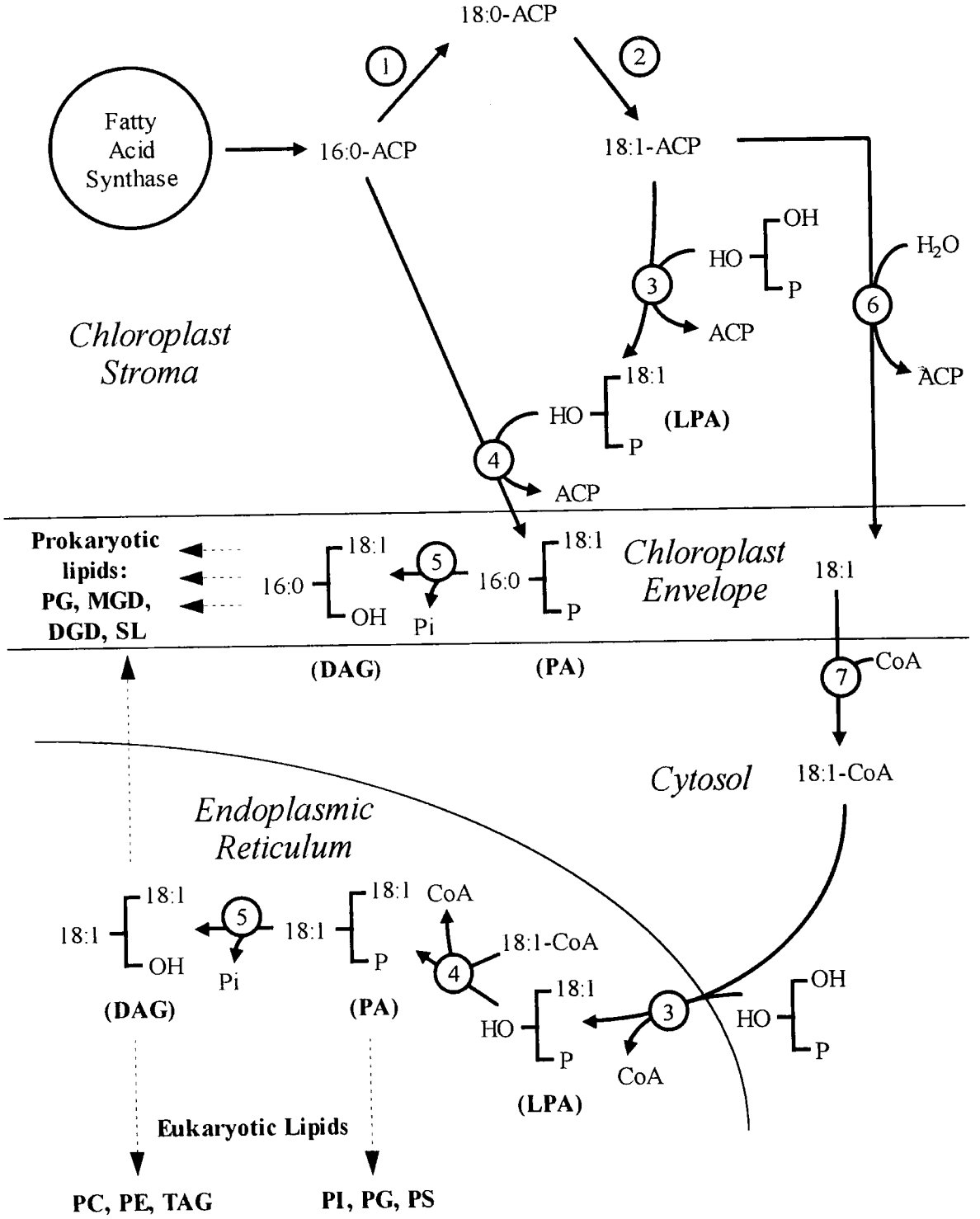
18:0-ACP
1
2
Fatty Acid Synthase
16:0-ACP
18:1-ACP
OH
HO
P
3
ACP
H_2O
6
ACP
Chloroplast Stroma
18:1
HO
P
(LPA)
4
ACP
Prokaryotic lipids: PG, MGD, DGD, SL
16:0
18:1
OH
5
Pi
16:0
18:1
P
Chloroplast Envelope
18:1
(DAG)
(PA)
7
CoA
Cytosol
18:1-CoA
Endoplasmic Reticulum
18:1
18:1
OH
5
Pi
18:1
18:1
P
CoA
18:1-CoA
4
18:1
HO
P
(LPA)
3
CoA
OH
HO
P
(DAG)
(PA)
Eukaryotic Lipids
PC, PE, TAG
PI, PG, PS

Figure 1.2

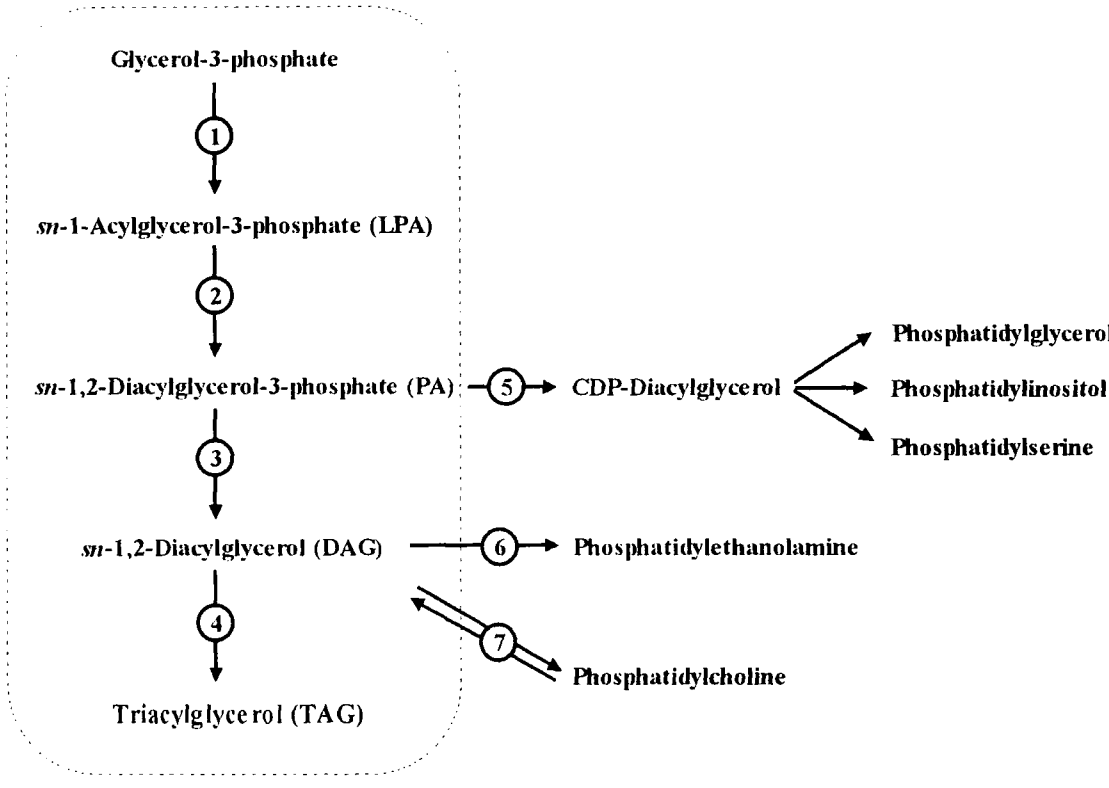
Glycerol-3-phosphate
1
sn-1-Acylglycerol-3-phosphate (LPA)
2
sn-1,2-Diacylglycerol-3-phosphate (PA)
5
CDP-Diacylglycerol
Phosphatidylglycerol
Phosphatidylinositol
Phosphatidylserine
3
sn-1,2-Diacylglycerol (DAG)
6
Phosphatidylethanolamine
4
7
Phosphatidylcholine
Triacylglycerol (TAG)

Plant seeds store TAG as food reserves for germination and post-germinitive growth of the seedling. The TAG is localised within small discrete intracellular organelles, called oil bodies, each having a diameter ranging from 0.5-2.5μm (Tzen and Huang, 1992). During soybean seed development, TAG levels increase from 0.4mg/seed at 18 days after flowering to 36mg/seed 42 days later; over the same period, phospholipids increase from 0.3 to 4.2mg/seed (Privett *et al.*, 1973). In field crops such as peanut, rapeseed and sunflower, approximately 45% of the seed weight is composed of oil (Somerville and Browse, 1991).

The TAG of currently used oil crops principally contain five different fatty acid species (Stymne *et al.*, 1993). These fatty acids are essentially the same as those seen in other lipid classes and are prevalent in all plant tissues. However, throughout the whole Plant Kingdom, there are a vast number of 'unusual' fatty acids within seed oils (Stymne *et al.*, 1993), which are excluded from membranes. Chemical modification to the acyl chain allows fatty acid diversity. Such modifications include: the degree of unsaturation; the position of the double/triple bonds along the acyl-chain; the length of the chain; and the addition of hydroxyl groups (Somerville and Browse, 1991). Many of these 'unusual' fatty acids are desirable for industrial purposes (erucic acid in the paint and lubricant industries, for example), but would only be economically viable if they could be mass produced to a similar scale and efficiency as edible oils (Davies *et al.*, 1993). Unfortunately, most of these desirable lipids are produced in undomesticated species whose agronomic properties make them agriculturally unpracticable (Somerville and Browse, 1991). Consequently, the identification and transfer of genes that encode the enzymes responsible for the modification/synthesis of fatty acids from undomesticated species to a highly efficient oilseed crop has attracted much scientific interest. The feasibility of producing transgenic crops with altered lipid composition depends on the understanding of the biochemical processes involved in the biosynthesis and regulation of lipids in TAG and phospholipids (Dutta et al., 1992).

The fatty acid moieties in the storage lipid (TAG) in oil seeds are species specific and are distributed in a non-random manner in the three *sn*-positions. The non-random distribution of the fatty acyl moieties in TAG is governed by two main factors: the availability of the acyl-CoA's in the intracellular pool; and the relative specificities/selectivities of the acyltransferases (Ichihara *et al.*, 1987; Oo and Huang, 1989; Cao *et al.*, 1990; Bernerth and Frentzen, 1990; Laurent and Huang, 1992).

Glycerol-3-phosphate acyltransferase (GPAT) has a broad selectivity for acyl-CoA species (Griffiths *et al.*, 1985; Ichihara *et al.*, 1987). Both saturated and unsaturated acyl-CoA species are utilised for the acylation of position *sn*-1 of glycerol-3-phosphate. The acyl composition thus depends on the fatty acyl-CoA pool in the cell.

The *sn*-1-acylglycerol-3-phosphate acyltransferase (LPAAT) is both 'specific' and 'selective' towards acyl-CoA and LPA species (Ichihara *et al.*, 1987; Cao *et al.*, 1990). The term 'specificity' is used to denote comparisons of acylation rates measured in the presence of single acyl donors, while the term 'selectivity' is used when the acylation rates are measured in the presence of multiple thioesters(Frentzen *et al.*, 1983). Cao *et al.* (1990) found that LPAAT from meadowfoam, nasturtium, palm castor, soybean, maize and rapeseed could all utilise *sn*-1-erucoyl-LPA as the acyl acceptor. However, with the exception of meadowfoam (*Limnanthes alba*), none of these plants could use erucoyl-CoA as the second substrate, and thus *sn*-1,2-dierucoyl-PA was not produced. Bernerth and Frentzen (1990) showed that LPAAT from rapeseed (*Brassica napus*) positively discriminated against erucic acid. Oo and Huang (1989) also showed that the acyl group in the *sn*-1 position (LPA acceptor type) influenced the subsequent acyl-CoA specificity in the *sn*-2 position.

sn 1,2-Diacylglycerol acyltransferase (DAGAT) from safflower seed has in contrast to LPAAT (Frentzen *et al.*, 1983; Bernerth and Frentzen, 1990; Cao *et al.*, 1990; Frentzen 1993), a very broad specificity/selectivity for acyl-CoA species irrespective of the DAG acceptor species, and the choice of acyl moiety used is governed by the acyl-CoA pool (Ichihara *et al.*, 1987). Cao and Huang (1987) reported that the DAGAT of *Cuphea*, maize, rapeseed and canola all possessed a slight degree of selectivity. More recently however, Vogel and Browse (1996) showed that the DAGAT of castor, safflower, rapeseed and *Cuphea* had no specificity towards acyl-CoA species.

'Unusual' fatty acids are targeted exclusively to triacylglycerol, with the acyl specificity of TAG assembly believed to arise in the first two acylation steps of the Kennedy Pathway. However, PA and DAG are common intermediates for both TAG and phospholipid (PL) biosynthesis within the endoplasmic reticulum. This means that both acyl moieties of phospholipids and two (of the three) in TAG must have been established, prior to being channelled into their subsequent syntheses (Battey and Ohlrogge, 1989). The partitioning mechanism between TAG and PL is unknown.

Vogel and Browse (1996) showed that CDP-choline:DAG cholinephosphotransferase from various oleaginous plants does not discriminate against different DAG species so that specificity of this enzymes was not the main factor in the prevention of 'unusual' fatty acids from becoming incorporated into PL. However, newly synthesised phosphatidylcholine containing C10:0 or 18:1-OH acyl moieties were found to be rapidly degraded in castor and *Cuphea* microsomes. This supported the speculation of Laurent and Huang (1992) that the control of fatty acid flow from PA to either TAG or PL may be due to the instability of the phospholipid containing unusual fatty acids. Laurent and Huang (1992) also considered that fatty acid channelling was likely to be due to the expression of different isozymes for the individual 'luxury' (TAG) and 'housekeeping' (PL) functions.

As was shown in Figure 1.2, phosphatidate phosphatase, CDP-DAG synthase and CDP-choline:DAG cholinephosphotransferase (CPT) are located at the branchpoint between TAG and phospholipid biosynthesis. These enzymes are believed to exert an effect on the channelling of glycerolipids towards TAG or PC (Battey and Ohlrogge, 1990; Kocsis and Weselake, 1996). Phosphatidate phosphatase is of particular importance because it's activity could be potentially responsible for the flux of glycerolipids between the individual phospholipid groups. If phosphatidate phosphatase is down regulated, PA will accumulate. This will lead to an increase in CDP-DAG synthesis by CDP-DAG synthase and ultimately the production of PI, PG and PS (Figure 1.2). Alternatively, if phosphatidate phosphatase is active, DAG is produced, which is the precursor for TAG, PC and PE. The relative fluxes of TAG and PC may then be determined by the activities of either DAGAT or CPT. PC readily interconverts into DAG for incorporation into TAG (Stobart and Stymne, 1985). During TAG biosynthesis, it has been shown that PC can still interconvert with DAG, enabling PAP and CPT to control the levels of DAG used in TAG biosynthesis (Griffiths *et al.*, 1985, 1988).

Considering the potential metabolic importance of phosphatidate phosphatase, it is surprising that there is only a limited amount of data concerning its enzymic properties, regulation and precise role in TAG/PL biosynthesis (Kocsis and Weselake, 1996). The mechanism(s) by which the syntheses of TAG and PL are controlled, along with the acyl- content of an oil seed remains unclear. This reiterates the need to study phosphatidate phosphatase due to it's role at the branchpoint in TAG and PL biosynthesis.

Recently, Kocsis and Weselake (1996) produced a comprehensive treatise of the current understanding of phosphatidate phosphatase from plants, yeast, and mammalian tissues. Biochemical developments of various mammalian and microbial

areas of research often precede the development in the same areas of plant research (Kocsis and Weselake, 1996). For this reason the current understanding of all eukaryotic PAP will be considered prior to the study of plant PAP.

1.4 Phosphatidate phosphatase in mammalian systems.

Phosphatidate phosphatase (PAP, EC 3.1.3.4) catalyses the hydrolysis of PA to produce DAG and inorganic phosphate (Pi). As already shown, this is an important step in the synthesis of glycerolipids. PAP is ubiquitous in eukaryotic (see Kocsis and Weselake, 1996) and prokaryotic (Icho, 1988a and b; Cabacungan *et al.*, 1988) organisms.

Jamal *et al.*, (1991) demonstrated the existence of two PAP isozymes in rat liver which could be distinguished from each other with respect to *N*-ethylmaleimide (NEM) inhibition and Mg^{2+} dependency. One of the isozymes exists (as two isoforms) within the microsomes and cytosolic fractions, and is NEM-sensitive and Mg^{2+} dependent (Martin *et al.*, 1991). This form was designated PAP-1 (Gomez-Muñoz *et al.*, 1992a), and was found to translocate from between the cytosol to the microsomes upon various stimuli, such as fatty acid accumulation within the microsomes (Butterwith *et al.*, 1985; Hopewell *et al.*, 1985; Asiedu *et al.*, 1992; Gomez-Muñoz *et al.*, 1992a). Following the addition of unsaturated fatty acids to the culture medium, rat hepatocyte PAP-1 translocated to the endoplasmic reticulum, where it became membrane associated and metabolically functional (Gomez-Muñoz *et al.*, 1992b). The cytosolic isoform of the enzyme is biologically active *in vitro*, but would have no effect on glycerolipid synthesis *in vivo* as this is located exclusively within the membranes. Cytosolic PAP therefore forms a physiologically inactive reservoir for the enzyme, which can be rapidly translocated to the microsomes upon stimulation. Martin *et al.* (1986) showed that by displacing the membrane-associated PAP back to

the cytosol by the addition of chlorpromazine, the synthesis of TAG in rat hepatocytes was terminated. Similar displacement was demonstrated with okadaic acid (Gomez-Muñoz *et al.*, 1992a). Saggerson (1986) showed that noradrenaline increased the PAP activity in the microsomes. As there was no change in the total homogenate activity, it was concluded that translocation had occurred between the soluble and microsomal enzyme pools. Noradrenaline caused the accumulation of fatty acids, which in turn resulted in the translocation, by creating a negative charge to the membranes, explaining why chlorpromazine displaced PAP activity to the cytoplasm (by creating a net positive charge). Pittner *et al.* (1986) and Gomez-Muñoz *et al.* (1992b) were able to demonstrate that the translocation from the cytosol to the membranes was decreased by cAMP and glucagon and increased by insulin, suggesting that protein phosphorylation-dephosphorylation mechanisms exist in the control of translocation.

Martin-Sanz *et al.* (1984) reported that the control of translocation of PAP by fatty acids and cAMP was similar to that observed for CTP:phosphocholine cytidyltransferase. It is apparent that a co-ordinated translocation of PAP and the cytidyltransferase occurs, and thus with a rise in fatty acids, more TAG and PC are produced.

The second PAP isozyme, named PAP-2, is NEM-insensitive, independent of Mg^{2+} and is an integral membrane protein, situated within the plasma membrane (Gomez-Muñoz *et al.*, 1992a). This isozyme is believed to be involved in signal transduction (Jamal *et al.*, 1991; Gomez-Muñoz, *et al.*, 1992a; Kanoh *et al.*, 1993). The agonist-stimulated phospholipase D catalyses the hydrolysis of PC to PA (Billah and Anthes 1990; Kanoh *et al.*, 1993). English *et al.* (1996) reported that PA is a second messenger involved in the modulation of several protein kinases, calcium mobilisation and cell proliferation. PAP removes the signal by converting PA into DAG, and is thus involved in these cellular functions (Billah and Anthes 1990). However, DAG is also involved in signal transduction as a second messenger, and it is

associated with the ultimate activation of protein kinase C (Kanoh *et al.*, 1993). Therefore PAP may play pivotal roles in the generation and removal of lipid signalling molecules.

Most of the studies of both PAP-1 and PAP-2 have been conducted with crude preparations of the enzymes, and the properties of the isozymes have remained largely unknown. Only the PAP-2 isoform, implicated in signal transduction, has been purified to homogeneity from porcine thymus (Kanoh *et al.*, 1992), and rat liver (Fleming and Yeaman, 1995). PAP-2 has also been purified, but not to homogeneity, from rat liver by Waggoner *et al.* (1995) and Seiss and Hofstetter (1996). The cDNA encoding the 31kDa isoform identified by Seiss and Hofstetter (1996) has recently been cloned by Kanoh and co-workers (Kai *et al.*, 1996). The isoform responsible for glycerolipid biosynthesis, has not been purified from animals.

1.5 Phosphatidate phosphatase from Yeast.

Arguably the most pioneering biochemical research in this field has been conducted by Carman and co-workers with PAP from *Saccharomyces cerevisiae*. They reported the first purification of PAP from any source to homogeneity (Lin and Carman, 1989) and have since conducted detailed biochemical analyses with homogenous protein in an attempt to ascertain it's role in glycerolipid metabolism. The 91kDa enzyme was dependent on Mg^{2+} and reducing agent (2-mercaptoethanol) for catalytic activity. The monomeric enzyme was inhibited by diacylglycerol, TAG and CDP-DAG. The formation of CDP-DAG from PA is the primary route for phospholipid synthesis in yeast, and as such the inhibition of PAP, which would otherwise dephosphorylate PA would be expected in PL synthesis (Lin and Carman, 1989). DAG and TAG inhibition of PAP was indicative of feedback inhibition.

Spacial or different temporal compartmentation may also play roles in the control of PA dephosphorylation by PAP.

Using antibodies raised against the homogenous 91kDa protein, Morlock *et al.* (1991) demonstrated that the 91kDa protein was a proteolytic product of a 104kDa protein. The 104kDa protein was purified to homogeneity from a protease deficient strain of *S. cerevisiae* using the 91kDa protein purification strategy of Lin and Carman (1989). The 104kDa protein was found to be enzymatically indistinguishable from the previously purified 91kDa protein (Morlock *et al.*, 1991). Immunoblot analysis of cell extracts using the anti-91kDa antibodies revealed that an additional 45kDa isoform existed within the mitochondrial and microsomal fractions. This was purified following the same procedure (Morlock *et al.*, 1991; Carman and Quinlan, 1992), and showed that the enzymatic properties were similar to the 91kDa protein (Morlock *et al.*, 1991)

The 104kDa and 45kDa isoforms were however differentially regulated with phosphorylation by cAMP-dependent protein kinase (Quinlan *et al.*, 1992). The 45kDa protein was phosphorylated by the cAMP-dependent protein kinase *in vitro* resulting in a 2.4-fold stimulation in activity. The action of alkaline phosphatase on the 45kDa protein resulted in the 1.6-fold reduction in PAP activity. To test the *in vivo* significance of these findings, cAMP-dependent protein kinase mutant strains were used. In mutant strains where cAMP-dependent protein kinase activity was elevated, a 1.6-fold higher V_{max} was observed for the immunoprecipitated 45kDa PAP isoform than the wild type enzyme. In mutant strains containing no cAMP-dependent protein kinase activity, PAP activity was 1.7-fold lower. This *in vivo* regulation thus corroborated the *in vitro* findings that the 45kDa was regulated by cAMP-dependent protein kinase. The 104kDa protein was not phosphorylated. The 104kDa and 45kDa PAP isoforms were therefore differentially regulated by protein phosphorylation. A similar differential regulation through gene expression was observed with the addition

of inositol to the yeast growth medium. The addition of inositol increased the 45kDa protein expression with no change in the 104kDa isoform observed (Morlock *et al.*, 1992)

In addition to the microsomal and mitochondrial PAP isoforms in yeast, a cytosolic isoform has been reported with an apparent native molecular mass (as determined by gel filtration) of 75kDa (Hosaka and Yamashita, 1984). Lin and Carman (1989) reported that the basic enzymatic properties of the 91kDa microsomal protein were comparable to the soluble activity as previously reported by Hosaka and Yamashita, (1984). However, Morlock *et al.* (1991) were unable to demonstrate the translocation of either the 45kDa or the 91kDa isoforms, as reported for mammalian systems.

Other mechanisms for regulation of activity have been investigated for the homogenous yeast enzyme. The inhibition of the 104 and 45kDa proteins by sphingoid bases was demonstrated and the kinetic analysis showed that the K_i values of phytosphingosine and sphinganine were in the *in vivo* concentration range, suggesting that these may regulate the activity of PAP *in vivo* (Wu *et al.*, 1993). Similarly, Wu and Carman (1996) have recently shown that anionic phospholipids such as cardiolipin, CDP-DAG and PI stimulated PAP activity at approximately the *in vivo* concentrations of each.

The addition of inositol to the growth medium of wild type yeast caused a 2-fold increase in 45kDa PAP activity (Morlock *et al.*, 1988; Morlock *et al.*, 1991). Overall PAP activity also increased 2-fold as the cells entered stationary phase of growth (Hosaka and Yamashita, 1984b; Morlock *et al.*, 1988). At the stationary phase of growth, CDP-DAG synthase and PS synthase activities were reduced (Morlock *et al.*, 1991). The increase of PAP activity at the stationary phase correlated with the flux of glycerolipid into TAG at the expense of PL. The addition of inositol

to the growth media also resulted in the reduction of CDP-DAG synthase and PS synthase activities. The addition of inositol to the media during exponential growth phase, caused an increase in 45kDa PAP activity, and the channelling of glycerolipid into PI at the expense of TAG and PS (Morlock *et al.*, 1988 and 1991). The differential regulation of PAP and CDP-DAG synthase, possibly at a genetic level, appears to be a mechanism by which glycerolipid is channelled into DAG, or different PL species.

It is clear that the activities of PAP, CDP-DAG synthase and PS synthase are an important factor in the partitioning of glycerolipid synthesis in *S. cerevisiae*. The ability to produce homogenous PAP protein preparations has facilitated the study of these mechanisms.

1.6 Phosphatidate Phosphatase in Plants.

Since the first identification (from any tissue) of PAP in spinach by Kates (1955), PAP has received little attention in plant biochemistry. The study of PAP in plant tissues has been limited to the use of crude sub-cellular preparations (Kocsis and Weselake, 1996). PAP has been localised in various sub-cellular fractions of plants. However, there are three main locations in which PAP activity has been documented; these are in the cytosol, the microsomes and plastids (Kocsis and Weselake, 1996).

1.6.1 Cytoplasmic and microsomal PAP in plants.

The temporal expression of PAP activity during safflower embryogenesis was investigated by Ichihara *et al.* (1990). In this system, highest activity was seen during maximal TAG deposition. Cytoplasmic PAP activity in safflower was found to be highest during the early stages of seed development, prior to TAG deposition. Levels

of cytoplasmic PAP activity fell sharply as the seed matured. Conversely, the microsomal PAP activity was low during the early stages of seed development, but as the TAG deposition increased, the majority of cellular PAP activity became microsomal. After TAG deposition, the PAP levels in both compartments decreased. The activity profile of PAP within the microsomal fraction during seed maturation of groundnut has also been reported (Sukumar and Sastry, 1987) where maximal PAP activity was slightly more prolonged than that of DAGAT during maximal TAG biosynthesis, suggesting that DAGAT could be rate limiting with respect to PAP during TAG biosynthesis. Both in safflower and groundnut, PAP activity is highest during maximal TAG biosynthesis. In the developmental profiles for PAP and DAGAT in *B. napus*, safflower and groundnut a common feature is that there is a marked decrease of these enzymes following maximal TAG biosynthesis (Weselake *et al.*, 1993).

Ichihara *et al.* (1990) demonstrated that translocation of safflower cytoplasmic PAP to the microsomes could be induced *in vitro* upon the addition of oleate, palmitate and stearate. Laurate and linoleate were found not to induce translocation, suggesting that only fatty acids (and/or fatty acyl-CoAs) produced by the proplastids mediated this phenomenon. Oleate was found to be the most effective fatty acid tested in promoting translocation. Safflower cytosolic fractions were incubated with the microsomal preparations from soybean, rapeseed, and sunflower. Even in the presence of oleate, the safflower cytosolic PAP activity did not translocate to the soybean or rapeseed microsomal fractions. However, a low level of PAP translocation was observed between the safflower cytoplasm and sunflower microsomes. Sunflower and safflower both belong to the Compositae family. This led to the conclusion that there is a species specific mechanism for PAP translocation. It was also speculated that there was a species specific receptor on the endoplasmic reticulum surface. BSA was shown to reverse the translocation, indicating that the translocation was a transient and

inducible process. However, the above physiological concentrations of fatty acids used in this study make true *in vivo* interpretation of the data difficult.

A common observation of cytosolic and microsomal PAP is that the enzyme properties are different for both compartments. Kocsis *et al.* (1995) showed that the pH and temperature optima of the cytosolic and microsomal enzymes of *B. napus* were pH 5.0 at 50°C and pH 6-7 at 40°C, respectively. It was speculated that the cytoplasmic activity was attributable to non-specific acid phosphatases, accounting for the different enzymatic characteristics observed in both cellular compartments. The observation that the microsomal enzyme has an approximately neutral pH optimum as opposed to the cytoplasmic enzyme of around pH 5.0, has been made in castor bean (Moore and Sexton, 1978) and in mung bean cotyledons (Herman and Chrispeels, 1980). The soluble and microsomal enzymes of safflower were shown to be similar to their mammalian counterparts with respect to pH and Mg^{2+} optima, polyamine inhibition, and subcellular distribution (Ichihara *et al.*, 1990; Ichihara, 1991). There is limited data concerning the divalent cation requirement of PAP. Microsomal PAP from safflower have been shown to be dependent on Mg^{2+} for catalysis (Griffiths *et al.*, 1985; Ichihara *et al.*, 1989). Soluble PAP activity in castor bean was inhibited at concentrations of $\geq$ 1mM Mg^{2+} (Moore and Sexton, 1978). It is therefore apparent that the data of plant isoforms of PAP are not the same. This may be due to a species specificity of each enzyme, multiple isozymes within each cell type or experimental artefact in the characterisation of very crude cellular preparations.

1.6.2 Plastidial PAP in plants.

Plastids form a major compartment for glycerolipid biosynthesis, and an isoform of PAP has been identified in the envelope membranes (Joyard and Douce, 1977; 1979). The plastidial PAP isoform exhibits biochemical properties different

from those described from any organism. The enzyme is integrated within the inner envelope membrane (Joyard and Douce, 1979; Block *et al.*, 1983; Andrews *et al.*, 1985). PAP activity within the chloroplasts constitute the first branchpoint in the biosynthesis of galactolipids and phospholipids (Joyard and Douce, 1979). Alban *et al.* (1989) demonstrated that in sycamore, the envelope membranes of non-green plastids contained very low levels of PAP activity, when compared to those of cauliflower. This means that in sycamore, little plastidial DAG (containing C16:0 acyl moieties) is made available for MGDG synthesis. The DAG required for MGDG synthesis is therefore obtained from the Eukaryotic pathway which contains predominantly C18:1 moieties. Cauliflower plastids contain high levels of PAP activity, and allow the generation of sufficient plastidial DAG for MGDG synthesis. Sycamore is a $C_{18:3}$ plant and cauliflower is a $C_{16:3}$ plant. This reiterated the previous observation (Frentzen *et al.*, 1983) that the level of PAP activity within the plastid envelope membrane is responsible for the distinction between $C_{18:3}$ and $C_{16:3}$ plants.

The biological properties of the membrane-bound plastidial enzyme have been well documented in comparison to the extracellular isozymes (Joyard and Douce, 1979; Malherbe *et al.*, 1992; 1995). The plastidial enzyme is highly membrane bound and optimum catalysis is observed at pH 9.0, as opposed to glycerolipid synthesising isoforms of PAP (PAP-1) from all other eukaryotes (Joyard and Douce, 1979). This pH optimum is similar to the optimum stromal pH for the fatty acid synthesising enzymes (Kocsis and Weselake 1996). The enzyme is strongly inhibited by Mg^{2+} (Joyard and Douce, 1979), and more noticeably with Mn^{2+}, Zn^{2+} and Cu^{2+} ions (Malherbe *et al.*, 1995). Malherbe *et al.*(1992) demonstrated that DAG was a powerful inhibitor of plastid PAP activity. This feedback inhibition is likely to be a regulatory mechanism of PAP activity in the channelling of glycerolipid to PG synthesis at the expense of SL and MGDG (Malherbe *et al.*, 1992).

It has become apparent that PAP activity in all organisms is highly regulated through a variety of mechanisms. Knowledge of these and the biochemical properties of PAP will facilitate future manipulations of the seed oil content in plants. No form of PAP has been purified from any plant source. Attempts to increase the TAG production in transgenic oilseeds through modification of the acyltransferases may prove fruitless if PAP activity regulatory mechanisms prevent the PA dephosphorylation. Considering the strategic and important positioning of PAP, it is surprising that there is only a limited amount of data concerning its enzymology, regulation and precise role in TAG and PL biosynthesis. In comparison, the acyltransferases have been subjected to greater scientific research (Frentzen *et al.*, 1983; Ichihara *et al.*, 1989, 1990; Frentzen 1993). The lack of knowledge PAP has been largely due to two main factors: the inherent errors and lack of reliability in the measurement of PAP activity within crude enzyme preparations (Sturton and Brindley, 1978; Ide and Nakazawa, 1989; Kocsis and Weselake, 1996); and the membrane-association of the enzyme/substrate, making purification and substrate presentation for assaying difficult (Verger, 1980; Malherbe *et al.*, 1995; Kocsis and Weselake, 1996).

1.7 The study of membrane bound enzymes.

A large proportion of cellular enzymes are located within membranes (Verger, 1980). Most enzymes involved in glycerolipid bioassembly are integral membrane proteins. Increased efforts to gain molecular insights into the functions and assembly of membrane proteins has been hindered by the hydrophobic or amphipathic nature of both protein and substrate (Hjelmetad and Bell, 1991; Thomas and McNamee, 1990, Carman *et al.*, 1995). The study of such enzymes is further complicated by the involvement of hydrophobic or amphipathic activators, inhibitors and products of such enzymes (Carman *et al.*, 1995).

The methods of membrane bound protein purification are similar to those used in the purification of soluble proteins (Thomas and McNamee, 1990). However, unique properties of membrane bound enzymes make application of these techniques difficult and invariably unsuccessful (Thomas and McNamee, 1990). The range of separation techniques is small and enzyme stability is an additional limiting factor during membrane protein fractionation (Schägger, 1994). Due to the difficulties of purifying membrane bound proteins, knowledge of the kinetic behaviour of these enzymes has been limited (Verger, 1980).

Theoretical and experimental considerations must be addressed in order to kinetically characterise membrane bound enzymes (Carman *et al.*, 1995). Lipid dependent enzymes act *in vivo* in an interfacial environment within large discrete aggregated structures (Deems *et al.*, 1975; Verger, 1980) where catalysis occurs within the two-dimensional interfacial surface. Any kinetic modelling of lipid-dependent enzymes must therefore account for the three-dimensional bulk and two-dimensional interfacial interactions during catalysis (Carman *et al.*, 1995). For this reason, the traditional Michaelis-Menten kinetic model is inappropriate for studying the catalysis of membrane proteins (Verger, 1980). The surface dilution kinetic model was developed by Deems *et al.* (1975) for the action of cobra venom phospholipase A_2 on phospholipid/detergent micelles. The model applies to all lipid interfaces, including micelles, vesicles, liposomes, membranes and detergent mixed micelles (Carman *et al.*, 1995). However, the presentation of lipid substrate within detergent-lipid mixed micelles offers a consistent means of examining surface active enzymes and substrates, at precise molar and surface substrate concentrations. The mixed micelle system is believed to provide an environment that mimics the physiological surface of the membrane (Robson and Dennis, 1977; 1983), where the detergent acts as a neutral dilutor (Carman *et al.*, 1995). The physical properties of Triton X-100 and Triton X-100/Phospholipid mixed micelles have been well documented (Robson and Dennis, 1977 and 1983). At concentrations above the critical micellar concentration (CMC),

Triton X-100 forms micelles of uniform size and shape. With the addition of up to 15mol% phospholipid, the micelles are similar to the structure of pure Triton X-100 (Lichtenberg *et al.*, 1983; Carman *et al.*, 1995). Physical properties of Triton X-100/PA mixed micelles have been reported by Lin and Carman (1990), and are in agreement with other Triton X-100/phospholipid mixed micelles. Such detailed understanding of the physical characteristics of mixed micelles is fundamental to the success of the interfacial kinetic analysis. Changes in the shape or size of the micelles could dramatically affect the enzyme activity and complicate the kinetic analysis (Carman *et al.*, 1995).

The surface dilution kinetic model has been used in the study of many lipid dependent enzymes including PAP from *S. cerevisiae* (Lin and Carman, 1990). In the study of many lipid dependent enzymes, the model has; allowed the identification of lipid activators and inhibitors, demonstrated structural requirements for activation and inhibition, illustrated substrate specificity, determined inhibition/activation mechanisms, and provided insights into the regulatory roles of lipid activators and inhibitors *in vivo* (Carman *et al.*, 1995). The capability of the surface dilution kinetic model in the elucidation of enzyme-lipid interactions during phospholipid metabolism was clearly demonstrated by Bae-Lee and Carman (1990). The effects of various phospholipid intermediates on PS synthase and PI synthase were examined with inhibition or activation constants derived for each lipid tested. This enabled the involvement of these enzymes to be assessed during the flux of glycerolipids through the primary, auxiliary and TAG pathways. Detailed biochemical investigations such as this on homogenous plant PAP will enable important information of the regulatory role of PAP in plant glycerolipid biosynthesis to be elucidated. Substrate specificity studies of the enzymes involved in phospholipid biosynthesis are required to delineate the mechanism by which these enzymes contribute to the molecular species distribution in membranes (Hjelmestad and Bell, 1991).

Triton X-100 forms micelles of uniform size and shape. With the addition of up to 15mol% phospholipid, the micelles are similar to the structure of pure Triton X-100 (Lichtenberg *et al.*, 1983; Carman *et al.*, 1995). Physical properties of Triton X-100/PA mixed micelles have been reported by Lin and Carman (1990), and are in agreement with other Triton X-100/phospholipid mixed micelles. Such detailed understanding of the physical characteristics of mixed micelles is fundamental to the success of the interfacial kinetic analysis. Changes in the shape or size of the micelles could dramatically affect the enzyme activity and complicate the kinetic analysis (Carman *et al.*, 1995).

The surface dilution kinetic model has been used in the study of many lipid dependent enzymes including PAP from *S. cerevisiae* (Lin and Carman, 1990). In the study of many lipid dependent enzymes, the model has; allowed the identification of lipid activators and inhibitors, demonstrated structural requirements for activation and inhibition, illustrated substrate specificity, determined inhibition/activation mechanisms, and provided insights into the regulatory roles of lipid activators and inhibitors *in vivo* (Carman *et al.*, 1995). The capability of the surface dilution kinetic model in the elucidation of enzyme-lipid interactions during phospholipid metabolism was clearly demonstrated by Bae-Lee and Carman (1990). The effects of various phospholipid intermediates on PS synthase and PI synthase were examined with inhibition or activation constants derived for each lipid tested. This enabled the involvement of these enzymes to be assessed during the flux of glycerolipids through the primary, auxiliary and TAG pathways. Detailed biochemical investigations such as this on homogenous plant PAP will enable important information of the regulatory role of PAP in plant glycerolipid biosynthesis to be elucidated. Substrate specificity studies of the enzymes involved in phospholipid biosynthesis are required to delineate the mechanism by which these enzymes contribute to the molecular species distribution in membranes (Hjelmestad and Bell, 1991).

1.8 The aims of this research.

There is great interest in the production of 'tailor-made' lipids in oilseed crops (Slabas *et al.*, 1995). Most agriculturally produced oleaginous seeds currently contain TAG with C18 and C16 fatty acids. These fatty acids are also prevalent within the phospholipids in all tissues of plants. However, there are also 'unusual' fatty acids which are exclusively found within TAG (Dutta *et al.*, 1992). These fatty acids are often family specific such as erucic acid (C22:1) in *Cruciferae* and petroselinic acid ($C18:1^{\Delta 6}$) in *Umbelliferae* (Dutta *et al.*, 1992), and can be desirable for industrial purposes. Trierucoyl-TAG is a desirable starting material in the production of high temperature lubricants, nylon and plasticizers (Kocsis and Weselake, 1996). *Brassica napus* produces erucoyl-CoA, but the acyltransferase machinery excludes it from position *sn-2* of the glycerol backbone of TAG (Bernerth and Frentzen, 1990). Plants of the genus *Limnanthes* can produce low levels of trierucin (Cao *et al.*, 1990). A cDNA has been isolated from maize which complemented an *E. coli* LPAAT mutant JC201 (Brown *et al.*, 1994). This was used as a heterologous probe in the identification of a cDNA encoding LPAAT from *Limnanthes douglasii* (Brown *et al.*, 1995). A second *Limnanthes douglasii* cDNA encoding a different LPAAT activity was identified by complementation of the *E. coli* JC201 mutant. Membranes isolated from the complemented *E. coli* mutant were found to be able to synthesise erucoyl-PA (Brown *et al.*, 1995). Recently, Lassner *et al.* (1995) transformed a high erucic acid cultivar of *B. napus* with a cDNA encoding *Limnanthes alba* LPAAT. Low levels of trierucin were produced in the transgenic seeds. This demonstrates the potential to genetically modify the fatty acid content and possibly the overall TAG level within oilseed crops. However, the elucidation of the glycerolipid flux and the intricate regulation mechanisms is a prerequisite of biotechnological strategies for seed oil modification.

Phosphatidate phosphatase is a key enzyme in glycerolipid biosynthesis in all eukaryotic cells. The dephosphorylation of PA to DAG is common to TAG and PL synthesis. PAP lies at a theoretical branchpoint in glycerolipid biosynthesis. Studies in yeast and mammalian tissues have shown it to be highly regulated. Identified mechanisms which alter PAP activity are as follows: protein-phosphorylation/dephosphorylation, the action of hormones, sub-cellular translocation, lipid activation/inhibition, product feedback inhibition. Such diverse regulatory mechanisms are indicative of the importance of this enzyme in the 'house-keeping' and 'luxury' synthesis of glycerolipids. The isoform of PAP implicated in glycerolipid synthesis has not been purified in animals, with most of the research directed towards an isoform implicated in signal transduction.

There is little biochemical information regarding PAP in plants. All of the currently available data was obtained with the use of crude enzymatic preparations. There have been no reported attempts to purify the enzyme to homogeneity from any plant source and there is currently conflicting data concerning the biochemical properties of PAP in plants.

The aim of the research in this thesis was to purify and characterise PAP from a TAG rich plant tissue. In this way the enzyme involved in glycerolipid biosynthesis could be positively identified, characterised and purified to homogeneity for the first time from any oleaginous tissue.

In order to study this enzyme, an accurate, sensitive and reproducible assay was developed, based on the assaying system used by Lin and Carman (1989). This was based on following the release of aqueous soluble [^{32}P]Pi from aqueous insoluble [^{32}P]PA. The [^{32}P]PA was not commercially available and would need to be synthesised in the laboratory. Owing to the short half life of ^{32}P (14.2 days), the

synthesis of [^{32}P]PA needed to be undertaken regularly and efficiently, throughout the course of this study.

With the [^{32}P]PA, and using the assaying procedure Lin and Carman (1989), PAP activity was located in differentially centrifuged cell extracts of an oleaginous plant. Ripening avocado (*Persea americana*) fruit was used as the source of cell extracts as it is very rich in TAG, and as such it would be expected that the TAG synthesising machinery would also be highly expressed. Once the activity was established, the measurement was optimised so that all future studies of the enzyme were accurate and reliable. The appropriate cellular fraction was chosen for the purification of the enzyme.

A novel purification strategy was employed in order to obtain a homogenous preparation of the enzyme. The development of a purification strategy was undertaken with a small avocado preparation. If the success of further manipulations (such as characterisation studies or N-terminal amino acid sequencing) was dependent on the quantity of homogenous protein, the scale of the fractionation was increased accordingly.

Once homogenous PAP was obtained, the research was focused towards detailed kinetic characterisation of the homogenous protein. It was hoped that with such studies, pertinent scientific questions could then be addressed in order to gain an insight into the regulation and activity of this elusive enzyme.

Chapter 2

Materials and Methods

2.1 Materials

With the exception of those listed below, all materials used throughout this study were obtained from either the Sigma Chemical Company Ltd., Fancy Road, Poole, Dorset, BH17 7NH, or BDH Chemicals Ltd., Merck Ltd., Merck House, Poole, Dorset, BH15 1TD. All reagents were of Molecular Biology or Ultrapure standard.

Acrylamide, sodium dodecyl sulphate, ammonium persulphate, Coomassie R-250 and N,N,N'N'-tetramethylethylene diamine (TEMED) were from Bio-Rad Laboratories Ltd., Bio-Rad, Maylands Avenue, Hemel Hempstead, Hertfordshire, HP2 7TD.

[γ-^{32}P]ATP (30Ci/mmol) and [U-^{14}C]Glycerol (159mCi/mmol) were purchased from Amersham International Plc., Little Chalfont, Amersham, Buckinghamshire, HP7 9NA.

Avocados (usually Type Haas) were purchased locally from Safeways, Milburngate, Durham, or from Hutchinson and Sons, Stanhope Street, Fenham, Newcastle Upon Tyne.

DAG Kinase was from Calbiochem-Novabiochem (UK) Ltd., Boulevard Industrial Park, Padge Road, Beeston, Nottingham, NG9 2JR.

DTT was obtained from Melford Laboratories Ltd., Chelsworth, Ipswich, Suffolk, IP7 7LE.

Fuji X-Ray film was from Fuji Photo Film [UK] Ltd., Fuji Film House, 125 Finchley Road, Swiss Cottage, London, NW3 6JH. Developer and fixer were from H.A. West [X-Ray] Ltd., 41 Watson Crescent, Edinburgh, EH11 1ES.

Mono Q, Mono S, Superose 12, Q-Sepharose, S-Sepharose, Phenyl-Sepharose and Phenyl Superose were all obtained from Pharmacia LKB Biotechnology, 23 Grovesnor Road, St. Albans, Hertfordshire, AL1 3AW, and used on Pharmacia Hi-Load, FPLC or Smart chromatography systems. Affi-Gel Blue was purchased from Bio-Rad Laboratories Ltd. Amicon dye-ligand matrices were from Amicon Corp., Lexington, Mass., USA.

Silica TLC plates (K6F Silica Gel 60 Å) were from Whatman International Ltd., St. Leonard's Road, Maidstone, Kent, ME16 0LS

Ecoscint A scintillation fluid was purchased from National Diagnostics, and used in conjunction with 5ml scintillation vials and a 1600TR Liquid scintillation counter that were supplied by Canberra Packard Ltd., Brook House, 14 Station Road, Pangbourne, Berks, RG8 7DT.

Glass centrifuge tubes (13ml) with Teflon-lined screw caps were purchased from Fisons, and the bottom of each subsequently tapered into a point by the Glass Blowing Department, University of Durham. The customised tubes were used for all radiochemical enzymatic assays.

Glycerol-3-Phosphate Acyltransferase was produced from the *Escherichia coli* strain BL21(DE3) containing the plasmid pET-AR1, which results in the enzyme overexpression (Nishida *et al.*, 1993) and was a gift from J.M. Kroon (University of Durham, Durham, UK).

Ultrafree®-MC filters were purchased from Millipore (UK) Limited, The Boulevard, Blackmoor Lane, Watford, Hertfordshire, WD1 8YW.

2.2 Synthesis of radiolabelled assay substrates

2.2.1 The synthesis of *sn*-1,2-dioleoyl-3-[^{32}P]phosphate

[^{32}P]PA was synthesised from [γ-^{32}P]ATP and *sn*-1,2-diacylglycerol with DAG kinase (10 μmol PA produced/min/mg; 1mg/ml) using an adaptation of the procedure described by Walsh and Bell (1986; 1992). In a 100μl final volume, the reaction mixture consisted of 51mM (15g/L) octylglucoside, 1mM cardiolipin, 60mM imidazole-HCl (pH6.6), 50mM NaCl, 12.5mM $MgCl_2$, 1mM EGTA, 0.3mM DTPA, 2mM DTT, 2mM dioleoylglycerol and 50μM [γ-^{32}P]ATP (30Ci/mmol, 10mCi/ml, 150μCi total) and 0.05 unit DAG kinase. The reaction was initiated with the addition of 5μl DAG Kinase.

The exact procedure used was as follows: DAG (10μl of 12.5mg/ml in $CHCl_3$) was transferred into a glass reaction vial and the $CHCl_3$ removed by evaporation under a stream of N_2 gas. The DAG was dissolved by vigorously mixing in 20μl of 5 x cardiolipin/octylglucoside solution (5mM Cardiolipin, 255mM Octylglucoside and 1mM DTPA), 50μl 2 x reaction buffer (100mM Imidazole-HCl pH6.6, 25mM $MgCl_2$, 100mM NaCl and 2mM EGTA) and 2μl 100mM DTT (freshly prepared) and an appropriate volume of ddH_2O. [γ-^{32}P]ATP (15μl) was then added and the mixture briefly incubated at 25°C prior to the addition of DAG Kinase. After 60minutes at 25°C, the reaction was terminated with the addition of 60μl 10% perchloric acid. The [^{32}P]PA was extracted from the [γ-^{32}P]ATP using the method of Rajasekharan *et al.* (1988) in which 2.5ml $CHCl_3$:CH_3OH (1:1) was added to the terminated reaction mixture, and vigorously mixed for 5 seconds. Two phases were then created with the addition of 1ml 0.2M H_3PO_4 in 1M KCl. The two phases were placed in separate

clean glass reaction vials. The $CHCl_3$ phase washed with fresh aqueous phase, and the aqueous phase was washed with $CHCl_3$ phase. The $CHCl_3$ phases were pooled and washed once more with fresh aqueous phase, resulting in a $CHCl_3$ phase that contained pure [^{32}P]PA. The volume was reduced by removing the chloroform under a stream of N_2 gas. This was stored at -20°C in $CHCl_3$ until use, and routinely synthesised approximately every 45 days.

2.2.2 The synthesis of *sn*-1-oleoylglycerol-3-[^{32}P]phosphate

[^{32}P]LPA was produced in an enzymatic reaction at 25°C for 60minutes, containing the two enzymes glycerokinase and glycerol-3-phosphate acyltransferase. The reaction mixture (100µl final volume) was as follows: 250mM HEPES-NaOH (pH7.5), 2mM glycerol, 2.5mM $MgSO_4$, 0.4mM oleoyl-CoA, glycerol kinase (2 units), glycerol-3-phosphate acyltransferase (2 units) and 0.1mM ATP containing 100µCi [γ-^{32}P]ATP. Oleoyl-CoA was prepared as a 8mM stock in 10mM sodium acetate (pH6.0). The reaction was terminated with the addition of 60µl 10% perchloric acid, phase extracted and stored as for the [^{32}P]PA (described above).

Alternatively, [^{32}P]LPA was synthesised from *sn*-1-monooleoylglycerol and [γ-^{32}P]ATP with DAG Kinase under otherwise identical conditions as used in the synthesis of [^{32}P]PA. The yield from both syntheses are comparable (approximately 60%).

2.2.3 The synthesis of *sn*-1-oleoyl[^{14}C]glycerol-3-phosphate

[^{14}C]LPA was synthesised from [U-^{14}C]glycerol, ATP and oleoyl-CoA by the action of glycerokinase and glycerol-3-phosphate acytransferase. The reaction conditions were similar to those used for the synthesis of [^{32}P]LPA. The reaction mixture (100µl final volume) was as follows: 250mM HEPES-NaOH (pH7.5), 5mM

ATP, 2.5mM $MgSO_4$, 0.4mM oleoyl-CoA, glycerol kinase (2 units), glycerol-3-phosphate acyltransferase (2 units) and 0.16mM [U-^{14}C]glycerol. The reaction was terminated with the addition of 60µl 10% perchloric acid, phase extracted and stored as for the [^{32}P]PA (described above).

2.2.4 The synthesis of Ceramide-1-[^{32}P]phosphate and *sn*-2-oleoylglycerol-3-[^{32}P]phosphate.

Ceramide-1-[^{32}P]phosphate and *sn*-2-oleoylglycerol-3-[^{32}P]phosphate were synthesised from 0.1mM[γ-^{32}P]ATP and ceramide or *sn*-1-monooleoylglycerol, respectively using DAG kinase as described by Waggoner *et al.* (1996). The reaction conditions for the synthesis of either compound were otherwise identical to those used for the synthesis of [^{32}P]PA, as described in section 2.2.1. In a 100µl final volume, the reaction mixture consisted of 51mM (15g/L) octylglucoside, 1mM cardiolipin, 60mM imidazole-HCl (pH6.6), 50mM NaCl, 12.5mM $MgCl_2$, 1mM EGTA, 0.3mM DTPA, 2mM DTT, 2mM ceramide or *sn*-2-MAG and 0.1mM [γ-^{32}P]ATP (10mCi/mmol, 20µCi total) and 0.05 unit DAG kinase. The reaction was initiated with the addition of 5µl DAG Kinase and incubated at 25°C for 12hours. The reaction was terminated with the addition of 2.5ml $CHCl_3$:CH_3OH (1:1), and the lipid extracted by the addition of 1ml 0.2M H_3PO_4 in 1M KCl. The lower chloroform phase was removed and dried under a stream of N_2 gas. The dried sample was resuspended in 100µl chloroform, applied to a silica TLC plate alongside standards, and developed in $CHCl_3$:CH_3OH:H_2O (12:6:1). The developed TLC plates were exposed to x-ray film, to determine the migration position for the radiolabelled reaction products. The corresponding radioactive spots were scraped off the TLC plate, extracted into 1 ml $CHCl_3$ and stored at -20°C.

The Rf values of the various lipids/compounds used in this when developed on silica K6F Silica Gel 60Å TLC plates (Whatman Int.) in $CHCl_3$:CH_3OH:H_2O (12:6:1) are shown in Table 2.1.

Compound	Rf Value
ATP	0
Oleoyl-CoA	1.0
sn-1,2-diacylglycerol (DAG)	0.9
sn-1,2-diacylglycerol-3-phosphate (PA)	0.4
sn-1-monoacylglycerol (MAG)	0.8
sn-1-acylglycerol-3-phosphate (LPA)	0.2
sn-2-monoacylglycerol (*sn*-2-MAG)	0.79
sn-2-acylglycerol-3-phosphate (*sn*-2-LPA)	0.18
Ceramide	0.85
Ceramide-1-phosphate	0.28

Table 2.1: The separation of various lipids on Silica TLC plates using the $CHCl_3$:CH_3OH:H_2O (12:6:1) solvent system. All freshly synthesised substrates were analysed by TLC with the appropriate authentic lipid standards.

2.3 Assaying for PAP activity.

2.3.1 The yeast standard PAP assay reaction conditions.

PAP activity was measured by following the release of [^{32}P]Pi from [^{32}P]PA according to the procedure described by Lin and Carman (1989). In a typical assay, sample protein was added to a final reaction volume of 0.1ml, containing: 50mM Tris-maleate buffer pH 7.0, 5mM Triton X-100, 10mM 2-mercaptoethanol, 2mM $MgCl_2$, 0.5mM [^{32}P]PA (1000-2000 decays per minute(DPM)/nmol, 50nmoles total, 50 000-100 000 DPM/assay).

PA (stock solution 5mg/ml in $CHCl_3$, 7µl/assay) was transferred into a glass reaction vial. An appropriate amount of undiluted [^{32}P]PA stock (30Ci/mmol, considered a negligible molar concentration) was added to the vial to give a final radioactivity of 50 000-100 000DPM/assay, and the $CHCl_3$ removed by evaporation under a stream of N_2 gas. The PA was solubilised with the addition and vigorous mixing of 50µl 10mM Triton X-100, 20µl 5 x stock reaction buffer (250mM Tris-maleate buffer pH7.0 and 10mM $MgCl_2$), 7µl 140mM 2-Mercaptoethanol and an appropriate volume of ddH_2O. The reaction was initiated with the addition of enzyme sample and allowed to proceed for 20 minutes at 30°C. If more than one assay reaction was required, an appropriate multiple of the above mixture was prepared and aliquotted for each reaction prior to the addition of enzyme sample to reduce variability. This reduced the assay preparation time and ensured that all reactions were the same.

The reactions were terminated and the [γ-^{32}P]ATP and [^{32}P]PA separated as described by Carman and Lin (1991). The reactions were stopped with the addition of 0.5ml 0.1N HCl in Methanol. Chloroform (1ml) and 1M $MgCl_2$ (1ml) were added to the terminated reaction and mixed to create two phases. Aliquots (100µl) of each phase were withdrawn and added to 5ml scintillation vials containing 4ml Ecoscint A. The radioactivity was determined by scintillation counting. One Unit of PAP activity was defined as the amount of enzyme that catalyses the formation of 1µmol of product per minute.

2.3.2 The avocado standard PAP assay reaction conditions.

Avocado PAP activity was measured using an adaptation of the procedure of Lin and Carman (1989) and Carman and Lin (1991). The reaction consisted of 0.5mM

[^{32}P]PA (1000-2000 DPM/nmol), 50mM Tris-maleate pH 6.0, 2-5mM Triton X-100, 2mM $MgCl_2$, and protein sample in a total volume of 100µl at 25°C. Stock solutions of dioleoyl-PA (5mg/ml in $CHCl_3$, 7µl/assay), 10mM Triton X-100 (50µl/assay) and 5x reaction buffer (250mM Tris-maleate pH 6.0 and 10mM $MgCl_2$) were prepared. The PA stock solutions and all other stock solutions were stored at -20°C and room temperature, respectively.

The reactions were prepared, terminated and phase extracted as in the Yeast standard assay conditions, described in the previous section. Where increased assay sensitivity was required, the specific activity of [^{32}P]PA was increased. The reaction contained 50µM [^{32}P]PA (15 000 DPM/nmol) and 0.2mM Triton X-100 in the otherwise unchanged assay procedure.

After reaction termination and phase extraction, the total volume of the $CHCl_3$ and aqueous phases were 1.0 and 1.3ml, respectively. The radioactivity in both phases was measured using a 100µl aliquot from each phase. Where no enzyme was added, both phases were respectively uncontaminated. PAP activity was calculated by measuring the total ^{32}P in each phase (i.e. that of [^{32}P]PA and [^{32}P]Pi in the $CHCl_3$ and aqueous phases, respectively). This enabled the calculation of the fraction of Pi from total [^{32}P]. The 20minute reaction initially contained 50nmoles substrate. The fraction of [^{32}P]Pi formed was multiplied by 50 to obtain the nmoles of Pi formed during the reaction. This was then divided by 20 to obtain a value of nmoles Pi/min. One Unit of PAP activity is defined as the amount of enzyme that catalyses the formation of 1µmol of Pi per minute.

2.4 Protein methods

2.4.1 The preparation of dialysis tubing

To remove chemical contaminants, dialysis tubing was boiled in 20 % (w/v) sodium bicarbonate and 1 mM EDTA for 10 minutes. The tubing was then boiled in 1 mM EDTA for a further 10 minutes. After cooling, it was stored in 50 % ethanol and 1 mM EDTA at room temperature. Prior to use, tubing was thoroughly washed in ddH_2O and handled with the use of gloves. The protein sample was retained within the tubing during dialysis with the combined use of plastic clamps and a knot tied at each end of the tube;

2.4.2 Microdialysis of protein samples.

Protein samples with a volume of less than 1ml were dialysed using the lid of an eppendorf tube as illustrated in Figure 2.1. A 1.5 or 0.5ml eppendorf tube was cut just below the neck and the sample transferred into the cap receptacle. A single layer of dialysis membrane was layered over the cap/protein sample and fixed into place with the remaining neck which acted as a sleeve over the outside of the dialysis membrane. The sealed unit was placed in the appropriate dialysis buffer and stirred at 4°C.

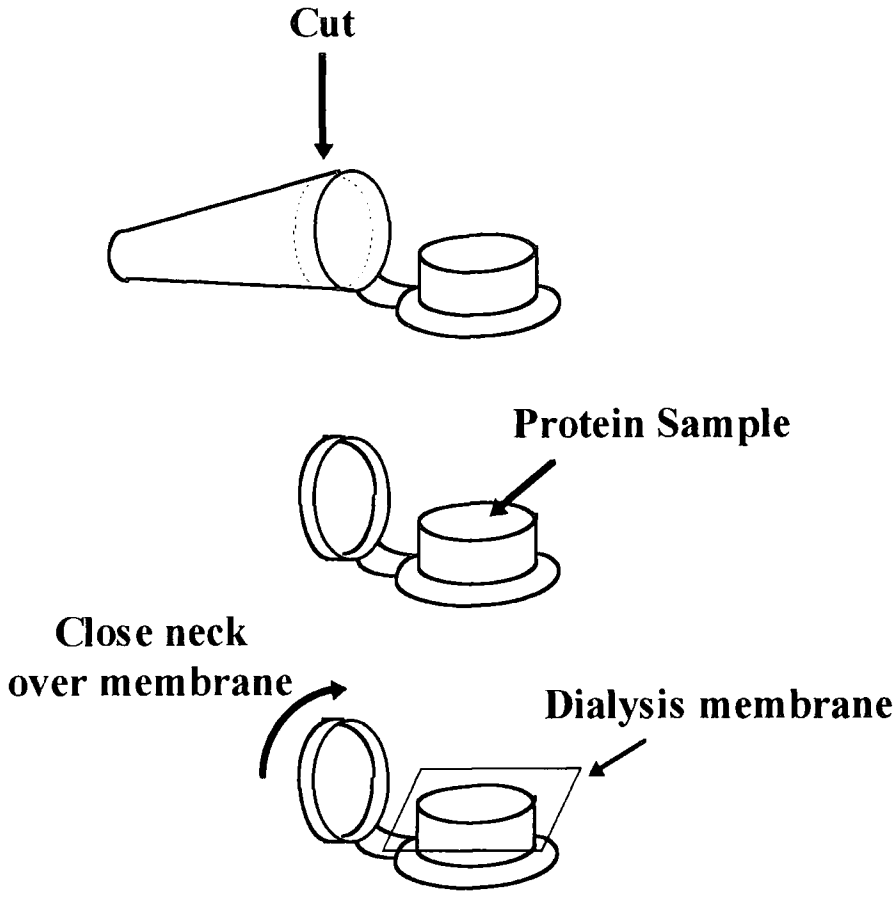

Figure 2.1: The assembly of the microdialysis apparatus from an eppendorf tube.

2.4.3 Determination of protein concentration.

The total protein concentration of a sample was measured using an adaptation of the Folin phenol method of Lowry *et al.* (1951) as described by Peterson (1983). The Folin phenol method is based on the reduction of molybdic-tungstic mixed acid chromagen (Folin and Ciocalteu reagent) caused by the aromatic amino acids, tyrosine and tryptophan and the reaction with copper chelates of polar groups and peptide chains. The reduction of acid chromagen causes an increase in the absorption at 750nm (Lowry *et al.*,1951; Peterson, 1983). To remove potentially interfering

compounds such as lipids and detergents, the quantitative deoxycholate-trichloroacetic acid (DOC-TCA) precipitation procedure of Peterson (1983) was conducted prior to protein measurement. The DOC-TCA adaptation of the Lowry assay was used for all protein samples during the course of this study, with BSA as standard.

Stock solutions were prepared as follows:

Reagent A: 2% (w/v) Na_2CO_2 in 0.1M NaOH (Store at RT)

Reagent B: 0.5% (w/v) $CuSO_4.5H_2O$ in 1% Sodium Tartrate (Store at RT)

Reagent C: Mix 50ml Reagent A and 1ml Reagent B (freshly prepared)

Reagent D: Folin-Ciocalteu reagent diluted 1:1 with ddH_2O

All samples/standards were precipitated and assayed for total protein in duplicate. 0.1ml of 0.15% (w/v) deoxycholate was added to a 1ml protein sample, vigorously mixed and allowed to stand at room temperature for 10 minutes. TCA (0.1ml of 72% w/v) was then added, and the sample centrifuged for 15 minutes at 3000*g*. After centrifugation, the supernatant was removed by aspiration. The pellets were resuspended in 1ml Reagent C and allowed to stand for 10 minutes (or longer) at room temperature. Reagent D (0.1ml) was added and vigorously mixed, and after at least 30 minutes at room temperature, the absorption at 750nm was measured. A protein standard curve was constructed and the protein concentrations of each sample calculated. An example of a protein standard curve is shown in Figure 2.2.

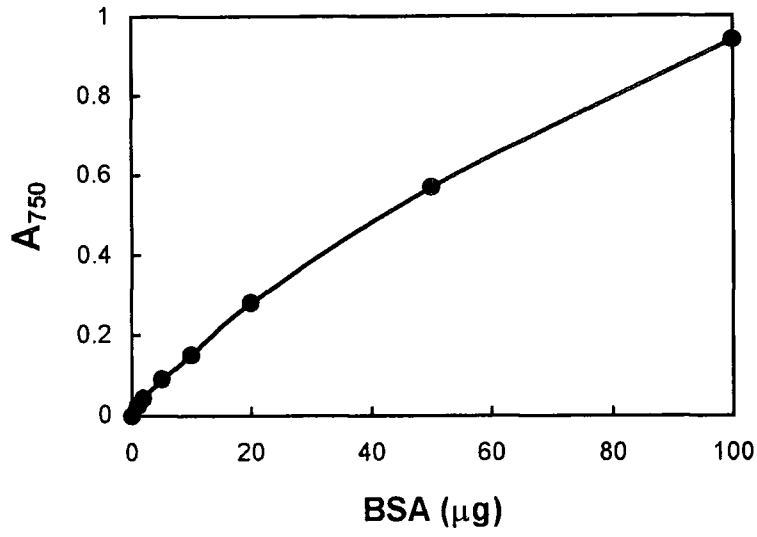

Figure 2.2: A typical Lowry assay protein standard curve. Total protein was measured using the TCA-deoxycholate adaptation of the Lowry method described by Peterson (1983). All standards and samples were routinely measured in duplicate.

2.4.4 Chloroform-methanol precipitation of proteins.

Protein samples were routinely precipitated using the quantitative chloroform-methanol precipitation technique described by Wessel and Flügge (1984). This enabled the concentration, delipidation and removal of interfering substances (i.e. detergent and salt) of protein samples prior to polyacrylamide gel electrophoresis.

The procedure was conducted as follows: 0.4ml of methanol was added to 0.1ml protein sample, vortexed for 2 seconds, and centrifuged for 10 seconds at 9000*g*. Then 0.1ml chloroform was added to the total sample, and centrifuged after vortexing. After centrifugation, 0.3ml ddH_2O was added and the sample vigorously mixed prior to centrifugation at 9000*g* for 1minute, to create two phases. The upper phase was carefully removed (leaving protein precipitate at the interface) and discarded. Methanol (0.3ml) was added to the lower chloroform phase, mixed and

centrifuged at 9000*g* for 5 minutes. The supernatant was removed and the pellet air-dried. When the pellets were completely dry, they were resuspended into SDS-PAGE sample buffer.

In larger protein samples (1ml), the procedure was adapted with the same relative amounts of each reagent added (Wessel and Flügge, 1981). For convenience, a 15ml Falcon tube was used. After centrifugation and removal of the upper phase, the lower phase and interfacial protein, was transferred into a 1.5ml eppendorf tube and the subsequent procedures continued, allowing easier resuspension of the final protein pellets.

2.4.5 Separation of proteins by SDS-PAGE.

SDS-PAGE was conducted with discontinuous gels, routinely with a 10% resolving gel (70 x 100 x 0.75mm) and a 5% stacking gel, using the buffer system of Laemmli (1970) and a Bio-Rad Mini Protean II vertical electrophoresis apparatus, unless otherwise stated.

The resolving gel was prepared in a 15ml Falcon tube, with 3.33ml 37.5:1 acrylamide:bis-acrylamide in, 0.375 M Tris-HCl (pH 8.8), 0.1 % (w/v) SDS, 0.014 % (w/v) ammonium persulphate (freshly prepared) and 0.2 % v/v TEMED. Acrylamide polymerisation was initiated with the addition of TEMED (catalyst). The solution was mixed by inversion and poured into the casting apparatus to not more than 2.5 cm from the top of the gel former. To ensure a level surface, water-saturated *n*-butanol was layered onto the top of the gel and allowed to stand at room temperature. Once the gel was set, the *n*-butanol was washed off with ddH_2O.

The stacking gel was prepared with 0.8ml 37.5:1 acrylamide:bis-acrylamide in, 0.125M Tris-HCl (pH 6.8), 0.1 % (w/v) SDS, 0.014 % (w/v) ammonium persulphate and 0.4 % (v/v) TEMED. This was poured on top of the resolving gel and an appropriate comb was inserted to create loading wells. After polymerisation at room

temperature, the comb was gently removed, and any unpolymerised acrylamide was washed away with ddH_2O.

All Protein samples were chloroform-methanol precipitated prior to electrophoresis. The pellets were resuspended in 1 x SDS sample buffer (62.5mM Tris-HCl (pH 6.8), 2 % w/v SDS, 60m M DTT, 0.01 % (w/v) bromophenol blue, and 10 % (v/v) glycerol). The samples were boiled for 2 minutes and maintained on ice.

The running buffer contained 25mM Tris-HCl buffer (pH 8.3), 192mM glycine and 0.1 % (w/v) SDS (stored as a 10 x solution). A current of 100V was applied across the gel until the protein had migrated to the interface. Electrophoresis was then conducted at 200V until the dye front reached the bottom of the gel.

Proteins were routinely visualised by staining with Coomassie Blue R-250. The gels were removed from the Protean II apparatus and immersed in hot Coomassie stain (25 % (v/v) propan-2-ol, 10% (v/v) glacial acetic acid and 0.04% (w/v) Coomassie R-250) in a microwave-safe container. The gels were gently agitated for 20minutes, whereupon the loosely covered container was placed in a microwave and reheated at a medium setting for 1-2 minutes. The gels were gently agitated as before, and allowed to cool.

Once cool, the coomassie stain was removed, the gels briefly rinsed in ddH_2O, and gently agitated in hot destaining solution (10 % v/v acetic acid and 1 % v/v glycerol). A small piece of sponge was included in the container to soak up Coomassie Blue until the background stain was completely removed. The gels were dried using a Easy Breeze Gel Drier (Hoefer Scientific Instruments).

2.4.6 Visualisation of proteins by Silver staining

In samples where there is insufficient protein sample to allow Coomassie staining (i.e. $\leq 0.1\mu g$ protein per band), the protein was visualised by the more sensitive silver staining. All glassware was thoroughly cleaned with ethanol and HNO_3 prior to use. For this reason, acrylamide gels were never handled with ungloved hands. The gel was removed from the electrophoresis apparatus, or from the Coomassie destaining container, and placed in fixing solution (ethanol: acetic acid: water 4:1:5) and gently agitated for at least 30 minutes. It was then placed in Incubation solution (75ml ethanol, 17g sodium acetate, made up to 250ml with ddH_2O) for a minimum of 30 minutes and then washed in ddH_2O for 5 x 5 minutes. The gel was then placed in silver solution (0.25g silver nitrate, 50µl formaldehyde (added prior to use), in 250ml ddH_2O) for 40 minutes. The images were developed by placing the gel in developing solution (6.25g sodium carbonate, 25µl formaldehyde, in 250ml ddH_2O) for up to 15 minutes, depending on the background darkening. The developing process was stopped by replacing the developing solution with stopping solution (2.5mM EDTA). The gel was then preserved in coomassie destaining solution(10% v/v acetic acid and 1% v/v glycerol) before drying as before.

In the event of over development of the image, the gel was totally destained with the addition of 50% photographic fixer solution (containing ammonium thiosulphate, Sodium sulphite, aluminium chloride and acetic acid; H.A. West [X-ray] Ltd.) The fixer solution was then removed by repeated washes in ddH_2O, and the staining procedure repeated.

2.4.7 The separation of proteins by native PAGE.

The separation of protein according to native molecular mass (and isoelectric point) was performed using the method described by Rock *et al.* (1981). This was

essentially the same as SDS-PAGE described above, except with the total exclusion of SDS and reducing agent. Protein samples were prepared for electrophoresis with the addition of 5 x native gel sample buffer (5 x solution: 250 mM Tris-HCl (pH 6.8), 50 % (v/v) glycerol, 0.3 M DTT, 0.5 % w/v bromophenol blue) to make a 1 x concentration and incubated at on ice for 5 minutes. The running buffer consisted of 3.1g Tris and 14.4g glycine in 1 litre ddH_2O (final pH 8.3). Electrophoresis was conducted at 4°C at 25mA until the tracking dye reached the bottom of the gel. The protein was visualised by coomassie staining as before. Monomeric and dimeric BSA, and ovalbumin were loaded along side to assess the efficiency of protein migration through the gel. Native PAGE separates proteins according to charge and size, therefore these proteins were not used as molecular mass standards. The accurate measurement of native molecular mass was obtained by separating the proteins further by SDS-PAGE. A sample lane containing resolved protein (unstained) was cut into 5mm slices and each slice boiled in 2 x SDS-PAGE sample buffer for 2minutes. The slices were then each paced into an SDS-PAGE sample well and the protein transferred into the SDS-PAGE gel and separated by electrophoresis. The separated protein was then visualised by coomassie or silver staining.

2.4.8 Electrophoretic transfer of protein to PROBLOT® PVDF membrane for N-Terminal amino acid sequencing.

N-Terminal amino acid sequencing was attempted using protein that had been immobilised on a PROBLOT PVDF membrane. HPLC and Ultrapure electrophoresis-grade reagents (Bio-Rad) were used throughout. An SDS-PAGE gel (5% stacking/10% resolving gel) was prepared and stored over night at 4°C to remove free radicals. The running buffer was freshly prepared, with 200μM thiodiglycolic acid added to the buffer in the upper chamber. The gel was 'pre-run' with the application of 100V across the gel for 20 minutes prior to sample/control protein loading. The

protein was separated through the gel until the dye front had reached the bottom of the gel.

The gel was removed from the electrophoresis apparatus, and soaked for 10 minutes in transfer buffer (2.21g CAPS buffer, 10% CH_3OH and 0.1% (w/v) SDS, adjusted to pH11 with 2M NaOH in 1litre final volume). A piece of PROBLOT membrane and six pieces of filter paper were cut to the size of the gel (approximately 100 x 75mm). The filter paper, and two pieces of nylon gauze were soaked in Transfer buffer. The PROBLOT membrane was briefly immersed in methanol and equilibrated for 2minutes in transfer buffer. The gel holder of a Trans-Blot electrophoretic Transfer Cell (Bio-Rad) was opened with the 'clear' side facing downwards. The blotting 'sandwich' was assembled onto the clear side (anode) of the apparatus as follows: A nylon gauze was placed on the apparatus, followed by 3 pieces of filter paper. Air bubbles were removed from the layers with the use of an 'artists screen-printing' plastic roller. The PROBLOT membrane was then placed on the sandwich, followed by the SDS-PAGE gel. The assembly was completed with addition of 3 more pieces of filter paper, and the second nylon gauze. The cassette was closed and placed in the electrophoresis tank in the correct orientation with the clear side of the assembly facing the anode, and the grey side towards the cathode. The electrophoretic transfer was conducted at 40mA for 16 hours. During the transfer, the transfer buffer in the gel tank was gently stirred.

After transfer of the protein, the apparatus was dismantled. The PROBLOT membrane was washed by immersion in ddH_2O and allowed to completely dry in an evacuated desiccator. To ensure complete electrophoretic transfer, the gel was coomassie stained with the total transfer of protein confirmed with the inability to detect protein sample or protein molecular mass standards. The dried blot was briefly immersed in methanol and then placed in Sulphorhodamine B stain (0.005% Sulphorhodamine B, 30% methanol and 0.2% acetic acid in ddH_2O). for 10 seconds. The membrane was then washed/destained in ddH_2O and dried as before. Protein

bands were detected once the membrane was completely dry. The protein band of interest were excised from the membrane with a sterile razor blade for N-Terminal amino acid sequencing.

As an alternative to Sulphorhodamine B staining, the blotted protein was detected with Fast Coomassie Staining. The gel was placed in fast Coomassie Blue stain (0.1% Coomassie Blue R-250, 40% methanol and 10% acetic acid) for 25 seconds, then briefly destained (until pale blue background is obtained) in 50% methanol and finally allowed to dry as before. Upon drying, the background faded from pale blue to white enabling protein detection.

2.4.9 Ammonium Sulphate precipitation of protein

Protein samples were routinely precipitated with $(NH_4)_2SO_4$ at 4°C following the procedure of Bollag and Edelstein (1991). Ultrapure $(NH_4)_2SO_4$ powder was finely ground in a mortar and the amount of required to bring the sample to the desired % saturation weighed out. The vessel containing the sample was placed on ice on a magnetic stirrer and gently stirred. $(NH_4)_2SO_4$ was slowly added in increments to the stirring sample solution. Each addition of salt was made only after the previously added amount has completely dissolved. Once all of the salt had been added, the solution was gently stirred for at least 45 minutes to allow the equilibration of the solvent and protein. The mixture was then centrifuged (in a Beckman 0650 Rotor) at 21 000*g* for 5 minutes at 4°C. After centrifugation, the supernatant was decanted and retained if the sample required further fractionation. The wet precipitate was resuspended in the original sample buffer. If further fractionation was desired, the appropriate amount of finely ground $(NH_4)_2SO_4$ was added to the supernatant and the procedure repeated as before.

2.5 The preparation of plant cell extracts

2.5.1 The preparation of Avocado sub-cellular fractions.

Avocado sub-cellular fractions were routinely prepared by differential centrifugation. The preparation of avocado homogenate was based on Sheldon *et al.* (1990), with the buffering conditions specifically adapted for avocado from Lin and Carman (1989). Avocado fruit (usually Hass variety) were ripened at 30°C until the skin started to turn black. At this stage the mesocarp tissue was green/yellow in appearance. The fruit were then incubated at 4°C for at least 1hour prior to tissue extraction. If the avocados were already at this stage of development when purchased, they were maintained at 4°C until use. All stages of the preparation were conducted on ice or at 4°C. The procedure outlined here was for the mesocarp tissue of three medium-sized ripened avocados (200-250g total tissue). The volumes of buffers used were altered as appropriate depending on the relative scale of the preparation.

Between 200-250g mesocarp tissue was finely chopped and soaked for 5min in 300ml chilled homogenisation buffer (50mM Tris-maleate buffer (pH 6.0), 1mM EDTA, 20% glycerol). This was then squeezed through 2 layers of muslin to form a homogenous suspension. More homogenisation buffer was added to a final avocado:buffer (g/ml) ratio of 1:2. Aliquots (100ml) of the slurry were taken and intermittently homogenised on ice, using a polytron (20mm probe, setting 5; Kinematica, Switzerland) for five 10sec periods . The temperature of the homogenate was monitored and never allowed to rise above 10°C. The homogenate was centrifuged at 5000*g* for 15min. This resulted in two supernatant layers (fat layer and cell extract) which were decanted from the cellular debris pellet through 1 layer of miracloth in order to separate by filtration the two supernatant layers. Miracloth retained the fat layer, and the filtrate was centrifuged again at 30 000*g* for 30 minutes to remove remaining organelles, cellular debris and fat layer. The supernatant was decanted through miracloth as before to create the cell extract (30 000*g* supernatant).

The cell extract was then further fractionated into the soluble and microsomal fractions.

The cell extract was centrifuged at 105 000*g* for 90min. (6 x 70 ml fixed angle rotor, Beckman L-70 Ultracentrifuge). The 105 000*g* supernatant, or soluble fraction, was decanted from the microsomal membrane pellets. The microsomal pellets, enriched in endoplasmic reticulum, were resuspended with the aid of a glass homogeniser, in 300ml membrane buffer (50mM Tris-maleate (pH 6.0), 10mM $MgCl_2$ and 20% glycerol). This was then centrifuged as above, in order to remove trapped soluble protein from the microsomal fraction. The supernatant containing the released soluble protein was removed and the microsomal pellets resuspended to 1/10 the original volume in the buffer as above, and stored at -80°C until use.

Chapter 3

The Preparation of Assay Substrates

3.1 Introduction.

Any biochemical study of PAP requires an accurate and sensitive procedure for measuring enzyme activity. Since the enzyme's identification by Kates (1955), there have been many different ways of following the PAP catalysed reaction, through spectrophotometric, direct substrate/product visualisation and radiochemical methods. A variety of techniques have been developed with PA presented as an emulsion, membrane-bound, or in detergent micelles (Sturton and Brindley, 1978). The underlying principles of the many assay procedures are the same: PAP activity is measured by following the PA conversion into DAG and Pi. Figure 3.1 shows a schematic representation of the PAP catalysed hydrolysis of PA (*sn*-1,2-diacylglycerol-3-phosphate). The measurement of PA or either of the products enables the direct quantification of PAP activity, assuming that PAP is solely responsible for PA hydrolysis.

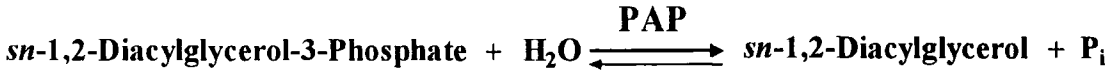

Figure 3.1: The hydrolysis of PA by PAP.

The colorimetric analyses of PAP activity are based on the spectrophotometric visualisation of inorganic phosphate in a phosphomolybdate complex. The addition of ascorbic acid to the phosphomolybdate complex causes its reduction with a formation

of colour (visualised at 820nm after 1.5-2 hours). This mode of phosphate determination was originally described by Chen *et al.* (1956), and has since been employed in the study of plant PAP (Ichihara *et al.*, 1989; Ichihara *et al.*, 1990; Kocsis *et al.*, 1996). A high degree of experimental uncertainty is inherent with this procedure, leading to erratic data, as reported by Kocsis *et al.*, (1996). Erroneous Pi can be formed from phospholipid breakdown, increasing the error within the assay further. All samples, including the enzyme sample must be void of appreciable concentrations of inorganic phosphate. Endogenous phosphate is removed from enzyme samples by dialysis, prior to assaying for enzyme activity, thus further increasing the duration of the assay. With a high degree of experimental uncertainty, it would be difficult to achieve the accurate evaluation of PAP activity required throughout the purification and characterisation of this enzyme. For these reasons the colorimetric assay as used by Ichihara *et al.* (1989) was deemed inappropriate for this study of the PAP protein.

The direct visualisation of reaction substrates and products is not an accurate means of quantifying PAP activity. Kocsis *et al.* (1996) monitored the appearance of DAG in the reaction mixtures using TLC, using the protocol reported by Ichihara *et al.* (1989). The reactions were terminated with 6M HCl, washed and applied to a silica TLC plate prior to being developed. The separated lipid classes were visualised by spraying with 30% H_2S0_4 (w/w) and incubating at 145°C for several minutes. This method enables the identification of PAP activity with the visualisation of reaction products. This method enables the identification of PAP activity, but does not allow its accurate quantification because of the potential error of sample application to the TLC plate, and the limited sensitivity of the image development.

Radiolabelled assay substrates have been widely employed for the determination of PAP activity in mammalian (see Sturton and Brindley, 1978), yeast (Lin and Carman, 1989) and plants (Malherbe *et al.*, 1995) systems. Different forms

of radiolabelled PA species have been used. Table 3.1 shows four potential radiolabelled moieties on the PA molecule, used for the radiochemical assay. Using radiolabelled substrates to follow the PAP assay reaction, allows both the emergence of products and the concomitant depletion in substrates to be measured. This acts as a dual measurement of PAP activity and enables a more accurate quantification of the reaction.

Where *sn*-1,2-diacylglycerol-3-[^{32}P]phosphate is used as the substrate, the reaction is monitored through the release of [^{32}P]Pi, with a reduction in [^{32}P]PA. [^{32}P]Pi is water-soluble, whereas PA and DAG are essentially insoluble, thus allowing an instant separation of Pi from the other reaction components. Separation and extraction is achieved using a two phase separation system (aqueous and organic solvent phases), such as those proposed by Bligh and Dyer (1959), Nishijima and Raetz (1979) and by Carman and Lin (1991), as follows: chloroform and methanol are added to the reaction mixture. The two phases are created by the addition of an aqueous solution. After vigorous mixing, the [^{32}P]Pi is located in the aqueous (upper) phase, whilst the [^{32}P]PA (and DAG) remain in the chloroform (lower) phase. The total radioactivity is then established for both phases by scintillation counting, enabling the calculation of PAP activity.

PA and DAG are essentially insoluble in water. Consequently, DAG can not be separated from PA using the rapid two-phase system. This necessitates an alternative reaction-monitoring method when *sn*-1,2-[^{14}C]diacylglycerol-3-phosphate or *sn*-1,2-diacyl[^{14}C/^{3}H]glycerol-3-phosphate are used as the radiolabelled substrate. The [^{14}C/^{3}H]DAG is therefore separated from [^{14}C/^{3}H]PA and analysed by TLC, alongside authentic DAG and PA standards. The TLC plates are exposed to iodine vapour, with the positions of the standards detected. The corresponding regions of the sample lanes are scraped off the TLC plates, resuspended, and the radioactivity counted.

Radiolabelled PA Species	Position of Label	Reaction Rate Measurement	Example Reference
sn-1,2-diacylglycerol-3-[^{32}P]phosphate	[^{32}P]Phosphate	[^{32}P]Pi formation	Lin and Carman, (1989)
sn-1,2-[^{14}C]diacylglycerol-3-phosphate	[^{14}C]-Fatty Acid	[^{14}C]diacylglycerol formation	Tzur and Shapiro, (1976)
sn-1,2-diacyl[^{14}C]glycerol-3-phosphate	[U-^{14}C]Glycerol	diacyl[^{14}C]glycerol formation	Ide and Nakazawa, (1989)
sn-1,2-diacyl[^{3}H]glycerol-3-phosphate	[2-^{3}H]Glycerol	diacyl[^{3}H]glycerol formation	Lin and Carman, (1989)

The procedure is time consuming with potential errors. A loss in yield due to the scraping of radiolabel from the TLC plates can, in conjunction with pipetting error during the application of the samples to the TLC plate, cause erroneous results. Rapid hydrolysis of DAG has also been shown to occur in rat liver microsomal and cytosolic fractions, during the PAP assay, due to lipase activities (Ide and Nakazawa, 1989). It was concluded that rat liver PAP activity can only be reliably measured through Pi release from PA (Ide and Nakazawa, 1989). Tzur and Shapiro (1976) reported that the measured rate of DAG formation was only 23-34% of the Pi release, due to deacylation. Ichihara *et al.* (1989) showed that in safflower microsomes, free fatty acids did not accumulate during the assay, indicating that deacylation did not occur (under the cited assay conditions) and that the Pi released reflected PAP activity.

With considerations towards the speed, sensitivity and accuracy of the assay, *sn*-1,2-diacylglycerol-3-[^{32}P]phosphate was deemed the most appropriate radiolabelled substrate, with activity measured as a function of [^{32}P]Pi release and concomitant [^{32}P]PA reduction. [^{32}P]PA is not available commercially, and therefore had to be synthesised.

Diacylglycerol kinase (EC 2.7.1.107, DAG kinase) catalyses the ATP-dependent phosphorylation of *sn*-1,2-diacylglycerol, producing PA (Pieringer and Kunnes, 1965; Walsh and Bell, 1986). In *Esherichia coli* the enzyme is tightly membrane bound protein(Loomis *et al.*, 1985) and there are both cytosolic and microsomal isoforms in mammals (Kanoh *et al.*, 1983; Kanoh *et al.*, 1993). In both systems it has been reported as being involved in both recycling DAG during phospholipid turnover(Rotering and Raetz, 1983; Kanoh *et al.*, 1993) and signal transduction (Walsh *et al.*, 1986; Kanoh *et al.*, 1993). The structural gene encoding *Esherichia coli* DAG kinase (*dgk*A locus) has been cloned, sequenced and overexpressed (Loomis *et al.*, 1985). The overexpressed protein has been well characterised (Walsh and Bell, 1986), and is commercially available. [^{32}P]PA can be

synthesised using [γ-^{32}P]ATP and DAG with DAG kinase in what is essentially the reverse of the PAP reaction. The aim of the research in this chapter was to synthesise [^{32}P]PA using DAG kinase under optimal conditions. Once synthesised, this [^{32}P]PA could be used in the assay for PAP activity. Throughout the course of the research presented in this thesis, PAP activity was tested for the ability to hydrolyse lysophosphatidic acid using *sn*-1-acylglycerol-3-[^{32}P]phosphate and *sn*-1-acyl[^{14}C]glycerol-3-phosphate. The synthesis of these substrates is described in Chapter 2, under *Materials and Methods*.

3.2 The Assay and Linearity of DAG Kinase.

Prior to the bulk preparation of [^{32}P]PA with DAG kinase, the linearity of the reaction was established using the assay procedure of Walsh and Bell (1986). This ensured that the eventual bulk preparation had a maximum efficiency. *Escherichia coli sn*-1,2-diacylglycerol kinase was purchased from Calbiochem Novabiochem (UK) Ltd. (Highfields Science Park, Nottingham, UK) with a specific activity of greater than 2μmol DAG/min/mg protein. The enzyme sample was aliquotted and frozen at -20°C until use.

A schematic representation of the DAG kinase assay reaction is shown in Figure 3.2. DAG kinase activity was determined by following ^{32}P incorporation into [^{32}P]PA from [γ-^{32}P]ATP (and DAG) at 25°C under the reaction conditions as previously described (Walsh and Bell, 1986 and 1992). The stock solutions and assay procedure were prepared according to Walsh and Bell (1992) and are described under *Materials and Methods*, Chapter 2.2.1. The DAG kinase standard assay conditions of Walsh and Bell (1986, and 1992) were used throughout the study of DAG kinase unless otherwise stated. The final volume of the reaction mixture was 100μl and contained 51mM Octylglucoside, 1mM cardiolipin, 60mM Imidazole (pH6.6), 50mM

NaCl, 12.5mM $MgCl_2$, 1mM EGTA, 0.3mM DTPA, 2mM DTT, 2mM DAG and 5mM [γ-^{32}P]ATP (2mCi/mmol) and DAG kinase (0.1Unit).

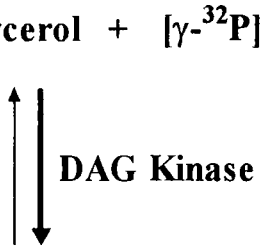

Figure 3.2: The Production of [^{32}P]PA by DAG Kinase.

Assay reactions were conducted in order to assess the DAG kinase activity, and to ensure that the radioactive product was not a result of chemical artefact. Reactions were prepared in duplicate alongside the various controls in glass reaction vials with Teflon-lined screw caps (centrifuge grade, Fisons Ltd., UK.), and assayed for enzyme activity. The reactions are summarised in Table 3.2, and each contained the standard reaction conditions, with the exceptions indicated in the table. The reactions were initiated by the addition of enzyme sample, incubated at 25°C and terminated after 20 minutes with 60µl 10% $HClO_4$. The terminated reaction mixtures were phase separated using an acidic modification (Rajasekharan *et al.*, 1988) based on the procedure reported by Bligh and Dyer (1959), with the PA separated into chloroform. This was conducted with the addition of 2.5ml $CHCl_3$:CH_3OH (1:1). After vigorously mixing the mixture for 5 seconds, 1ml 0.2M H_3PO_4 in 1M KCl was then added. This was mixed as before, prior to centrifugation at 500 *g* for 2 minutes creating two distinct phases. The chloroform phase (lower phase; 0.5ml) was removed and pipetted into a scintillation vial, with 4ml Ecoscint A and the radioactivity counted by scintillation counting.

This method was used instead of the original phase extraction described by Walsh and Bell (1992) for the following reason. The total volume of the phase extraction solutions used by Walsh and Bell (1992) was 5.7ml. The total capacity of a reaction vial in this study was 13ml. This presented a problem during the vigorous mixing of the solutions after reaction termination, where the Teflon-lined screw caps became heavily contaminated with radioactivity. The procedure of Rajasekharan *et al.* (1988) uses 3.5ml of extraction solutions and when subjected to vigorous mixing, all of the radioactivity is contained within the vial. Unless otherwise stated, this phase extraction procedure was used for the separation of [^{32}P]PA and [γ-^{32}P]ATP.

The results from Table 3.2 show that the production of PA was dependent on enzyme concentration, and the presence of both ATP and DAG. However, the addition of 2 x the enzyme concentration only caused a 1.5-fold increase in relative PA production. This suggested that at enzyme concentrations of between 0.1-0.2units, the reaction had become saturated. Where ATP was omitted (*Reaction 3*), no radioactivity was present in the reactions. This served as a negative control for the scintillation counting, where an expected radioactivity of zero was seen. Traces of radioactivity were observed in reactions where DAG had been omitted. This may be indicative of slight DAG contamination within the enzyme sample or more likely [γ-^{32}P]ATP contamination within the chloroform phase. It is possible that traces of [γ-^{32}P]ATP become dissolved in the $CHCl_3$ phase, causing an over estimation of DAG kinase activity, as the observed ^{32}P is incorrectly believed to be from [^{32}P]PA. This exemplifies the need to wash the chloroform phase in the bulk synthesis of [^{32}P]PA, to remove all traces of [γ-^{32}P]ATP.

Reaction	Conditions	Relative Activity (%)
1.	Normal assay conditions	100 (± 7)
2.	2 x Enzyme concentration	148 (± 19)
3.	No [γ-^{32}P]ATP or ATP	0
4.	No DAG	8 (± 1)
5.	Pre-boiled enzyme	3.5

Table 3.2: DAG kinase activity with various control reactions. *Reaction 1* was conducted under the standard assay conditions using 0.1 Unit of DAG kinase (0.1 μmol DAG/min). *Reaction 2* contained 0.2 Unit DAG kinase in an otherwise unchanged reaction; *Reactions 3-5* contained the standard reaction mixtures as in *Reaction 1*, but each with one variable as indicated in the table. The relative activities are calculated using the [^{32}P]PA radioactivity measured from *Reaction 1* (8460 DPM) as 100%. All subsequent activities are calculated as relative to *Reaction 1*. The data are calculated as the mean of duplicate assays, with the experimental variance shown in parenthesis.

3.2.1 DAG Kinase assay linearity with time and protein concentration.

The production of [^{32}P]PA appeared to be dependent on the concentration of enzyme (Table 3.2). In order to optimise the eventual bulk synthesis of [^{32}P]PA, the linearity of the DAG kinase reaction was considered, enabling an accurate quantification of DAG kinase activity.

The effect of time on DAG kinase activity was investigated for up to 1 hour, using 0.05 Units of enzyme and 100 000 DPM total radioactivity per reaction. A final reaction mixture of 600µl (6 x normal assay volume) was prepared in a glass reaction vial. The reaction was initiated with the addition of DAG Kinase (0.3 Units) and incubated at 25°C. A 100µl aliquot was immediately removed and pipetted into a second vial containing 60µl 10% $HClO_4$ thus terminating the reaction. At set time intervals, 100µl aliquots were removed from the reaction vial and placed in fresh vials each containing 60µl 10% $HClO_4$. Each terminated reaction was phase extracted. The formation of [^{32}P]PA from [γ-^{32}P]ATP was determined by scintillation counting of 500µl chloroform and aqueous phases respectively, with the mean results of duplicate experiments shown in Figure 3.3. The activity of DAG kinase was calculated as conversion of total ^{32}P into [^{32}P]PA, and was expressed in terms of percentage conversion. The production of [^{32}P]PA was found to be linear for up to 20 minutes, whereupon an increase in the experimental variance was observed.

The effect of enzyme concentration on [^{32}P]PA synthesis was also examined. Duplicate assays were performed with increasing concentrations of DAG kinase protein. After 20 minutes, the reactions were terminated with the addition of 60µl 10% $HClO_4$, prior to phase extraction. Two 100µl aliquots of the chloroform phase were removed from each reaction tube. One of the aliquots was directly added to 4ml Ecoscint A and the radioactivity measured. The second aliquots were pipetted into

empty 5ml scintillation vials and the chloroform removed under a steady stream of N_2 gas in a fume hood. The dried samples were resuspended in 100µl 10% methanol by vigorously mixing and 4ml Ecoscint A was added, prior to scintillation counting. A 100µl aliquot of the aqueous phase for each reaction was also measured for radioactivity, to determine the remaining unreacted [γ-^{32}P]ATP.

The effect of enzyme concentration on PA synthesis is shown in Figures 3.4 and 3.5, Figure 3.4 shows the effect of chloroform in the radioactive measurement, when compared to samples where it had been substituted with an equal volume of 10% methanol. The presence of chloroform quenched the radioactivity. Figure 3.5 is a replot of the unquenched data (chloroform-free) from Figure 3.4, and shows that PA synthesis is approximately linear in respect to enzyme concentration up to 0.05 units. At higher enzyme concentrations the rate decreased, as the substrate became limiting.

From Figure 3.4, it is clear that the presence of chloroform in the sample quenched the radioactivity measurement efficiency, thus underestimating the [^{32}P]PA produced. There are two possible ways of circumventing this quenching effect. Firstly, all chloroform can be removed from each sample prior to counting. However, drying the samples prior to radioactivity measurement is time consuming. Secondly, a quench standard curve can be created which accounts for the change in the spectral index of the sample when chloroform is present. The spectral index value decreases as quench increases (Packard Instrument Company technical bulletin, 1992). The quench standard curve allows the scintillation counter to adjust the measured radioactivity according to the spectral index itself, converting measured CPM into absolute sample radioactivity, DPM. It was decided to construct a quench standard curve for chloroform on the scintillation counter, in order to negate its effect on radioactive measurement. Once the quench standard curve is stored in the instrument computer, it was used for automatic DPM calculations (Packard Instrument Company technical bulletin, 1992).

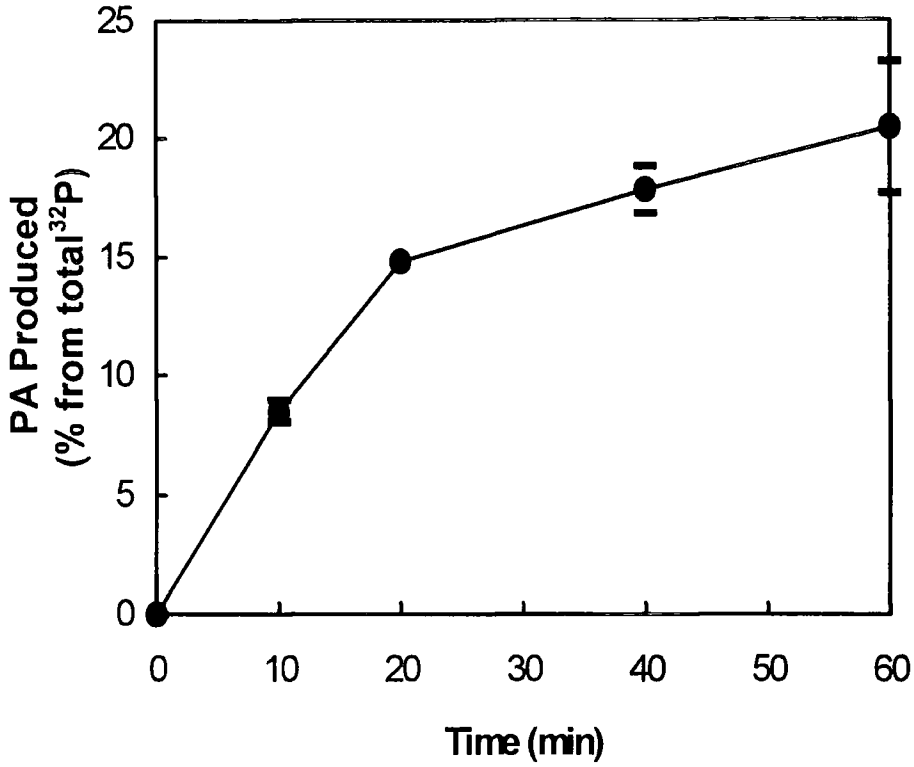

Figure 3.3: The effect of time on DAG kinase activity. The production of PA over time was investigated with 0.05 Units of enzyme per reaction for up to 60 minutes. Reactions were incubated at 25°C for the indicated times. The data was calculated by measuring the levels of [^{32}P]PA produced and the remaining [γ-^{32}P]ATP in duplicate experiments. The PA production represents the % conversion of total radioactivity (100 000 DPM) into product. At 60 minutes approximately 20% of total ^{32}P was [^{32}P]PA.

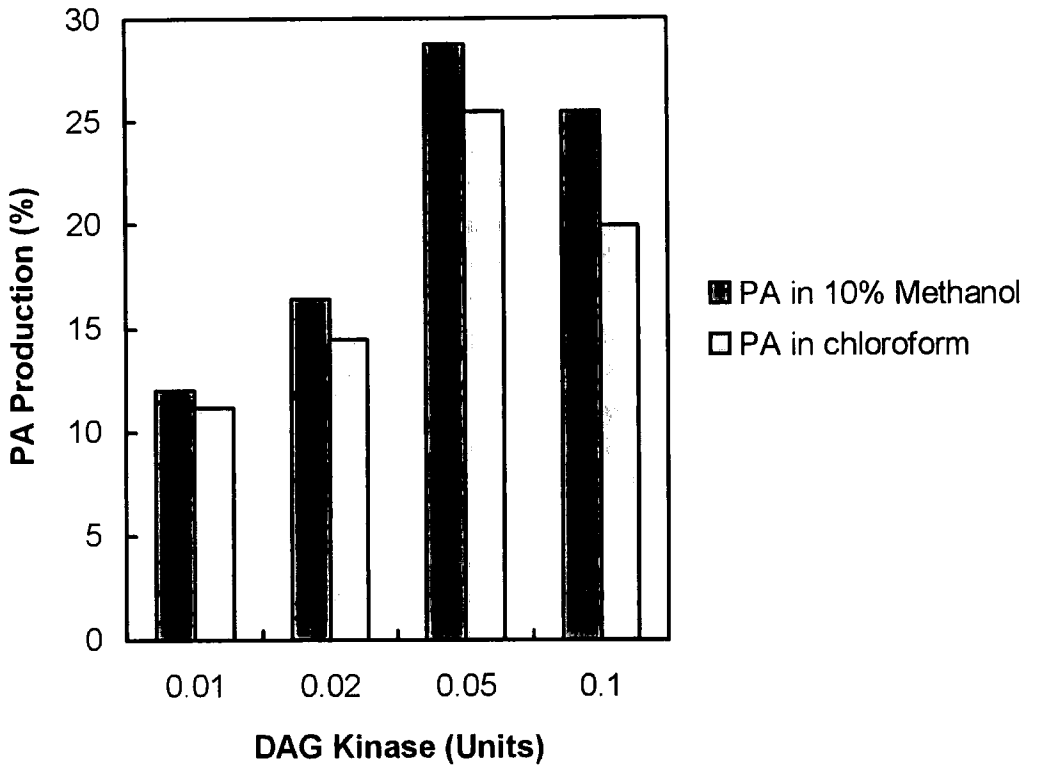

Figure 3.4: The effect of chloroform on the measurement of [^{32}P]PA. Reactions were prepared with various concentrations of DAG Kinase and 85 000 DPM total radioactivity per reaction. The terminated reactions were phase separated, and two 100µl aliquots of the PA-containing chloroform phase were taken from each reaction and placed in scintillation vials. Scintillation fluid (4ml) was added to the first set of aliquots, and the radioactivity measured. The chloroform in the second set of aliquots was removed by evaporation under a stream of N_2 gas. The dried samples were resuspended in 100µl 10% methanol and scintillation fluid added, prior to radioactivity counting. The measured radioactivity for both aliquots are shown. The PA production represents the % conversion of total radioactivity into product from duplicate experiments.

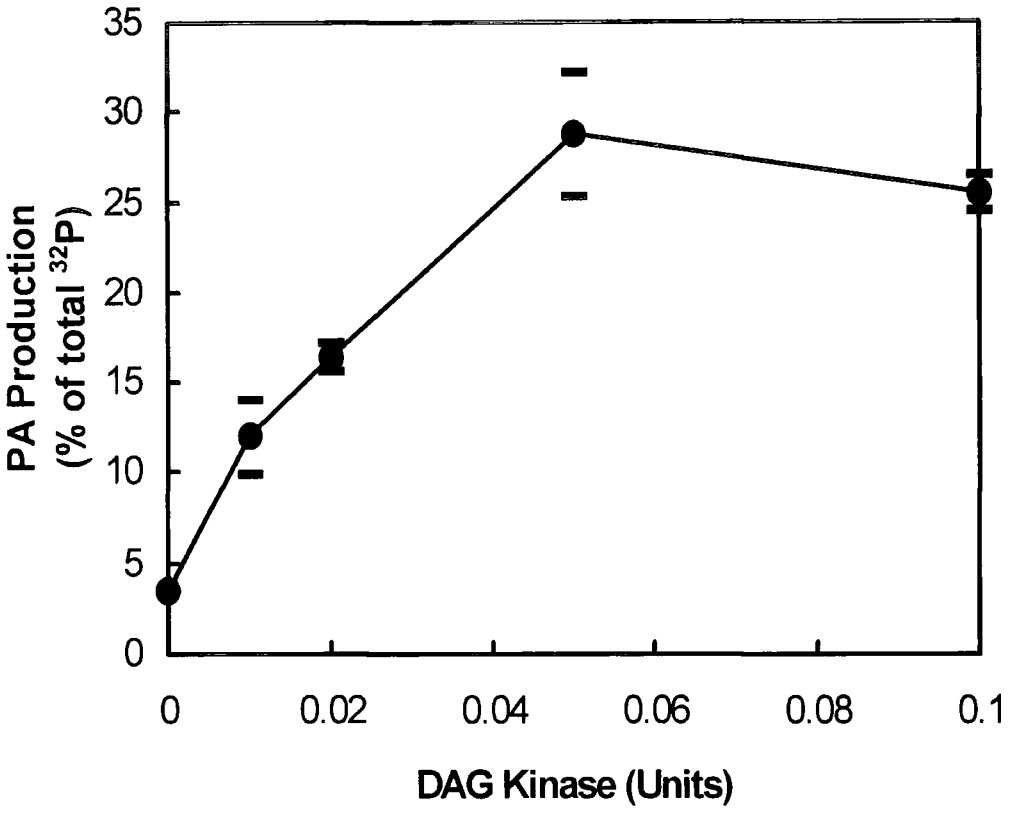

Figure 3.5: The effect of enzyme concentration on PA synthesis. A replot of the data shown in Figure 3.4 when chloroform had been removed from the [^{32}P]PA samples, prior to scintillation counting. The data was calculated by measuring the levels of [^{32}P]PA produced and the remaining [γ-^{32}P]ATP in duplicate experiments. The PA production represents the % conversion of total radioactivity (85 000 DPM) into product.

3.3 Eliminating Chloroform Quench in Scintillation Counting.

A chloroform quench standard curve was prepared according to the recommended procedure of Packard Instrument Company (1992). The quench indicating parameter (QIP) used to monitor quench was the spectral index of the sample (SIS). [γ-^{32}P]ATP (0.636μCi, 1.4 x 10^6 DPM) was added to 80ml Ecoscint A (National Diagnostics, UK) and thoroughly mixed by inversion. The mixture, with a known radioactivity, was aliquotted (4ml each) into 5ml scintillation tubes and the radioactivity measured by scintillation counting each tube for 1 minute. Each tube theoretically contained 70 000 DPM. This level of radioactivity was chosen for establishing the quench curve, because it is at this level that the PAP assay in Lin and Carman (1989) was conducted, and will be used in this study. This allows the quench curve also to apply in radioactivity quantification during the PAP assay. After measurement, any tube which deviated from the mean DPM value by more than 1% was discarded, leaving 9 tubes for the quench standards, each containing 63500 DPM (± 1%). Chloroform was added to tubes 2-9 in increasing amounts, and recounted for radioactivity, with tube 1 as control. Table 3.3 shows the effect of chloroform addition on the measurement of CPM and the SIS value. The CPM values were mainly unaffected, but decreased up to 5% upon the addition of 0.5 and 1ml $CHCl_3$. The quench standard curve was constructed within the scintillation counter computer, by plotting counting efficiency *versus* SIS value (Figure 3.6).

The addition of chloroform greatly decreased the spectral index of the samples (Table 3.3). The overall counting efficiency of these samples was, in effect, constant. Radioactive decay is converted into photons of light during the liquid scintillation process. The photons are converted into electrical pulses by photomultiplier tubes (Packard Instrument Company technical bulletin, 1992). The extremely high energy of

Sample	Volume of $CHCl_3$ added (μl)	CPM	SIS Value
1.	0	63135 (DPM)	1423
2.	10	63957	1256
3.	20	64872	1146
4.	50	63711	951
5.	100	63170	762
6.	150	63904	570
7.	200	63864	409
8.	500	62536	356
9.	1000	60823	183

Table 3.3: The effect of chloroform on the measurement of radioactivity and SIS values. All 4ml samples initially contained 63500 DPM(±1%). The indicated volumes of $CHCl_3$ were added and the CPM and SIS values were measured for 1 minute.

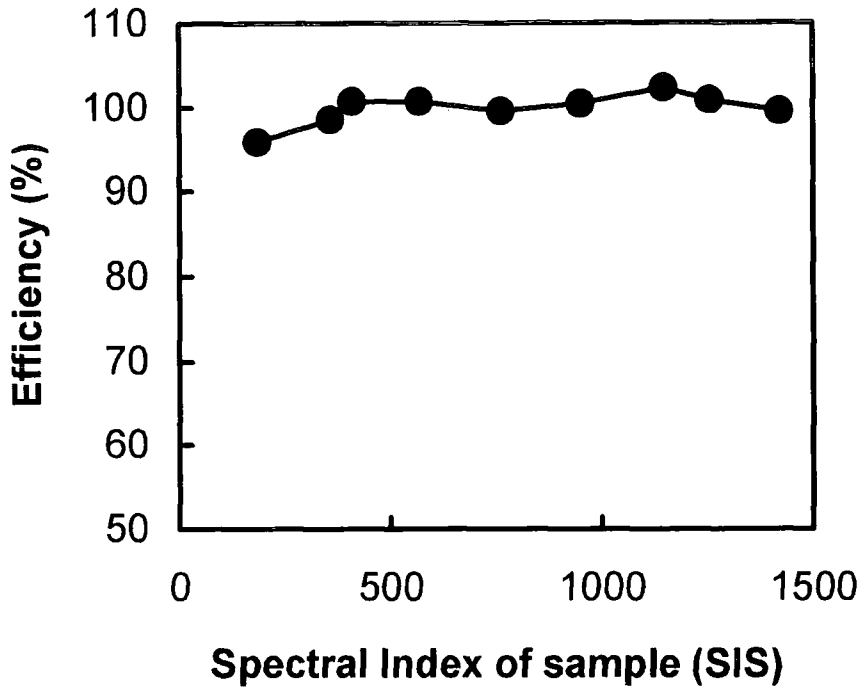

Figure 3.6: The chloroform quench standard curve. Using the data from Table 3.3, the counting efficiency (%) was calculated as (CPM/DPM) x 100 and plotted *versus* the corresponding SIS values.

β emission in ^{32}P means that even in the presence of chloroform, that the efficiency of light detection is almost 100%. This efficiency was only seen to be compromised in the presence of 0.5 and 1ml of chloroform. The quench standard curve was stored in the instrument computer, where it was used in all [^{32}P] measurements, enabling automatic DPM calculation.

3.4 Bulk synthesis of [^{32}P]PA.

For a characterisation and purification of PAP, a large amount of [^{32}P]PA is required for assaying purposes. The half life of ^{32}P is approximately 14 days, making it necessary to regularly synthesise [^{32}P]PA. The basic characterisation of DAG kinase, ensured that the [^{32}P]PA synthesis was reproducible and efficient, and could be conducted on a routine basis

Once the activity and assay for DAG kinase were established, the same reaction conditions were used for the bulk synthesis of [^{32}P]PA. This was with the exception that the [γ-^{32}P]ATP used in the bulk synthesis reaction was at a higher specific activity. Overall molar concentrations of the substrates remained the same. The reaction was prepared using the standard reaction conditions of Walsh and Bell (1986 and 1992), as described in section 3.2 above, with 0.05 Units of DAG kinase. The purchased [γ-^{32}P]ATP (Amersham International Plc., UK) had a specific activity of 30Ci/mmol with a concentration of 10mCi/ml. The 100μl reaction containing 50μCi, had a final concentration of 16μM [γ-^{32}P]ATP in a total ATP concentration 5mM. The final reaction [γ-^{32}P]ATP specific activity was therefore 100Ci/mol. The reaction was started with the addition of ATP, and incubated at 25°C. The reaction contained 200nmol DAG and 0.05μmol/min DAG kinase. The theoretical time taken for the reaction to go to completion was calculated as 4 minutes. However the observed activity in the assays was lower than the expected activity. It was futile to

increase the duration of the assay to more than 60 minutes, due to the inactivation of the enzyme at 25°C, as the half life of the enzyme is approximately 70 minutes, under these reaction conditions (Walsh and Bell, 1986). The reaction was therefore terminated after 60 minutes with 60µl 10% $HClO_4$, to ensure completion of the reaction. It was noted that traces of [γ-^{32}P]ATP contamination existed in the PA sample after phase extraction of the terminated reaction. Also, low levels of PA remained in the aqueous phase. Both phases were washed in order to maximise the PA yield, and eliminate ATP contamination. The three stages of PA extraction and washing are shown in figure 3.7. After extraction, the chloroform was removed from the PA under a steady stream of N_2 gas in a fume hood, resuspended into 1ml chloroform and stored at -20°C.

Aliquots of the final $CHCl_3$ and aqueous samples were analysed by TLC. The radioactive samples were applied to a silica TLC plate and developed in $CHCl_3$:CH_3OH:H_2O (12:6:1). The plate was then dried under a fume hood and exposed to pre-flashed x-ray film at -80°C for 12 hours. Authentic PA was loaded alongside as standard, and visualised by subjecting the TLC plate to iodine vapour. Figure 3.8 shows the autoradiogram of the TLC plate, illustrated with the position of authentic PA standard. The synthesis, extraction and washing resulted in the production of pure [^{32}P]PA.

The equilibrium constant for *E.coli* DAG kinase has not bee reported in the literature. Based on the assumption that there is no significant reverse reaction, the reaction would proceed in the direction of PA production to virtual completion. Under the reaction conditions of Walsh and Bell (1986 and 1992), the concentrations of ATP and DAG were 5mM and 2mM, respectively. The [γ-^{32}P]ATP was in a molar excess of DAG. This means that in the production of [^{32}P]PA, the theoretical maximum yield is 40%. From 50µCi [γ-^{32}P]ATP, 17.2µCi washed [^{32}P]PA was recovered, with a final yield of 34%, and similar to the theoretical value obtained with the above assumption.

Figure 3.7

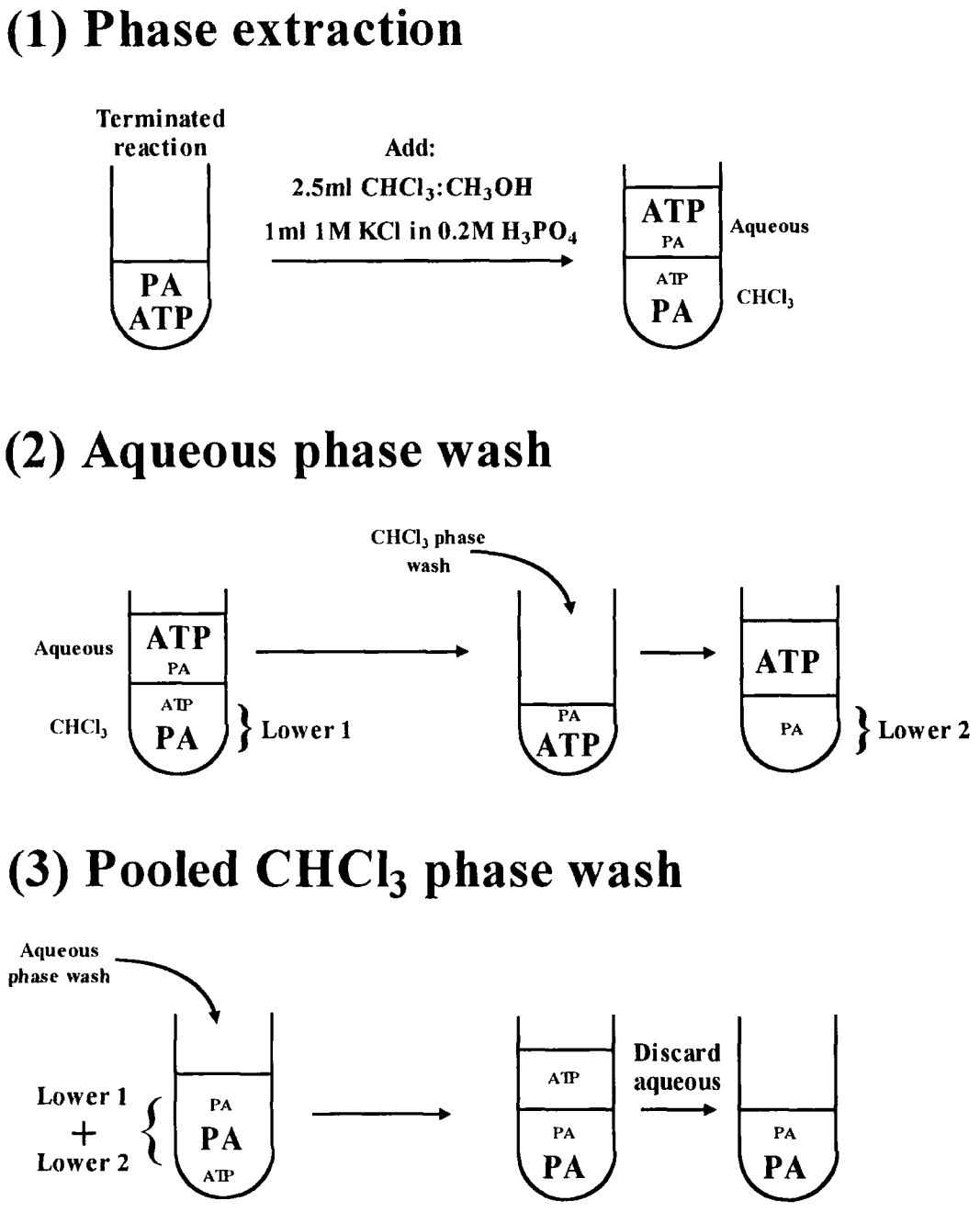
(1) Phase extraction
Terminated reaction
PA
ATP
Add:
2.5ml $CHCl_3$:CH_3OH
1ml 1M KCl in 0.2M H_3PO_4
ATP
PA
Aqueous
ATP
PA
$CHCl_3$
(2) Aqueous phase wash
$CHCl_3$ phase wash
Aqueous
ATP
PA
ATP
PA
$CHCl_3$
Lower 1
PA
ATP
ATP
PA
Lower 2
(3) Pooled $CHCl_3$ phase wash
Aqueous phase wash
Lower 1
+
Lower 2
PA
PA
ATP
ATP
PA
PA
Discard aqueous
PA
PA

Figure 3.8

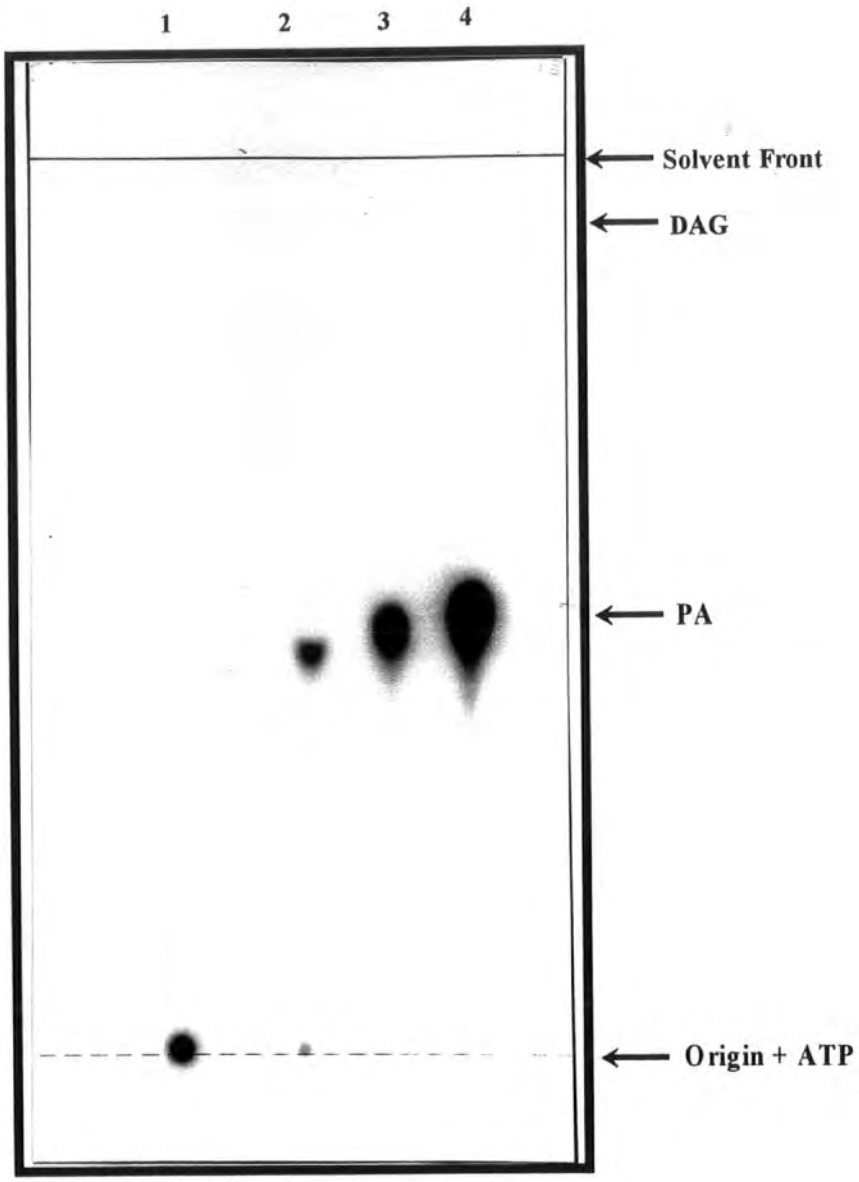

Owing to the short half life of ^{32}P, it would be necessary to synthesise [^{32}P]PA regularly and efficiently throughout the study of PAP. Under the above DAG kinase reaction conditions, 34% product formation was observed. This was because [γ-^{32}P]ATP was not the limiting substrate in the synthesis reaction. In order to maximise the [γ-^{32}P]ATP utilisation, an excess of DAG in the reaction mixture was required.

To achieve a greater efficiency, two further experiments were conducted in which there was an excess of DAG over ATP (Table 3.4). In both experiments, 50μCi ATP was used. In the first experiment, 6mM DAG and 5mM [γ-^{32}P]ATP was used and the other reaction components were identical to above. The second experiment had a gross excess of DAG over ATP, by using 2mM DAG and undiluted [γ-^{32}P]ATP (30Ci/mmol, 10mCi/ml). The second reaction therefore had a final ATP concentration of 16.6μM. Both experiments resulted in an increase in the recovery of [^{32}P]PA (Table 3.4).

Reaction	[γ-^{32}P]ATP (mM)	Total ATP (mM)	DAG (mM)	[^{32}P]PA Yield (%)
1.	16.6×10^{-3}	5	2	34
2.	16.6×10^{-3}	5	6	82
3.	16.6×10^{-3}	16.6×10^{-3}	2	95

Table 3.4: The effect of DAG:ATP ratio on [^{32}P]PA yield. All reactions contained 50μCi [γ-^{32}P]ATP, and were incubated for 60 minutes at 25°C, prior to termination and extraction of [^{32}P]PA. *Reaction 1*, was performed under identical conditions of Walsh and Bell (1986 and 1992). *Reactions 2 and 3*, were carried out under the same conditions as *reaction 1*, but at the indicated substrate concentrations. In *Reaction 3*, the [γ-^{32}P]ATP was carrier free.

The efficiency of [^{32}P]PA synthesis was noticeably improved by increasing the DAG:ATP ratio within the reaction mixture. Walsh and Bell (1986) used 6.9 mol% DAG in the enzyme reaction, despite reporting that concentrations of greater than 3.4 mol% DAG have an inhibitory effect on DAG kinase activity. However, at this concentration only minor inhibition occurs (Walsh and Bell, 1986). Reaction 2 had an increased DAG concentration of 18 mol%, and consequently resulted in an observed PA yield which was below the theoretical value. To achieve a maximum yield with 6mM DAG, more octylglucoside would have to be added, to reduce the DAG mol%. In reaction 3, the ATP concentration was reduced. This allowed the DAG concentration to be maintained at 6.9mol% and still be in gross excess of ATP. Under these conditions, the yield was routinely greater than 90%.

3.5 Discussion

The results in this section have shown that *sn*-1,2-diacylglycerol-3-[^{32}P]phosphate could be efficiently synthesised, extracted and recovered, and was identical to authentic *sn*-1,2-diacylglycerol-3-phosphate upon TLC analysis. The effects of protein concentration and time on [^{32}P]PA synthesis were examined. This enabled the final synthesis to be conducted under conditions where the rate was linear and maximal in respect to protein concentration. This prevented excessive and wasteful use of DAG kinase. The reaction was also optimised towards the substrate concentrations. The conditions cited by Walsh and Bell (1986), show [γ-^{32}P]ATP to be in excess of DAG. This had a maximum theoretical [^{32}P]PA yield of 40%. By altering the relative concentrations of the two substrates, the yield of [^{32}P]PA was increased from 34% to over 90%.

[γ-^{32}P]ATP was the sole source of ATP in the final optimised reaction, resulting in synthesised PA with the same specific activity, 30Ci/mmol (or 66 000

DPM/pmol) at a yield of above 90%. This [^{32}P]PA can be used as the substrate in the assay for PAP activity. As will be seen in the next chapter, each PAP assay contained 50 nmoles of substrate. The desired radioactivity per assay was 75 000 DPM, or 1.1 pmol [^{32}P]PA. The majority of PA in the assay mixture was derived from stock unlabelled PA. As the isotope decayed, more [^{32}P]PA was required. By creating [^{32}P]PA with a concentration of 30Ci/mmol (66 000 000 DPM/nmol), the amount added to each assay to give 100 000 DPM, had no significant effect on the overall PA concentration. Therefore, the appropriate radioactivity was added to 50 nmoles of unlabelled PA prior to each assay, with the final PA concentration remaining at 0.5mM irrespective of the amount of [^{32}P]PA added.

Chloroform was found to quench the efficiency of scintillation counting. A quench standard curve was constructed and programmed into the scintillation counter computer, so that all quench could be corrected. All ^{32}P measurement was conducted using the quench standard curve, enabling CPM to be analogous to DPM. The maximum quench seen in the standard curve was 5%, caused by the addition of 0.5ml and 1ml chloroform. By establishing the quench standard curve, the reduced scintillation counting efficiency was accounted for during the routine measurement of PAP activity.

Chapter 4

The Development and Optimisation of an Assay for Avocado Phosphatidate Phosphatase

4.1 Introduction.

It has been established that this is an important enzyme in phospholipid and TAG biosyntheses. A purified preparation of PAP is required for defined studies on the mechanism and regulation of this key enzyme of lipid metabolism. A homogenous enzymic preparation would also allow its positive identification, thus enabling amino acid analysis and the generation of antibodies, to be used in the subsequent isolation of the gene, encoding PAP. The purification of PAP depends on the ability to accurately assay protein samples for PAP activity. Without a suitably sensitive assay, the fractionation of the enzyme would not be possible. It is therefore important to be able to assay the enzyme reliably, accurately and reproducibly.

As previously discussed, there are inherent sources of error when assaying for PAP activity (Sturton and Brindley, 1978; Martin *et al.*, 1991) and, where possible, these must be considered, eliminated or accounted for in the measurement of PAP activity. Ide and Nakazawa (1989) concluded that it is essential to characterise the assay reaction products before employing specific assay conditions. Jamal *et al.* (1991) reiterated this point by stating that it is necessary to re-evaluate many of the published papers, because the innate problems of the assays had not been taken into consideration. Different tissues have different levels of phospholipases, lipases and phosphatases and will therefore have different effects on the PAP assay. Whether, the reaction is being monitored by the decrease of PA, or the increase of DAG or Pi, the effects of other enzymatic activities must be assessed.

As was described in Chapter 1.6, PAP is microsomally-associated and PA is insoluble in an aqueous environment, with *in vivo* catalysis occurring at the membrane interface. It is virtually impossible to consistently recreate the *in vivo* conditions for the assay, *in vitro*. The substrate therefore needs to be presented in a suitable form for measuring enzyme activity in aqueous solutions. The use of detergents is therefore almost unavoidable, and has enabled the study of many membrane bound enzymes and their insoluble substrates (Weselake and Jain, 1992). Detergents represent a neutral artificial 'membrane' in which the enzyme and substrate are integrated (Deems *et al.*, 1975), and have been successfully used for the study of PAP in *S.cerevisiae* (Lin and Carman, 1989 and 1990).

As was shown in Chapter 3, [^{32}P]PA was routinely and efficiently synthesised enzymatically in the laboratory. Using the data obtained from PAP characterisation studies with this substrate, the final optimal assay conditions can be refined, and used in the subsequent purification of the enzyme.

Prior to any characterisation studies, a suitable tissue source must be chosen, the enzyme identified, and its sub-cellular localisation established. Avocado mesocarp is extremely rich in triacylglycerol, and has been extensively used for the study and isolation of lipid metabolising enzymes (for example: Barron *et al.*, 1961; Barron and Stumpf, 1962; Weaire and Kekwick, 1975; Shine *et al.*, 1976; Griffiths *et al.*, 1988; Sheldon *et al.*, 1990; Gulliver and Slabas, 1994; Eccleston and Harwood, 1995). Despite being a fruit, it provides a model system for oilseed TAG biosynthesis, with a similar TAG-fatty acid composition to rapeseed (*Brassica napus*) oil (Gunstone *et al.*, 1994). Avocado has the advantage over rapeseed as the experimental material, in that it is much larger and readily available commercially. As avocado is rich in TAG, then the enzyme activities involved in its synthesis would be expected to be high. Avocado was therefore used for the characterisation and purification of PAP.

The knowledge of PAP from mammalian and yeast systems, is considerably more advanced than our present understanding of the plant enzyme (Kocsis and Weselake, 1996). The enzymic data for plant PAP isoforms are variable, with the reported pH optima and Mg^{2+} requirement inconsistent (Kocsis and Weselake, 1996). The assaying procedures used in the study of PAP from different species are equally variable. This makes comparison between the activities from different tissues very difficult and is further complicated with the occurrence of isoforms within each tissue. Positive advancement in the study of the plant enzyme could therefore be made, as with other fatty acid synthesising enzymes, by adapting methods already used in another system where the enzyme has been successfully purified and characterised. PAP has been extensively studied in yeast and the biochemical properties of the enzyme have been reported (Lin and Carman, 1989, 1990; Morlock *et al.*, 1991). In order to assess the initial sub-cellular localisation and relative abundance of PAP in avocado, the yeast PAP assay conditions as reported by Lin and Carman (1989), were used. These conditions were found appropriate in the initial study of PAP activity for the following reasons: (i) the same radioactive substrates were used, allowing an identical product identification; (ii) the assay mixture contained 10mM Mg^{2+} allowing the detection of Mg^{2+} dependent and independent activities; (iii) the reaction was conducted at pH 7.0 in order to reduce the activities of alkaline and acid phosphatases; (iv) PA emulsions are eliminated by Triton X-100 micellisation, allowing all PA molecules to theoretically interact with PAP at the protein-micelle interface (Verger, 1980).

4.2 PAP Activity Distribution in Avocado Fruit Extract.

Distribution of PAP activity was investigated in avocado sub-cellular fractions that had been prepared by differential centrifugation. The preparation of avocado homogenate was based on Sheldon *et al.* (1990) as described in Chapter 2.5.1, with the buffer conditions of Lin and Carman (1989).

The main aim of this section was to locate PAP activity from within the subcellular fractions obtained by differential centrifugation above. Using the information from the subcellular distribution, the optimal source of PAP for characterisation and purification can be determined. The differentially centrifuged fractions (post 30 000*g*) from above were assayed according to Lin and Carman (1990). In order to ensure that the assay was linear with respect to protein concentration, each sample was assayed for activity using 2µl of normal and diluted (1/10) sample. Control reactions were used in which water was substituted for enzyme sample. As shown in Table 4.1, phosphatase activity (with PA as substrate) was found predominantly in the soluble fraction (105 000*g* supernatant). It would be inaccurate to conclude that all of the Pi formation from PA is entirely attributable to PAP activity. Combinations of phospholipase and non-specific phosphatase activities can lead to Pi release and consequently an overestimation of PAP activity (Sturton and Brindley, 1978). The activities shown in table 4.1 therefore represent total phosphatase activity, with PA as the substrate. However, the overall distribution of phosphatase-type activity, with PA as substrate (termed PA-phosphatase as opposed to PAP) can be seen.

Estimation of the fat layer PA-phosphatase activity was difficult to accurately quantify, because of possible pipetting error and the high concentration of endogenous lipid. The lipid could severely dilute the substrate concentration, leading to an underestimation of phosphatase activity.

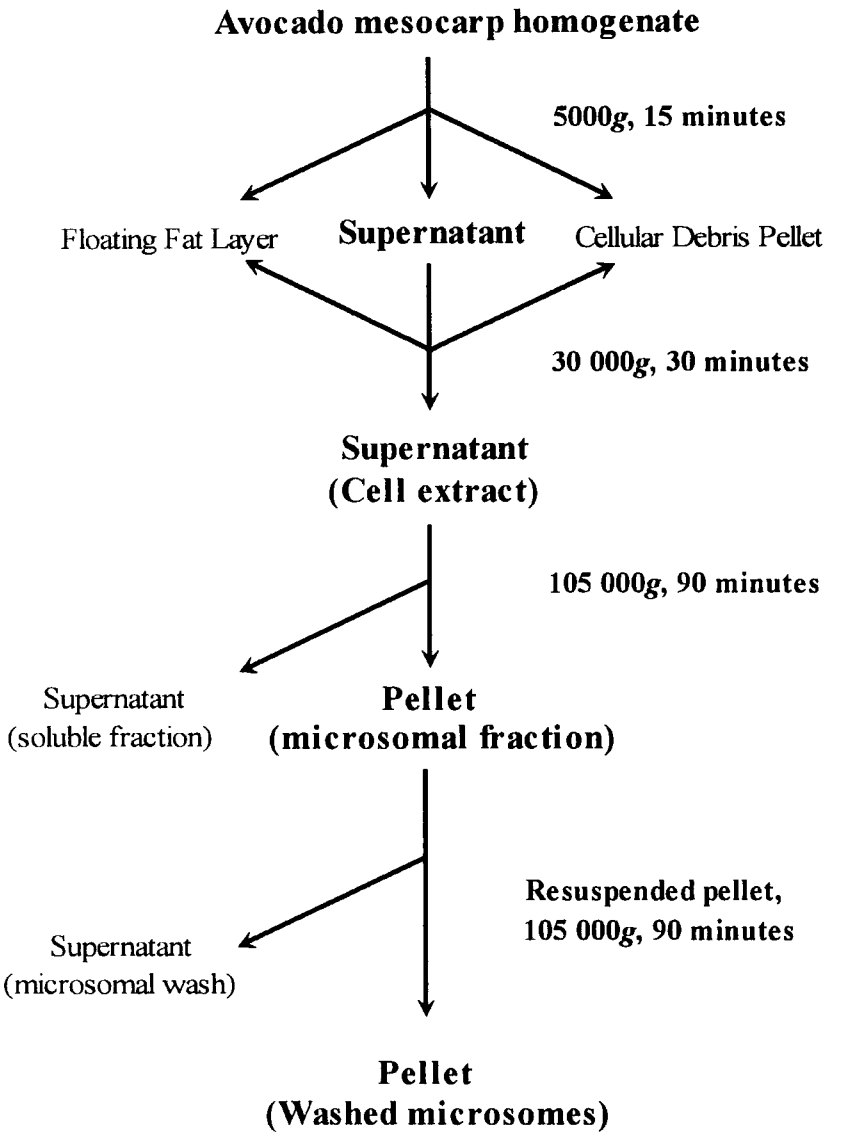

Figure 4.1: The diagrammatic representation of the preparation of washed microsomes. Washed microsomes were prepared by differential centrifugation as described in the text.

PA-phosphatase activity was predominantly found in two fractions, namely, the soluble (105 000*g* supernatant) and the washed microsomes (105 000*g* pellet). Nearly 10% of total phosphatase activity (from cell extract) was found in the washed microsomes ((ii) 105 000*g* pellet). This is in agreement with the activity distribution found in other lipid-rich plant species. Between 11-17% of total PAP activity was found in the microsomes of *Brassica napus* seed, microspore-derived and embryogenic cell-suspension cultures (Kocsis *et al.*, 1996) and 12% in developing safflower microsomes (Ichihara *et al.*, 1989). The activity contained within the microsomal wash resulted from the release of soluble protein, which had become trapped within the microsomal pellets.

Fraction	Total Protein (Mg)	Total Activity (Units; μmol Pi/min)	Specific activity (Units/mg protein)
30 000*g* Sup.	222	2.284	10.3×10^{-3}
(i)105 000*g* Pellet	38.1	0.29	7.0×10^{-3}
105 000*g* Sup.	200	1.912	9.6×10^{-3}
(ii)105 000*g* Pellet	26.3	0.215	8.2×10^{-3}
105 000*g* Sup.(wash)	10.9	0.105	9.6×10^{-3}
Fat Layer	5.2	0.01	1.9×10^{-3}

TABLE 4.1: Sub-Cellular Distribution of PAP in Avocado.

Phosphatase activity was found to be distributed throughout all differentially centrifuged fractions examined. However there was no noticeable increase in specific activity upon fractionation of the phases (Table 4.1). The 105 000*g* supernatant had the highest fractionated PA-phosphatase activity but with a corresponding high total protein concentration. Although the microsomes were found not to be the major source of the PA-phosphatase activity, they were used in this research for the

following reasons ; (i) the endoplasmic reticulum is believed to be the site of TAG/PL biosynthesis and involves a microsomally associated form of PAP (Stymne and Stobart, 1987; Browse and Somerville, 1991, Lacey and Hills, 1996); (ii) of the two respective activities, microsomal PAP is believed to be physiologically active; (iii) the 100 000*g* supernatant is most likely to contain non-specific acid phosphatases the majority of which are soluble (Schmidt, 1955; Long *et al.*, 1967; Herman and Chrispeels, 1980; Duff *et al.*, 1994; Staswick *et al.*, 1994), which have a very broad substrate specificity (Duff *et al.*, 1994) and can hydrolyse PA (Blank and Snyder, 1970), thus making it difficult to specifically attribute PA hydrolysis to PAP activity.

4.3 Partial Characterisation of Microsomal PAP.

4.3.1 Stability to freezing of PAP activity in Avocado Extracts.

Avocado cell extract (30 000*g* supernatant) and washed microsomes were prepared as above and examined for the stability of PAP activity after freezing at -80°C. The fresh extracts were assayed, rapidly frozen in liquid N_2, and stored at -80°C for 1 week. All assays were conducted in duplicate using the yeast standard assay conditions with the mean and variance shown in Table 4.2. The frozen samples were incubated under a flow of running tap water (approx. 18°C) until fully thawed. They were then assayed for PAP activity. Freezing of the cell free extract resulted in a decrease in specific activity of approximately 20%. Microsomal PAP showed no decrease in specific activity upon freezing. Stability of the microsomal fraction to a repeat cycle of freeze-thaw was investigated. The once-frozen microsomes were frozen and thawed immediately as above and assayed, with no significant change in activity seen (Table 4.2). Fresh microsomes were frozen in aliquots and used for characterisation studies. Despite the PAP stability after thawing, the aliquots were never refrozen but discarded. Instead, a fresh sample was thawed for each experiment, allowing all characterisation studies to be conducted with microsomes that had been

frozen once. Various microsomal fractions were prepared for use in the characterisation studies, accounting for the slight differences in specific activity.

Sub-Cellular Fraction	PAP Specific Activity (Units/mg protein)
Cell Free Extract (30 000g Sup.)	0.018 (±0.003)
Once-Frozen Cell Free Extract	0.0142 (±0.002)
Washed microsomes(105 000g Pt.)	0.065 (±0.04)
Once-Frozen Microsomes	0.07 (±0.02)
Twice-Frozen Microsomes	0.059 (±0.01)

TABLE 4.2: Effect of Freeze-Thaw Cycle on PAP activity.

4.3.2 Assay linearity with time and protein concentration.

For the accurate quantification of enzyme activity it is important to ensure that the conditions are linear with respect to time and protein (enzyme sample) concentration.

To determine the rate of Pi production with time, a 1.5ml assay mixture was initiated with approximately 120μg cell extract. At set time intervals, 100μl aliquots were stopped and analysed for PAP activity following the normal assay phase extraction procedure. Linearity towards protein concentration was determined with the addition of increasing concentrations of cell extract (30 000*g* supernatant) to assay reactions, under otherwise standard assay conditions.

Cell extract was found to have a linear PAP activity for up to 60 minutes (Figure 4.2) with up to 40μg protein (Figure 4.3).

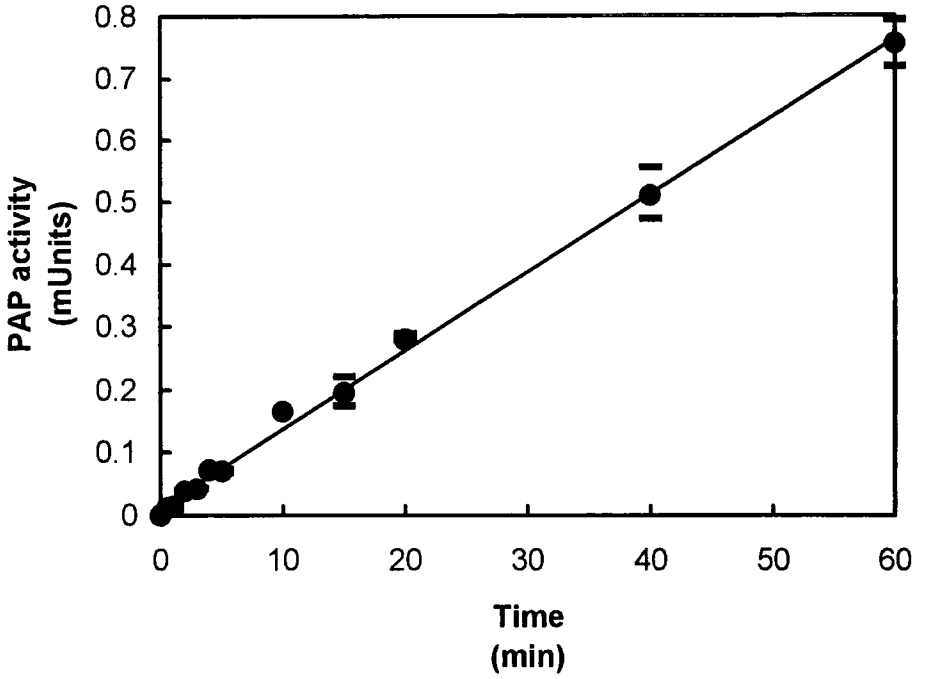

Figure 4.2: Linearity of PAP Activity with Time. An assay vial was prepared with 15 volumes of assay mixture and the reaction initiated with the addition of cell extract (30 000*g* supernatant). The final reaction (1.5ml) contained, 0.5mM [^{32}P]PA, 5mM Triton X-100, 50mM Tris-maleate pH7.0, 10mM 2-mercaptoethanol, 2mM $MgCl_2$, 120μg enzyme protein and was incubated at 30°C. At set time intervals, 100μl aliquots were withdrawn, the reaction terminated, and the activity measured as described in *Materials and Methods*, Chapter 2.3.1. Data are represented as the means of duplicate experiments with experimental variance also shown. The line is plotted as a result of least squares analysis of the mean data. One unit of PAP activity was defined as the amount of enzyme required to catalyse the formation of 1μmol Pi/min.

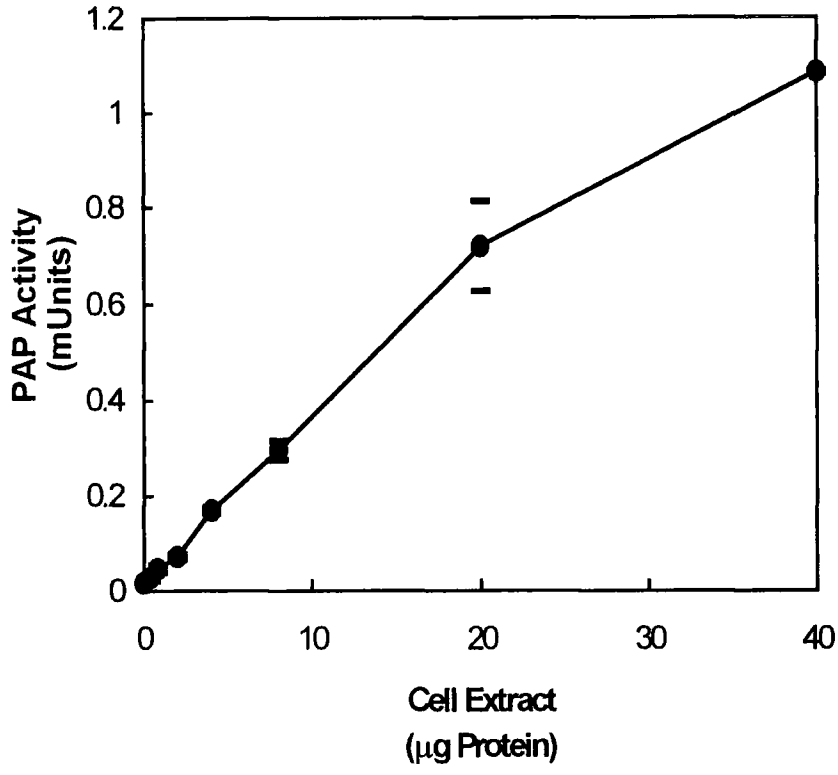

Figure 4.3: Linearity of PAP Activity with increasing Cell Extract. PAP activity was measured after 20 minutes at 30°C with various concentrations of cell extract (30 000*g* supernatant), under the standard yeast assay conditions. The *plot* is drawn using the means with experimental variance of the data from duplicate experiments. One unit of PAP activity was defined as the amount of enzyme required to catalyse the formation of 1µmol Pi/min.

4.3.3 The pH optimum of PAP.

The effect of pH on cell free extract and washed microsomal PAP activity was investigated, using 50mM Tris-maleate in a pH range of 5.0-8.5, in an otherwise unchanged assay mixture as above. Tris-maleate has an effective buffering range of pH 5.4 to 8.4 and was used in this preliminary characterisation study.

As shown in Figure 4.4, Microsomal PAP had a pH optimum of between 5.5-6.5, over a broad range of 5.0-7.0. Further increases in pH caused rapid reduction in specific activity, with virtually no activity seen at pH 8.5. The pH profile for cell free extract was broad with a slightly more acidic optimum between 5.0-5.5. The more acidic pH optimum of the total cell free extract is indicative of a more acidic cytosolic PA-phosphatase type activity as reported in *Brassica napus* extracts by Kocsis *et al.* (1996).

4.3.4 Effect of Mg^{2+} on PAP activity.

As was mentioned in Chapter 1, in yeast (Lin and Carman, 1989) and mammalian (Jamal *et al.*, 1991; Kocsis and Weselake, 1996) systems, an isoform of PAP exists that is totally dependent on the presence of Mg^{2+} ions for enzymatic activity. The dependence of plant PAP on the presence of Mg^{2+} ions for microsomal PAP activity has also been reported (Griffiths *et al.*, 1985; Sukumar and Sastry, 1988; Ichihara *et al.*, 1989). For purposes of assay optimisation, the Mg^{2+} requirement of PAP was examined in avocado microsomal preparations. An aliquot of microsomes (200µl) was dialysed in 50mM Tris-maleate pH 6.0 and 4mM EDTA (2 x 1 litre, 2 hours total), and then in 50mM Tris-maleate pH 6.0 (1 x 2 litres, 4 hours total) to remove any Mg^{2+} ions. The dialysed microsomes were then assayed in duplicate, with increasing concentrations of Mg^{2+}, with the results shown in Figure 4.5. In assays where no Mg^{2+} was added, 4mM EDTA was included in the mixture, to act as a chelator, ensuring the total removal of Mg^{2+} ions.

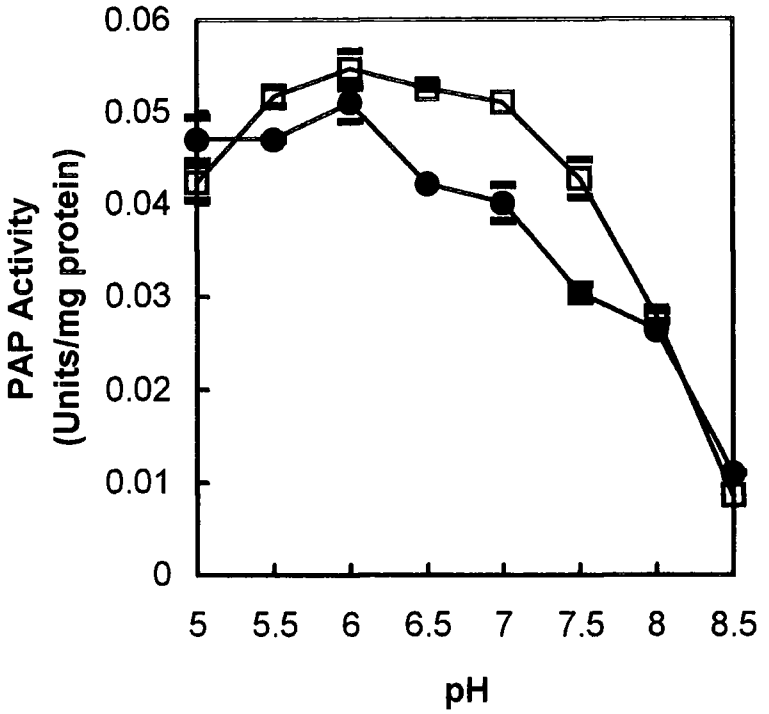

Figure 4.4: The effect of pH on PAP Activity. PAP activity in Cell Extract (30 000*g* supernatant) and washed Microsomes (105 000*g* pellet) was measured in 50mM Tris-maleate buffer from pH 5-8.5, under the otherwise standard yeast assay conditions described under *Materials and Methods*, Chapter 2.3.1. Each assay for cell extract activity (●) contained 4μg total protein and for microsomal activity (□), 6μg total protein. The mean data from duplicate experiments are plotted, with the experimental variance also shown. One unit of PAP activity was defined as the amount of enzyme required to catalyse the formation of 1μmol Pi/min.

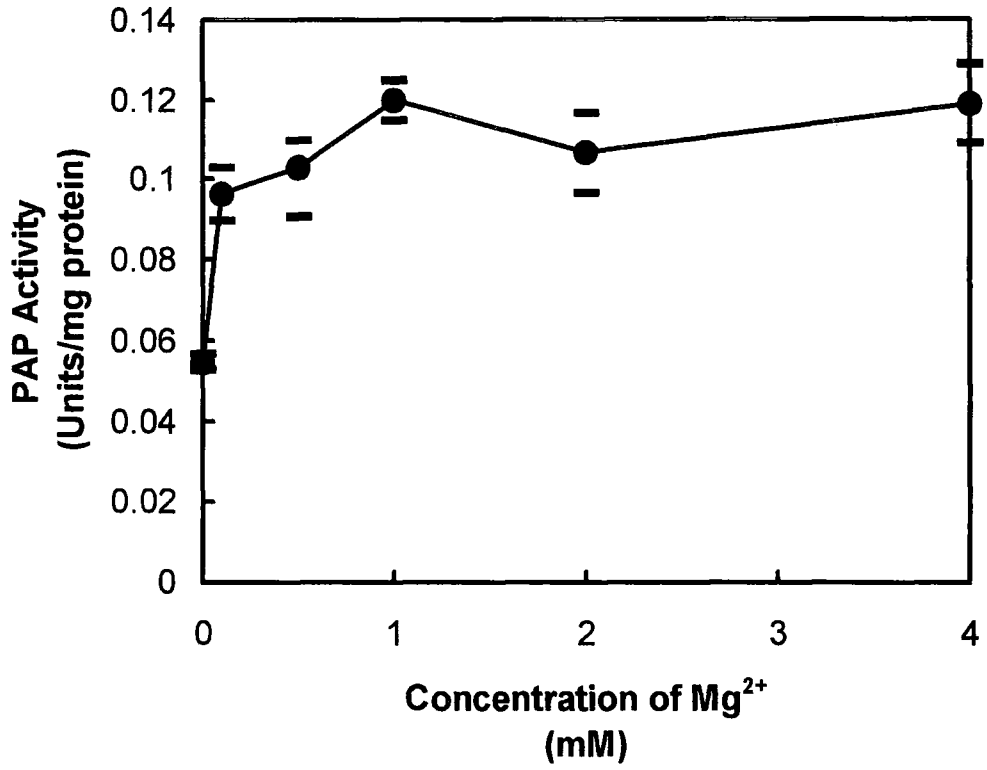

Figure 4.5: The effect of Magnesium on Microsomal PAP Activity. Microsomes (10μg) were assayed in duplicate for 20 minutes, with various concentrations of Mg^{2+}, with the mean and the variance of the data shown. In samples where Mg^{2+} was omitted, 4mM EDTA was added to the assay mixture. One unit of PAP activity was defined as the amount of enzyme required to catalyse the formation of 1μmol Pi/min

Avocado PAP showed no absolute dependence on the presence of Mg^{2+} ions, although a 2-fold stimulation in activity was observed with increasing Mg^{2+} concentrations. This result shows that PAP is essentially Mg^{2+} independent. However, due to the observed 2-fold stimulation of activity, it was decided to include 2mM $MgCl_2$ in the assay mixture. The reduced PAP activity with no Mg^{2+} (Figure 4.5) was not due to the presence of EDTA as a similar experiment was conducted in which EDTA was added to all reactions with Mg^{2+} added where required.

4.3.5 Thiol-reducing agents and PAP activity.

In *S.cerevisiae* (Lin and Carman, 1989) and mammalian systems (Jamal *et al.*, 1991) an isoform of PAP exists which is entirely dependent on thiol-reducing reagents for catalytic activity. The dependence of plant isoforms on thiol-reducing compounds has not been reported. Although avocado extracts were routinely prepared and assayed in the presence of 10mM 2-mercaptoethanol or 4mM dithiothreitol, the thiol-reducing agent requirement was unknown. The effect of DTT and the thioreactive compound, N-ethylmaleimide (NEM), on PAP catalytic activity was investigated. A fresh preparation of washed microsomes was prepared as described in Chapter 2.5.1 in the presence of 4mM DTT. The enzyme samples were pre-incubated with either 10mM NEM or 4mM DTT. The microsomes were assayed (2µl microsomes used per 100µl assay) in duplicate, in the presence of either 4mM DTT or 5mM NEM. As shown in Table 4.3, the addition or exclusion of DTT to the assay mixture had no significant effect on catalytic rate. Similarly, the addition of NEM to the assay mixture had no effect on avocado PAP activity over the 20minute assay duration. Microsomal PAP activity was independent of thiol-reducing agents, and insensitive to the thioreactive compound, NEM. This implies that a sulphydryl group is not required for enzyme catalysis in contrast to yeast and mammalian systems (Lin and Carman, 1989).

Sample	PAP Activity (Units/mg protein)
Microsomes	0.047 (± 0.006)
Microsomes + 4mM DTT	0.05(± 0.003)
Microsomes + 5mM NEM (no DTT)	0.051 (± 0.003)

Table 4.3: The effect of Thioreactive compounds on microsomal PAP activity.

4.3.6 Effect of temperature on PAP activity.

The effect of temperature on PAP activity was determined using the washed microsomal fraction at varying temperatures. The assay mixtures were pre-incubated at temperatures of between 0-60°C for 5 minutes prior to reaction initiation by the addition of 2µl microsomal enzyme sample. Reactions were terminated after 20 minutes and the activities measured, as shown in Figure 4.6.

Activity increased in a linear fashion to a maximum at 50°C, whereupon a further increase resulted in loss of enzyme activity through inactivation. The temperature coefficient (Q_{10}) was approximately 2.0 for temperatures up to 50°C. Greater variability in activity was seen as the temperature increased, most probably due to enzyme instability above 40°C. An Arrhenius plot was constructed (Cornish-Brown, 1995) using the mean data between 0-50°C from Figure 4.6. The data was plotted as Log_{10}(Activity) *versus* the reciprocal of the absolute temperature ($°K^{-1}$), with the resulting plot (Figure 4.7) used to calculate the reaction activation energy as 37.3 kJ/mol (8.9 kcal/mol). Kocsis and Weselake (1995) reported activation energies for microsomal and soluble PAP from *B.napus* of 15.6 kcal/mol and 9.4 kcal/mol, respectively. However, the assay reactions used by Kocsis and Weselake (1995) did not contain detergent and were conducted under different conditions, making comparison difficult. Lin and Carman, (1989) reported the activation energy of homogenous PAP from *S. cerevisiae* was 11.9kcal/mol under the identical assay conditions as described here.

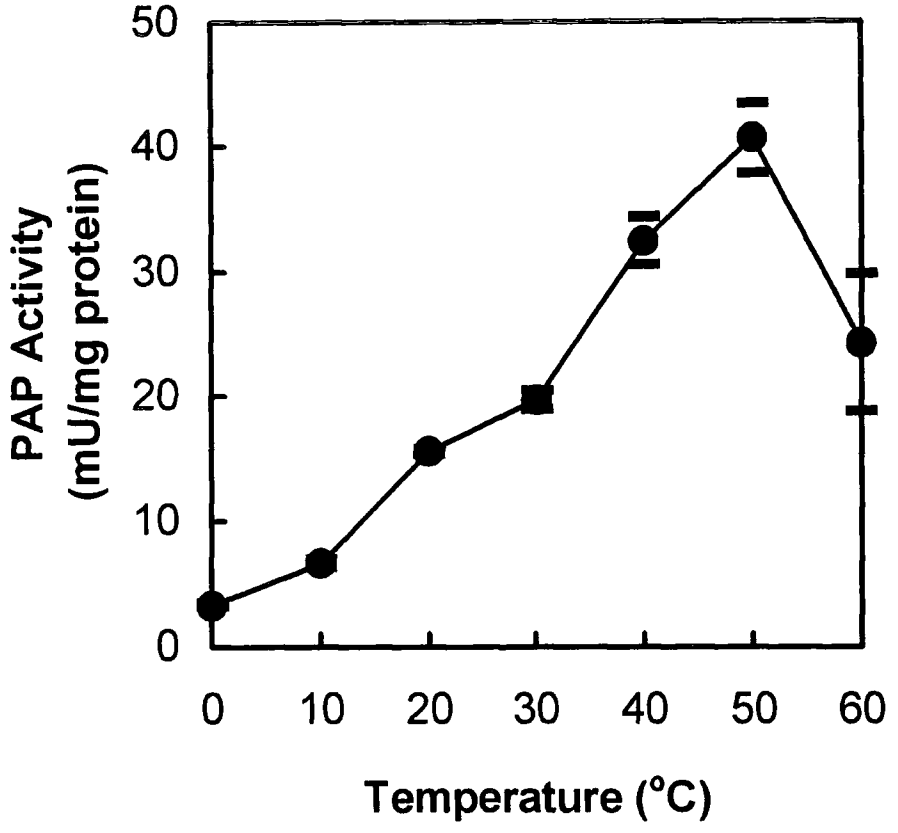

Figure 4.6: The effect of temperature on microsomal PAP activity. Standard yeast assay mixtures were pre-incubated at temperatures of between 0-60°C for 5 minutes prior to reaction initiation by the addition of pre-incubated (5 minutes) microsomal enzyme sample (2μg protein). Reactions were terminated after 20 minutes and the activities measured. Mean values with variance of the data from duplicate experiments are shown. One unit of PAP activity was defined as the amount of enzyme required to catalyse the formation of 1μmol Pi/min.

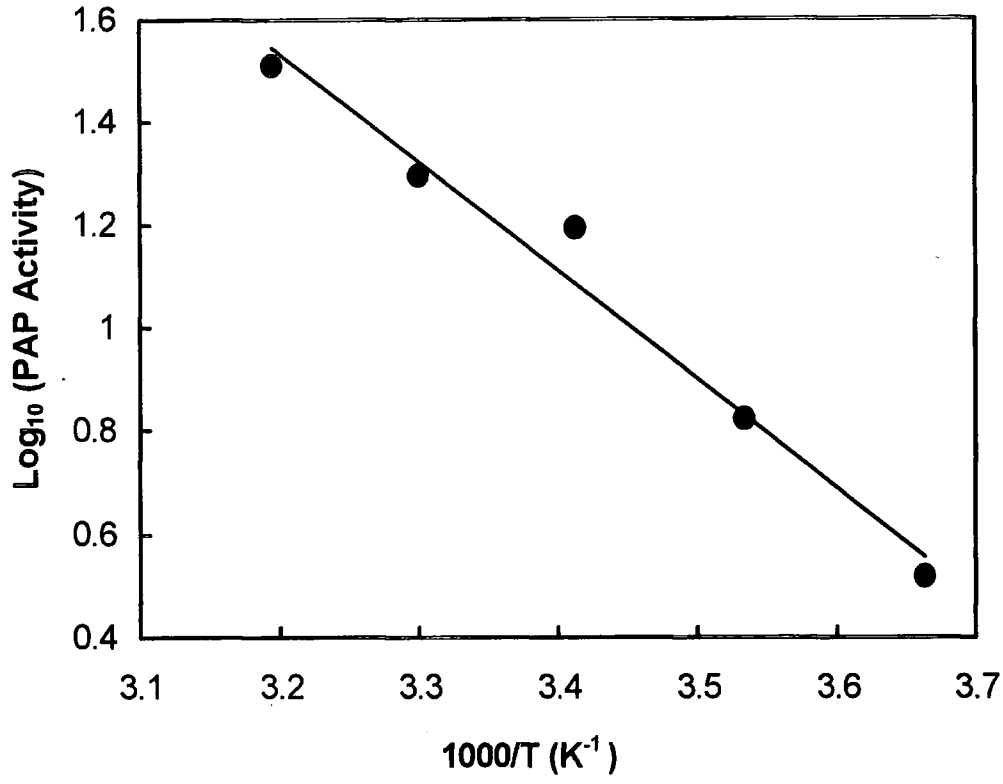

Figure 4.7: Arrhenius Plot for microsomal PAP temperature dependence. The plot was constructed using the mean data in the temperature range of 0-50°C from Figure 4.6. The plot was used to calculate the activation energy for the reaction as 37.3 kJ/mol (8.9 kcal/mol).

Although the optimum temperature was as high as 50°C, this was not a fundamental parameter, since the optimum temperature depends on the duration of the assay. At 50°C, PAP was only marginally stable, and consequently likely to be denatured. To ensure consistency, it was decided to conduct the standard assay at 25°C. This would allow for possible fluctuations in the stability of the PAP protein throughout purification, in which the enzyme is subjected to various stresses such as detergent solubilisation, in high salt and low protein concentrations.

4.3.7 Effect of detergent on PAP activity.

Both enzyme and substrate require detergent for solubilisation. For many detailed membrane bound enzyme studies, solubilisation is a prerequisite for reproducible assay conditions. It is for these reasons that the study of membrane bound enzymes and their immobilised substrates has been hindered (Verger, 1980). The optimisation and use of detergent is central to the study and purification of PAP. The use of detergent in the solubilisation of the PAP protein is discussed in the next chapter. This chapter is concerned with the use of detergent in the solubilisation of substrate, and its presentation to the enzyme as a substrate-mixed micelle complex. Triton X-100 has been successfully used with a variety of lipid-dependent enzymes (Carman *et al.*, 1995), and its physical properties are well documented (Robson and Dennis, 1977; Lichtenberg *et al.*, 1983).

The effect of Triton X-100 concentration on microsomal PAP specific activity was investigated and is shown in Figure 4.8. Duplicate assays were prepared with a constant PA concentration of 0.5mM. PA was dried under a stream of N_2 gas and resuspended by vigorous mixing with concentrations of Triton X-100 (0-40mM final assay concentration) and assayed. Microsomal PAP activity was stimulated by over 1.5-fold with maximum activity observed at 5mM Triton X-100. Further increases in Triton X-100 caused a reduction in activity, similar to the Triton X-100 effect seen with yeast PAP activity (Lin and Carman, 1989). The reduction in activity caused by additional Triton X-100 was due to substrate dilution within the detergent micelles and

is characteristic of substrate dilution kinetics (Deems *et al.*, 1975) at the micelle surface.

The PA surface concentration (or mole fraction) is the important factor for activity and not the bulk concentration of either substrate or detergent. Therefore the data from Figure 4.8 was replotted as PAP activity *versus* PA mole fraction ([PA]/[PA+Triton X-100]) in Figure 4.9, and demonstrates the dependence of PAP activity on the surface concentration of PA in Triton X-100/PA mixed micelles. The optimal surface concentration of PA for microsomal PAP is therefore 0.5mM in 5mM Triton X-100. This is calculated as 0.091 mole fraction (0.5/0.5 + 5) or 9.1 molar%. The detailed kinetic properties of PAP towards mixed micelles of PA/Triton X-100 were investigated and are described later.

The effect of substituting Triton X-100 for Tween-20, on microsomal PAP activity, was examined. PA-Tween-20 mixed micelles were prepared at 0.091 mole fraction and used in the otherwise identical assay as for above. The substitution of Tween-20 resulted in a 3% reduction in microsomal PAP specific activity when compared to PA-Triton X-100 mixed micelles. Triton X-100 was used for PA solubilisation in subsequent PAP assays.

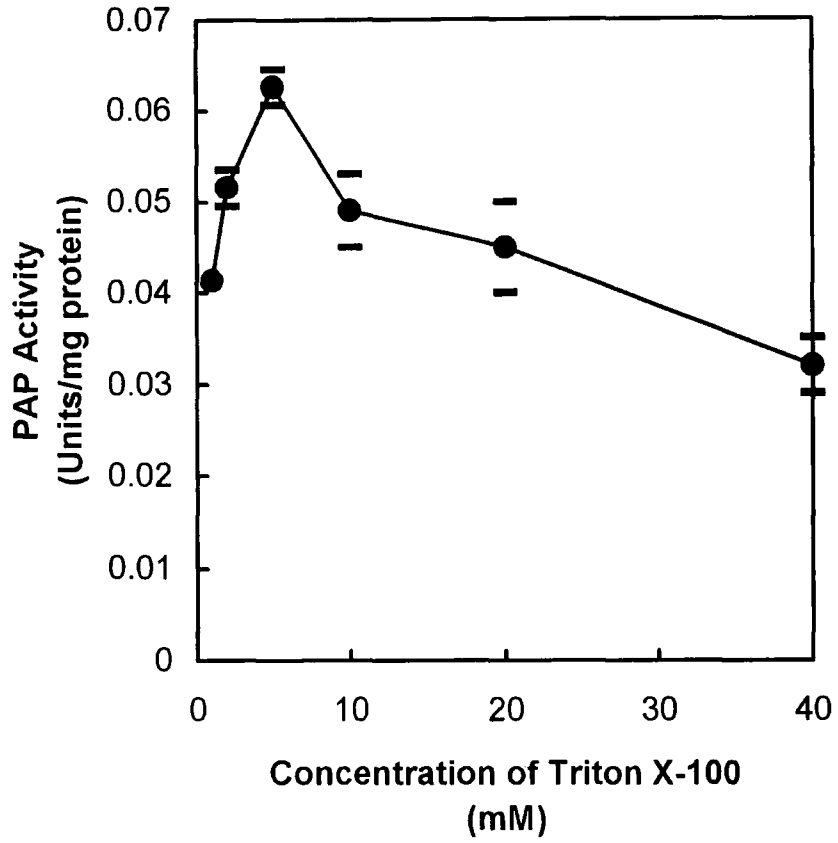

Figure 4.8: The Effect of Triton X-100 on PAP activity. Microsomal PAP specific activity was investigated at various concentrations of Triton X-100. Assays were prepared with a constant PA concentration of 0.5mM, and 4μg washed microsomal protein. PA was vigorously mixed with appropriate concentrations of Triton X-100 and assayed for 20 minutes at 30°C with the mean and variance of the data from duplicate experiments shown. One unit of PAP activity was defined as the amount of enzyme required to catalyse the formation of 1μmol Pi/min.

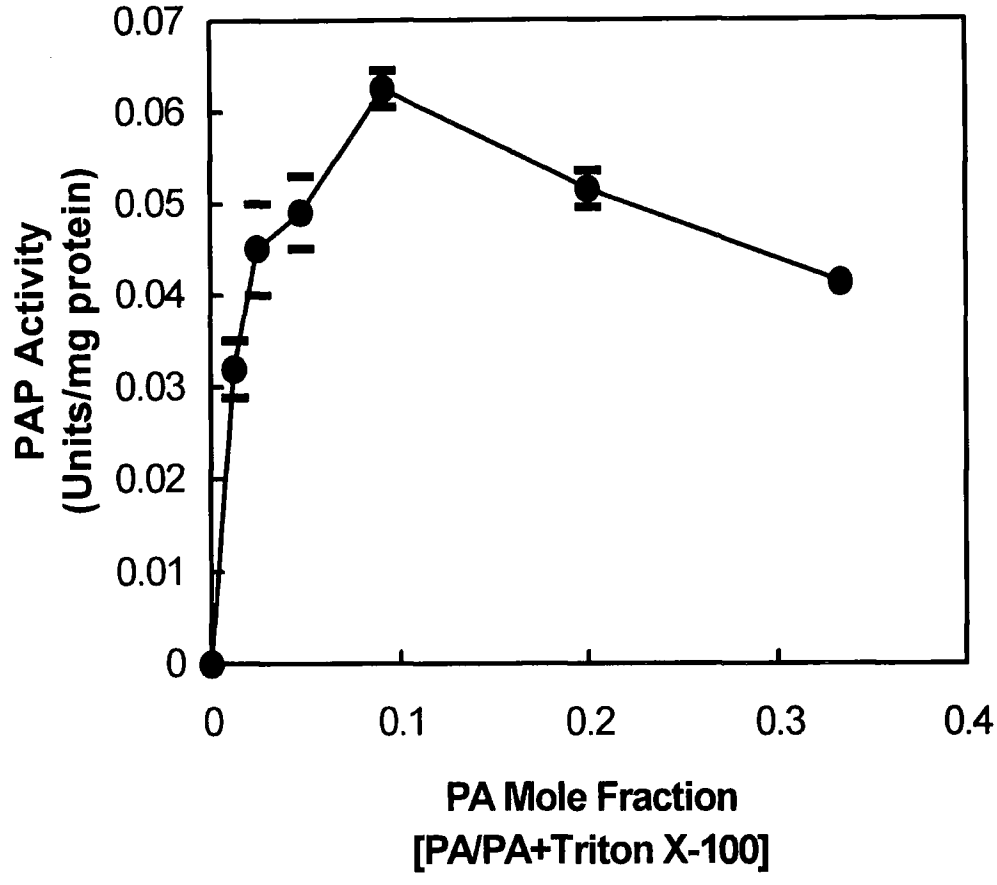

Figure 4.9: Dependence of PAP activity on the PA surface concentration in PA/Triton X-100 mixed micelles. The mean data from Figure 4.8 was replotted as PA mole fraction *versus* PAP specific activity. Using this plot, PAP activity is measured as a function of the surface concentration of PA, where the PA bulk concentration was held constant as the concentration of Triton X-100 was varied. One unit of PAP activity was defined as the amount of enzyme required to catalyse the formation of 1μmol Pi/min

4.3.8 The effect of substrate concentration and PAP activity.

As was shown in the previous section, variable concentrations of Triton X-100 (with PA concentrations remaining constant) affect the catalytic rate of PAP. The important factor is the PA:Triton X-100 ratio or mole fraction, and not the physical concentration of Triton X-100. The optimum PA mole fraction in mixed micelles of Triton X-100, for microsomal PAP was 0.091 (Figure 4.9). The kinetic analysis of microsomal PAP, was therefore conducted at a constant PA and Triton X-100 molar ratio of 1:10. PAP activity was assayed with increasing concentrations of dioloeoyl-PA in uniform Triton X-100 micelles. The effect of PA concentration (at the above mole fraction) was determined for microsomal PAP, with the mean results from two identical experiments shown in Figure 4.10. Under these conditions, PAP showed typical saturation kinetics with increasing PA concentrations, with the velocity tending to maximal at approximately 0.5mM PA.

A Lineweaver-Burk plot was constructed (Figure 4.11), linearising the data from Figure 4.10, by plotting 1/(activity) *versus* 1/[PA]. This allowed a kinetic analysis with the derivation of Michaelis-Menten kinetic constants of V_{max} and K_m. Values for V_{max} and K_m were calculated as 0.076 Units/mg protein and 160μM, respectively. The total microsomal fraction was used in this experiment, and consequently the V_{max} value is not representative of a homogenous PAP preparation. The K_m is independent of enzyme concentration.

Values for K_m have been reported for PAP from several plant species and are shown in Table 4.4. The K_m for avocado microsomal PAP is approximately halfway between the two reported values for microsomal PAP, although the experimental conditions used by the authors in Table 4.4 were vastly different, making a comparison difficult.

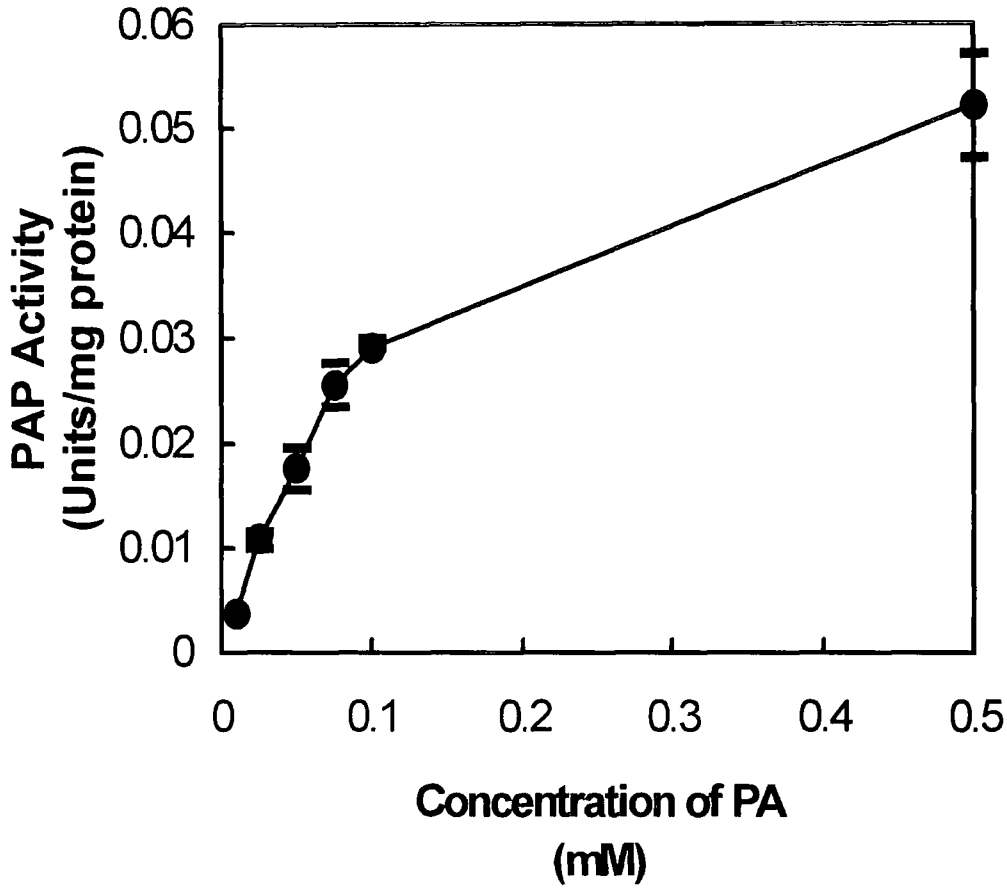

Figure 4.10: Effect of Substrate Concentration on PAP Specific Activity. Using a constant PA mole fraction of 0.091 in mixed micelles of Triton X-100, microsomal PAP activity was measured with increasing concentrations of PA. Reactions were initiated by the addition of 4μg washed microsomal protein and terminated after 20 minutes at 30°C. Mean results with variance of the data from duplicate experiments, are shown. One unit of PAP activity was defined as the amount of enzyme required to catalyse the formation of 1μmol Pi/min.

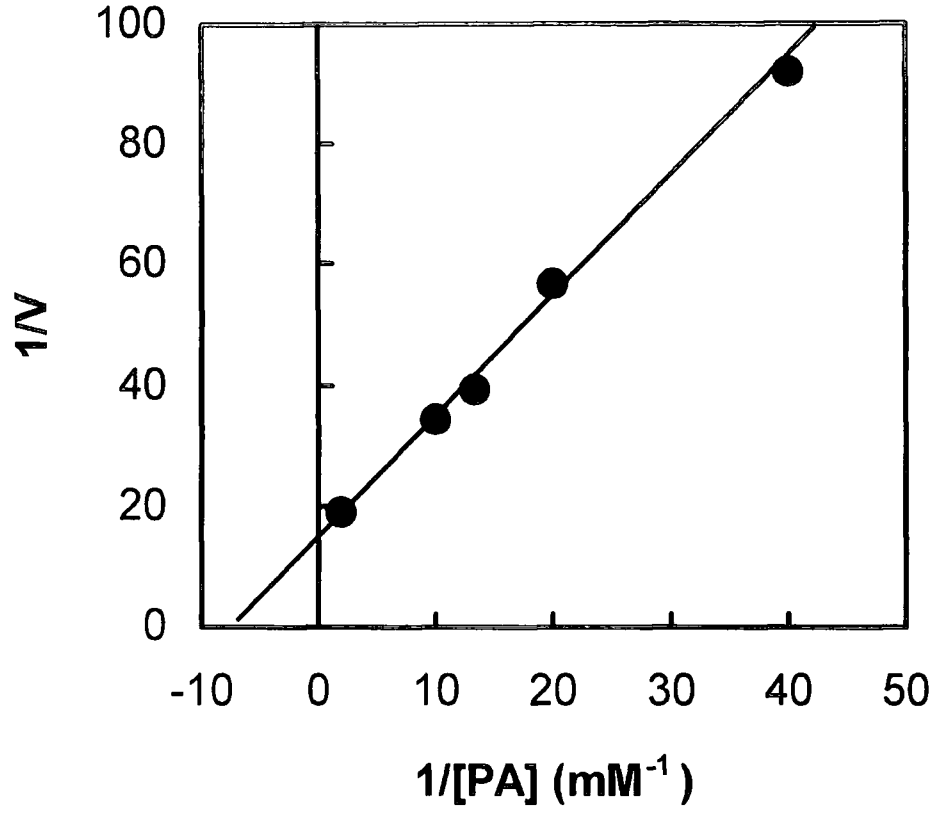

Figure 4.11: Lineweaver-Burk analysis of microsomal PAP. A double-reciprocal plot was constructed with the mean data from Figure 4.10, by plotting 1/(activity) *versus* 1/[PA]. This allowed a kinetic analysis with the derivation of Michaelis-Menten kinetic constants of V_{max} and K_m. Values for V_{max} and K_m were calculated as 0.076 μmol/min/mg protein and 160μM, respectively.

Subcellular Fraction	Plant Species	Km for PA (μM)	Reference
Cell extract	Broad bean	3.5	Königs and Heinz, 1974
Protein bodies	Mung bean	250	Herman and Crispeels, 1980
Microsomes	Ground nut	210	Sukumar and Sastry, 1987
Microsomes	Safflower	70	Ichihara, 1991
Chloroplast	Spinach	600	Malherbe *et al.* 1992

Table 4.4: Reported K_m values for plant PAP

The K_m of microsomally-associated PAP has been reported as 50μM in yeast (Lin and Carman, 1989), 200μM in porcine thymus (Kanoh *et al.*, 1992) and 300μM in rat liver (Fleming and Yeaman, 1995). Avocado microsomal PAP has a more than three times higher K_m for dioleoyl-PA than its yeast counterpart, when assayed under identical conditions (Lin and Carman, 1989). Avocado PAP requires higher concentrations of substrate to achieve maximal catalytic activity. Given that avocado mesocarp forms a large reservoir of lipid, it is possible that PA concentrations are higher than in yeast. The difference in K_m for yeast and avocado PAP reflects a possible difference in triacylglycerol biosynthesis, and the potential internal concentrations of PA in both tissues.

The kinetic results showed that at approximately 500μM PA, the substrate concentration exceeded the K_m value and the velocity was tending towards maximum. This meant that at this substrate concentration, the measured rate was dependent only on the enzyme concentration (Cornish-Bowden, 1995). Slight variations in substrate concentration would have had little effect on the rate of catalysis. Assays were not conducted with higher substrate concentrations as this would have resulted in an added cost of materials. For the routine measurement and quantification of PAP activity, it was decided that the concentration of PA used in the assay would be 500μM.

4.3.9 Final refined assay conditions for PAP activity

With the combined data from section 4.4, the final assay conditions were established for optimal and quantifiable measurement of PAP activity. The assay conditions were based on Lin and Carman (1989), but with slight alterations made in order to optimise the assay for the avocado system, with the final refined assay mixture described in Chapter 2.3.2, under *Materials and Methods*. The standard reaction mixture contained 0.5mM [^{32}P]PA (1000 - 2000 DPM/nmol), 5mM Triton X-100, 50mM Tris-maleate pH 6.0, 2mM $MgCl_2$. The reaction was initiated by the addition of enzyme sample ($\leq$20μg), and incubated at 25°C for 20 minutes.

To ensure that the measured enzyme catalytic activity was not due to chemical artefact, either during the reaction, termination or phase separation, an aliquot of microsomal fraction was incubated at 100°C for 5 minutes, and assayed in duplicate under the standard avocado assay conditions, alongside a positive control reaction containing an equal volume of normal untreated microsomal fraction. Absolutely no [^{32}P]Pi was detected after assaying with boiled microsomes, with an unaltered [^{32}P]PA level observed. The terminated and phase separated reactions were therefore free from non-enzymatically hydrolysed PA.

4.4 Characterisation of Assay reaction products.

Once the standard assay conditions were established, it was important to ascertain the extent of interference from lipases. The microsomal PAP reaction products were characterised using the standard avocado assay conditions. The reactions were initiated with the addition of microsomal fraction. After 60 minutes, the reactions were terminated and two phases created with chloroform as in *Materials and Methods* (Chapter 2.3.1). Two aliquots (50 and 200μl) of each phase were taken and dried under a stream of N_2 gas. They were then resuspended in 40μl of chloroform or 50% methanol depending on the phase (solvent or aqueous, respectively). The samples were then applied to a silica TLC plate and developed in

chloroform:methanol:water (12:6:1). Lipid standards were applied to a second plate and co-developed with the reaction products. The TLC plates were air dried and the sample plate exposed to pre-flashed X-ray film for 48hours. After film development, both of the TLC plates were evenly sprayed with Phloxene B and examined under UV light to identify lipid components. The autoradiograph of the TLC plate is shown in Figure 4.12, with the Ploxene B identified non-radioactive spots illustrated and superimposed onto the autoradiograph. The illustrated spots are proportional in size and position to the original spots seen. The migration positions of the lipid standards are shown alongside.

Figure 4.12 shows two areas of radioactivity, attributable to [^{32}P]PA and [^{32}P]Pi. Examination of the dyed non-radioactive products (illustrated and superimposed on Figure 4.12) revealed that DAG was the major product with traces of MAG. No other ^{32}P-containing PA degradation products, such as LPA and glycerol-3-phosphate were identified. This same phenomena was observed by Ide and Nakazawa (1989) in PAP assays with rat liver cytosolic and microsomal fractions, and strongly suggests that PAP (or phosphatase activity) was solely responsible for PA hydrolysis, leading to the production of DAG and Pi. A minor proportion of the DAG was then deacylated into MAG by the action of lipases. This slight hydrolysis of DAG would not effect the quantification of PAP activity provided [^{32}P]Pi release from [^{32}P]PA was measured. The reaction product profile showed that under the standard avocado PAP assay conditions, PA hydrolysis was caused by phosphatase and not phospholipase activity.

Figure 4.12

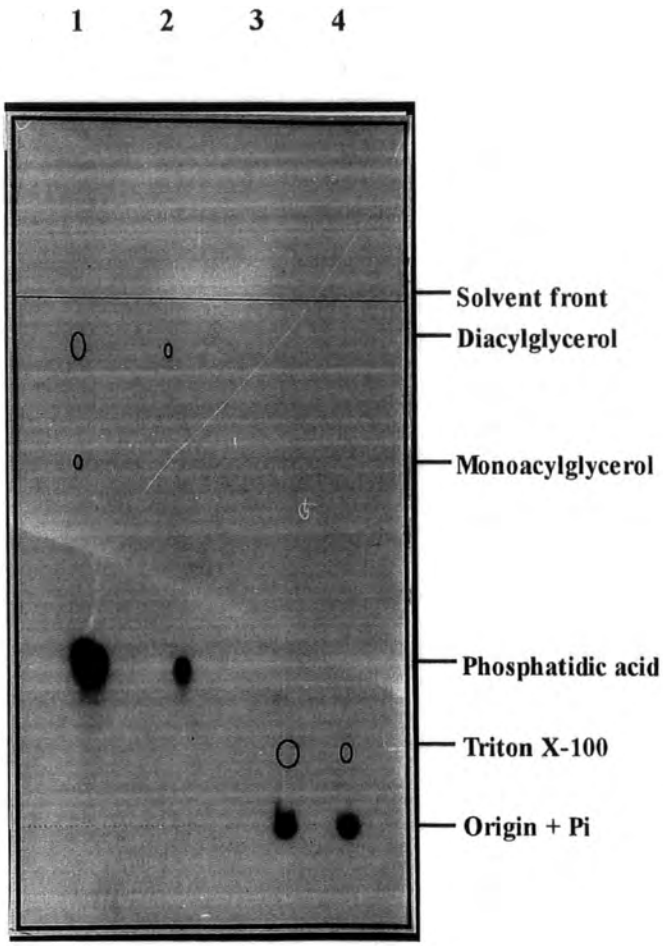
1
2
3
4
Solvent front
Diacylglycerol
Monoacylglycerol
Phosphatidic acid
Triton X-100
Origin + Pi

4.5 Discussion.

In this chapter, the research was directed towards the positive identification of PAP activity in avocado. Avocado mesocarp is an oil rich tissue whose lipid biochemistry has been well documented, and would be expected to be a rich source of lipid metabolising enzymes such as PAP. Using the assay procedure for yeast PAP (Lin and Carman, 1989; Carman and Lin, 1991), activity was found throughout differentially centrifuged fractions of avocado extract. The majority of the PAP was found in the soluble, or cytoplasmic fraction (105 000*g* supernatant), and approximately 10% of activity was located in the washed microsomal fraction (105 000*g* pellet). The microsomal activity was chosen for further characterisation because this form is most likely to be involved with glycerolipid biosynthesis.

These preliminary characterisation studies enabled the refinement of the yeast assay conditions so that the measurement of avocado PAP was linear with respect to time and protein concentration. The microsomal enzyme was found to be stimulated by, but not absolutely dependent on, Mg^{2+} ions. There are several possible explanations for this finding: (a) PAP is stimulated by Mg^{2+} ions as seen; (b) more than one enzyme activity is responsible for PA hydrolysis, one of which is Mg^{2+} dependent; (3) PAP may be Mg^{2+} dependent with traces of the ion trapped in the microsomal leaflets after dialysis, thus causing a basal activity with no added Mg^{2+}.

In mammalian systems, two isoforms of PAP have been identified, one of which is totally inhibited with thioreactive compound such as NEM and associated with glycerolipid biosynthesis. The NEM insensitive PAP has been implemented in signal transduction in mammals (Jamal *et al.*, 1991). The observed independence of avocado PAP activity on thiol-reducing agents suggests that there is only one isoform of PAP in plants. Only one distinct isoform of PAP has been identified in yeast. From this it would appear that the avocado system is more similar to yeast, but independent of reducing agents.

The temperature studies revealed that PAP has an 'optimum' temperature of 50°C. Ichihara *et al.* (1989) reported thermolability of safflower PAP at 55°C for both soluble and microsomal. Kocsis *et al.* (1996) reported that microsomal and soluble PAP in *B.napus*, have temperature optima of 45 and 50°C, respectively. However, the assay reactions of Ichihara *et al.* (1989) and Kocsis *et al.* (1996) were incubated at the set temperatures for up to 1hour, under detergent free conditions. Therefore accurate comparison is difficult under the different sets of circumstances. The 'optimum' for avocado PAP, however, is approximately the same as those previously reported in plants (Ichihara *et al.*, 1989; Kocsis *et al.*, 1996). Due its association with tropical climates, it would be expected that the 'optimum' temperature of avocado PAP to be higher, than the more temperate *B. napus*.

The effect of detergent on PAP activity was investigated using Triton X-100. The physical properties of Triton X-100 have been well documented (Robson and Dennis, 1977; Lichtenberg *et al.*, 1983), enabling its use in the detailed study of many enzymes (Carman *et al.*, 1996). The effect of Triton X-100 on PAP activity revealed that the detergent had a similar effect as reported for yeast PAP (Lin and Carman, 1989).

PAP activity decreased with increasing concentrations of Triton X-100. This reduction in activity was not attributable to Triton X-100 inhibition of the PAP protein, because as seen in Figure 4.10, PAP activity increased with PA concentration (in a constant PA:Triton X-100 mole fraction) with normal substrate saturation kinetics observed. Under these conditions the PAP protein was presented with increasing concentrations of Triton X-100, with no net decrease in activity.

PAP activity was dependent on the mole fraction of PA in Triton X-100 micelles. The critical micellisation concentration (CMC) of Triton X-100 is between 0.2-0.9 mM (Robson and Dennis, 1977; Neugebauer, 1994). By increasing the Triton X-100 concentration (at levels above the critical micellar concentration), the number of micelles increases, with PA evenly distributed between them. With a constant

concentration of PA, the overall PA surface concentration in the micelles decreases with increasing micelle numbers. This can be interpreted by the surface dilution kinetic model, proposed by Deems *et al.*, (1975). PAP specific activity decreased with increasing concentrations of Triton X-100 (with a constant PA concentration), indicating that it may follow the surface dilution kinetic model, where the substrate was diluted with increased micelle numbers. For a detailed kinetic analysis of the enzyme, a homogenous protein is required to derive meaningful data, and is therefore discussed later.

In order to derive the Michaelis-Menten constants, PAP activity was measured with increasing PA at a fixed mole fraction. As was shown in Figure 4.9, PAP activity is dependent on the surface concentration of PA in mixed micelles of Triton X-100. The PAP protein was therefore assayed with simultaneously increasing concentrations of PA and Triton X-100. Consequently, the Michaelis-Menten model is not strictly appropriate for the action of PAP towards PA/Triton X-100 micelles. A Michaelis-Menten analysis of the microsomal enzyme was conducted to provide sufficient K_m data for assay refinement only.

The characterisation allowed the refinement of the yeast assaying conditions, so that avocado PAP could be assayed under its optimal conditions. Under these conditions, during the characterisation of microsomal PAP reaction products, arguably the most important single observation was made. The reaction was essentially free from phospholipase activity under the avocado standard assay conditions. PA was subjected only to phosphatase hydrolysis. One of the products of the reaction, DAG, was further deacylated, but with no effect on the measurement of PAP activity. Therefore [^{32}P]Pi release was an accurate measure of phosphatase activity. This reiterates the conclusions of Ide and Nakazawa (1989), that following [^{32}P]Pi release is the only accurate means of PAP activity measurement.

Chapter 5

The Purification of PAP from Avocado Mesocarp

5.1 Introduction.

Since its identification by Kates in 1955, there have been many attempts to purify PAP from a variety of tissue sources. Despite this fact, the enzyme has only relatively recently been purified to homogeneity in yeast (Lin and Carman, 1989), porcine thymus (Kanoh *et al.*, 1992), and rat liver (Fleming and Yeaman, 1995). PAP has also been purified, but not to homogeneity, in rat liver by Waggoner *et al.* (1995) and Seiss and Hofstetter (1996). The isoform identified by Seiss and Hofstetter (1996) has recently been cloned by Kanoh and co-workers (Kai *et al.*, 1996). However, all of the PAP isoforms purified from mammalian sources have been implicated in signal transduction, in what has been a contentious field of research. The isoform responsible for glycerolipid biosynthesis, has not been purified from animals. PAP has not been purified from plants.

Solubilisation of the PAP protein is a prerequisite for its purification. There are many criteria that must be considered when choosing a suitable detergent for the solubilisation and purification of any protein (Neugebauer, 1990; Thomas and McNamee, 1990), including PAP. In choosing a suitable detergent for the solubilisation (and purification) of PAP, the following factors were considered:

Non-ionic and zwitterionic detergents are considered the most beneficial in the preservation of enzyme integrity upon solubilisation, and are often termed 'mild' (Helenius and Simons, 1975). Such non-ionic detergents include: octyl-β-D-glucopyranoside, Triton X-100 and Tween 20. CHAPS and LDAO are examples of zwitterionic detergents. If the solubilised enzyme requires the presence of detergent

for activity throughout purification, these detergents are also favoured because they have a smaller effect or interaction on chromatographic matrices, than seen with anionic or cationic detergents (Hjelmeland and Chrambach, 1984).

The critical micellar concentration (CMC) is the concentration of detergent at which the monomers aggregate (cluster) to form micelles. At concentrations below the CMC, detergents exist as monomers (Neugebauer, 1994). The number of monomers that form a micelle is termed the aggregation number of the detergent. This determines the micelle size. The solubilisation of an integral membrane protein is most effective at or near the CMC for most detergents (Hjelmeland and Chrambach, 1984). At these detergent concentrations, the subsequent purification can be hampered with detergent interference of the chromatographic matrices. It can be beneficial to reduce or totally remove the detergent after solubilisation for purification purposes. The removal of the detergent by dialysis is most effective in detergents that have a high CMC value (>1mM) and a small micelle size (aggregation number <30) (Neugebauer, 1994). It is beneficial if the physical properties of the detergent have previously been elucidated (Neugebauer, 1994).

There are additional problems when using detergents during protein purification. Many detergents contain aromatic groups and interfere with UV-VIS absorption. Triton X-100 absorbs light at 280nm, and affects protein measurement at this wavelength during chromatography (Hjelmeland and Chrambach, 1984). Ionic detergents if not removed, affect protein migration during electrophoresis, and some detergents interfere during staining procedures (Neugebauer, 1994). Many detergents have a limited solubility at 4°C, such as SDS and deoxycholate, or are precipitated at moderate pH values (Hjelmeland *et al.*, 1983). Such detergents are inappropriate for protein purification. The cost of purchasing the different detergents is also an important factor in the eventual choice of detergent. This is most noticeable under circumstances where detergent is constantly required for stability throughout the

purification process. Under these circumstances all of the solutions (including dialysis buffers) must contain the detergent.

There are therefore a number of criteria for choosing a suitable detergent. Even when these criteria are met or compromised, the enzyme may not be solubilised or may be totally inactivated by the detergent. Hjelmeland and Chrambach (1984) reported that it is advisable to undertake the initial solubility/stability studies of most functional membrane proteins with eight common detergents. These are shown in Table 5.1, with the data for Tween 20 also included. Hjelmeland and Chrambach (1984) later concluded that of these, octyl-β-D-glucopyranoside and CHAPS were often the most optimal.

The aim of the research in this chapter was to purify the microsomal enzyme. To achieve this aim, the following would be required: detergent solubilisation of the PAP protein, estimation of the native molecular weight, the designing and undertaking of a suitable purification strategy.

Property	Sodium cholate	CHAPS	BigCHAP	Digitonin	Zwittergent t3-14	octyl-β-D-glucopyranoside	Triton X-100	Tween 20	Lubrol PX
Detergent type	anionic	zwitt.	zwitt.	non-ionic	zwitt.	non-ionic	non-ionic	non-ionic	non-ionic
Monomer Mr	431	615	862	1229	364	292	650	1228	582
Aggregation Number	4	10	10	60	83	84	138	unknown	110
Critical Micelle Conc.:									
% (w/v)	0.36	0.49	0.12	unknown	0.011	0.73	0.02	0.007	0.006
(mM)	8	5	3	unknown	0.2	25	0.3	0.059	0.1
Dialysability	+	+	+	-	-	+	-	-	-
Use in ion exchange	-	+	+	+	+	+	+	+	+
Significant A_{280}	-	-	±	-	-	-	+	-	-
Protein assay interference	-	-	+	unknown	-	-	+	+	+

Table 5.1

5.2 The solubilisation of microsomal PAP.

By analysing the properties of the many detergents reported in Neugebauer (1994) and Hjelmeland and Chrambach (1984), it was decided that CHAPS was the most acceptable detergent for initial solubilisation studies of microsomal PAP. The physical properties of this bile salt derivative are well documented (Hjelmeland *et al.*, 1983; Stark *et al.*, 1984), where, in the case of rhodopsin, it has been shown to preserve native conformation and to stabilise the protein from thermal denaturation (Stark *et al.*, 1984). CHAPS does not conduct electricity, contribute to electrophoretic mobility, bind to ion-exchange matrices, contribute to the ionic strength of the solution or mask the ionic properties of proteins to which they are bound (Hjelmeland *et al.*, 1983). These properties make it an ideal detergent for solubilising and purifying membrane-bound proteins.

Thomas and McNamee (1990) reported that peripheral membrane proteins can be released from the membranes with the addition of salt. The addition of NaCl to the microsomes causes the interruption of electrostatic interactions between the membrane and protein, causing the subsequent release of protein from the microsomes. If PAP is membrane associated, the use of detergents could be circumvented by solubilisation with NaCl. However, the success of NaCl solubilisation is totally dependent on the resulting enzyme stability after solubilisation. The detergent micelle surface is analogous to the membrane surface on which solubilised proteins associate allowing stability (Thomas and McNamee, 1990).

The ability of NaCl and detergent to solubilise microsomal PAP was investigated. Solubilisation studies were conducted using washed microsomal fractions with 0.5% (w/v) CHAPS or Tween 20, and 2M NaCl at 4°C. The CMC of CHAPS is 0.49% (w/v), and is believed to be the concentration for optimal membrane bound protein solubilisation. At this concentration, delipidation of the protein sample

can be achieved. Maximum solubilisation of membrane-bound protein occurs at or above the CMC (Helenius and Simons, 1975). At 0.5%, the concentration of Tween 20 is in excess of its CMC, so solubilisation is theoretically maximal. Tween 20 was used in this experiment to allow a comparison between the detergents in terms of PAP and total protein solubilisation.

All procedures were conducted at 4°C. Aliquots (0.5ml) of washed microsomes were centrifuged at 200 000*g* for 30 minutes. The resulting microsomal pellets (twice washed) were resuspended using a glass homogeniser to a 0.5ml final volume in 0.5% CHAPS/Tween 20 or 2M NaCl in 50mM Tris-maleate pH 6.0, 10mM $MgCl_2$ and 20% glycerol. The final microsomal protein concentration was 5mg/ml. A control experiment was conducted in which the microsomes were resuspended in the same buffer, but with no detergent/salt added. All samples were placed on a Vortex Genie™ with 'multihead' attachment, and gently agitated for 45 minutes, whereupon they were centrifuged at 200 000*g* for 30 minutes. The supernatant from each was removed and retained. Microsomal pellets were resuspended to 0.5ml, in buffer ± detergent/salt as before. The solubilisation mixture, 200 000*g* supernatant and pellet were assayed for PAP activity for each sample, and the total solubilised protein measured, as described under *Materials and Methods*, Chapter 2.4.4, using the modified method based on Lowry *et al.* (1951), as described by Peterson (1983).

As can be seen in Table 5.2, 0.5% CHAPS and Tween 20 solubilised the majority of microsomal PAP. CHAPS was the more effective detergent, with a 85% PAP activity recovered in the 200 000*g* supernatant. The total solubilised protein was lower in samples that had been solubilised with CHAPS than with Tween 20, and the

Sample	TOTAL PAP ACTIVITY (nmol/min)			PAP activity in the 200 000*g* supernatant after 12 hours at 4°C (mU)	Solubilised Protein (mg)	PAP Solubilisation (%)
	Solubilisation Mixture	200 000*g* pellet	200 000*g* supernatant		200 000*g* Supernatant	
0.5% CHAPS	26.7	4.5	25.9	25.0	0.55	85.2
0.5% Tween 20	27.5	6.8	25.4	23.2	0.78	78.9
2M NaCl	23.2	6.1	15.3	6.0	0.43	71.5
Control	21.0	17.2	4.3	2.1	0.08	20.0

Table 5.2

CHAPS extract had a higher PAP specific activity calculated as 0.047 μmol/min/mg protein. A 20% release of microsomal protein was observed in samples where detergent was omitted. The microsomal fractions had been washed twice, so it was unlikely that this activity was attributable to the release of soluble enzyme that had been trapped within the microsomal membranes. Kocsis *et al.* (1996) reported a 21% release of PAP activity, from washed microsomes, upon further washing. NaCl caused the release of 70% total PAP activity into the 200 000*g* supernatant. The data from Table 5.2 strongly suggests that avocado PAP, as seen in yeast (Lin and Carman, 1989), is membrane-associated and not an integral membrane protein (Thomas and McNamee, 1990).

The stability of the enzyme after solubilisation, was dependent upon the presence of detergent (Table 5.2). A 60% loss in the NaCl solubilised activity was observed after 12 hours. This was most likely due to the removal of a 'membrane' support in the form of lipid or detergent, causing the protein to become denatured (Thomas and McNamee, 1990). CHAPS was deemed a suitable detergent for the solubilisation of microsomal PAP, and it was apparent that its constant presence was required for enzyme stability. Consequently, a purification strategy in the presence of CHAPS, would have to be elucidated, to ensure enzyme integrity throughout the protein fractionation process.

5.3 The Determination of the Native Molecular Mass of PAP.

To date, all reported isoforms of PAP from all organisms have been reported as being monomeric proteins. The approximation of the native molecular mass of microsomal PAP would greatly assist in the subsequent purification of microsomal PAP. Assuming plant PAP is monomeric with a known native mass, the area of an SDS-PAGE gel corresponding to this molecular mass can be analysed for protein band enrichment, after each fractionation step. Once homogenous, the molecular mass

determined by SDS-PAGE can be compared to the native molecular mass. This can enable association of the homogenous protein band to PAP activity, and the elucidation of the subunit composition of the native protein. This helps to ensure that the PAP activity is not attributable to another protein that is not visible on the gel.

To achieve an estimation of the native molecular weight of PAP, both gel filtration and native-PAGE were conducted on CHAPS solubilised microsomal enzyme.

5.3.1: Gel Filtration analysis of solubilised PAP.

Microsomal PAP was solubilised with 0.5% CHAPS, and the resulting CHAPS extract was used for gel filtration analysis, in order to measure the native molecular weight of the enzyme. The CMC of CHAPS is 0.49%. The solubilised protein within the CHAPS extract would be predominantly in CHAPS micelles. The interpretation of data after gel filtration chromatography, in the presence of micellar detergent, is difficult. The exact micelle/protein size must be established, and the sum molecular mass of the CHAPS monomers subtracted to give the native molecular mass of the protein of interest. This relies upon the assumptions that all micelles are equal in size (i.e. the detergent has a constant aggregation number), and that each micelle contains only one protein molecule. Therefore size exclusion chromatography in the presence of micellar detergent can be erroneous. For this reason, the gel filtration analysis of the samples and protein standards was conducted in the presence of 0.1% CHAPS. At this concentration, CHAPS is monomeric. This eliminated any complications caused by the formation of protein-detergent micelles during chromatography.

Prior to chromatography, all samples/solutions were filtered through a 0.22μm filter to remove particles and eliminate the risk of blockages in the column. All procedures were performed at 4°C. The Superose 12 (PC 3.2/30) gel filtration column (Pharmacia LKB Biotechnology) was equilibrated with 50mM Tris-maleate pH 6.0,

10mM $MgCl_2$, 150mM NaCl and 0.1% (w/v) CHAPS using a Pharmacia SMART system. This reduced the CHAPS concentration to considerably lower than the CMC, and removed the glycerol, which would cause an unacceptable column back pressure during the separation. NaCl (150mM) was included in the buffer to prevent unwanted protein-gel matrix ionic interactions during the separation.

The Superose 12 (PC 3.2/30) gel filtration column (Pharmacia LKB Biotechnology) was equilibrated with the above buffer, prior to the calibration of the column with various protein molecular weight standards. Each protein standard (gel filtration grade) was prepared as 1mg/ml in the above buffer. A 20µl aliquot of an individual standard was loaded onto the column at a flow rate of 40µl/min. The elution peak was monitored by measuring the absorbance at 280nm and the elution volume (V_e) recorded. This was repeated for all of the standards until a retention time for each was elucidated. The void volume (V_0) for the column was 0.8ml. The mean elution volumes and the relative elution volumes (V_e / V_0) for the molecular mass standards from duplicate calibration experiments are shown Table 5.3.

Protein Standard	Molecular Mass (kDa)	V_e (ml)	Relative elution volume (V_e / V_0)
Ferritin	443	1.1	1.38
BSA	66	1.29	1.61
Ovalbumin	45	1.37	1.71
RNAase	13.7	1.58	1.98

Table 5.3: Gel Filtration retention volumes for molecular mass standards.

A 1ml aliquot of CHAPS extract was dialysed (2 x 2 litres, 4 hours total) into the same buffer, to reduce the CHAPS concentration to 0.1% and to totally remove the glycerol. A 20µl aliquot of filtered dialysed CHAPS extract was loaded onto the

column at a flow rate of 40µl/min, and 100µl fractions were collected. The fractions were assayed for PAP activity with the peak of PAP elution (V_e) between 1.3-1.4 ml (Figure 5.1). The mean relative elution volume from duplicate experiments was calculated with a V_e of 1.35 and had a value of 1.69 ml. The molecular mass of each protein standard was plotted against V_e/V_o, and using the relative elution volume for PAP as 1.69, an apparent native molecular mass was estimated as being between 50-55 kDa (Figure 5.2). In both gel filtration runs, PAP activity eluted over two fractions, making the precise quantification of the relative elution volume difficult. The absence of PAP activity in the 1,000,000kDa molecular mass range showed that true solubilisation and total delipidation had taken place (Thomas and McNamee, 1990).

The gel filtration analysis was repeated in the total absence of detergent. Solubilised PAP had a limited stability in the absence of detergent, however, the activity was detectable, allowing the gel filtration analysis of PAP with the CHAPS removed. The procedure was identical to above, with the exception that the standards, elution buffer, and PAP sample contained no detergent. The Superose 12 column was calibrated using the identical standards as before. A 1ml aliquot of CHAPS extract was dialysed (2 x 2 litres, 4 hours total) in 50mM Tris-maleate pH 6.0, 10mM $MgCl_2$, 150mM NaCl, to remove detergent and glycerol. The sample (20µl) was injected onto the column and eluted as before. Under these conditions, the retention times of the standards and PAP were identical (Table 5.4) to the previous gel filtration analysis, which contained 0.1% CHAPS. Figure 5.2 could therefore be directly used to calculate the PAP molecular mass with the data obtained when detergent was omitted. The apparent molecular mass was determined as between 50-55kDa.

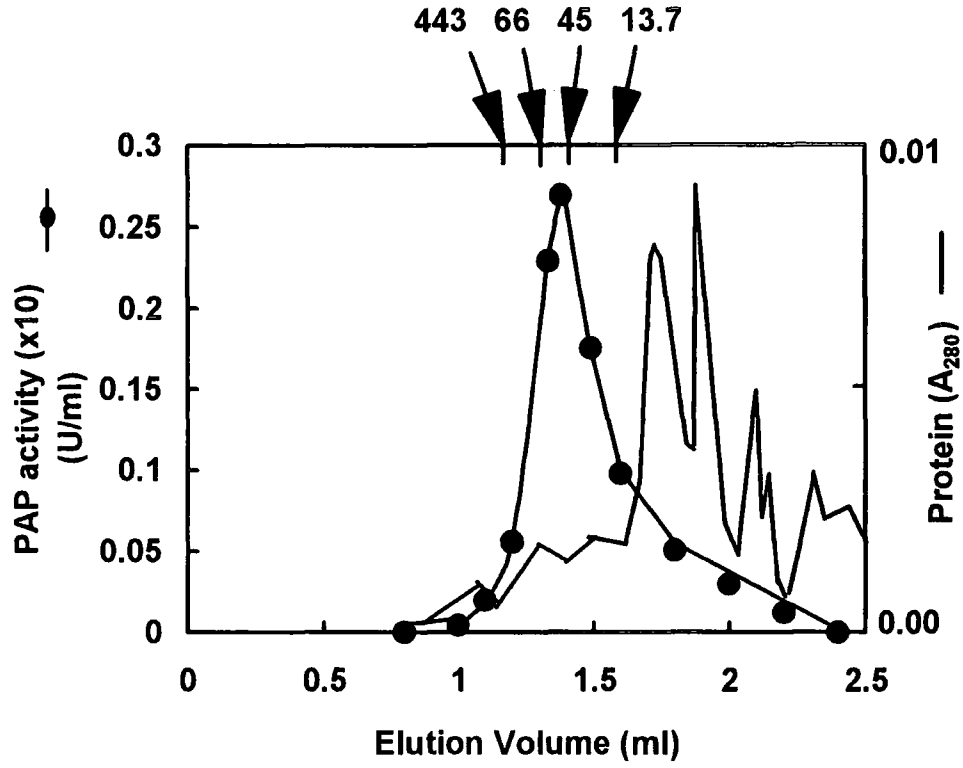

Figure 5.1: Superose 12 Gel Filtration analysis of microsomal PAP. A solubilised microsomal preparation was subjected to size exclusion chromatography in the presence of 0.1% CHAPS. Fractions (100µl) were collected and assayed for PAP activity (●). The column was calibrated with ferritin (443kDa), BSA (66kDa), ovalbumin (45kDa) and ribonuclease A (13.7kDa) with the elution volumes indicated with *arrows*.

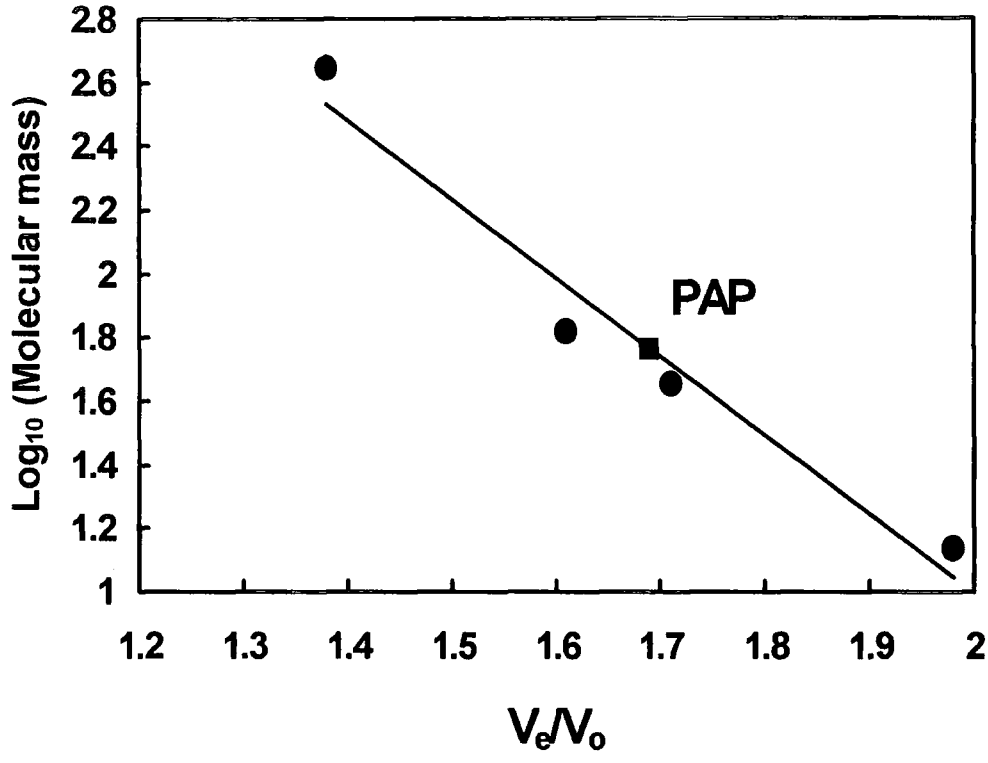

Figure 5.2: Determination of the molecular mass of native PAP by gel filtration. A Superose 12 gel filtration column was calibrated with molecular mass standards (●) (Ferritin, 443kDa; BSA, 66kDa; Ovalbumin, 45kDa; and ribonuclease A, 13.7 kDa) in the presence of 0.1% CHAPS. The Log_{10} of the molecular mass of each protein was plotted against V_e/V_o. The V_e/V_o for PAP, calculated from Figure 5.1, was positioned on the standard curve (■), allowing the determination of the apparent molecular mass.

5.3.2 The approximation of PAP molecular mass by Native/SDS-PAGE.

The aim of this section was to corroborate the molecular mass of PAP obtained by gel filtration. For this, non-denaturing PAGE was used in conjunction with SDS-PAGE. Non-denaturing PAGE was followed by the SDS-PAGE of the region of native gel containing PAP activity. The native electrophoresis conditions were based on Rock *et al.* (1981), which contained no SDS or reducing agent during the non-denaturing separation. Solubilised microsomal protein was loaded onto the gel. Once the protein migrated through the gel, one of the lanes containing protein sample was cut into segments and each slice assayed for PAP activity. A second lane was cut into segments and each boiled in SDS-PAGE sample buffer. The equivalent segment containing maximum PAP activity was then layered onto an SDS-PAGE gel and the protein separated by SDS-PAGE alongside protein standards. The migration of protein by native PAGE was dependent on the isoelectric point and molecular mass of the protein.

A 3mm thick 10% resolving gel was cast in a BioRad Maxi-gel apparatus, according to the manufacturer's guidelines, using the solutions of Rock *et al.* (1981) as described under *Materials and Methods*, chapter 2.4.8. A 5% stacking gel was poured over the resolving gel and allowed to polymerise. The running buffer (pH 8.3)and gel were chilled to 4°C, prior to sample loading. Solubilised microsomal PAP (100μg protein each), was loaded into 3 lanes on the gel in sample loading buffer containing no SDS or reducing agent (Rock *et al.*, 1981). BSA and ovalbumin were loaded alongside to act as native protein standards, showing the efficiency of migration and separation. Gels were run at 15mA and maintained at 4°C (Schägger, 1994) until the dye front reached the bottom of the gel after approximately 5 hours.

The lanes containing protein standards and one sample lane were cut away from the remaining gel and coomassie stained (see under *Materials and Methods*, Chapter 2.4.6). The remaining 2 lanes containing solubilised microsomal sample were

cut into 10mm slices. Each slice from one lane was homogenised in an eppendorf tube with 500µl 100mM Tris-maleate pH6.0, 10mM $MgCl_2$ and 0.1% CHAPS.

Protein Standard/Sample	Molecular Mass (kDa)	V_e/V_o
Ferritin	443	1.375
BSA	66	1.625
Ovalbumin	45	1.7
Ribonuclease A	13.7	2
Solubilised PAP	Calculated as 50-55	1.68

Table 5.4: Gel Filtration analysis in the absence of CHAPS. Relative elution volumes for protein standards and solubilised PAP were determined in the absence of CHAPS, and were found to be identical to the values obtained when the same experiment was conducted in the presence of 0.25% CHAPS (Table 5.1). Accordingly, the V_e/V_o value for PAP was used in conjunction with Figure 5.2 to determine the apparent native molecular mass as between 50-55kDa.

Undiluted [^{32}P]PA (40 000 DPM/assay) was added to each tube in 10mM Triton X-100 micelles to identify PAP activity. The samples were incubated at 25°C for 12 hours. Aliquots (200µl) were removed from the assay mixture, terminated and the [^{32}P]Pi measured. The remaining sample lane was cut into 10mm slices, and each placed in an eppendorf tube containing 100µl 2 x SDS-PAGE sample buffer.

PAP activity was distributed throughout the upper part of the gel (most likely through protein smearing during electrophoresis) up to segment 8 where it was maximal (Figure 5.3). The segment containing the highest PAP activity, was boiled in 2 x SDS-PAGE sample buffer and layered onto a SDS-PAGE gel. The denatured protein was separated by electrophoresis through the 10% gel and the protein visualised by silver staining. It was necessary to grossly overdevelop the gel in silver stain in order to visualise any sample protein. For this reason a photograph of the gel is not presented in this thesis. Several protein bands were identified in the molecular mass region of 45-66kDa.

A large amount of protein precipitated at the interface of the native resolving gel, and consequently, the coomassie staining failed to detect any migrated protein bands through the gel. This experiment was repeated under identical conditions, except with a smaller gel, using the Protean Mini-Gel Kit (BioRad) with identical results. Again, the SDS-PAGE gel required over development of silver stain in order to visualise the sample protein

In both non-denaturing PAGE experiments PAP activity was observed, and the SDS-PAGE analysis of this region showed protein bands predominantly in the 45-66kDa region. This appeared to corroborate the findings of the gel filtration, and suggested that PAP has a native molecular mass of around between 45 and 66kDa. With this information, the successful identification of PAP upon further chromatographic fractionation would be made easier.

Figure 5.3

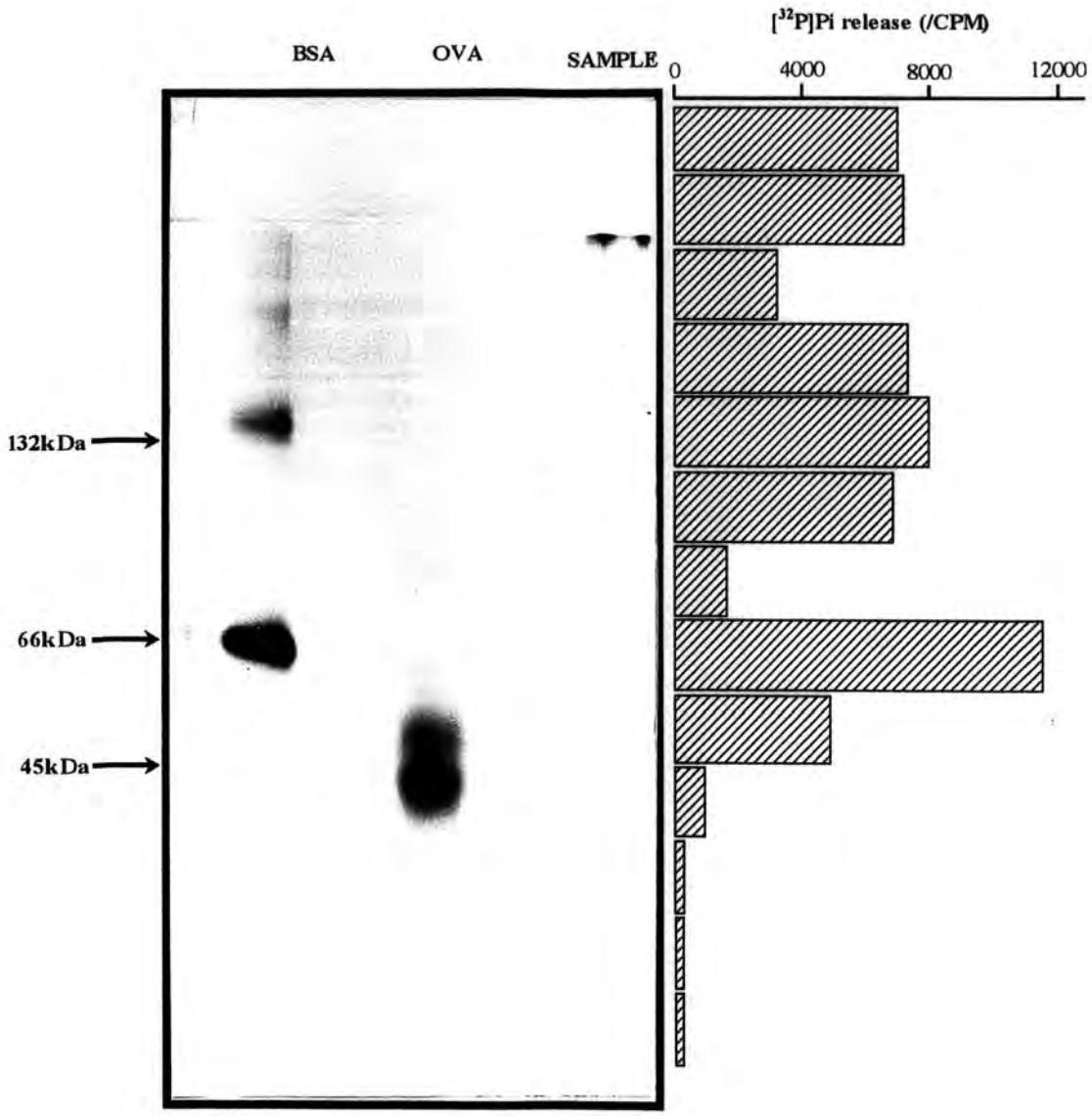
BSA
OVA
SAMPLE
[32P]Pi release (/CPM)
0
4000
8000
12000
132kDa
66kDa
45kDa

5.4 Purification studies of microsomal PAP from avocado.

The isoelectric point of PAP was unknown. At a certain pH, the net ionic charge of the PAP protein was unknown. This eliminated the possibility of predicting enzyme interaction with ion exchange matrices. The uncertainty of binding conditions was further increased with the requirement for CHAPS throughout purification. Although the detergent has a limited ionic effect on protein (Hjelmeland *et al.*, 1983) the CHAPS could still disrupt protein-exchanger group interactions or interact with the matrix backbone, thus interfering with overall protein binding.

The simplest way in which to determine the choice of chromatographic matrix was to conduct the 'test-tube method' for the selection of resin and starting conditions, as described by Pharmacia LKB Biotechnology technical bulletin (1991). Using this method, the binding conditions of PAP to any chromatographic gel matrix could be investigated. The method is based on the addition of protein sample at a certain pH/ionic strength/concentration to loose equilibrated gel matrix in a test-tube, and monitoring the relative amount of activity that binds or remains unbound. The method is not absolute, but general trends in enzyme binding can be determined. Various resins can be tested, and the binding conditions for each recorded. These conditions can then be adopted on a preparative scale for the isolation of homogenous protein, using a combination of the resins tested. The aim of this section was to purify PAP to homogeneity, with optimal yield. With sufficient homogenous protein the amino acid sequence can be derived from N-terminal sequencing. This will allow the generation of oligonucleotide primers encoding a region of the PAP protein and these used for the identification of the cDNA (encoding PAP) through screening of an avocado cDNA library. The homogenous protein could also be used for the generation of antibodies and in a detailed kinetic analysis of the enzyme.

5.4.1 The effect of NaCl and $(NH_4)_2SO_4$ on PAP activity.

Throughout the purification of PAP using ion exchange and affinity chromatography, the protein sample is eluted from the column with concentrations of NaCl. It is important to determine the effect that NaCl has on enzyme activity. A NaCl standard curve can be constructed and used in the measurement of PAP activity where known salt concentrations are present. This allows for accurate quantification of NaCl-eluted samples without the need to remove the salt by dialysis prior to assaying.

Similarly, the effect of $(NH_4)_2SO_4$ on PAP activity was also examined. Since $(NH_4)_2SO_4$ precipitation is routinely used in the fractionation of proteins and as for NaCl, a standard curve will allow the accurate measurement of PAP activity in the presence of $(NH_4)_2SO_4$.

Stock solutions of 4M NaCl and 4M $(NH_4)_2SO_4$ in 50mM Tris-maleate (pH6.0) and 10mM $MgCl_2$ were prepared and added to duplicate PAP assay reaction mixtures to create various final salt concentrations (0-1M NaCl and 0-2M $(NH_4)_2SO_4$). The reactions were initiated with the addition of CHAPS extract, and incubated for 20 minutes at 25°C, and the reactions measured for PAP activity (Figure 5.4). Both NaCl and $(NH_4)_2SO_4$ caused a reduction in PAP activity. At a concentration of 1M both NaCl and $(NH_4)_2SO_4$ caused a 60% decrease in PAP activity. The overall reduction in activity up to 1M salt was similar. At 2M $(NH_4)_2SO_4$, PAP activity was 26% of that observed when no salt was added.

The reduction in activity with both salts, was probably due to several factors. The solubility of PA is lowered in high salt, resulting in PA aggregation, and the reduction in catalysis due to substrate availability within the aggregates(Verger, 1980). The salt also causes a reduction in the CMC of Triton X-100 (Neugebauer, 1994) and thus an increased number of micelles are formed, causing a dilution of the substrate (Carman *et al.*, 1995). High concentrations of salt reduce the solubility of proteins

(Arakawa and Timasheff, 1985). The increased ionic strength of the protein solution is likely to cause a salting out effect of both protein and detergent-substrate micelles (as mentioned above).

5.4.2 The selection of chromatography resins for the purification of PAP.

The ability of PAP protein to bind to ion and affinity exchange groups was investigated using various chromatographic resins. The determination of chromatography starting conditions was based on the procedure recommended in Pharmacia LKB Biotechnology (1991), in which the enzyme is batch-bound to loose matrix gel, under various experimental conditions. The procedure was identical for all resins studied, with the data obtained from the batch-binding analysis of S-Sepharose used as an example below. The binding conditions for all of the tested matrices will be shown later.

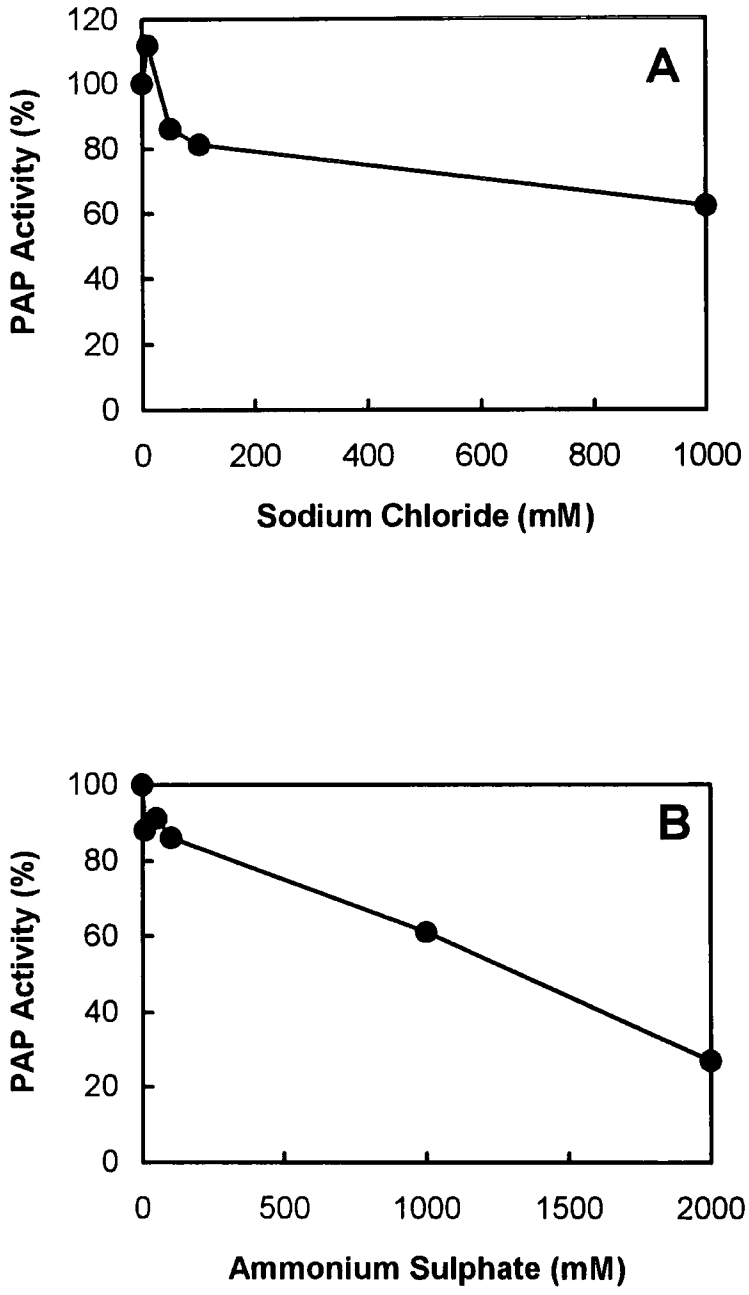

Figure 5.4: The effect of NaCl and $(NH_4)_2SO_4$ on solubilised PAP activity. CHAPS extract was assayed for 20 minutes at 25°C at various concentrations of NaCl (**A**) and $(NH_4)_2SO_4$ (**B**), with the mean *data* shown from duplicate experiments.

All resins were regenerated with 1M NaCl, and washed with ddH_2O prior to batch binding analysis. A series of 7 1.5ml eppendorf tubes was each prepared with 200µl bed volume of Fast Flow S Sepharose (Pharmacia LKB Biotechnology). The gel in each tube was equilibrated to a different pH by washing 5 times with 1ml of 50mM Tris-maleate (pH 5.5-8), 10mM $MgCl_2$, 20% Glycerol and 0.1% CHAPS. After each wash, the contents of each eppendorf tube were gently mixed for 1 minute and allowed to settle, prior to the removal of supernatant buffer. Aliquots (200µl) of CHAPS extract (in 10mM Tris-maleate (pH 6.0), 10 mM $MgCl_2$, 20% glycerol and 0.25% CHAPS) were added to each of the equilibrated tubes and gently mixed for 5 minutes at 4°C. The samples were then allowed to settle for a further 5 minutes. The supernatant, containing unbound enzyme, was removed and retained for assaying. The gel was washed with 2 x 200µl of equilibration buffer and the supernatant discarded. The gel was then washed in equilibration buffer containing 2M NaCl and the supernatant, or elutant, was retained. The unbound enzyme and elutant from each pH were assayed for PAP activity (at pH 6.0), and the % binding calculated from the total activity recovered in the unbound and eluted fractions (Figure 5.5). As was shown in the previous chapter, PAP activity is dependent on pH. The effect of pH on the determination of PAP activity was negligible because the binding was expressed as a % of the total recovered at that pH. Under these conditions, PAP-S Sepharose binding was at a maximum at pH 5.5, with a subsequent decrease in the binding observed as the pH increased. Binding at lower pH values was not investigated.

There was a substantial reduction in PAP binding between pH 6.0-6.5. This suggests that there was a shift in the net charge of the protein. However, the role that

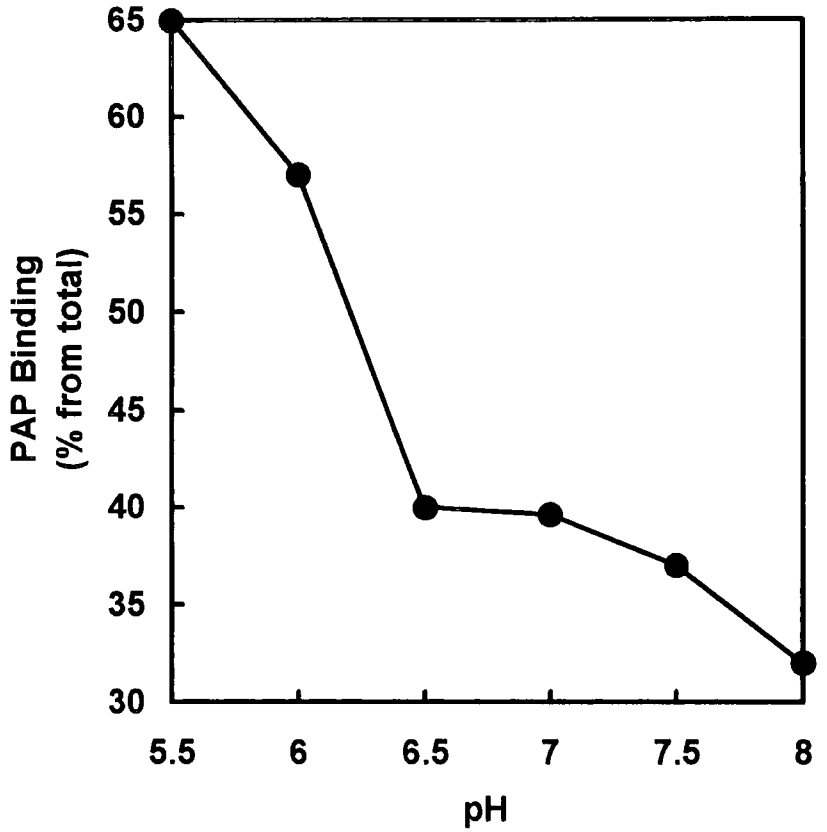

Figure 5.5: The effect of pH on PAP binding to S-Sepharose. CHAPS extract was applied to Fast Flow S Sepharose gel, which had been equilibrated to the indicated pH. Unbound protein and 2M NaCl elutant were assayed for PAP activity, and the % binding calculated.

CHAPS had on protein binding was unknown. A change in pH could equally effect the net charge of the zwitterionic detergent, and disrupt matrix-detergent-protein interactions.

This identical test was conducted using different gel matrices, and the binding conditions elucidated (Table 5.5). The affinity matrices proved to be effective in the binding of the PAP protein. Under the above conditions, the majority of PAP activity remained unbound in the presence of Fast Flow Q Sepharose at pH 8.0. Using the data from Figure 5.5, one would feasibly predict that PAP binds to Q-Sepharose at pH 8.0. However this is clearly not the case, and shows that the presence of detergent in the sample/equilibration buffer plays an influential role in PAP binding to ion exchange gels.

Hydroxylapatite has a requirement for low ionic strength for protein absorption, and thus PAP remained unbound. This experiment was conducted under different ionic conditions, with an otherwise identical procedure. CHAPS extract (2ml) was dialysed (2 x 2 litres, 4 hours total) into 10mM Phosphate buffer, 5mM $MgCl_2$ and 0.01% CHAPS. The sample was then applied to equilibrated hydroxylapatite and eluted using 800mM sodium phosphate. The unbound/eluted samples (200µl) were dialysed (2 x 200ml) in 50mM Tris-maleate pH6.0, 10mM $MgCl_2$, 20 % glycerol and 0.1% CHAPS, and assayed for PAP activity, with virtually no PAP absorption with the resin observed (Table 5.5).

The highest level of solubilised PAP binding to any one resin was 76%. Higher levels of association were not seen. This was most likely due to saturation of the 200µl gel with protein, preventing the remaining PAP protein from binding to the matrix. It was therefore important to ensure that the theoretical protein binding capacity of the matrix was taken into account when the batch analysis was scaled up to preparative scale. With the data from Table 5.5, a purification strategy using, Affi-Gel Blue (BioRad), S-Sepharose (Pharmacia) and Amicon Green A (Whatman) chromatography was decided. This combined both ionic and affinity matrices and offered a varied chromatographic approach to protein fractionation.

Chromatographic Matrix	Nature of gel functional group	Optimum pH for binding	% PAP bound
Fast Flow S-Sepharose	cationic exchanger	5.5	65
Fast Flow Q-Sepharose	anionic exchanger	8.0	35
Affi-Gel-Blue	Affinity	5.5	75
Amicon Blue A	Affinity	6.0	75
Amicon Blue B	Affinity	5.0	65
Amicon Green A	Affinity	5.0/5.5	70
Hydroxylapatite	Absorption	7.0	10

Table 5.5: The Batch-binding analysis of chromatographic resins. CHAPS extract was applied to the indicated gel matrices, which had been equilibrated in a pH range of 5.5-8.0. Unbound protein and 2M NaCl elutant were assayed for PAP activity, the % binding calculated. The maximum % value for bound PAP at the corresponding pH is shown. The binding conditions were identical for all matrices except for hydroxylapatite, where the ionic conditions were altered to suit the absorption limitations of the resin, with all procedures described in the text.

5.4.3 The partial purification of microsomal PAP - Purification Strategy No. 1.

Using the data from the batch-binding analyses of the various chromatographic matrices, the purification of PAP was attempted using 1 medium-sized Avocado mesocarp (100g, Type Haas). The preparation of washed microsomes was carried out at 4°C, using the procedure described in Chapter 2.5.1. From 100g tissue, 9.75 units of PAP activity were found in the 30 000*g* cell extract, and from this 1.13 units was subsequently recovered in the washed microsomal fraction (100 000*g* pellet). The washed microsomal fraction was centrifuged at 200 000*g* for 30 minutes and resuspended (second wash) to 2mg/ml (microsomal protein/buffer) in 50mM Tris-maleate pH6.0, 10mM $MgCl_2$, 20% glycerol and 0.5% (w/v) CHAPS. The solubilisation mixture was gently shaken at 4°C for 1 hour prior to centrifugation at 200 000*g* for 30 minutes. The resulting CHAPS extract (supernatant) contained 0.79 units of PAP activity with 70% of the microsomal PAP solubilised.

SDS-PAGE analysis of the differentially centrifuged samples and the CHAPS extract, demonstrated the high degree of protein enrichment and fractionation obtained upon the CHAPS solubilisation of the washed microsomes (Figure 5.6). After the 100 000*g* centrifugation of the cell extract, the majority of cellular protein was located in the supernatant (Figure 5.6, lanes 1 and 2). CHAPS solubilisation of the washed microsomal fraction, released 70% of PAP activity, but the main bulk of protein remained membrane bound (Figure 5.6, lanes 3-5). It can be seen that many of the microsomal protein bands were fractionated from the PAP sample due to the discriminatory behaviour of the CHAPS solubilisation. This observation was typical for all subsequent solubilisations undertaken using the above conditions, of 0.5% CHAPS (in buffer) at a microsomal protein concentration of 2-10mg/ml.

Figure 5.6

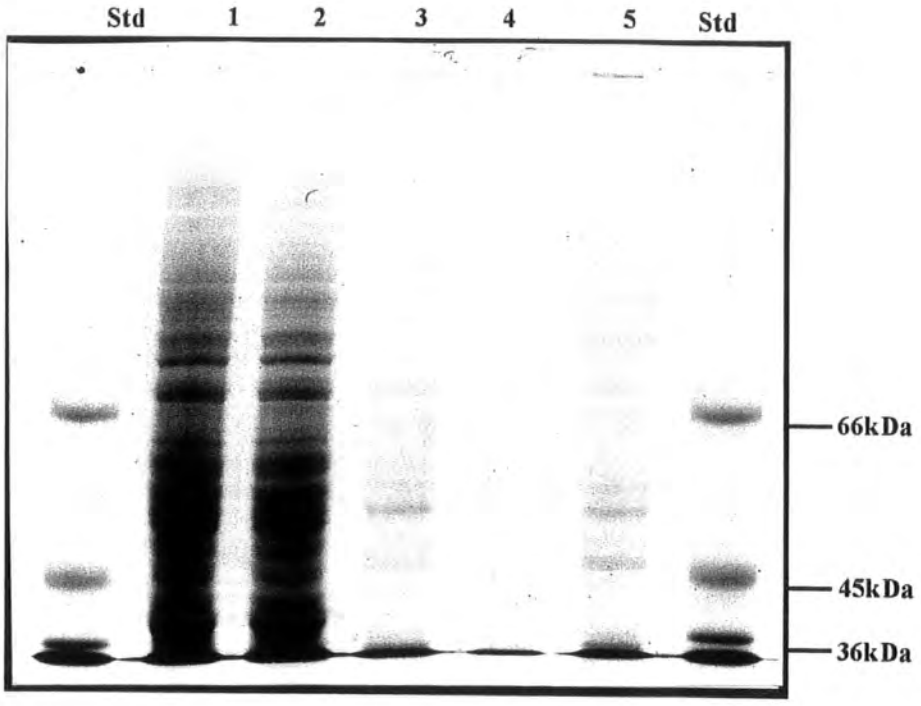

Solubilisation was conducted above the micellising concentration of CHAPS, ensuring that the solubilised protein was delipidated (Helenius and Simons, 1975). This allowed the subsequent chromatographic manipulations to be undertaken. For all chromatographic steps, the solutions and protein samples were filtered through 0.22μm filter disks (Sartorious) to prevent column blockages during chromatography. The overall recovery and enrichment of PAP activity will be shown as a purification table at the end of the purification. The protein concentration at each stage was determined using the trichloroacetic acid/deoxycholate adaptation of the Lowry assay(Lowry *et al.*, 1951), as described by Peterson (1983) and under *Materials and Methods*, Chapter 2.4.4, with BSA as the standard.

Affi-Gel Blue Chromatography: The CHAPS extract (20ml, 9mg total protein) was dialysed (2 x 2 litres) against 50mM Tris-maleate pH5.5, 10mM $MgCl_2$, 20% glycerol and 0.1% (w/v) CHAPS at 4°C. An Affi-Gel Blue column (1 x 4cm) was prepared and equilibrated with the buffer from the second dialysis (Buffer A), using a Pharmacia Hi-Load system (Pharmacia LKB Biotechnology, Uppsala, Sweden). The sample was loaded at 1ml/min onto the column using a peristaltic pump, and washed with 30ml Buffer A. The protein was eluted with Buffer B (Buffer A containing 2M NaCl) over a total 38ml step gradient (Figure 5.7) at a flow rate of 1ml/min as follows: A 9ml gradient (0-600mM NaCl) was applied to the column and held at 600mM NaCl (30% Buffer B) for 8ml, prior to continuation of the gradient to 2M NaCl. The fractions (1ml each) were collected and assayed for PAP activity (Figure 5.7). The majority of the CHAPS extract protein did not bind to the column. PAP eluted from the column at 600mM NaCl, with a recovery of 86% (0.673 units in pooled fractions 6-15).

Figure 5.7

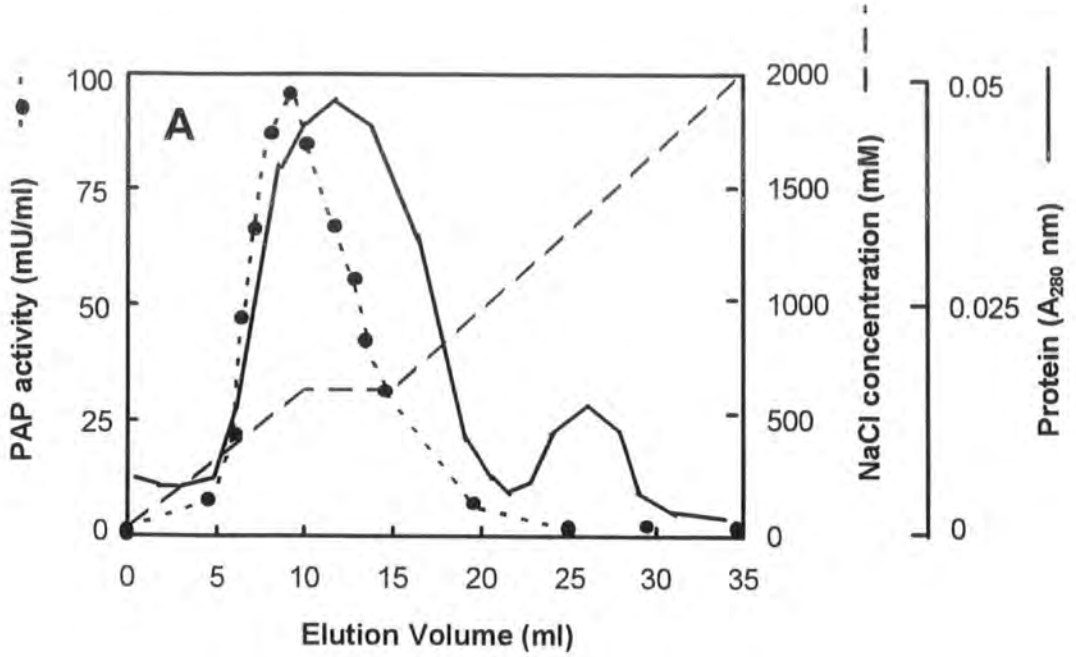
A
PAP activity (mU/ml)
NaCl concentration (mM)
Protein (A_{280} nm)
Elution Volume (ml)
0
25
50
75
100
500
1000
1500
2000
0.025
0.05
0
5
10
15
20
25
30
35

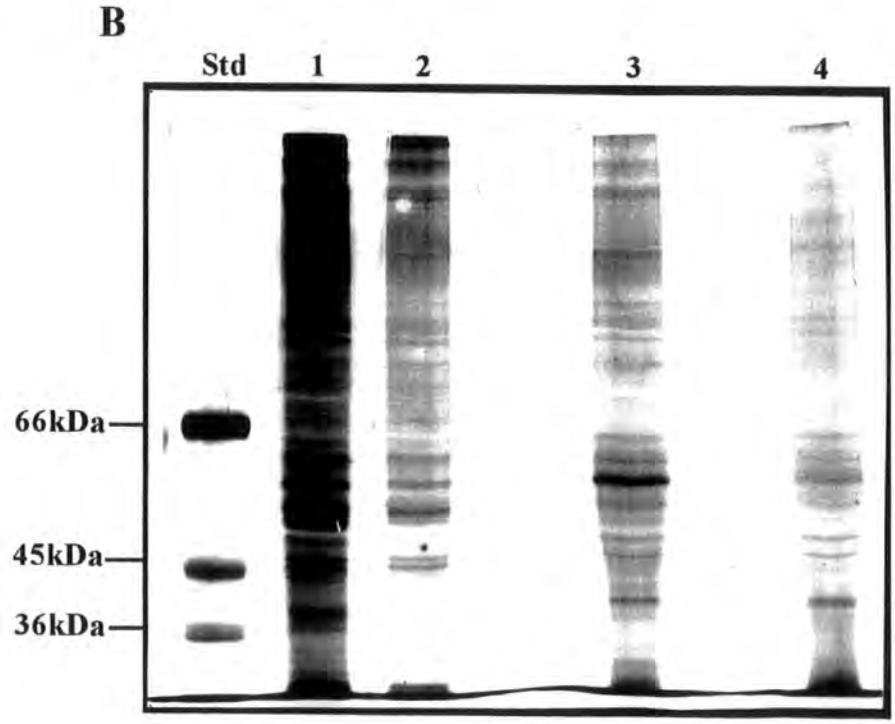
B
Std
1
2
3
4
66kDa
45kDa
36kDa

Aliquots of the CHAPS extract, the unbound protein, and pooled fractions 6-10 and 11-15 were chloroform:methanol precipitated using the procedure of Wessel and Flugge(1984) as described under *Materials and Methods*, Chapter 2.4.4. This served to remove detergent and NaCl from the samples and to concentrate the protein in the pooled fractions. The degree of protein enrichment/removal from the fractionated sample was investigated by visualising the migrated protein by silver staining (Figure 5.7). The majority of proteins within 45-66kDa did not bind to the column. There was no significant difference in the number of protein bands in the pooled fractions 6-10 and 11-15. Consequently, fractions 6-15 were pooled and used for the next purification step. The protein eluted from the column with a low resolution, with PAP eluting with the bulk of the bound protein. Only 30% of CHAPS extract protein bound to the column making this step useful for the removal of the majority of CHAPS extract protein.

Mono-S Chromatography: The Affi-Gel Blue purified PAP (10ml, 2.88mg total protein) sample was dialysed (2 x 2litres, 4 hours total) against 50mM Tris-maleate pH 5.5, 10mM $MgCl_2$, 20% glycerol and 0.075% (w/v) CHAPS at 4°C. A large reduction in activity was observed after dialysis, with the activity reduced from 0.67 to 0.291 units. A Mono-S HR5/5 column (Pharmacia) with a 1ml column volume, was equilibrated in the above buffer (buffer A) on a Pharmacia FPLC system. The dialysed sample was loaded onto the column at 1ml/min, and the column washed with 10ml Buffer A. A linear 30ml gradient (0-1M NaCl) of Buffer B (Buffer A containing 1M NaCl) was applied to the column, and 1ml fractions were collected. The elution of total protein was monitored by absorbance at 280nm. The fractions were assayed for PAP activity, with the broad peak of PAP elution observed at 350mM NaCl (Fractions 10-11, Figure 5.8). The fractions containing the peak of PAP activity (fractions 10-15) were pooled and used in the next purification step, and contained

Figure 5.8

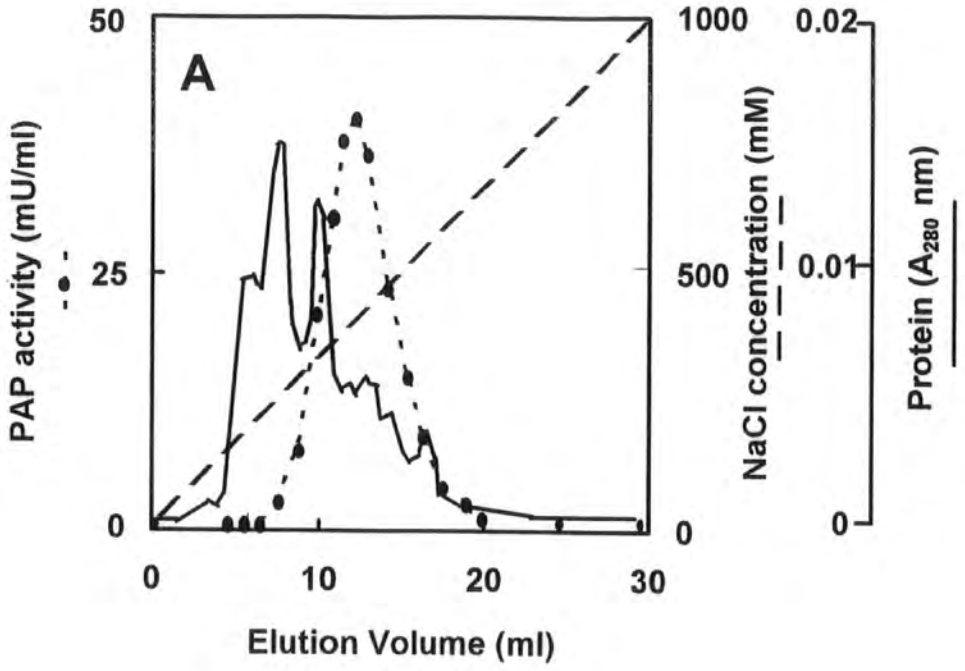
A
PAP activity (mU/ml)
NaCl concentration (mM)
Protein (A_{280} nm)
50
25
0
1000
500
0
0.02
0.01
0
0
10
20
30
Elution Volume (ml)

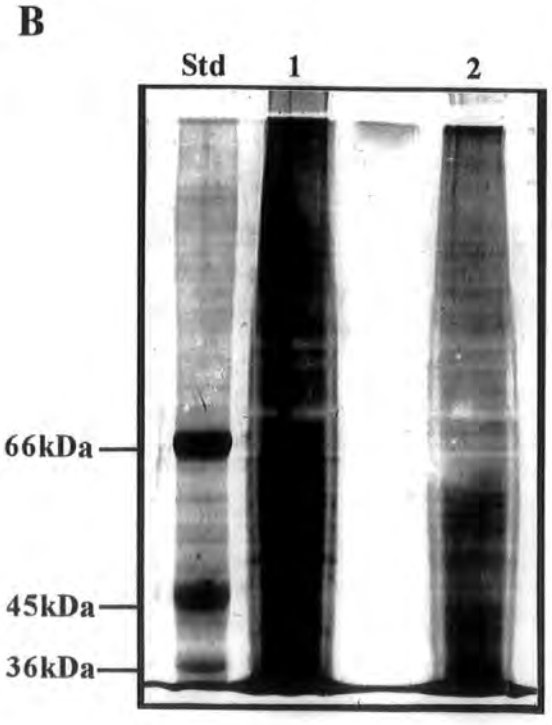
B
Std
1
2
66kDa
45kDa
36kDa

0.226 units in a 78% step recovery. The load (post Affi-Gel blue) and the pooled fractions (500µl of each) were chloroform:methanol precipitated, prior to analysis by silver stained SDS-PAGE. Mono-S chromatography caused a significant reduction in the total protein, most notably in the region of 45-66kDa (Figure 5.8).

Amicon Green A: The most active fractions from the Mono-S step (fractions 6-15, 10ml total, 0.226 units, 0.75mg total protein) were pooled and dialysed at 4°C against 2 litres (2 hours) of Buffer A (50mM Tris-maleate pH 5.5, 10mM $MgCl_2$, 20% glycerol and 0.075% (w/v) CHAPS). An Amicon Green A column (1cm x 2cm, 1.5ml bed volume) was prepared, regenerated with 2M NaCl and equilibrated in Buffer A using a Pharmacia FPLC system. The dialysed sample was loaded onto the column at 1ml/min, and washed with 15ml Buffer A. A linear 25ml gradient of 0-500mM NaCl (in buffer A) was applied to the column and the eluted protein measured with absorbance at 280nm. Fractions (1ml) were collected and assayed for PAP activity (Figure 5.9). The peak of PAP activity eluted at fraction 11 with 200mM NaCl. Fractions 6-14 were pooled and had a total PAP activity of 0.11 units, with a step recovery of 50%.

SDS-PAGE analysis of fractions 6-14 (500µl chloroform:methanol precipitated) showed a considerable enrichment of several protein bands in the molecular mass region of 45-66kDa (Figure 5.9), with the removal of most of the other protein. Coomassie Blue was used to visualise the SDS-PAGE separated samples, in order to allow relative abundance of each protein band to be assessed, as silver staining is non-linear with respect to protein concentration (Bollag and Edelstein, 1991). Several minor protein bands were present and further fractionation of the sample was required. As fewer proteins were in the sample it was decided to repeat the Mono-S purification step, allowing a better resolution. With fewer proteins in the sample it was hoped that the separation of individual peaks might be achieved. Affi-Gel blue was the most effective purification step in this strategy, but did not offer

Figure 5.9

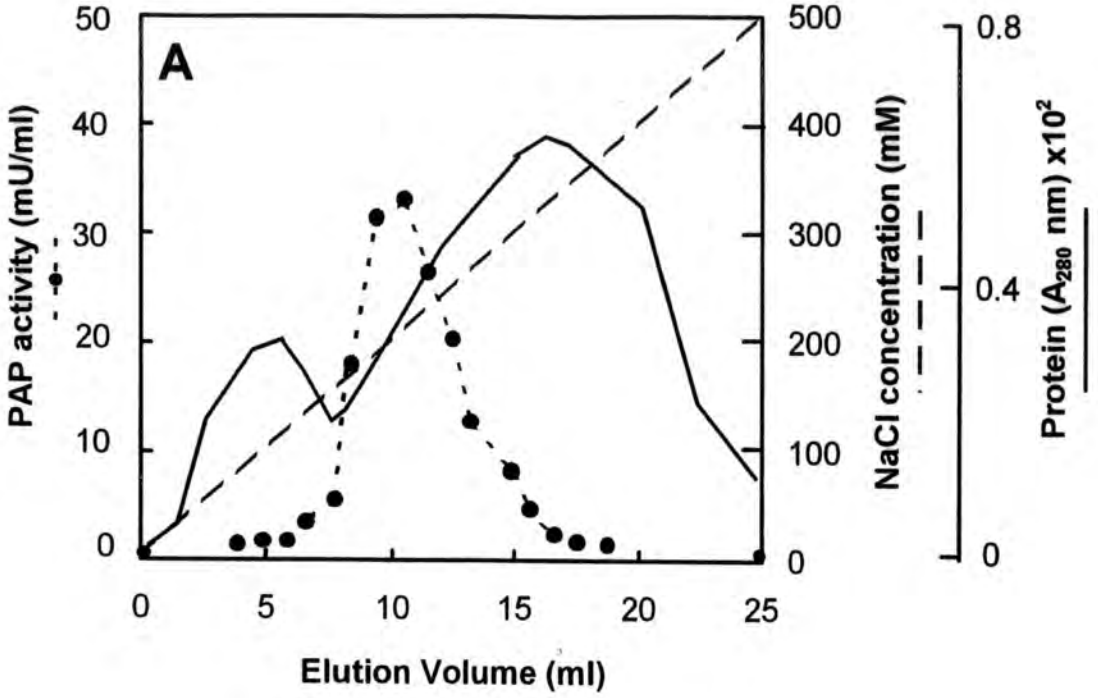
A
PAP activity (mU/ml)
NaCl concentration (mM)
Protein (A_{280} nm) x10^2
Elution Volume (ml)
0
10
20
30
40
50
100
200
300
400
500
0.4
0.8
0
5
10
15
20
25

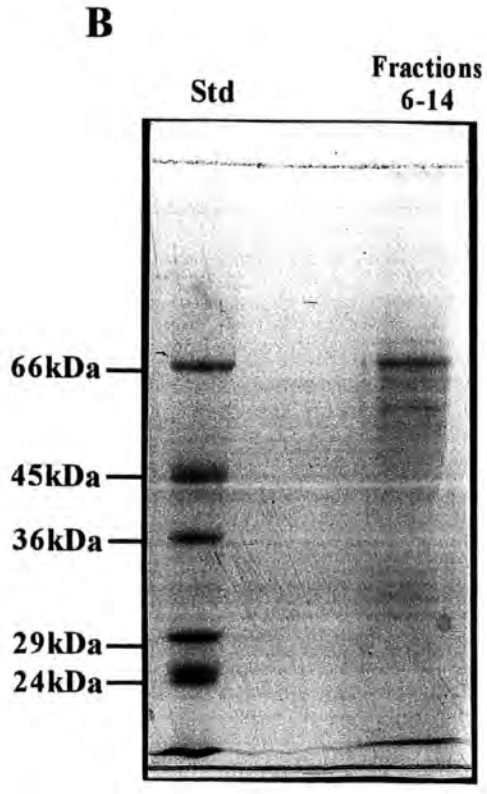
B
Std
Fractions 6-14
66kDa
45kDa
36kDa
29kDa
24kDa

the superior resolution properties associated with Mono-beads, and as such was not used.

Mono-S (2): The pooled fractions from the Amicon Green A step (9ml, 0.11 units, 0.24mg total protein) were dialysed against 2 litres of 50mM Tris-maleate pH 5.5, 10mM $MgCl_2$, 20% Glycerol and 0.075% CHAPS at 4°C. The Mono-S column was regenerated with 2M NaCl using a Pharmacia FPLC system, and equilibrated in the above buffer. The sample was loaded onto the column at 1ml/min and eluted with 1M NaCl (in the above buffer) with a linear 0-1M NaCl gradient (10ml). The eluted protein was monitored with absorbance at 280nm, and the collected fractions (0.5ml) were assayed for PAP activity, with the peak of PAP elution at 500mM NaCl (Figure 5.10). A large proportion (40%) of protein did not bind to the column, which was unexpected as this protein had bound under identical conditions earlier in the purification. The bulk of the protein eluted at 400mM NaCl, with a small sharp peak of protein eluting at 500mM which contained PAP activity (Figure 5.10). The fractions (10-15) containing PAP activity were pooled and had a total PAP activity of 0.062units with a step yield of nearly 60%.

The pooled fractions were analysed for protein purity using SDS-PAGE (Figure 5.11). The pooled fractions (500µl) were chloroform:methanol precipitated and loaded onto a 10% polyacrylamide gel. The protein was visualised with coomassie blue, allowing the relative abundance of each protein band to be assessed. The coomassie stained gel showed seven weak protein bands, of which five had a molecular mass of between 45 and 66kDa (Figure 5.11).

The total protein of the sample was determined as 10µg. The purification summary of avocado microsomal PAP, is shown in Table 5.6. PAP was purified by 163-fold from avocado microsomes with a final yield of 5.5%. The yield was considerably reduced as a result of PAP instability, prior to the first Mono-S step. This was most likely to be due to the reduction in CHAPS from 0.1% to 0.075%.

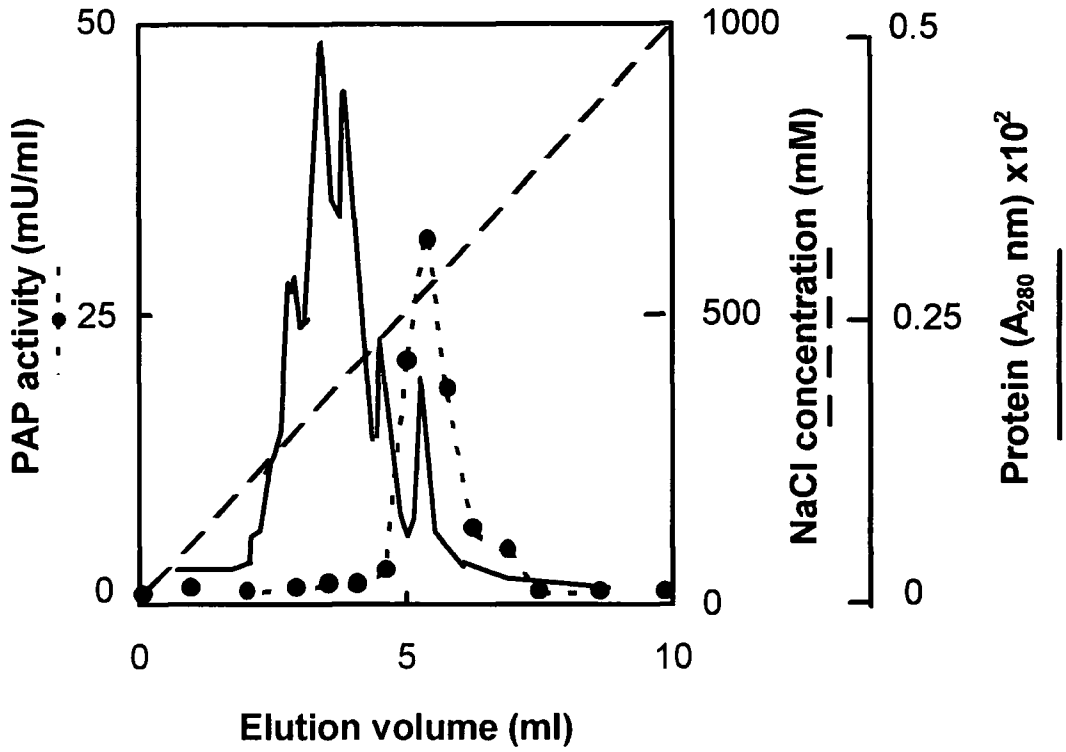

Figure 5.10: The elution profile of PAP using Mono-S chromatography (2). The dialysed Amicon Green A purified sample was loaded onto a 1.0ml equilibrated Mono-S column at pH5.5. After washing with 10ml of loading buffer, protein was eluted with a linear 10ml gradient of 0-1M NaCl (– –). The fractions (0.5ml) were assayed for PAP activity (●) and total protein was measured by A_{280} (—). The peak of PAP activity eluted from the column with 500mM NaCl.

Figure 5.11

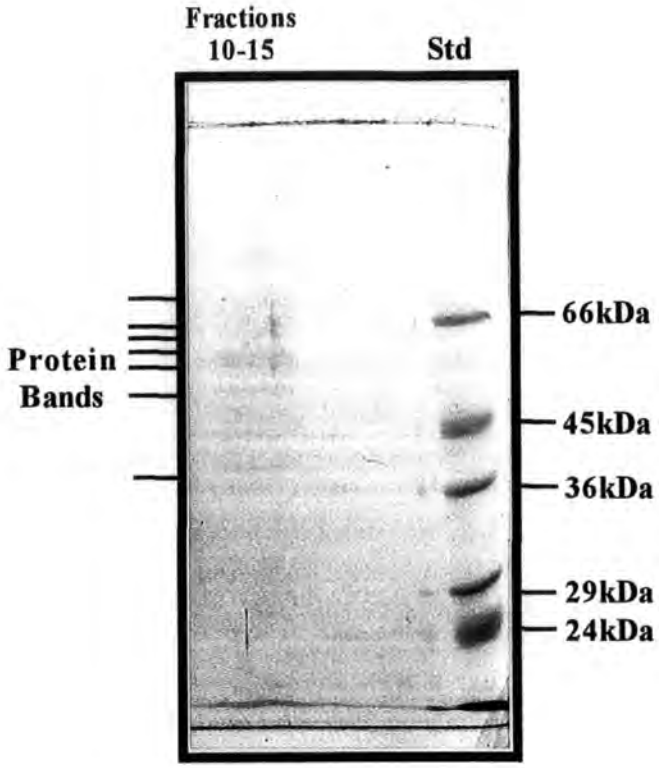

Figure 5.11: The SDS-PAGE analysis of the Mono-S (2) purified sample. The fractions containing PAP activity after elution from Mono-S (2), were pooled, 500µl was chloroform:methanol precipitated prior to loading onto a 10% polyacrylamide gel. The protein was visualised by coomassie staining. The pooled fractions consisted of seven protein bands(lane 1), with their positions indicated (—). The molecular masses of the protein standards are indicated with *arrows*.

Purification Step	Total Units (μmol/min)	Protein (mg)	Specific Activity (Units/mg protein)	Yield (%)		Purification (fold)	
1.Cell Extract	9.75	800	0.012	100	—	1	—
2.Microsomes	1.13	30	0.038	11.5	100	3.2	1
3.CHAPS extract	0.79	9	0.087	8	70	7.25	2.3
4.Affi-Gel Blue	0.67	2.88	0.223	7	59	19	5.9
5.Mono-S	0.23	0.75	0.301	2.3	20	25	7.9
6.Amicon Green	0.11	0.24	0.44	1	9.7	116	11.6
7.Mono-S	0.062	0.01	6.2	0.64	5.5	517	163

Table 5.6

There were seven main bands each of approximately equal intensity. If one of these protein bands was PAP, it could be inferred that 0.062 units PAP corresponds to 1.4μg protein, which would give a specific activity of homogenous PAP to be 43 units/mg protein (23μg protein/unit). It was possible that this was an over estimate as inactivated PAP protein may have co-purified. The apparent native molecular mass was 50kDa as determined by gel filtration analysis. This shows that the sample was inadequate for purposes of amino acid sequencing or the generation of high titre antibodies, where 100pmoles (5μg) are ideally required for N-terminal sequencing. To further purify this sample would be futile as a resulting decrease in yield would make identification of the homogenous protein by SDS-PAGE difficult due to the low protein levels. It was decided that there was insufficient protein to continue with this purification.

Using this specific activity (23μg protein/unit) the amount of PAP protein in the microsomal fraction (1.13units) was 26μg. With the low yield observed in this purification, more microsomal PAP protein would be initially required to obtain a final yield of protein, sufficient for N-terminal sequencing and/or the generation of antibodies.

Under the conditions used in the above purification, approximately 50% reduction in recovery was observed after each Mono-S and Amicon Green A purification step. The reduction in PAP total units after Affi-Gel blue was due to enzyme instability and loss of activity and poor chromatographic recovery. A new purification strategy was therefore considered in an attempt to improve the fractionation and the step yield. Two procedures were tested: ammonium sulphate fractionation, and hydrophobic interaction chromatography with Phenyl Superose.

5.4.4 Ammonium Sulphate Precipitation of PAP.

At high ionic strengths, protein solubility decreases. As the salt increases in a protein solution, the molecules of solvation are competed away from the protein to dissolve the salt, and the protein becomes 'salted out'(Arakawa and Timasheff, 1985) The solubility of different proteins at certain salt concentrations vary. $(NH_4)_2SO_4$ is routinely used in protein purification 'salting out' procedures to fractionate and concentrate protein samples, because it has a high solubility (up to 3.9M in water at 4°C) and it is cheap (Bollag and Edelstein, 1991).

To determine the approximate $(NH_4)_2SO_4$ concentration at which PAP precipitates, an experiment was conducted at 4°C with 25ml CHAPS extract (in sample buffer, containing: 50mM Tris-maleate pH 6.0, 10mM $MgCl_2$, 20% glycerol and 0.1% CHAPS). The ammonium sulphate precipitation was conducted following the procedure of Bollag and Edelstein (1991) and Jakoby, (1984), as described under *Materials and Methods*, Chapter 2.4.10. Finely ground $(NH_4)_2SO_4$ was slowly added to gently mixing CHAPS extract to 35% saturation (5.2g into 25ml). The mixture was gently stirred for 45 minutes prior to centrifugation at 21 000*g* for 5 minutes. The pellet, containing precipitated protein was resuspended in sample buffer and retained. $(NH_4)_2SO_4$ was added to the supernatant to 55% saturation (3.2g), and after stirring for 45min the centrifugation was repeated as before. The 55% supernatant was slowly brought to 85% saturation with the addition of 5.38g $(NH_4)_2SO_4$, and the whole process repeated. The CHAPS extract, 35%, 55% and 85% saturation supernatants and resuspended pellets were assayed for PAP activity (Table 5.7). At 35% saturation of $(NH_4)_2SO_4$, all PAP activity was recovered in the 21 000*g* supernatant. When $(NH_4)_2SO_4$ was added to 55% saturation to the mixture, one third of the activity precipitated. At 85% saturation no activity was recovered in the 21 000*g* supernatant, with all PAP protein located in the 21 000*g* pellets. Under these

Ammonium Sulphate	Fraction	PAP activity (μmol/min/mg)
35% Saturation	21 000*g* Pellet	0.001
	21 000*g* Sup.	0.086
55% Saturation	21 000*g* Pellet	0.015
	21 000*g* Sup.	0.059
85% Saturation	21 000*g* Pellet	0.037
	21 000*g* Sup.	0.000

Table 5.7: The ammonium sulphate precipitation of solubilised PAP. $(NH_4)_2SO_4$ was added to CHAPS extract to 35%, 55% and 85% saturation. At each % saturation, the mixture was centrifuged at 21 000*g* for 5 minutes, the pellet retained, and the supernatant brought up to the next % saturation. After centrifugation the pellet and supernatant (Sup.) were measured for PAP activity.

conditions the majority of PAP protein precipitated between 55-85% saturation of $(NH_4)_2SO_4$. The observed precipitation at 55% saturation indicates that the precipitation point of PAP was just above 55%.

5.4.5 Hydrophobic interaction chromatography of solubilised PAP.

Considering the microsomal association of PAP, and the requirement of detergent for solubility, it would be expected that regions of the protein are hydrophobic. The PAP protein would be expected to bind to a hydrophobic interaction column matrix. The ability of PAP to bind to Phenyl Superose was investigated using the 55% $(NH_4)_2SO_4$ 21 000*g* pellet from above and a 1ml Phenyl Superose HR5/5 column (Pharmacia). Many proteins, especially lipid binding proteins, have exposed hydrophobic regions/groups, theoretically allowing interaction with hydrophobic ligands attached to chromatographic resins This interaction is enhanced by high ionic strength buffers, allowing desorption to occur by reducing the salt concentration. The 55% $(NH_4)_2SO_4$ pellet (4ml total) containing 0.1unit of PAP was dialysed (2 x 1 litre, 4hours total) into Buffer A, consisting of 50mM Tris-maleate pH 6.5, 10mM $MgCl_2$, 20% glycerol, 0.1% CHAPS and 1.7M $(NH_4)_2SO_4$ (35% saturation). After dialysis the sample was centrifuged at 21 000*g* for 10 minutes and filtered through a 0.22μm filter to remove denatured/precipitated protein. The sample was loaded onto the column that had been equilibrated in the above dialysis buffer at a flow rate of 0.3ml/min. The column was washed with 10ml Buffer A, and the protein eluted from the column with a reversed linear gradient of 1.7-0M $(NH_4)_2SO_4$ in the otherwise identical buffer. The protein eluted from the column, was measured by absorbance at 280nm. The 1ml fractions were assayed for PAP activity, with a peak of activity observed at 0mM $(NH_4)_2SO_4$ (Figure 5.12) and a step recovery of 87%.

Figure 5.12

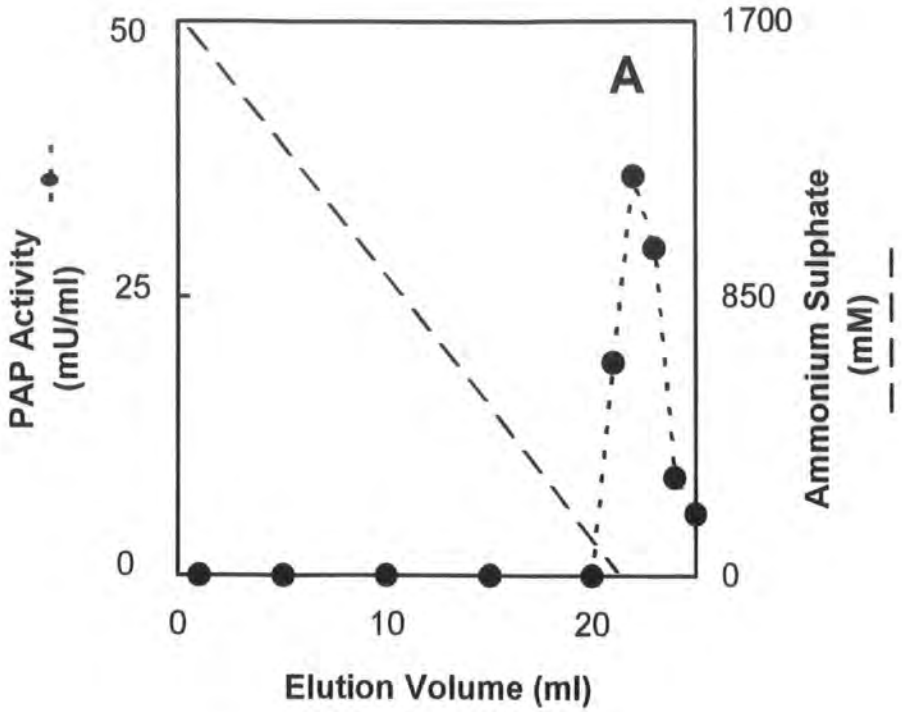
A
50
25
0
1700
850
0
0
10
20
PAP Activity (mU/ml)
Ammonium Sulphate (mM)
Elution Volume (ml)

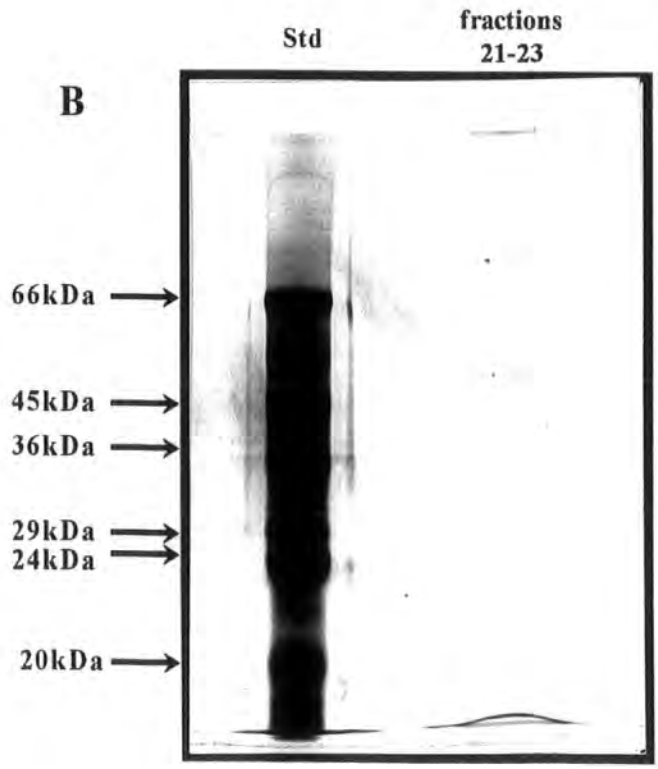
B
Std
fractions 21-23
66kDa
45kDa
36kDa
29kDa
24kDa
20kDa

The measurement of protein at A_{280} produced an erratic trace, and was excluded from Figure 5.12. This was probably due to the combination of detergent and high concentrations of $(NH_4)_2SO_4$, causing an interference in the A_{280} measurement. SDS-PAGE analysis of 400µl of the pooled fractions 21-23, revealed that there was very few protein bands in the eluted sample with one of the prominent bands having an estimated molecular mass of 50kDa (Figure 5.12). Phenyl Superose, in conjunction with $(NH_4)_2SO_4$ precipitation was found to be highly efficient in the purification of PAP.

5.4.6 The partial purification and identification of PAP - Purification Strategy No.2.

The Mono-S and Amicon green A steps in the previous fractionation yielded poor recovery of PAP protein. For these reasons, the ion exchange and Amicon Green A chromatography steps from the previous purification were exchanged for a purification strategy that combined Affi-Gel Blue chromatography, ammonium sulphate precipitation and Phenyl-Superose hydrophobic interaction chromatography. With these resins, a higher recovery of the PAP protein was expected. Once a successful strategy is obtained, the scale of purification can be increased for the subsequent bulk preparation of homogenous PAP protein. The large preparation of Avocado microsomes was time consuming and was considered inappropriate until a successful purification strategy had been elucidated.

The mesocarp from two ripe large avocados, with a fresh weight of 400g, was used for the purification of PAP, using a revised purification strategy. The preparation of CHAPS extract was conducted at 4°C or on ice, as described under identical conditions as in the previous purification.

Affi-Gel Blue Chromatography: The CHAPS extract (19ml, 0.61units, 4.35mg total protein) was dialysed (2 x 2 litres, 4 hours total) against 50mM Tris-maleate pH5.5, 10mM $MgCl_2$, 20% glycerol, and 0.1% CHAPS. A 5.5 ml bed volume Affi-gel Blue column (1 x 7.0cm) was prepared and equilibrated in the above buffer using a Pharmacia Peristaltic Pump P-1 at 4°C. The dialysed CHAPS extract was loaded onto the column at a 1ml/min flow rate, and washed with 10ml of equilibration buffer. As it has been shown, the resolution of eluted protein from Affi-Gel Blue, was poor, with the peak of PAP elution coinciding with maximal protein elution, so the protein was eluted in one step from the column with the addition of 5 column volumes of the above buffer containing 1M NaCl. The eluted sample was assayed for total protein and PAP activity, and found to contain 0.38units in 4.35mg protein, with a step recovery of over 60%. PAP activity (0.1units) was also located in the unbound fraction, indicating that the column had been saturated with bound protein. The protein binding capacity of Affi-Gel Blue was apparently reduced under these conditions (i.e. in the presence of 0.1% CHAPS).

Ammonium Sulphate fractionation: The Affi-Gel Blue purified sample (25ml, 0.38units) was dialysed (2 x 2litres for 1hour each) against 50mM Tris-maleate pH6.0, 10mM $MgCl_2$, 20% glycerol and 0.1% CHAPS at 4°C in order to remove the NaCl which could otherwise interfere with the 'salting out' by $(NH_4)_2SO_4$ (Arakawa and Timasheff, 1985;). Finely ground $(NH_4)_2SO_4$ (6.5g) was slowly added to the dialysed sample to 35% saturation. After 45 minutes of gentle stirring on ice, the sample was centrifuged at 21 000*g* for 5 minutes. The pellet were resuspended in the above buffer. The supernatant was raised to 55% and then 65% saturation with the addition of 4g and 2.3g $(NH_4)_2SO_4$, respectively, using the same procedure at each stage. The $(NH_4)_2SO_4$ fractionated samples were assayed for PAP activity, with 0.21 units recovered in the 55-65% $(NH_4)_2SO_4$ pellet. PAP activity (0.08units) was also detected in the 35-55% $(NH_4)_2SO_4$ pellet but was discarded.

Phenyl-Superose Chromatography: The 55-65% $(NH_4)_2SO_4$ pellet (7ml, 0.21 units, 0.244mg total protein) was dialysed against (2 x 1 litre, 2 hours total) of buffer A, consisting of 50mM Tris-maleate pH6.5, 10mM $MgCl_2$, 5% glycerol, 0.1% CHAPS and 1M $(NH_4)_2SO_4$ at 4°C. The Glycerol concentration was reduced to avoid excessive column back pressure during chromatography. A Phenyl-Superose HR5/5 (1ml bed volume) column was equilibrated at room temperature, in buffer A, using a Pharmacia FPLC system. The dialysed sample was applied to the column at a flow rate of 0.3ml/min followed by 15ml of Buffer A to wash unbound protein from the column. The bound protein was eluted with a step gradient with Buffer B (Buffer A without $(NH_4)_2SO_4$) as follows; 80% Buffer B (200mM $(NH_4)_2SO_4$ concentration) was applied to the column for 6ml, followed by a 4ml gradient to 100% Buffer B (0mM $(NH_4)_2SO_4$ concentration) prior to the further addition of 8ml 100% Buffer B (Figure 5.13). The eluted fractions were collected (1ml) and each assayed for PAP activity. The peak of PAP activity eluted between 50-0mM $(NH_4)_2SO_4$, predominantly in fractions 26-30 (Figure 5.13).

The fractions that eluted from the column immediately before any of the PAP activity (fractions 20 and 21), and the pooled fractions containing PAP activity (fractions 25-31) were chloroform/methanol precipitated (500µl of each) and the protein analysed by SDS-PAGE (Figure 5.14). In the pooled fractions containing PAP activity, three protein bands were seen after silver staining, all of which were in the molecular mass range of 45-66kDa. However, when the lane containing the protein which had eluted immediately prior to PAP activity, was examined, two of the protein bands were identical to those in the pooled sample (Figure 5.14). The PAP protein was therefore concluded to be the lowest of the three protein bands in the sample lane. The degree of protein enrichment/fractionation from the CHAPS extract, Affi-Gel Blue and Ammonium Sulphate precipitation steps are shown in Figure 5.14.

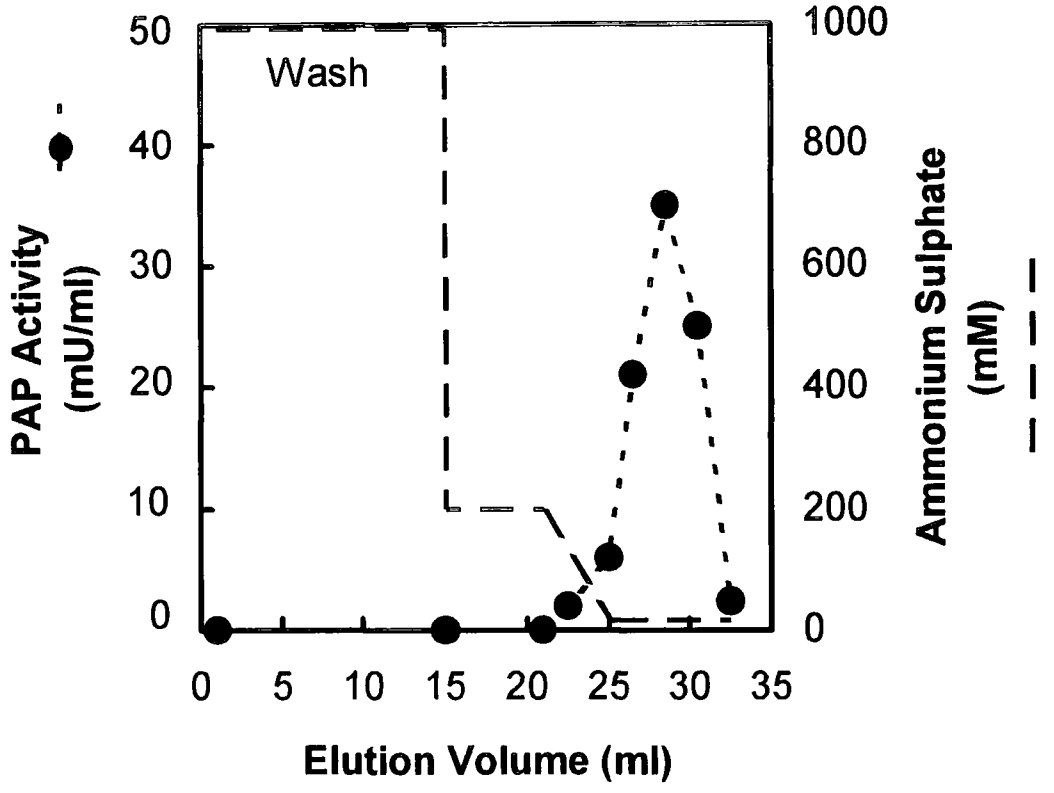

Figure 5.13: The Elution Profile of PAP from Phenyl-Superose. The 55-65% Ammonium Sulphate pellet was loaded onto an equilibrated 1ml Phenyl-Superose column at 1M $(NH_4)_2SO_4$. The column was washed with 15ml of Buffer containing 1M $(NH_4)_2SO_4$, and the unbound eluted fractions collected (1ml each, indicated as Wash). The bound protein was then eluted stepwise (— —) with 200mM $(NH_4)_2SO_4$ in buffer for 6ml, followed by a linear 4ml reversed gradient to 0mM $(NH_4)_2SO_4$. At 0mM $(NH_4)_2SO_4$, the column was washed for a further 8ml. The fractions were assayed for PAP activity (--●--). The measurement of total protein absorption at 280nm was erratic and indiscernible and was not shown.

Figure 5.14

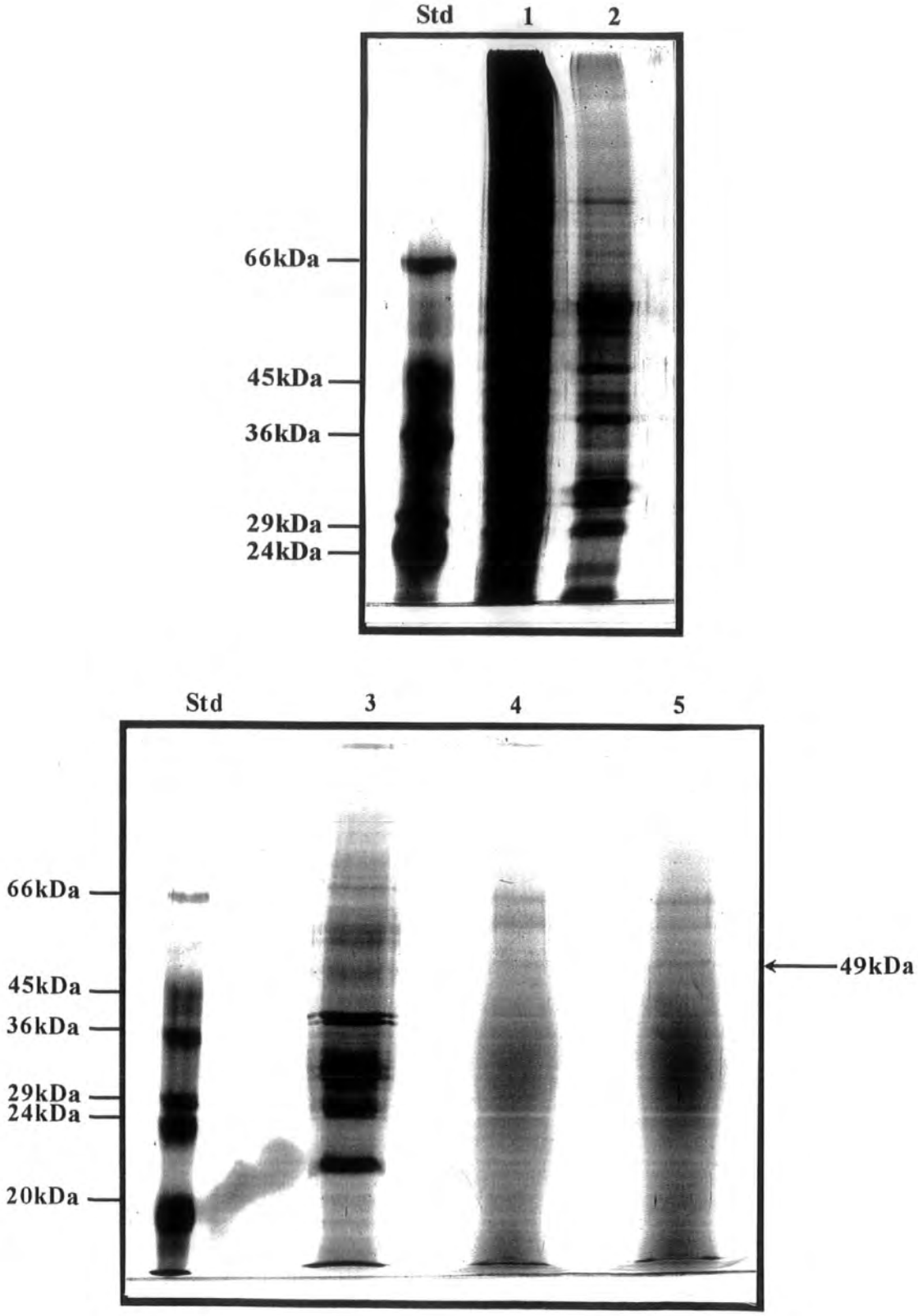
Std
1
2
66kDa
45kDa
36kDa
29kDa
24kDa
Std
3
4
5
66kDa
45kDa
36kDa
29kDa
24kDa
20kDa
49kDa

After each stage of the purification a marked reduction in the number of protein bands were observed, of which Phenyl-Superose was the most noticeable. The pooled fractions from the Phenyl-Superose chromatography had a PAP specific activity of 12.3units/mg protein, resulting from a 300-fold purification from the washed microsomal fraction as shown in the purification summary (Table 5.8)

The smallest of the three protein bands shown in Figure 5.14 was concluded to be that of PAP. As was shown before in the previous purification attempt, a final protein sample with seven protein bands was produced (Figure 5.11). With hindsight, one of these bands, having the same apparent molecular mass could now be identified as being PAP.

The apparent molecular mass of PAP was calculated by plotting the molecular masses of the protein standards (in Log_{10}) versus the Rf value for each protein (Figure 5.15). The Rf value of the PAP protein band (0.42) was interpolated onto the molecular mass standard curve, and the corresponding Log_{10}(molecular mass) determined. The apparent molecular mass of PAP was calculated as 49kDa. This, in conjunction with the data obtained with gel filtration and native PAGE, show the PAP protein to be monomeric.

Silver-staining is non-linear with respect to protein concentration making quantification of the relative concentration of each protein band difficult. The sample containing three protein bands had a specific activity of 12.3Units/mg. If all three bands in the sample were of equal protein concentration, the specific activity of PAP could be estimated as 37units/mg. This value was similar to that obtained from the previous purification (43units/mg protein). The sample consisted of approximately 3.25μg PAP protein, which according to the molecular mass of 49kDa, is 66pmoles.

Purification Step	Total Units (μmol/min)	Protein (mg)	Specific Activity (Units/mg)	Yield (%)		Fold Purification (-fold)	
1. Cell Extract	11.17	356.7	0.0313	100	—	1	—
2. Microsomes	1.63	39.3	0.0414	14.5	100	1.3	1
3. CHAPS extract	0.613	4.35	0.14	5.4	37.6	4.47	3.4
4. Affi-Gel Blue	0.38	0.752	0.505	3.4	23.3	16.13	12.2
5.55-65% $(NH_4)_2SO_4$	0.210	0.244	0.861	1.88	12.8	27.5	19.56
6. Phenyl-Superose	0.12	0.0098	12.3	1.1	7.4	392	297

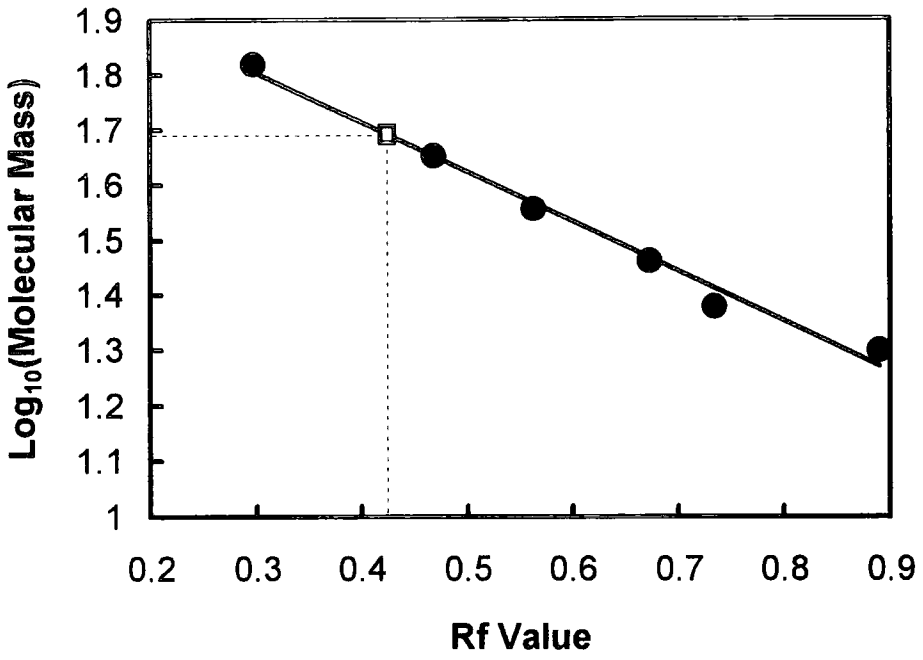

Figure 5.15: The determination of the apparent molecular mass of PAP from SDS-PAGE. Using the data from Figure 5.14, the Log_{10} of the molecular masses of the protein standards(kDa) was plotted *versus* the Rf values of each standard (●) with a line of best fit constructed. The Rf value of the identified PAP protein (0.42) was interpolated onto the molecular mass standard curve(□), and the corresponding Log10(Molecular Mass) noted (---). The apparent molecular mass of the PAP protein was calculated as 49kDa.

The Phenyl Superose purified sample had a volume of 5.5ml. It was decided to attempt N-Terminal sequencing of the 49kDa protein. The sample was within the lower concentration limits for sequencing, but it was hoped that there was sufficient protein to obtain N-terminal amino acid sequence. The sample required a concentration step and to achieve this, it was decided to freeze dry the sample. The sample was dialysed in 2 x 1 litre of 5mM Tris-maleate pH6.0, 1mM $MgCl_2$ and 0.01% CHAPS to remove the glycerol, excess detergent and buffering salts which would otherwise become very concentrated with the lyophilisation (Schägger, 1994). The total removel of buffer and detergent was avoided in order to reduce the risk of denaturation (and loss) of protein during the dialysis.

The dialysed sample was placed in a small round-bottomed flask and 'shell-frozen' by rotating the flask in a bath of liquid N_2. The neck of the flask was then covered with parafilm and small holes pierced to allow free movement of moisture during lyophilisation. The lyophilisation was kindly conducted by John Gilroy. The dried sample was resuspended into 100µl of SDS-PAGE sample buffer, which had been freshly made with ultrapure reagents. A 10% polyacrylamide mini-gel was prepared, and pre-run under normal SDS-PAGE conditions (using ultrapure reagents) in the presence of 200µM Thiodiglycolic acid at 100mV for 20 minutes prior to sample loading. The protein sample was loaded into 4 lanes of the gel, alongside protein standards and resolved through the gel. The protein was transferred to a PVDF membrane by 'wet blotting' using the BioRad Mini-Protean Blotting apparatus as described under *Materials and Methods*, Chapter 2.4.9. After blotting, The 10% gel was silver stained and no sample protein was detected. The blotted protein was stained with Sulphorhodamine B, and destained in 10% CH_3OH. No sample protein was detected on the membrane upon staining/destaining with Sulphorhodamine B. It was believed that the loss occurred during the resuspension of the lyophilised sample, where inadequate pipette access to the flask interior prevented efficient resuspension.

5.5 The purification to homogeneity of avocado microsomal PAP.

With the first positive identification of microsomal PAP from any plant source, the purification could be scaled up for the bulk preparation of PAP protein, enabling N-terminal amino acid sequencing and/or the generation of antibodies, and the detailed enzymological characterisation. Whereas the previous protein fractionations used 1-2 avocados as the starting material, it was decided to repeat the second purification strategy with 18 avocados, and assuming a similar yield was obtained, a recovery of 30μg PAP protein (600pmol) was expected.

Due to the increase in mesocarp tissue at the start of the purification, it was decided to incorporate Fast Flow Q Sepharose chromatography at the start of the purification strategy. As determined by the batch binding analysis of CHAPS extract with Fast Flow Q Sepharose, PAP activity did not associate to the gel at pH8.0. Many proteins with isoelectric points below this pH will associate to the exchanger groups, thus removing a substantial amount of protein in the sample. This would make the scaling up process easier and more reliable, as the sizes of the subsequent columns could be reduced, allowing a better resolution. The step was also added to the strategy in the hope that the two co-purifying proteins in the previous purification would be fractionated away from PAP. Ammonium sulphate precipitation of protein is affected by the protein composition of the sample. With the scaling-up of the preparation and the addition of an extra column to the purification strategy, the protein composition of the sample would be different from the previous purification. There was a danger that some proteins would not be fractionated away during the $(NH_4)_2SO_4$ precipitation step, that would later co-purify with PAP during Phenyl Superose chromatography. The Phenyl Superose step was very effective in the purification of PAP. As was shown in Chapter 5.4.5, Phenyl Superose chromatography of the ammonium sulphate precipitate of a crude CHAPS extract resulted in near homogenous PAP protein, without the use of other chromatography matrices.

Therefore the danger of contaminatory protein bands co-purifying with PAP was eliminated by the extremely efficient fractionation of Phenyl Superose, in conjunction with Q-Sepharose, $(NH_4)_2SO_4$ precipitation and Affi-Gel Blue chromatography.

The mesocarp from 18 small-medium ripened avocados (1460g) was homogenised and the cell extract (1150ml, 42units, 4087mg protein) and washed microsomal fraction (130ml, 3.9units, 585mg protein) prepared by centrifugation at 4°C, as before. The washed microsomes were resuspended in 130ml (4.5mg/ml) Tris-maleate pH6.0, 10mM $MgCl_2$, 20% glycerol and 0.5% (w/v)CHAPS, and gently shaken at 4°C for 1hour. The mixture was centrifuged at 105 000*g* for 90 minutes and the resulting CHAPS extract (125ml, 3.2units, 66mg protein), was dialysed (3 x 2litres, 5 hours total) in 50mM Tris-maleate pH8.0, 10mM $MgCl_2$, 20% glycerol and 0.1% (w/v)CHAPS at 4°C. The CHAPS solubilised 82% of the microsomal PAP.

Fast Flow Q Sepharose Chromatography: Using a Pharmacia Hi-Load system, a 70ml bed volume Fast Flow Q Sepharose column (2 x 16cm) was equilibrated in the dialysis buffer from above (Buffer A), and the dialysed CHAPS extract was applied to the column at 1ml/min at 4°C, with the unbound protein collected from the column. The column was washed with 1 column volume of buffer A, and the wash pooled with the other unbound protein. The bound protein was eluted from the column with a linear 250ml 0-2M NaCl gradient (in buffer A) at 2ml/min. The protein elution was monitored at A_{280}nm and the fractions (4ml each) assayed for PAP activity in groups of 10. PAP activity (2.88units, 24.3mg total protein) was exclusively found in the unbound fraction (Figure 5.16), and resulted in a recovery of PAP of 90%.

Affi-Gel-Blue Chromatography: The post Fast Flow Q Sepharose sample (unbound) was dialysed (2 x 2litres, 10 hours total) into Buffer A consisting of 50mM Tris-maleate pH5.5, 10mM $MgCl_2$, 20% glycerol and 0.1% (w/v)CHAPS at 4°C. A 30ml bed volume Affi-Gel Blue column (1.5 x 20cm), attached to a Pharmacia

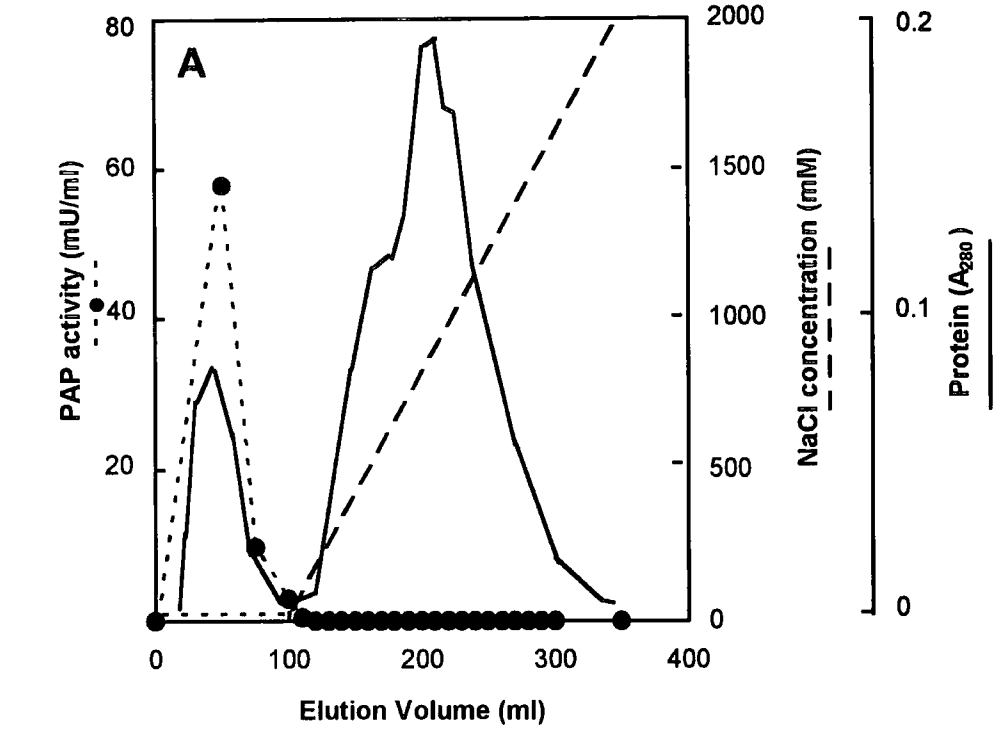
A
80
60
40
20
PAP activity (mU/ml)
2000
1500
1000
500
0
NaCl concentration (mM)
0.2
0.1
0
Protein (A_{280})
0
100
200
300
400
Elution Volume (ml)

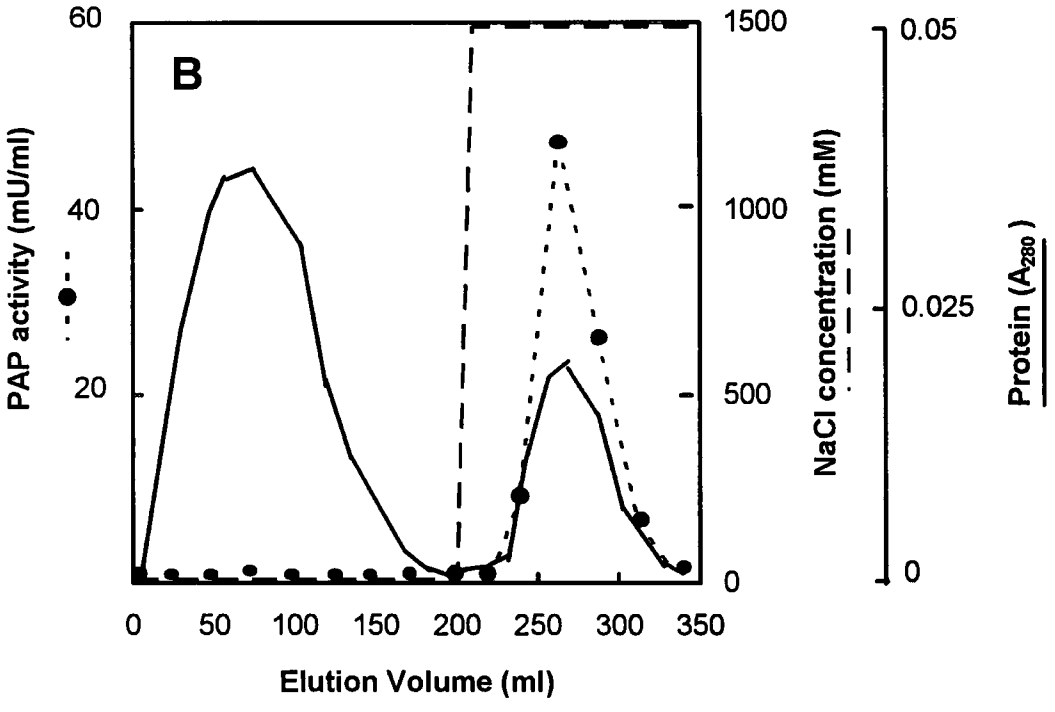
B
60
40
20
PAP activity (mU/ml)
1500
1000
500
0
NaCl concentration (mM)
0.05
0.025
0
Protein (A_{280})
0
50
100
150
200
250
300
350
Elution Volume (ml)

Hi-Load system, was equilibrated in Buffer A and the dialysed sample loaded at 1ml/min. The total protein was measured by the absorbance at 280nm. The protein was eluted stepwise from the column with four column volumes of 1.5M NaCl. The eluted sample was assayed for total protein and PAP activity, and found to contain 2.57units in 5.29mg protein, with a step recovery of PAP of 89% (Figure 5.16).

Ammonium Sulphate precipitation: The sample from the Affi-Gel Blue purification step was dialysed (2 x 2 litres, 4 hours total) in 50mM Tris-maleate pH6.0, 10mM $MgCl_2$, 20% glycerol and 0.1% (w/v)CHAPS at 4°C. The ammonium sulphate precipitation was conducted as in the previous purification attempt, at 45% saturation and 65% saturation. The 45% and 45-65% $(NH_4)_2SO_4$ pellets were assayed for PAP activity and contained 0.72 and 1.47units, respectively. As the 45% $(NH_4)_2SO_4$ pellet contained a large proportion of PAP activity, it was pooled with the 65% pellet. The resulting 0-65% $(NH_4)_2SO_4$ pellet (2.2units of PAP, 3.8mg total protein, 25ml) was used for the next stage of the purification.

Phenyl Superose Chromatography: The nature of the gradient was slightly altered to resolve the eluted protein more effectively in an attempt to purify PAP to homogeneity. The 65% $(NH_4)_2SO_4$ pellet, was dialysed (2 x 2 litres, 4 hours total) into buffer A, consisting of 50mM Tris-maleate pH6.5, 10mM $MgCl_2$, 10% glycerol, 0.1% (w/v)CHAPS and 1M $(NH_4)_2SO_4$, at 4°C. On a Pharmacia FPLC system, a 1ml Phenyl-Superose HR 5/5 column was cleaned, following the manufacturers guidelines (Pharmacia LKB biotechnology, Uppsala, Sweden), with 5ml 1% Trifluoroacetic acid in 100% acetonitrile followed by 20ml MQ water. The regenerated column was equilibrated in buffer A and the 25ml sample was loaded in 5ml sample aliquots (with a 5ml sample loop) onto the column at a flow rate of 0.5ml/min. The column was washed with 5ml buffer A, to remove unbound protein. A step gradient of 1.0-0M $(NH_4)_2SO_4$ was applied to the column using buffer B (buffer A without $(NH_4)_2SO_4$) as shown in Figure 5.17. This was as follows: A linear 5ml reversed gradient 1.M-0.3M

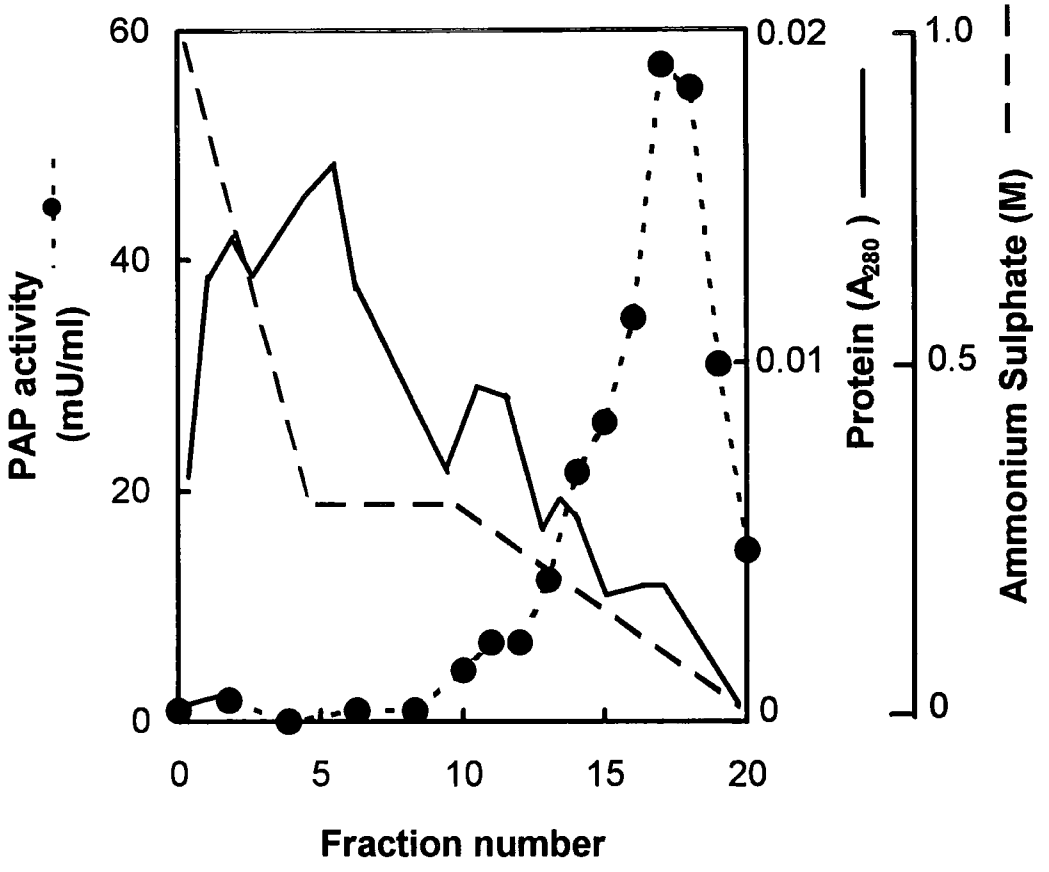

Figure 5.17: The elution of microsomal PAP from Phenyl-Superose. The 45-65% Ammonium Sulphate pellet was loaded onto an equilibrated 1ml Phenyl-Superose column in 1M $(NH_4)_2SO_4$. The column was washed with 5ml equilibration buffer. A linear 5ml reversed gradient of 1.0M-0.3M $(NH_4)_2SO_4$ was applied to the column at 0.5ml/min (— —). The concentration was held at 0.3M $(NH_4)_2SO_4$ for 5ml, prior to the application of a 10 ml linear gradient of 0.3M-0M $(NH_4)_2SO_4$ to the column. The fractions(1ml) were assayed for PAP activity (--●--). Total protein was measured by absorption at 280nm (—).

$(NH_4)_2SO_4$ was applied to the column at 0.5ml/min at room temperature. The concentration was held at 0.3M $(NH_4)_2SO_4$ for 5ml. A second 10ml linear gradient of 0.3M-0M $(NH_4)_2SO_4$ was then applied to the column (Figure 5.17). The unbound protein and the eluted fractions (1ml) were assayed for PAP activity. PAP eluted (0.118units total) from the column at 100mM $(NH_4)_2SO_4$. The decrease in $(NH_4)_2SO_4$ caused a decrease in the absorption irrespective of protein concentration. The measurement of protein at 280nm was achieved by setting the chart recorder to 50% of the full scale deflection as the zero value of absorption. Serendipity was a major factor in the ability to produce a discernible A_{280} trace, as the combination of CHAPS and $(NH_4)_2SO_4$ affected the absorption.

The majority of PAP (1.57 units) did not bind to the column, and was recovered in the unbound fraction. This was due to the low binding capacity of the matrix under these conditions (most likely as a result of CHAPS and glycerol interaction with the phenyl groups). The unbound sample was therefore split into less than 1mg aliquots and each aliquot individually fractionated under the identical conditions as above. In this way all PAP activity was eventually purified by phenyl superose. Prior to every run, the column was regenerated, as before. For each sample, the PAP elution profile was identical to Figure 5.17. Under these loading conditions, the peak of PAP activity eluted in 100mM $(NH_4)_2SO_4$ (typically fractions 15-20). Fractions 15-20 from the 5 Phenyl Superose runs were pooled and contained a combined PA activity of 1.12 units. This was dialysed (30ml into 2 x 2 litres, 4 hours total) 50mM Tris-maleate pH6.0, 10mM $MgCl_2$, 20% glycerol and 0.1% CHAPS. After dialysis, the sample had increased in volume to 37ml and was frozen in aliquots at -80°C. SDS-PAGE analysis was conducted on the consecutive fractions that eluted from one of the Phenyl Superose steps. The fractions that contained the majority of PAP activity (fractions 15-20) were pooled. The fractions preceding and after the peak of PAP elution were pooled in consecutive groups of two fractions. After chloroform/methanol precipitation of 1.5ml of PAP sample(0.03units) and 2ml of each set of two fractions, the protein was analysed by SDS-PAGE (Figure 5.18).

Figure 5.18

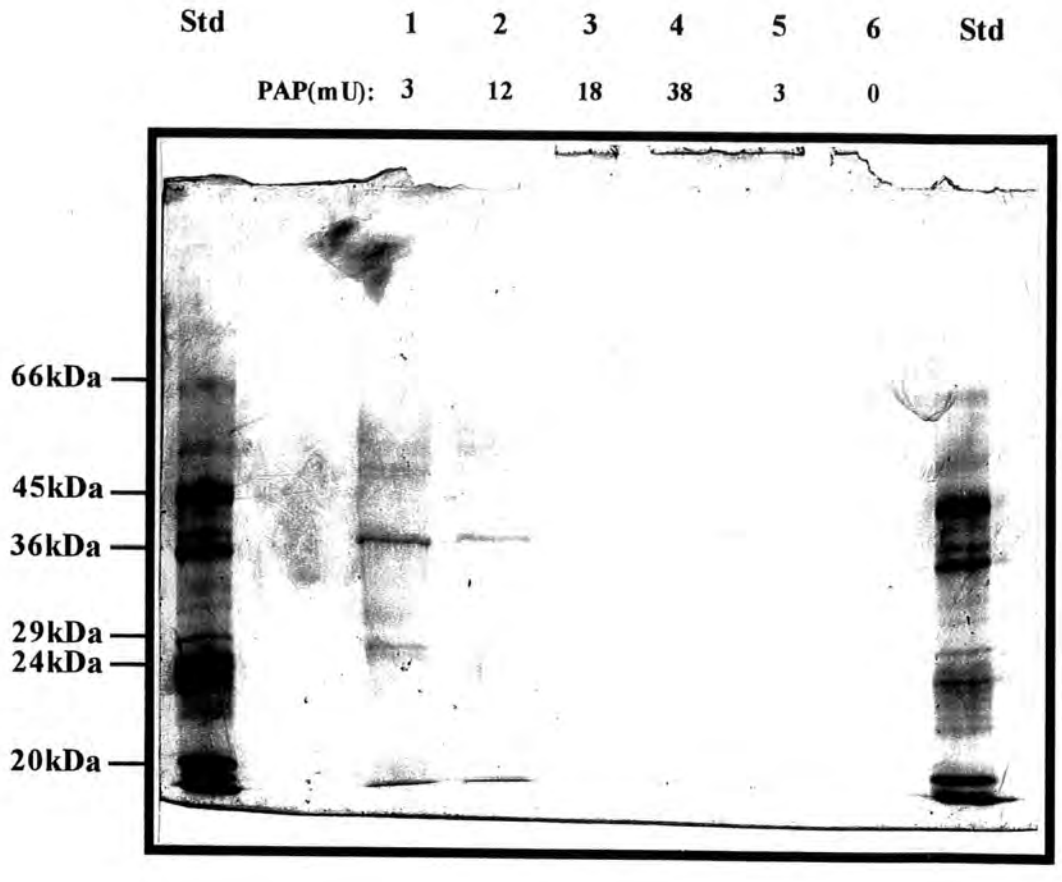
Std
1
2
3
4
5
6
Std
PAP(mU):
3
12
18
38
3
0
66kDa
45kDa
36kDa
29kDa
24kDa
20kDa

SDS-PAGE analysis of the pooled active fractions revealed that the Phenyl Superose chromatography resulted in homogenous PAP protein with a molecular mass of 49kDa. In the preceding fractions which contained slight PAP activity, the emergence of the PAP protein during elution was observed. This allowed the association between PAP activity and the 49kDa protein band to be made. The molecular mass of the protein was calculated as in the previous purification attempt, with identical results.

The total protein of the sample was measured (in duplicate) and the specific activity calculated for homogenous PAP as 48.7 units/mg protein (Table 5.9). The purification resulted in homogenous PAP with a molecular mass of 49kDa, which had been purified 7380-fold from washed microsomes, with a final yield of nearly 29%.

The degree of total protein enrichment after each stage of the purification was examined by coomassie stained SDS-PAGE (Figure 5.19). The PAP protein can be seen in the samples purified by Affi-Gel Blue and $(NH_4)_2SO_4$ precipitation. The Phenyl Superose step was the most effective purification step in the fractionation of PAP. The low protein binding capacity of Phenyl Superose meant that the Q-Sepharose and Affi-Gel Blue steps were important in reducing the overall protein content of the sample, and were essential for the final purity of the sample. Two additional feint bands of contaminatory protein (M_r of 57kDa and 66kDa) were observed in the Phenyl Superose purified sample (Figure 5.19). This was unique to this gel, and was believed to be keratin (Ochs, 1983) or similar contamination during the preparation of the sample for electrophoresis.

The dialysed pooled fractions, contained 23μg of PAP protein in 37ml of buffer. This was equivalent to 460pmoles of PAP protein. It was decided to attempt N-terminal sequencing of the enzyme. The protein concentration was too low to allow this directly, so a Affi-Gel blue concentration step was conducted.

Purification Step	Total units (μmol/min)	Protein (mg)	Specific activity (Units/mg)	Yield (%)		Purification (fold)	
1. Cell Extract	42	4087	0.0102	100	—	1	—
2. Microsomes	3.9	585	0.0066	9.3	100	0.647	1
3. CHAPS extract	3.2	65.8	0.049	7.6	82.1	4.8	7.4
4. Q-Sepharose	2.88	24	0.119	6.8	73.8	11.7	18.0
5. Affi-Gel Blue	2.56	5.29	0.484	6.1	65.6	47.5	73.3
6. $(NH_4)_2SO_4$ (65%)	2.2	3.8	0.578	5.2	56.4	56.6	87.6
7. Phenyl Superose	1.12	0.023	48.7	2.7	28.7	4775	7379

Table 5.9

Figure 5.19

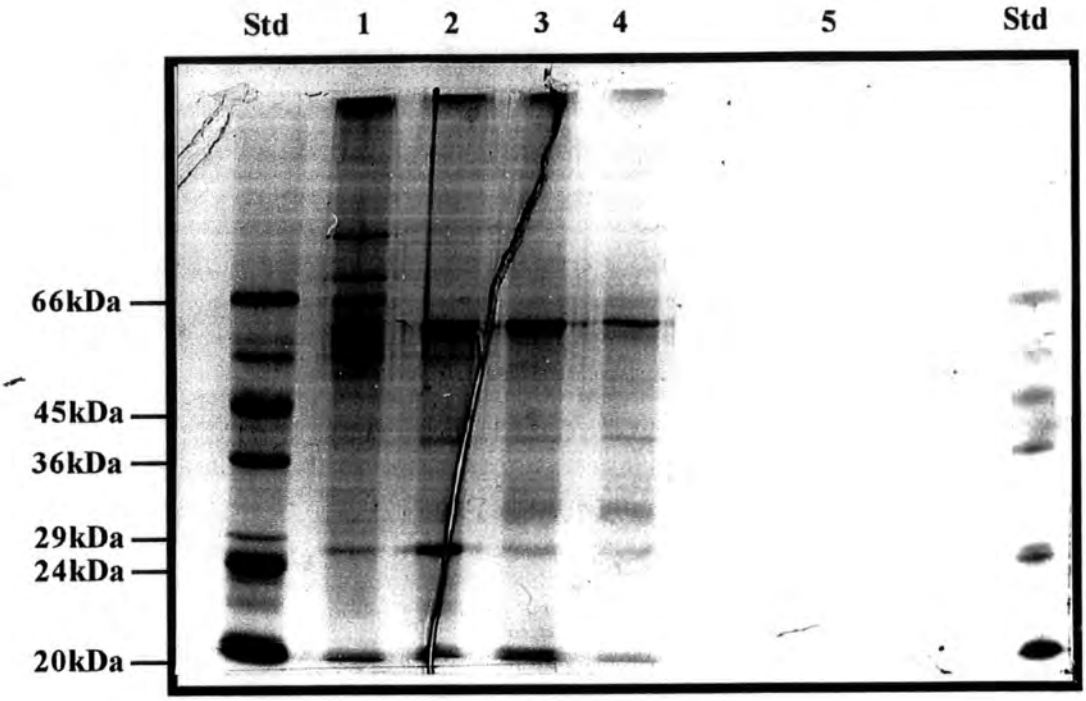

Affi-Gel Blue concentration step: A 1ml Affi-Gel Blue column was prepared using unused resin. The column was equilibrated in 50mM Tris-maleate pH 5.5, 10mM $MgCl_2$, 0.1% CHAPS, and 20% glycerol at 4°C. The dilute homogenous PAP sample (37ml) was loaded onto the column and step-eluted at 1ml/min with 2M NaCl in the above buffer. The eluted protein was manually collected in 1ml fractions. The loaded sample, the unbound protein and the eluted fractions were assayed for PAP activity. 1.10units of PAP activity was loaded onto the column and 0.130 units did not bind to the column. Fraction 3 contained the peak of bound PAP activity, with pooled fractions 3-6 containing a total of 0.276units PAP activity. The column was washed with buffer containing 4M NaCl, and 1M guanidium-HCl, with no release of PAP protein detected by SDS-PAGE and enzymatic assays. Passive sites on the column back-bone were blamed for this loss of protein, even though the manufacturers product information had described Affi-Gel Blue as a pre-blocked matrix. A dry-run with crude enzyme sample would have eliminated passive protein binding sites. It was decided to use the PAP sample for characterisation studies as there was insufficient protein to allow N-terminal amino acid sequencing. Fractions 3-6 were pooled and dialysed into 1x 1litre of in 50mM Tris-maleate pH 5.5, 10mM $MgCl_2$, 0.1% CHAPS, and 20% glycerol at 4°C, to remove the NaCl. The dialysed sample was stored at -80°C in 100µl aliquots, and used in the characterisation studies described later.

5.5.1 The repeated purification of microsomal PAP to homogeneity.

The concentration of the Phenyl-Superose purified PAP sample using Affi-Gel Blue, resulted in the loss of sufficient protein for N-terminal amino acid sequencing. It was decided to repeat the purification under identical conditions, with the inevitable concentration step being conducted using Phenyl-Superose chromatography. In this way, the eluted and very dilute PAP from the several Phenyl-Superose purification steps, would be pooled and re-applied to the column, and eluted as one step. Using this technique, the eluted protein from several Phenyl-Superose runs could be concentrated as one elution which was equivalent to 5ml.

Eighteen medium-small avocados (type Haas, 1620g mesocarp tissue) were purchased locally, and the purification was repeated. The purification procedure was conducted under identical conditions as before, as seen in the purification summary (Table 5.10), and the SDS-PAGE analysis of the homogenous protein (Figure 5.20). A Pharmacia 7.5% PhastGel was used for the SDS-PAGE analysis with the PhastSystem™. This allowed the visualisation of the protein with 200µl of PAP sample (Figure 5.20), and reduced PAP wastage.

A large loss in PAP activity was observed after 65% $(NH_4)_2SO_4$ precipitation. In the previous purification, the 45% and 65% $(NH_4)_2SO_4$ precipitates had been pooled, so that the combined sample was a 0-65% $(NH_4)_2SO_4$ precipitate. In this purification, the $(NH_4)_2SO_4$ fractionation was performed as one step with 65% $(NH_4)_2SO_4$. Under these conditions, a large floating detergent pellet was observed after centrifugation, which CHAPS adhered to the side of the glass sample flask, and was inadvertently discarded. A loss in PAP activity resulted, probably due to enzyme inactivation during the formation of the CHAPS floating pellet. It was therefore important to perform the 65% $(NH_4)_2SO_4$ fractionation in two stages, at 45% and 65% saturation. Using the two stage precipitation method, CHAPS precipitated at 45% saturation, and all detergent was thus removed from the sample, preventing the

formation of a floating pellet and the large loss of PAP activity/protein at 65% saturation.

The homogenous protein (14μg, 0.29μg/ml) from the combined Phenyl Superose chromatography purification steps was in a final volume of 47ml, and required concentration. A stock solution of 4M $(NH_4)_2SO_4$ in 50mM Tris-maleate pH6.5, 10mM $MgCl_2$, 10% glycerol and 0.1% CHAPS was prepared and 6.7ml added to the sample to make a final concentration of 500mM $(NH_4)_2SO_4$ in the same buffer. The 1ml Phenyl Superose HR5/5 column was equilibrated in the above buffer containing 500mM $(NH_4)_2SO_4$. The sample was applied to the column at a flow rate of 0.3ml/min using a 50ml sample loop. The sample was eluted from the column with a linear 10ml reversed gradient of 500-0mM $(NH_4)_2SO_4$ with the above buffer containing no $(NH_4)_2SO_4$, followed by an additional 5ml wash at 0mM $(NH_4)_2SO_4$. The eluted protein was collected in 1ml fractions, and assayed for PAP activity. The peak of PAP activity eluted at 100mM $(NH_4)_2SO_4$. The fractions containing the majority of PAP activity were pooled and contained 0.46units of PAP activity in a total volume of 6ml. This was equivalent to a PAP protein concentration of 1.6μg/ml, and required further concentration.

The sample was again concentrated with Phenyl Superose chromatography, but with a smaller column on a Pharmacia SMART system. The stock solution containing 4M $(NH_4)_2SO_4$ was added to the PAP sample to a final concentration of 1M $(NH_4)_2SO_4$ in 50mM Tris-maleate pH6.5, 10mM $MgCl_2$, 10% Glycerol and 0.1% CHAPS. A Phenyl Superose PC 1.6/5 column with a bed volume of 0.1ml, was equilibrated at 50μl/min in the above buffer containing 1M $(NH_4)_2SO_4$, using a Pharmacia SMART System. The sample (0.46units) was loaded onto the column at 50μl/min and eluted in a 1.5ml gradient of 1.0-0M $(NH_4)_2SO_4$ in 50mM Tris-maleate pH6.5, 10mM $MgCl_2$, and 0.1% CHAPS. Glycerol was excluded from the elution buffers in order to reduce the back pressure of column.

Purification Step	Total units (μmol/min)	Protein (mg)	Specific activity (Units/mg)	Yield (%)		Purification (fold)	
1. Cell Extract	45.1	4763	0.0095	100	—	1	—
2. Microsomes	3.68	632	0.0058	8.2	100	0.61	1
3. CHAPS extract	3.82	54.2	0.070	8.5	104	7.4	12.1
4. Q-Sepharose	2.58	18.3	0.14	5.7	70.1	14.7	24.1
5. Affi-Gel Blue	2.27	5.8	0.39	5.0	61.7	41.1	67.2
6. $(NH_4)_2SO_4$ (65%)	1.06	2.9	0.37	2.3	28.8	38.9	63.8
7. Phenyl Superose	0.71	0.014	50.7	1.5	19.3	5337	8741

Figure 5.20

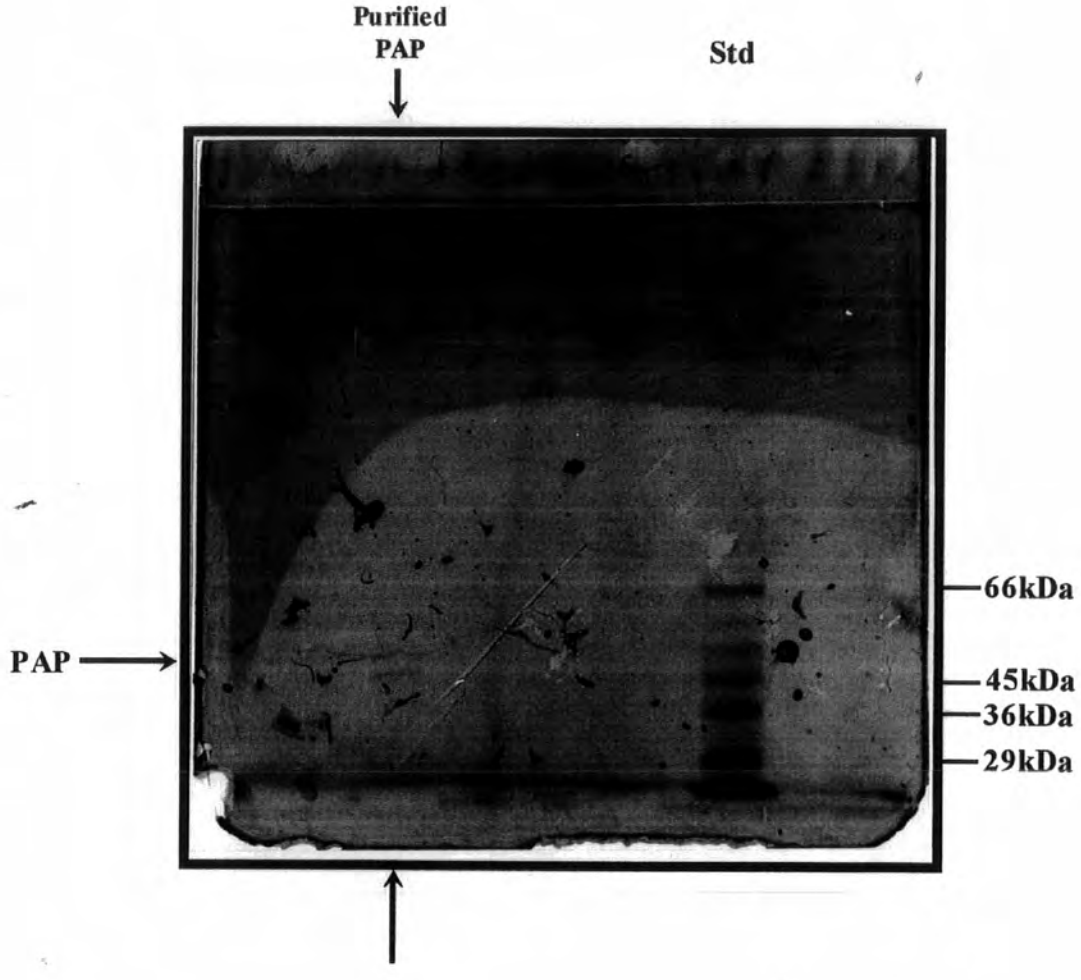

The eluted protein was collected in 100µl fractions and assayed for PAP activity. The peak of PAP activity eluted at 100mM $(NH_4)_2SO_4$ and the pooled fractions contained 0.13units (2.6µg) in 300µl.

A large loss of PAP activity was observed from both Phenyl Superose concentration steps. The resulting 2.6µg of PAP protein was deemed insufficient for N-terminal amino acid sequencing, and was considered to be more useful for the characterisation studies of the homogenous enzyme. The nature of the purification strategy meant that the homogenous enzyme was recovered as an extremely dilute solution. The Phenyl Superose chromatography caused a significant enrichment and purification of the enzyme, at the price of a diluted sample. Concentrating the protein using Phenyl Superose enabled the recovery of PAP protein but at the expense of large losses.

It has already been discussed that PAP is a ubiquitous enzyme. In avocado, approximately 10% of phosphatase activity (with PA as substrate) was located in the washed microsomes. This is similar to *B.napus* (Kocsis *et al.*, 1996) and safflower (Ichihara *et al.*, 1990). Ichihara *et al.* (1990) reported the translocation of PAP from the cytoplasmic pool to the microsomes with the addition of free fatty acids. The cytoplasm formed a physiologically inactive reservoir for PAP protein. Considering that the avocado 105 000*g* supernatant (soluble fraction) forms the major source of PA-phosphatase activity, it was decided to apply the purification strategy to this fraction, under identical conditions as used for the microsomal enzyme fractionation.

The soluble isoform of PAP has not been isolated from any tissue. This is partly due to the inability to attribute the phosphatase activity directly to PAP. With detailed information regarding the microsomal enzyme, the identical purification strategy could be used to identify the soluble enzyme, if in fact they are the same enzyme. It was not expected that the strategy, designed for the elimination of microsomal protein, would result in homogenous cytosolic PAP, although it was

hoped that the enzyme could be identified during the purification. It is unknown how translocation of PAP is controlled in plants. Purification of the cytosolic enzyme would allow further studies to be conducted in order to gain an insight into the control of translocation.

5.6 The partial purification of cytosplasmic PAP.

The 105 000*g* supernatant from the mesocarp of 2 avocados was used for the purification of cytoplasmic PAP which was conducted under identical conditions as the microsomal enzyme, described in Chapter 5.5.1. The summary of the purification is shown in Table 5.12, with the SDS-PAGE analysis of the protein purity after each chromatographic step shown in Figure 5.21.

The purification was briefly as follows; the soluble fraction (25.6 units), prepared as before, was filtered to remove all traces of fat layer, and dialysed into 50mM Tris-maleate pH 8.0, 10mM $MgCl_2$, 20% glycerol and 0.1% CHAPS and applied to a 50ml Fast Flow Q Sepharose column. The unbound fraction (16.9units) was adjusted to pH 5.5 and loaded onto an equilibrated 50ml Affi Gel Blue column at pH 5.5, and step eluted with 2M NaCl. The eluted protein (16.0units) was dialysed (to remove NaCl) prior to ammonium sulphate fractionation, at 45% and 65% saturation. The combined 45 and 65% precipitates (5.3units) contained 32.2mg protein. The binding capacity of Phenyl Superose was low under these conditions a maximum of 2mg of sample was used for each separation. A Phenyl Sepharose step was incorporated into the purification strategy to reduce the total protein and allow the subsequent Phenyl Superose chromatography to be conducted in fewer separations. The combined ammonium sulphate precipitates were dialysed into a buffer containing 1.0M $(NH_4)_2SO_4$ and loaded onto a 50ml equilibrated Phenyl Sepharose column and eluted with a 1.0-0M $(NH_4)_2SO_4$ gradient. Cytosolic PAP eluted at 500mM $(NH_4)_2SO_4$, and the fractions containing the peak of PAP activity

(3.6units, 7.7mg protein) were pooled and used for the Phenyl Superose chromatography. The sample was made up to 1M $(NH_4)_2SO_4$ (with the slow addition of solid $(NH_4)_2SO_4$) and loaded in 2mg aliquots directly onto a 1ml Phenyl Superose column using an FPLC system, which had been equilibrated in buffer containing 1M $(NH_4)_2SO_4$. The protein was eluted from the column, using a stepwise gradient of 1.0-0M $(NH_4)_2SO_4$, as before. PAP activity eluted from the column in 100mM $(NH_4)_2SO_4$.

The SDS-PAGE analysis of the purified soluble protein showed that there were many protein bands within the sample after Phenyl Superose chromatography (Figure 5.21). The purification strategy was designed to purify PAP from the microsomal fraction, and as such, it would not be expected for cytosolic PAP to fractionate to homogeneity using the same strategy. However, PAP activity was observed in the final sample, and had column binding and elution characteristics, identical to that of the microsomal enzyme. This shows that a proportion of the activity observed in the soluble fraction can be attributed to PAP. It was unlikely that such high levels of activity found in the soluble fraction were entirely due to PAP-dissociation from the microsomes upon centrifugation of the cell extract at 105 000*g*. Previously, the association of the cytosolic and microsomal enzymes was made purely on both fractions' ability to hydrolyse PA and the observed translocation of PAP activity between the two sub-cellular fractions (Brindley, 1984; Ichihara *et al.*, 1990).

After each step of the purification, an enrichment of certain proteins was seen. This was most noticeable with a protein at 33kDa (Figure 5.21). After Phenyl Sepharose, two protein bands were enriched, at approximately 50kDa (Figure 5.21, *Lane 4*). Using the calculated Rf values and the molecular masses of the protein standards, the upper of these protein bands was calculated as 49kDa. The intensity of the 49kDa band (after Phenyl Superose chromatography, Figure 5.21 *Lane 4*) was comparable to the protein standards alongside (0.1μg/band), and the total amount of that protein in the sample was calculated as approximately 100μg. The sample

contained 3.6Units of PAP activity. With the assumption that the 49kDa protein was PAP, the specific activity was calculated as approximately 36 Units/mg.

The 49kDa protein was seen after the final stage of purification, and formed a negative image after silver staining, making the estimation of the relative abundance difficult. This protein therefore had the same molecular mass, co-purified with microsomal PAP, and had a similar estimated specific activity to homogenous microsomal enzyme. This indicated that the 49kDa cytosolic protein was PAP. However, as the protein sample was not homogenous, this 49kDa protein could not be absolutely identified as being PAP.

As with the purification of the microsomal enzyme, losses in enzyme activity were seen at every stage of the purification (Table 5.12). The major losses in PAP activity were seen after the ammonium sulphate precipitation and Phenyl Superose steps. Only one peak of PA-phosphatase activity was seen at each step. This suggests that the loss in activity was due to inactivation and not fractionation/removal of different PA-phosphatase activities.

Purification Step	Total units (μmol/min)	Protein (mg)	Specific activity (Units/mg)	Yield (%)	Purification (fold)
1. Cell Extract	29.4	302	0.097	100	1
2. 105 000*g* Sup.	25.6	285	0.090	87	—
3. Q-Sepharose	16.9	147.2	0.115	57.5	1.2
4. Affi-Gel Blue	16.0	90.8	0.176	54.4	1.8
5. $(NH_4)_2SO_4$ (65%)	5.3	32.2	0.165	18.0	1.7
6. Phenyl Sepharose	3.6	7.73	0.47	12.2	4.8
7. Phenyl Superose	0.8	0.027	29.63	2.7	305

Table 5.11

Figure 5.21

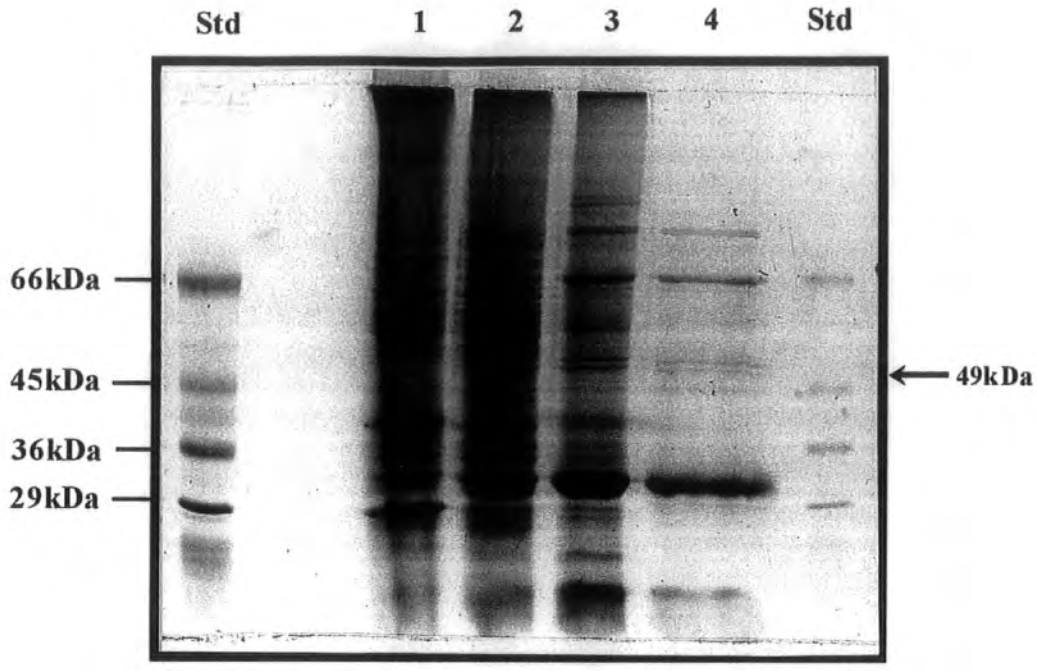
Std
1
2
3
4
Std
66kDa
45kDa
36kDa
29kDa
49kDa

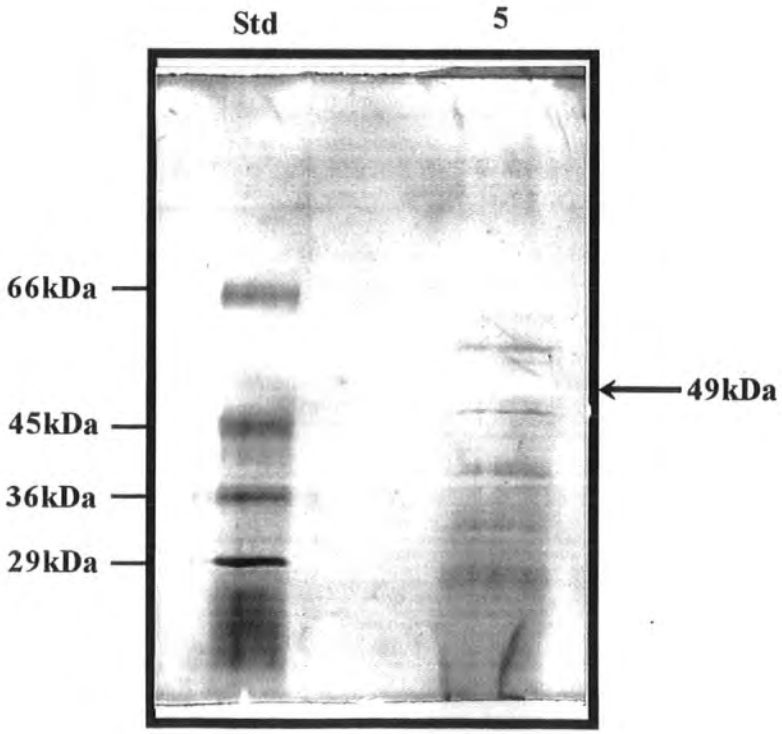
Std
5
66kDa
45kDa
36kDa
29kDa
49kDa

5.7 Discussion

In this chapter, the first positive identification of plant PAP protein was obtained, and it's subsequent purification to homogeneity shown. PAP was shown to be microsomally-associated, and required detergent or salt for solubilisation. CHAPS was chosen for use as a surfactant in the solubilisation of microsomal PAP, primarily because it resulted in stable solubilised PAP, but also because it fitted the theoretical criteria required for subsequent manipulations. The solubilised protein was found to be stabilised in the presence of CHAPS. Disassociation of PAP protein from the microsomes in NaCl, resulted in unstable enzyme activity. This clearly shows that the enzyme was the microsomal isoform and not a soluble activity trapped within the membrane leaflets.

To facilitate the purification, the native molecular mass of the solubilised enzyme, was determined by: (i)size-exclusion chromatography, and (ii) native-PAGE followed by SDS-PAGE of the region of the native gel containing PAP activity. The data from both analyses indicated that avocado microsomal PAP has a native molecular mass of approximately 50kDa. This corroborates the data from several of the isoforms reported in different species. The gel-filtration analysis of *B. napus* solubilised microsomal PAP revealed that the enzyme had a minimum native molecular mass of 40kDa (Kocsis *et al.*, 1995). Similarly, purified isoforms of PAP from yeast mitochondria (Morlock *et al.*, 1991) and rat liver plasma membranes (Waggoner *et al.*, 1995) were reported to have a molecular mass of 45kDa and 51kDa, respectively.

Phenyl Superose, in conjunction with $(NH_4)_2SO_4$ precipitation was found to be highly efficient in the purification of PAP. The extent to which PAP bound to Phenyl Superose was indicative of strong hydrophobicity. The interaction of many detergents within detergent-protein micelles, with Phenyl-Sepharose was reported by Robinson *et*

al. (1984). For this reason the involvement of CHAPS in the enzyme binding to Phenyl-Superose can not be ruled out.

A purification of microsomal PAP from two avocados was conducted, and incorporated CHAPS solubilisation, Affi-Gel Blue chromatography, $(NH_4)_2SO_4$ precipitation and phenyl Superose chromatography. The purification resulted in the emergence of three proteins after Phenyl Superose. In the immediately preceding fractions (that contained no PAP activity), two of the protein bands were present. This lead to the first positive identification of the PAP protein from any plant tissue. The molecular mass of PAP was calculated as 49kDa, using a standard curve of the Rf values of the molecular mass standards. There was insufficient protein in the sample to attempt N-terminal amino acid sequencing.

The binding capacity of a 1ml Phenyl Superose HR5/5 column was $\leq$10mg protein (Pharmacia LKB Biotechnology technical bulletin, 1993). The binding capacity of the column was found to be lower under these conditions, most likely due to detergent binding to the hydrophobic ligands (Schägger, 1994). To prevent column saturation, the sample was loaded and eluted in $\leq$1mg aliquots onto the column. The reduction in the protein binding was believed to be due to CHAPS saturation of the phenyl-ligands.

The purification (with an added Q-Sepharose step) was repeated under the same conditions, with 18 avocados as the starting material. The purification resulted in homogenous PAP protein with a calculated molecular mass of 49kDa and was found to be highly reproducible.

During the purification of this enzyme, only one peak of PAP activity was seen at each step. Only one microsomal PAP activity was identified, leading to the conclusion that it is most probably involved in glycerolipid biosynthesis as avocado

mesocarp is a major site of glycerolipid biosynthesis and forms a huge reservoir for triacylglycerol.

The purification strategy was then directed towards the potential fractionation of the cytoplasmic enzyme (100 000*g* supernatant). There has been no reported attempts to isolate or identify the soluble enzyme. The purification did not yield homogenous enzyme. The elution profiles of the soluble PAP was identical to the microsomal enzyme, throughout the purification. A 49kDa protein was identified during the purification. It has already been shown that the microsomal enzyme activity was not attributable to microsomally-trapped soluble enzyme. The emergence of a protein band at 49kDa, in a purification where soluble PAP activity showed the exact purification characteristics of the microsomal isoform, lead to the conclusion that this 49kDa protein could be PAP. A further enrichment or the use of anti-microsomal PAP antibodies may allow the precise identification of cytosolic PAP.

The research in this chapter demonstrated the first purification to homogeneity of PAP from any plant source. It became apparent that the purification strategy would require adjustment if amino acid analysis was to be conducted on the purified protein. Given the limited time of study, it was decided to conduct a detailed enzymological study on the partially purified and homogenous microsomal protein, rather than address the problems of PAP stability during the purification. As already discussed, this enzyme has been largely ignored within lipid research. There is little enzymological information regarding the kinetics, regulation or substrate specificity of the enzyme. With this detailed information, an insight can be obtained into PAP from the microsomes of a tissue whose main role is to synthesise TAG.

Chapter 6

Characterisation and Substrate Specificity Studies of Microsomal PAP

6.1 Introduction.

There is currently great interest in the production of 'tailor made' triacylglycerols through genetic modification of the acyltransferases. The final acylation step in the Kennedy pathway can not occur until the phosphate moiety is hydrolysed from the glycerol backbone. The means by which glycerolipid is channelled into phospholipid or triacylglycerol is not currently known. PAP lies at a theoretical branch-point in TAG and PL biosyntheses. The enzymatic properties of PAP are largely unknown in respect to substrate specificity, regulation of activity and co-factor dependence. Until all of the enzymes responsible for the assembly of TAG are well characterised, the production of industrially desirable lipids is an inexact science. A preliminary characterisation of the enzyme was therefore undertaken in order to readdress the scientific obscurity regarding this enzyme.

The characterisation studies were mainly conducted prior to the successful purification to homogeneity of PAP. Unless otherwise stated, a partially purified preparation of PAP was used for characterisation studies, because homogenous enzyme was unavailable. The PAP sample was purified (following the procedure already described in chapter 5.5) up to, and including, the ammonium sulphate precipitation stage. In this way, the sample was solubilised, free from endogenous lipid and highly enriched. TLC analysis of the [^{32}P]PA assay reaction products of this sample, showed no phospholipase degradation products. The partially purified sample was frozen in aliquots and stored at -80°C until use. When required, each aliquot was

thawed at room temperature, placed on ice, and discarded after use. In this way, the enzyme was never re-frozen, with all aliquots identically treated.

6.1.1 The effect of Mg^{2+} ions and pH on partially purified PAP activity.

The glycerolipid metabolising PAP isoform from all mammalian and yeast tissues have been reported to be Mg^{2+}-dependent and have pH optima within one pH unit of neutrality (Kocsis and Weselake, 1996). The requirement for Mg^{2+} ions for catalytic activity has been used as a means of PAP isoform classification in mammalian systems (Jamal *et al.*, 1992; Gomez-Muñoz *et al.*, 1992a). In different plants, Mg^{2+} has been reported to be inhibitory (Moore and Sexton, 1978; Malherbe *et al.*, 1995) and stimulatory(Griffiths *et al.*, 1985; Sukumar and Sastry, 1987; Ichihara *et al.*, 1989) on PAP activity.

The effect of $MgCl_2$ on partially purified avocado PAP activity is shown in Figure 6.1, where all reactions were conducted under the identical conditions as already described in Chapter 4. Mg^{2+} ions were removed from the sample (1ml) by dialysis (2 x 1litre each) against buffer containing 4mM EDTA and 0.1% CHAPS, followed by buffer and 0.1% CHAPS. In agreement with the data obtained using microsomal PAP, enzyme catalysis was independent of the presence of Mg^{2+} in the reaction. In reactions where Mg^{2+} was omitted (and 4mM EDTA added), PAP activity was 0.48units/mg protein. The addition of 0.1mM $MgCl_2$ to the reaction mixture caused an increase in PAP activity to 0.68units/mg protein. Maximal catalysis (0.8 units/mg protein) was observed in the presence of $\geq$ 1mM Mg^{2+}. This shows that PAP was not dependent on the cation for catalysis, but was stimulated nearly 2-fold by $\geq$ 1mM Mg^{2+}.

The effect of pH on PAP activity is shown in Figure 6.1. PAP was assayed under the standard assay conditions at various pH values, with the buffer changed accordingly, to enable the effective buffering of the mixture at each pH. The buffer

concentration was 50mM throughout all experiments. As with the washed microsomal preparation, the solubilised enzyme exhibited a broad pH optimum between pH5.0 and 7.0, with a maximum activity observed at pH6.0. The detergent solubilisation (and delipidation) of the enzyme did not effect the Mg^{2+} or pH optima for catalysis, when compared to the profiles of the microsomal enzyme (shown earlier).

6.2 The identification of lysophosphatidate as a substrate for PAP.

The selectivity and specificity for different acyl-CoA moieties for the acyltransferases in the Kennedy Pathway has been well documented (Frentzen, 1993). The specificity of PAP towards different PA species has largely been ignored in glycerolipid research.

During the initial purification of PAP (shown in the previous chapter), a dual assay was devised in order to resolve PAP activity from so called non-specific phosphatase activity. Each protein sample was assayed under standard assay conditions with 0.5mM PA or lysophosphatidate (LPA). It was assumed that PAP would be highly specific towards PA, and that the hydrolysis of LPA would be negligible. The microsomal fraction was found to contain Lyso-Phosphatidate Phosphatase (LPAP) activity. The observed 'LPAP' activity co-purified with PAP activity (Table 6.1). As will be shown later, LPAP activity was observed with the homogenous enzyme.

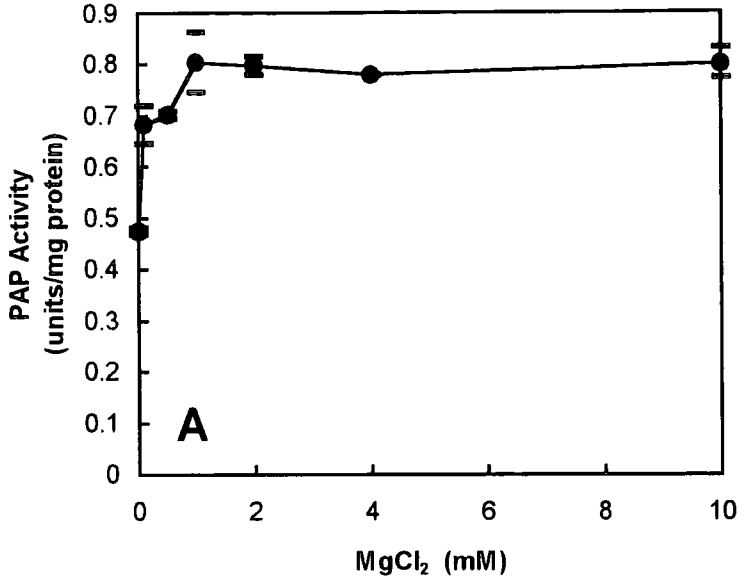
PAP Activity
(units/mg protein)
0.9
0.8
0.7
0.6
0.5
0.4
0.3
0.2
0.1
0
A
0
2
4
6
8
10
MgCl2 (mM)

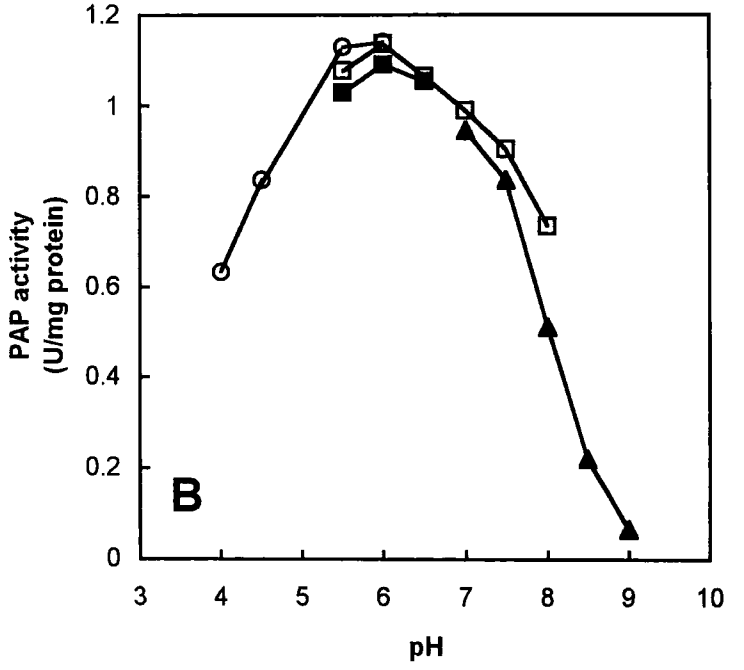
PAP activity
(U/mg protein)
1.2
1
0.8
0.6
0.4
0.2
0
B
3
4
5
6
7
8
9
10
pH

LPAP activity was not observed in assays that had no enzyme added, or in which the microsomes had been pre-incubated at 100°C for 5 minutes. This eliminated the possibility that LPA, which is slightly water-soluble, was not entirely removed from the phase-extracted aqueous layer of the terminated reaction. In this case, the LPA would be detected in the upper aqueous phase and incorrectly assumed to be [^{32}P]Pi. LPAP activity was consistently higher than that of PAP in each sample tested throughout the purification.

Sample	PAP Activity (μmol/min/mg)	LPAP Activity (μmol/min/mg)
Cell Extract	0.012	0.014
Microsomes	0.038	0.062
CHAPS extract	0.087	0.149
Affi-Gel Blue	0.223	0.38
Mono-S	0.301	0.496
Amicon Green A	0.44	not tested
Mono-S (2)	6.2	6.7
No enzyme	0.001	0.002
Boiled Microsomes	0.001	0.003

Table 6.1: The co-purification of LPAP activity with PAP.

In an attempt to explain the physiological significance of this broad specificity, it was decided to characterise PAP with both oleoyl-PA and oleoyl-LPA as substrates, with the respective activities referred to as PAP and LPAP.

6.3 The effect of Triton X-100 on PAP and LPAP activity.

The effect of Triton X-100 concentration on the activity of PAP with both LPA and PA as substrates is shown in Figure 6.2. The addition of Triton X-100 caused a stimulation (1.6-fold) in PAP activity to a maximum at 2mM (or 20mol% PA) whereupon at higher concentrations of Triton X-100 (or lower PA mol%) a decrease in activity is seen. Maximum PAP activity was observed between 2-4mM Triton X-100 (20-11mol% PA). LPAP activity had no stimulation with Triton X-100, and a reduction in activity occurred (as with PA) with increasing concentrations of detergent (or lower LPA mol%). LPAP activity was observed in reactions that had no Triton X-100 added. The observed difference in LPAP activity when compared to PAP activity in the previous section was because the assays had been conducted with 5mM Triton X-100 (9mol% substrate). LPAP activity is higher than PAP activity, when measured at 9mol% substrate.

PAP/LPAP activity was dependent on the surface concentration of PA and LPA in Triton X-100 micelles. This suggests that the enzyme follows the surface dilution kinetic model towards both substrates, as proposed by Deems *et al.* (1975) for the action of phospholipase A_2 from cobra (*Naja naja naja*) venom.

6.3.1: The effect of bulk substrate concentration on enzyme activity.

As seen in Figure 6.2, the two enzyme activities were dependent on the substrate surface concentration, and had approximately equal activities with 20mol% substrate. For this reason, when the two activities were compared, a substrate:Triton X-100 molar ratio of 1:4 (20mol%) was used. To confirm this similarity, the effect of bulk substrate concentration was investigated at the constant substrate surface dilution of 20mol%. The effect of bulk PA and LPA concentration at 20mol% in Triton X-100 micelles, is shown in Figure 6.3. The initial velocity for LPAP activity is higher than for PAP, and both show a similar

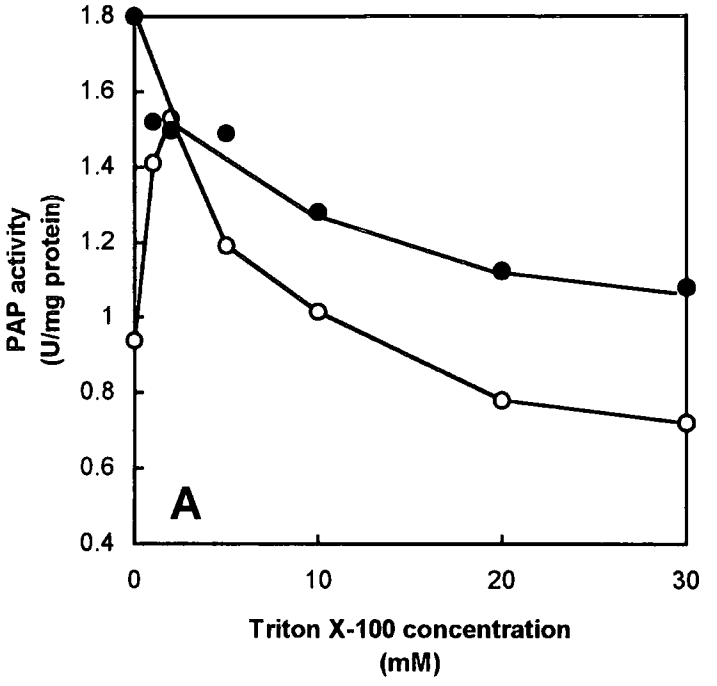
1.8
1.6
1.4
1.2
1
0.8
0.6
0.4
PAP activity
(U/mg protein)
A
0
10
20
30
Triton X-100 concentration
(mM)

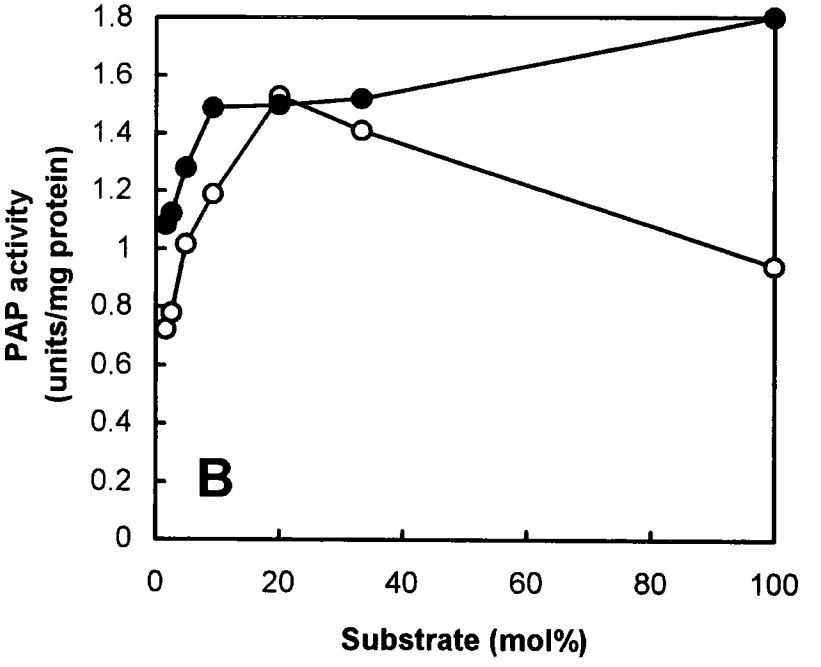
1.8
1.6
1.4
1.2
1
0.8
0.6
0.4
0.2
0
PAP activity
(units/mg protein)
B
0
20
40
60
80
100
Substrate (mol%)

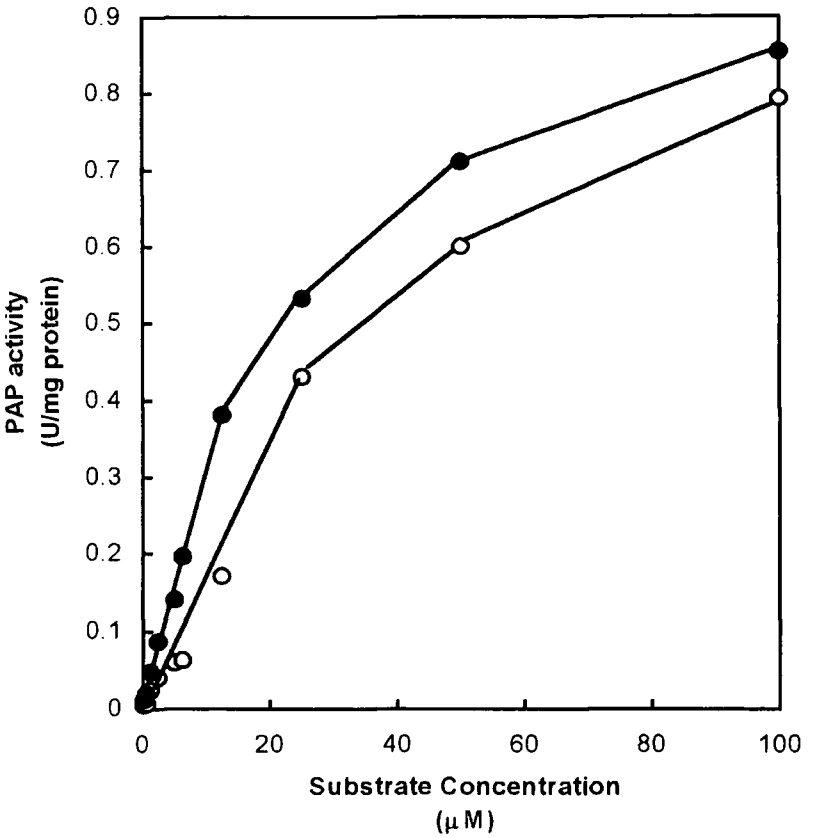

Figure 6.3: The effect of bulk concentrations of PA and LPA on PAP activity. Partially purified PAP activity was measured with increasing concentrations of PA (O) and LPA (●) in a constant substrate:Triton X-100 molar ratio of 1:4. The experiments were conducted in triplicate, under the otherwise standard assay conditions with the mean data shown (variance of ≤5%). One unit of PAP activity was defined as the amount of enzyme required to catalyse the formation of 1μmol Pi/min.

maximum velocity. Enzyme activity towards both substrates was dependent on the bulk substrate concentration.

This data shows that at a substrate surface concentration of 20mol% (in Triton X-100), the two enzyme activities were similar in respect to bulk substrate concentration. This validates the data obtained during experiments in which the activity towards both substrates are compared.

6.4. Substrate Selectivity of homogenous PAP.

In an attempt to understand the relevance of LPA and PA catalysis by PAP, experiments were conducted in which the homogenous enzyme was simultaneously presented with equimolar high specific activity [^{14}C]LPA and [^{32}P]PA. The rates of catalysis for both substrates were simultaneously measured. This assay with dual labelled substrates provided the means of assessing the substrate selectivity of the PAP protein.

[^{14}C]LPA and [^{32}P]PA were synthesised as already described in Chapter 3. [^{32}P]PA and [^{14}C]LPA in mixed micelles of Triton X-100 were added to a 2ml final reaction volume containing: 25μM [^{32}P]PA and 25μM [^{14}C]LPA (50μM total substrate, 15 000 DPM/nmol), 0.2mM Triton X-100, 50mM Tris-maleate pH 6.0, 2mM $MgCl_2$. The reaction was started with the addition of 60ng homogenous enzyme. At set time intervals, 100μl aliquots were removed and the reaction stopped by the addition of 20μl 10% perchloric acid (Figure 6.4). Terminated aliquots were: (a) tested for total radioactivity; (b) measured for [^{32}P]Pi and [^{32}P]PA levels under the normal assay conditions, and; (c) resolved on silica TLC plates, as summarised in Figure 6.4. The remainder of the terminated reaction mixtures was discarded.

The total radioactivity (^{32}P and ^{14}C) at each time point was measured by scintillation counting of 5μl of the terminated aliquots, ensuring that each sample

contained a known level of each radiolabel. The accurate measurement of [^{32}P]Pi and [^{32}P]PA levels at each time point were taken by phase extracting 20µl of each terminated aliquot, under the normal conditions. This allowed the precise measurement of PAP activity to be determined.

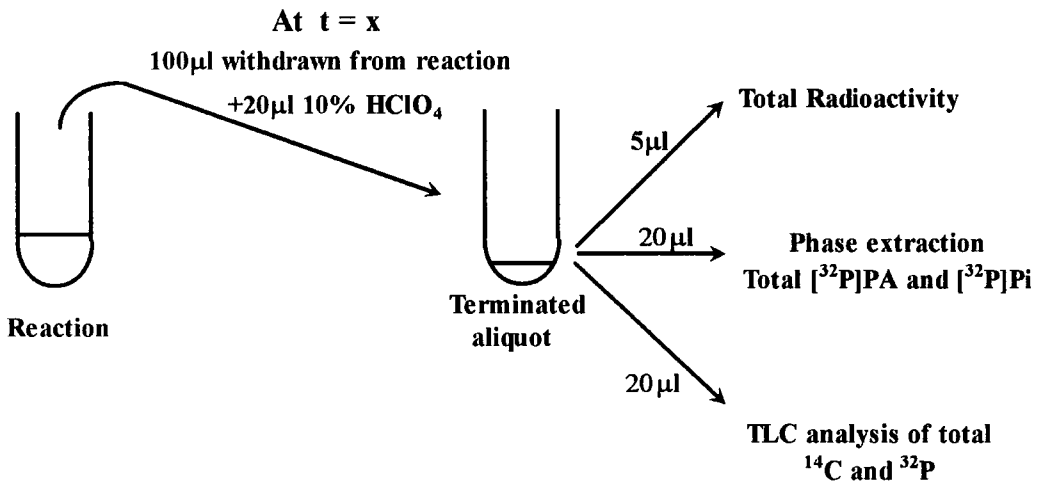

Figure 6.4: A summary of the dual labelled substrate assay procedure.

The ^{14}C and ^{32}P reaction substrates and products were identified by TLC analysis, allowing the measurement of LPAP/PAP activities simultaneously. For each sample in the time course, 20µl of the terminated reaction mixture was applied onto a silica TLC plate (alongside standards), developed in chloroform:methanol:water (12:6:1) and exposed to x-ray film. The ^{32}P and ^{14}C reaction substrates/products (i.e. LPA, PA MAG and Pi) were identified on the autoradiographs (Figure 6.5). The corresponding radioactive spots were scraped off the TLC plate, extracted with 100µl chloroform or 100µl 50%methanol depending upon the aqueous or chloroform solubility of the compound, and the radioactivity counted. In this way, LPAP activity could be measured through the production of [^{14}C]MAG from [^{14}C]LPA, and PAP activity assessed through [^{32}P]Pi emergence from [^{32}P]PA. Enzyme activity was

established by counting appropriate substrate and product spots on the TLC plate and expressed in terms of % product formation (product/[product+substrate] x 100). The rates for [^{32}P]Pi formation from [^{32}P]PA were also calculated using the standard assay phase separation procedure were comparable to the those calculated from [^{32}P]PA depletion in the TLC scrapings. The mean rates of PAP/LPAP activity are shown from duplicate experiments in Figure 6.6.

The rate of LPA dephosphorylation was far higher than with PA. As was shown earlier in this chapter, at 25μM bulk substrate, the catalytic rate was approaching maximal. Therefore in near saturating amounts of PA, the PAP protein had a preference for LPA as substrate. The initial rate of LPA hydrolysis was 4-fold higher than for PA. As can be seen in the autoradiograph, no traces of ^{32}P degradation products were seen in the sample after 3hours.

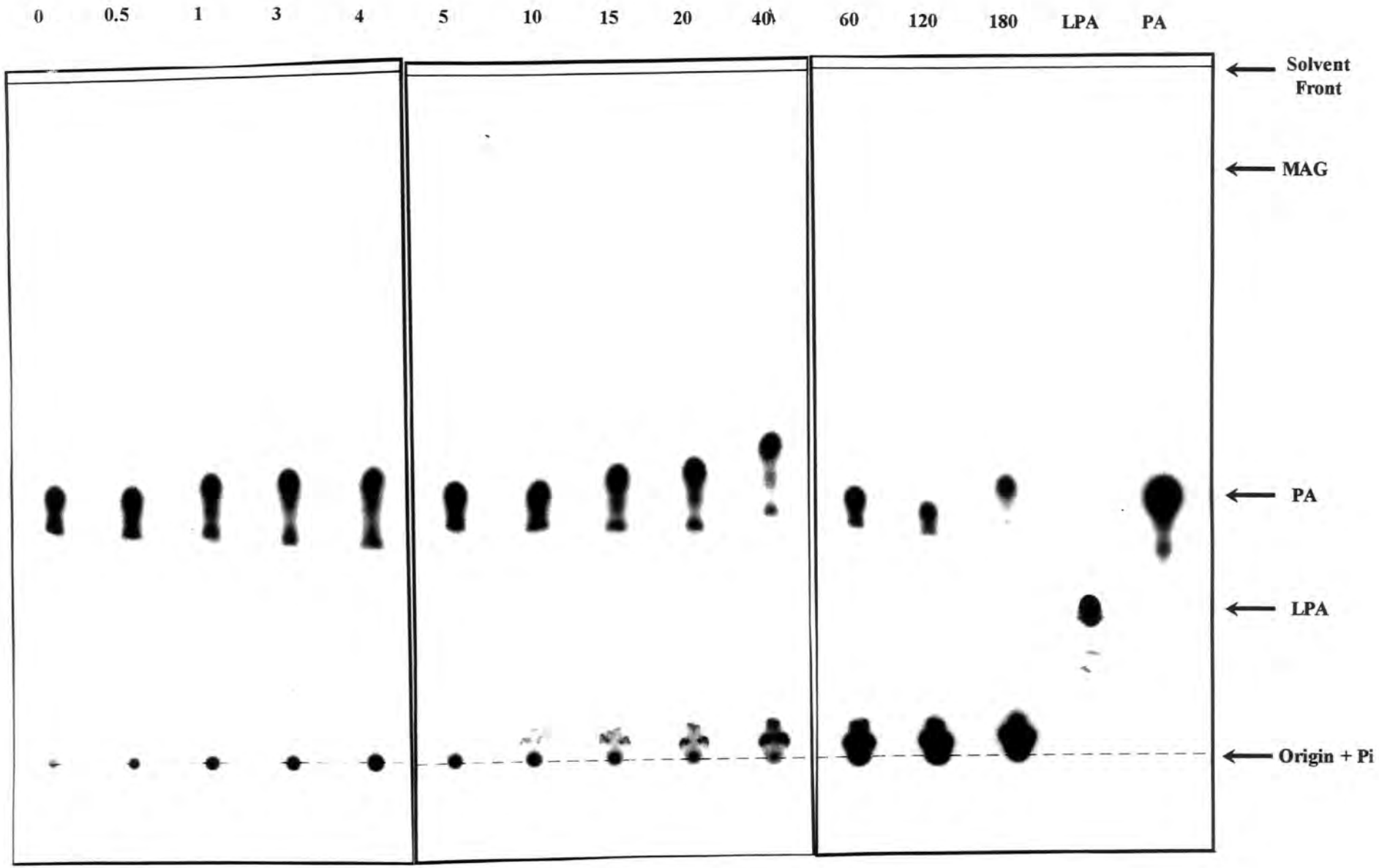
0
0.5
1
3
4
5
10
15
20
40
60
120
180
LPA
PA
Solvent Front
MAG
PA
LPA
Origin + Pi

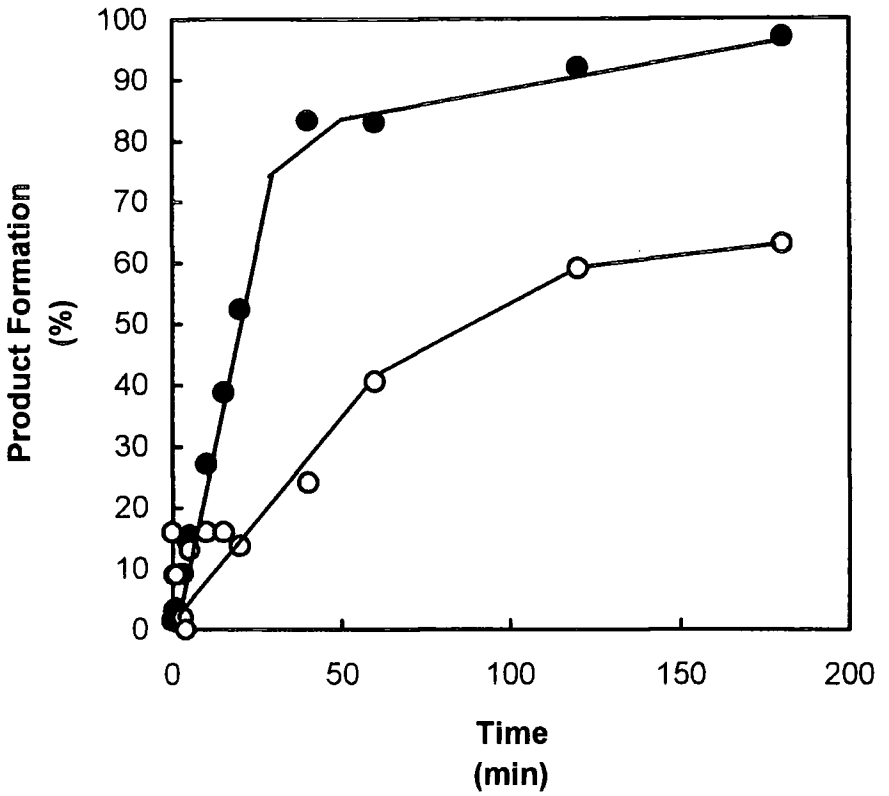

Figure 6.6: The simultaneous rates of equimolar LPA and PA catalysis. Using the autoradiograph from Figure 6.5, the corresponding radioactive spots were scraped off the TLC plates, extracted from the silica with 100µl chloroform or 100µl 50% methanol and the radioactivity counted. Consequently, the simultaneous catalytic rates for LPAP (●) and PAP (○) were calculated, and expressed in terms of % product formation (product/substrate+product x 100), from approximately 40 000DPM total radioactivity for each substrate.

6.5 *p*-Nitrophenyl-Phosphate as a substrate for PAP

Conflicting reports have arisen over the true identity of PAP in animals. A possible source for error in the identification and purification of PAP lies in the fact that there are non-specific acid phosphatases within the cell. It has been shown that wheatgerm acid phosphatase dephosphorylated phospholipids to a variable extent and that PA was a substrate for acid phosphatase but not alkaline phosphatase (Blank and Snyder, 1970). A soybean acid phosphatase has been purified and had a monomeric molecular mass of 51kDa (Staswick *et al.*, 1994). The specific activity of the soybean acid phosphatase was found to be 1353μmol *p*-nitrophenol released/min/mg protein (pH 6.4 at 25°C). A membrane bound acid phosphatase was purified from Yam tuber which had a molecular mass of 50kDa and a specific activity (with *p*NPP) of 1200 μmol/mg protein (Kamenan and Diopoh, 1983). Kocsis *et al.* (1996) reported the ability of *B.napus* extracts to hydrolyse *p*NPP; the 100 000*g* pellet of a developing seed extract hydrolysed *p*NPP with a considerably greater specific activity($\geq$20-fold) than seen when PA was the substrate.

With the clear indications that PAP could effectively utilise PA and LPA as substrates with a higher selectivity for the latter, several queries as to the identity of the purified enzyme were raised. The activity, which had until now been attributed to PAP, could have actually been due to non-specific phosphatase activity. The substrate specificity of PAP was therefore further characterised, by conducting assays with the synthetic phosphatase substrate analogue, *p*-nitrophenyl phosphate (*p*NPP). *p*NPP is routinely used in the study of phosphatase activity, enabling the relative activities of different phosphatases to be compared in terms of V_{max} and K_m (Duff *et al.*, 1994). In this way, the activity of PAP with *p*NPP as substrate could be compared to the already purified plant intracellular acid phosphatases as described by Duff *et al.* (1994), and the possibility of mis-identification eliminated.

6.5.1: The PAP catalysed phosphohydrolysis of *p*NPP.

Assays were prepared in duplicate, using conditions based on the standard assay procedure in order to assess the ability of partially purified PAP samples to hydrolyse *p*NPP. The hydrolysis of *p*NPP to *p*-nitrophenol (and Pi) was monitored by measuring a decrease in absorbance at 405nm, in 1ml (1cm light path) quartz cuvettes. In the *p*NPP assay, PA/Triton X-100 mixed micelles were substituted for 0.5mM *p*NPP ± 2mM Triton X-100, under otherwise unaltered standard assay reaction conditions, enabling the direct comparison to the rate of PA hydrolysis. As a control, an aliquot of enzyme sample was incubated at 100°C for 5min prior to assaying. The partially purified sample was found to hydrolyse 0.5mM *p*NPP with a specific activity of 0.39 units/mg protein and independent of Triton X-100 (Table 6.2). This was expected, as the substrate did not require the detergent for solubility and subsequently presentation to the enzyme. Also shown in Table 6.2 is the *p*NPP hydrolysis by homogenous PAP, with a specific activity of 1.192 Units/mg protein (with 0.5mM *p*NPP).

Duplicate assays were also conducted using the procedure of Kocsis *et al.* (1996), to enable the comparison with the similar activity in *B.napus* (Table 6.2). For assays using the conditions of Kocsis *et al.* (1996), reactions contained: 50mM Tris-maleate pH6.75, 0.1mM EDTA, 2mM $MgCl_2$, and enzyme sample in a final volume of 1ml. Reactions were initiated with the addition of *p*NPP (to 5mM) and incubated at 30°C. There was no observed difference in the rate of *p*NPP hydrolysis using this procedure, when compared to the standard assay procedure .

Reaction	Specific Activity (μmol/min/mg protein)
0.5mM *p*NPP	0.39 (± 0.05)
0.5mM *p*NPP + 2mM Triton X-100	0.38 (± 0.03)
5mM *p*NPP (using standard assay)	0.52 (± 0.05)
5mM *p*NPP (following Kocsis *et al.*, 1996)	0.48 (± 0.03)
Pre-Boiled enzyme sample	0.01
Homogenous PAP	1.192 (± 0.02)

Table 6.2: The hydrolysis of *p*NPP by partially pure and homogenous PAP.

As shown in the previous chapter, homogenous PAP had specific activity of 50μmol/min/mg protein with PA. The partially purified PAP sample had a specific activity with PA of 1.0μmol/min/mg (as seen in Figure 6.3). The specific activity of partially pure and homogenous PAP was found to be significantly lower with *p*NPP as substrate than seen with PA or LPA. The rate of *p*NPP hydrolysis by homogenous PAP was 40-fold lower than with PA. The difference for partially purified enzyme sample was nearly 3-fold. There was no significant difference in the catalytic rates of *p*NPP hydrolysis, when the reaction conditions were changed from the standard avocado assay conditions to those of Kocsis *et al.* (1996).

6.5.2: Effect of PA and DAG on *p*NPP hydrolysis.

To examine the effect of PA and DAG on 0.5mM *p*NPP hydrolysis, assays were conducted in duplicate with 0.5mM dioleoyl-PA, dioleoyl-DAG and 2mM dioleoyl-DAG in Triton X-100 mixed micelles. The effect of the addition of PA and DAG to the reaction is shown in Table 6.3. The presence of equimolar PA caused a

nearly 4-fold reduction in the rate of *p*NPP hydrolysis. This is indicative of substrate inhibition, as was seen for LPA and PA catalytic activities. The DAG, had no discernible effect in equimolar concentrations with *p*NPP. However, at 2mM, the rate of catalysis was reduced by 2.5-fold (i.e. 60% inhibition). DAG is the *in vivo* product of the enzyme catalysis, and as such would be expected to cause feedback inhibition as was seen in chapter 4. In the *p*NPP assay, DAG was not the product of the reaction, showing that the enzyme inhibited was infact PAP.

Reaction	Specific Activity (μmol *p*NPP/min/mg)
0.5mM *p*NPP	0.40 (± 0.07)
+ 2mMTriton X-100	0.41 (± 0.02)
+ 0.5mM PA/2mM Triton X-100	0.109 (± 0.04)
+ 0.5mM DAG/2mM Triton X-100	0.38 (± 0.01)
+ 2mM DAG/2mM Triton X-100	0.164 (± 0.06)

Table 6.3: Inhibition of *p*NPP hydrolysis by PA and DAG.

The inhibition of *p*NPP hydrolysis by PA was examined further, by measuring the rates of catalysis, at a fixed concentration of PA, with increasing concentrations of *p*NPP. *p*NPP assays were conducted in duplicate sets of 0.1-1mM *p*NPP each in the presence of 0, 0.1, 0.2, and 0.5mM PA. The effect of PA on *p*NPP catalysis is shown

in Figure 6.7. The addition of PA to the reaction caused a reduction in the catalytic rate. At high concentrations of *p*NPP, the maximum rate (V_{max}) was unaffected by the addition of PA. This clearly shows that PA(in Triton X-100 micelles) is competitively inhibiting *p*NPP hydrolysis.

A Lineweaver-Burk plot was constructed using the data from Figure 6.7 (Figure 6.8). The K_m and V_{max} of *p*NPP hydrolysis were calculated as 0.5mM *p*NPP and 0.7units/mg protein, respectively. The double reciprocal plot demonstrates that PA increased the K_m (reciprocal of -1/[*p*NPP] intercept) for *p*NPP hydrolysis. In saturating concentrations of *p*NPP, the V_{max} (reciprocal of 1/V intercept) was unaltered irrespective of the PA concentration. The K_i for PA was calculated as 2 x 10^{-4}M, using a replot of the slopes from Figure 6.8 *versus* the concentration of PA (Figure 6.9).

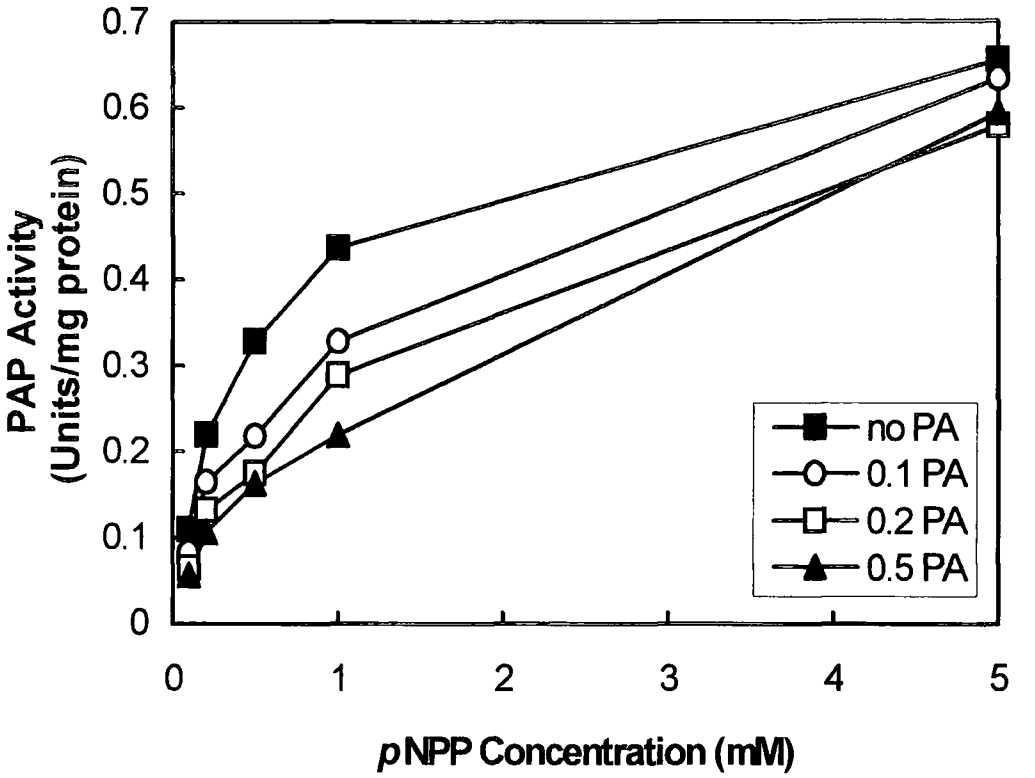

Figure 6.7: Effect of PA on PAP hydrolysis of *p*NPP. PAP activity was measured with increasing concentrations of *p*NPP in the presence of the following fixed concentrations of PA: 0mM (■); 0.1mM (○); 0.2mM (□); and 0.5mM (▲). *p*NPP hydrolysis was measured by a decrease in absorbance at 405nm. One unit of PAP activity was defined as the amount of enzyme required to catalyse the formation of 1μmol *p*-nitrophenol/min.

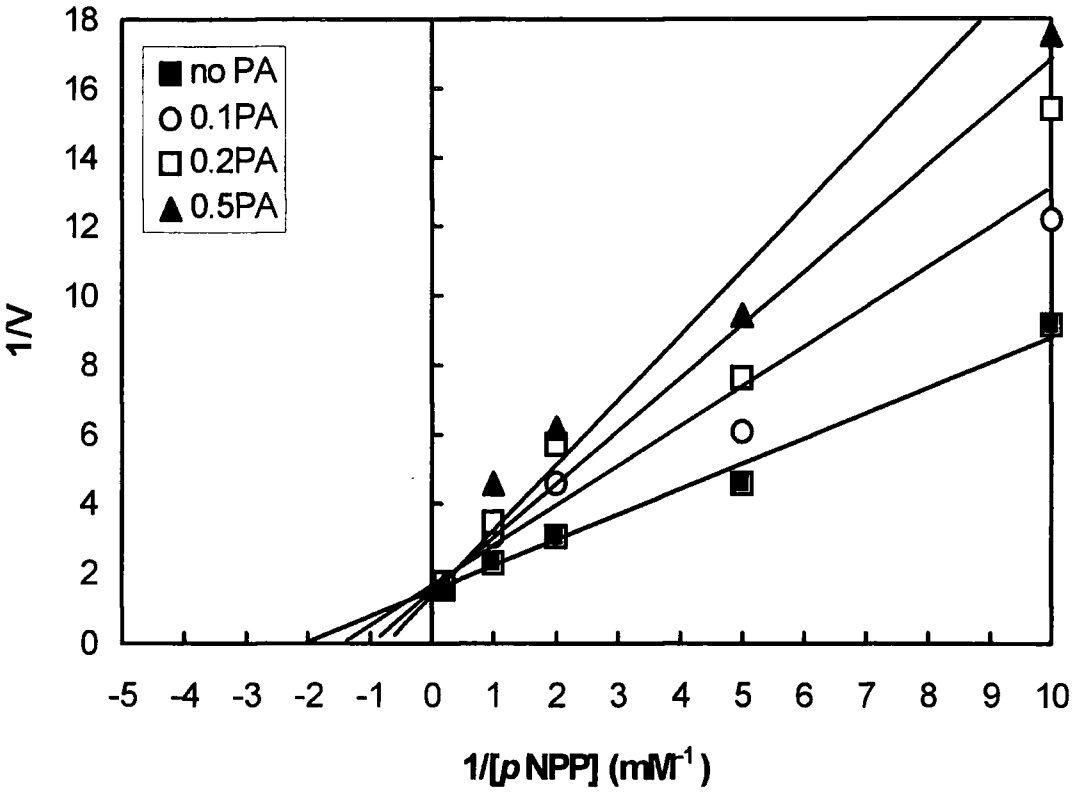

Figure 6.8: A Lineweaver-Burk plot showing the competitive inhibition of *p*NPP hydrolysis with PA. A double-reciprocal plot was constructed using the data from Figure 6.7. The data are shown for rates of *p*NPP hydrolysis in the presence of no PA (■); 0.1mM PA (○); 0.2mM PA (□); and 0.5mM PA (▲).

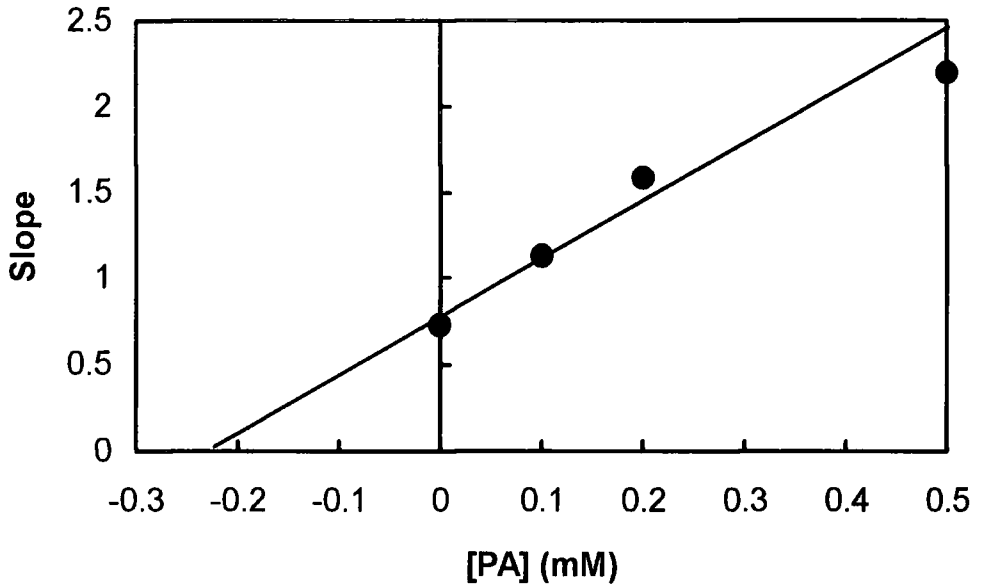

Figure 6.9: Determination of the K_i for PA in *p*NPP hydrolysis. The slopes of the Lineweaver-Burk plot (Figure 6.8), were plotted versus the corresponding concentration of PA. The K_i was calculated from the -[PA] intercept, and was found to be 0.22mM.

6.6 Substrate specificity for different PA species.

In plant TAG biosynthesis research, considerable attention has been focused on the acyl-chain selectivity and specificity of the acyltransferases (Ichihara *et al.*, 1987; Oo and Huang, 1989; Cao *et al.*, 1990, Bernerth and Frentzen, 1990; Laurent and Huang, 1992; Frentzen, 1993). The acylation steps of the Kennedy Pathway are considered important in the final TAG composition of a plant. There has to date, been only one reported phosphatidate specificity profile of PAP from any plant species (Ichihara, 1991). The microsomal Safflower PAP was found to be selective and specific for unsaturated phosphatidates suggesting that PAP had little influence on the fatty acid composition of the final TAG pool. It was decided to test the acyl-preference of avocado PAP, with PA species containing acyl chains of between 12-18 carbons. It is possible that PAP conveys a specificity/selectivity over PA species containing acyl moieties of differing chain length.

In oilseed cotyledons, oleoyl-DAG can be reversibly converted into PC (Stymne and Stobart, 1984), whereupon the acyl chains undergo desaturation thus generating PC that contains poly-unsaturated fatty acids. These polyunsaturated species of PC are eventually incorporated into TAG via DAG (Stobart and Stymne, 1985b). The generation of such glycerolipids containing polyunsaturated fatty acids therefore occurs downstream and is independent of PAP. Stobart and Stymne (1985) demonstrated that oleoyl-PC desaturation in avocado mesocarp was very low. Avocado mesocarp produces TAG that is rich in oleate and very low in polyunsaturated fatty acids (Stobart and Stymne, 1985b). Therefore, TAG biosynthesis in avocado mesocarp proceeds via the conventional Kennedy pathway, where the acyl groups confronted by PAP are the same as those in the final TAG pool. The specificity/selectivity of PAP for PA with different acyl moieties may exert an influence in TAG biosynthesis in avocado mesocarp.

All *sn*-1,2-diacylglycerols (C12:0, C14:0, C16:0, C18:0 and C18:1) were purchased from Sigma Chemical Company. The *sn*-1,2-diacylglycerol-3-[^{32}P]phosphate substrates were produced following the procedure of Walsh and Bell (1986) as already described in Chapter 3, with the appropriate diacylglycerol moiety [γ-^{32}P]ATP and DAG kinase.

PAP was assayed for the ability to hydrolyse various PA species. For each PA tested, a reaction was prepared (1ml final volume), using the standard assay conditions, with 50μM PA (20mol% in Triton X-100). The reactions were initiated with the addition of 1.5μg partially purified PAP. At set time points, 100μl was withdrawn from the reaction, terminated, phase extracted and the activity measured. The effect of the acyl-chain length of PA on PAP activity from duplicate experiments is shown in Figure 6.10. The substrates were delivered to the enzyme in Triton X-100 mixed micelles. This eliminated the difference in solidity/fluidity between the fatty acid species. Maximal rates of PA hydrolysis were observed with dioleoyl- PA (C18:1), dilauroyl- PA (C12:0) and dimyristoyl- PA(C14:0). Catalysis of stearoyl- PA (C18:0) and palmitoyl- PA(16:0) was lower than dilauroyl- and dimyristoyl-PA. This suggests that PAP has a catalytic preference for PA species containing either unsaturated or short chain fatty acids. However this was only a preliminary study. To evaluate the precise catalytic specificity of each substrate, a kinetic analysis toward each substrate would be required.

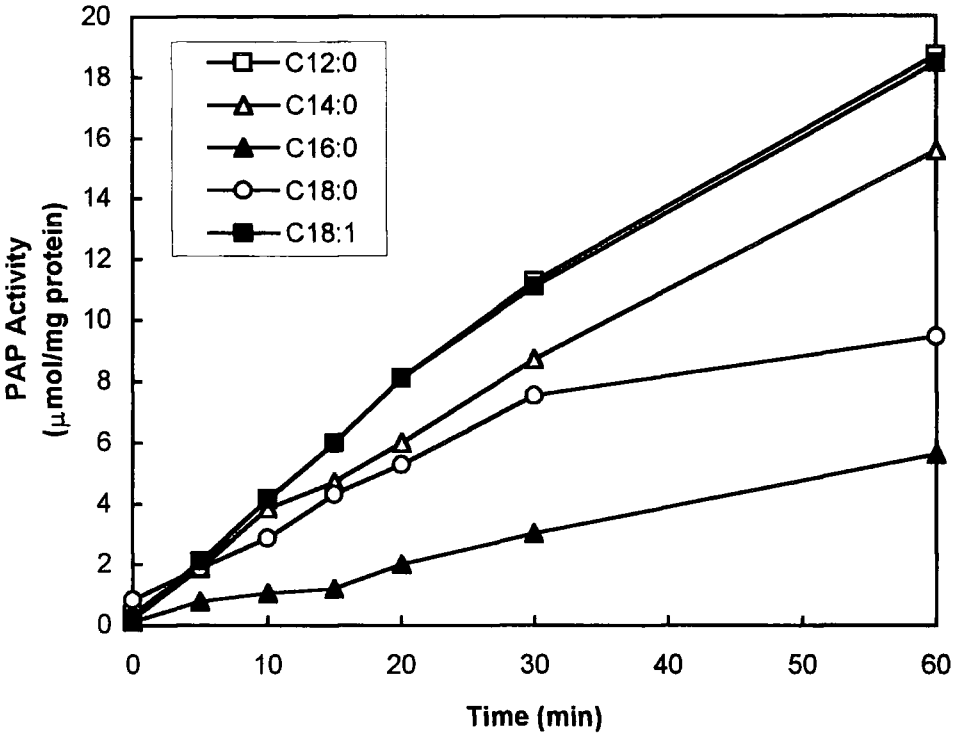

Figure 6.10: The effect of different PA species on the rate of hydrolysis. Release of [^{32}P]Pi from various molecular species of PA (50μM in 0.2mM Triton X-100) was measured using the standard assay procedure. A 1ml final volume reaction was initiated with the addition of 1.5μg partially purified PAP, and at various time points, aliquots were removed and the PAP activity measured. The acyl-moieties for the PA species are indicated in the *inset*. The data represent the means from duplicate experiments with the experimental variance ≤8%.

6.7 Discussion.

In this Chapter, the catalysis of LPA and *p*NPP was demonstrated with partially purified microsomal PAP, and confirmed with the homogenous enzyme. The activities were compared using a partially purified preparation. Hydrolysis of LPA was similar to that of PA at 20 mol%. However, at higher molar concentrations of LPA, hydrolysis exceeded the rate observed with PA as substrate.

Activity was dependent on the surface (Figure 6.2) and bulk (Figure 6.3) concentration of LPA and PA. The derivation of kinetic values of K_m and V_{max} from a double reciprocal plot of Figure 6.3, using the Michaelis-Menten kinetic model would have therefore been inappropriate (and inaccurate), as this model only accounts for the effect of bulk substrate concentration (Engel, 1977). Also, the enzyme preparation was not homogenous, making the kinetic characterisation arbitrary. This reiterates the suitability of the Surface Dilution Kinetic Model of enzyme catalysis (Deems *et al.*, 1975). The application of this kinetic model to homogenous PAP is shown in the next chapter.

The observation of LPA hydrolysis lead to the conclusion that PAP had a promiscuous specificity towards acylglycerol-3-phosphate species, irrespective of the presence of an acyl moiety in position *sn*-2 of the glycerol backbone. This has since been corroborated with many reports of the PAP catalysed hydrolysis of LPA. Kocsis *et al.* (1996) reported that erucoyl-LPA is dephosphorylated at a similar rate as erucoyl-PA by solubilised *B. napus* extracts. LPA also appears to be a substrate for the rat liver PAP, where it was shown to inhibit PA hydrolysis (Fleming and Yeaman, 1995). More recently, the 51kDa isoform of PAP, purified from rat liver plasma membranes, was shown to catalyse the phosphohydrolysis of ceramide-1-phosphate, sphingosine-1-phosphate and LPA (Waggoner *et al.*, 1996). Homogenous PAP from *S.cerevisiae* did not catalyse the hydrolysis of LPA (Lin and Carman, 1990)

The significance of LPA hydrolysis was demonstrated by presenting the enzyme with equimolar LPA and PA, and measuring the catalysis of both substrates simultaneously. The rate of LPA catalysis was far higher than that for PA. There are two possible explanations for the observed catalytic rates for both substrates. Firstly, the LPA causes inhibition of PA hydrolysis (i.e. competitive inhibition), with the inhibition reduced as LPA is catalysed. Secondly, when given both substrates simultaneously, the enzyme selectively catalyses LPA. It is also possible that a combination of the both of these situations gives rise to the rates of catalysis. The interaction/inhibition of LPA towards PAP activity was investigated using the surface dilution kinetic model and is described in the next chapter. In this way any inhibition could be kinetically characterised allowing a better interpretation of the substrate specificity.

The specific activity of the 51kDa soybean acid phosphatase was reported to be 1353μmol *p*-nitrophenol released/min/mg protein at pH 6.4 and 25°C (Staswick *et al.*, 1994). The findings presented here revealed that purified avocado PAP had a considerably lower specific activity towards *p*NPP of 1.19 μmol/min/mg protein, under conditions which were similar to those of the soybean acid phosphatase (Staswick *et al.*, 1994) . Similarly, the specific activity of a 55kDa membrane bound acid phosphatase from Yam Tuber was 1200μmol/min/mg protein (Kamenam and Diopoh, 1983). The level of PA dephosphorylation caused by wheatgerm acid phosphatase was less than 1% of that seen with the phosphatase substrate, *O*-carboxyphenyl phosphate (Blank and Snyder, 1970). The specific activity of PAP towards PA was more than 40-fold higher than that seen with *p*NPP. The presence of PA reduced the rate of *p*-nitrophenol formation further. The addition of 2mM DAG, the *in vivo* product of PAP, was also found to inhibit *p*-nitrophenol production by greater than 60%. This could be due to feedback inhibition as seen in spinach chloroplastic PAP (Malherbe *et al.*, 1992). These results support the conclusion that the enzyme is

indeed PAP, and eliminate the possibility that this activity represented an acid phosphatase contamination from within the washed microsomal preparations. PAP was microsomally-associated and required the presence of detergent for solubilisation and stability.

*p*NPP is soluble in an aqueous environment and it's hydrolysis was found to be independent of Triton X-100. This indicated that the substrate was not a surface active compound requiring intercalation into a lipid (or detergent) interface. A standard Michaelis-Menten Kinetic analysis of the *p*NPP hydrolysis reaction was therefore appropriate for the reaction. The K_m of the *p*NPP reaction was 0.5mM. PA was found to be a potent competitive inhibitor with a K_i of 0.2mM, and caused the dramatic increase in the K_m of *p*NPP hydrolysis. The inhibition shows that the PA and *p*NPP were competing for the same enzyme, indicating further the positive identification of PAP and not non-specific phosphatase activity.

In both partially pure and homogenous enzyme samples, PA hydrolysis was in excess of *p*NPP hydrolysis. There was a large difference in the PA:*p*NPP activity ratio between the two enzyme samples. This suggests that the partially purified sample contained another phosphatase activity, which could predominantly catalyse *p*NPP over PA, and which was fractionated away during Phenyl Superose chromatography. In the *B. napus* extracts used by Kocsis *et al.* (1996), *p*NPP hydrolysis was more than 20-fold higher than for PA. This clearly shows that the *B. napus* microsomal enzyme preparations were heavily contaminated with non-specific phosphatases, and raises the degree of uncertainty about the reported data.

A preliminary investigation of substrate specificity towards different PA species was conducted. The catalytic rates for the PA species indicated that PAP has a significant catalytic preference for PA species containing either unsaturated or short

chain fatty acids. Ichihara (1991) found that microsomal PAP from Safflower predominantly hydrolysed PA species containing unsaturated acyl moieties.

Chapter 7

Kinetic analysis of homogenous PAP

7.1 Introduction

The surface dilution kinetic model was proposed by Deems *et al.* (1975) for the action of lipolytic enzymes on mixed micelles of phospholipid and surfactant. The kinetic model accounts for the concept that the surface and the bulk substrate concentration play essential roles in defining the kinetic parameters of lipid-dependent enzymes. As already discussed in Chapter 1, it has been used in defining the kinetic parameters of many lipid-dependent enzymes (see Carman *et al.*, 1995) including homogenous microsomal PAP from *S. cerevisiae* (Lin and Carman, 1990; Wu *et al.*, 1993). It provides a useful and consistent means of assessing lipid effectors and inhibitors and can be used in the study of enzyme substrate specificity (Yu and Dennis, 1992; Wu *et al.*, 1993; Carman *et al.*, 1995). The surface dilution kinetic scheme is summarised in Equation 7.1.

$$\textbf{Bulk Step:} \quad E + A \underset{k_{-1}}{\overset{k_1}{\rightleftharpoons}} EA$$

$$\textbf{Surface step:} \quad EA + B \underset{k_{-2}}{\overset{k_2}{\rightleftharpoons}} EAB \xrightarrow{k_3} EA + Q$$

Equation 7.1: The Surface Dilution Kinetic Model (after Deems *et al.*, 1975)

According to this model, PAP(**E**) first binds to a mixed micelle of Triton X-100/PA (**A**), to form an enzyme-mixed micelle complex (**EA**). Once sequestered into the mixed micelle, the enzyme can associate with PA(**B**), resulting in an enzyme-Triton X-100-PA complex (**EAB**). This leads to catalysis and the formation of enzyme-mixed micelle complex(**EA**) and the release of products (**Q**). At the beginning of the

reaction, the formation of the enzyme-mixed micelle complex is dependent on the bulk concentration of enzyme, Triton X-100 and PA and is expressed as the sum of the molar concentrations of Triton X-100 and PA. The homogenous PAP protein was in a solution containing 0.1% CHAPS. At this concentration, CHAPS is monomeric and the PAP protein was considered to be free enzyme (**E**). The second step is dependent on the surface concentration of the PA, and PA is expressed in terms of mole fraction ([PA]/[Triton X-100]+[PA]) or mol% (mole fraction x 100). In conjunction with this two step scheme, the enzyme may also specifically and directly associate (in one step) with the substrate at the micelle surface. This has led to these two possible schemes within the surface dilution kinetic model being named: 'surface binding model' and 'phospholipid binding model', respectively (Roberts *et al.*, 1977; Carman *et al.*, 1995).

It was shown in the previous chapter that PAP was dependent on the bulk and surface concentrations of aqueous insoluble PA and LPA in Triton X-100 mixed micelles, and therefore followed interfacial enzyme kinetics. This suggested the suitability of the Surface Dilution Kinetic model for the kinetic characterisation of PAP. The aim of this chapter was to conduct a surface dilution kinetic analysis of PAP, with both PA and LPA as the catalytic substrates. Using this model, it was hoped that a greater insight into the substrate specificity could be obtained, with the derivation of kinetic data for LPA and PA, allowing the direct comparison of the catalysis of both substrates. It would also enable the precise determination of LPA inhibition of PA hydrolysis, as was speculated in the previous chapter. It was hoped that the overall analysis would provide information about the reaction mechanism, substrate specificity and inhibition of PAP within the detergent-water interface.

7.2 The kinetic analysis of homogenous PAP towards dioleoyl-PA in Triton X-100 mixed micelles.

The kinetic model assumes that the size, aggregation number and average surface area of the micelles remains constant throughout the analysis (Deems *et al.*, 1975). Lin and Carman (1990) demonstrated Triton X-100/PA mixed micelles with up to 15mol% PA were uniform in size and were similar to the structure of pure Triton X-100 micelles. As was shown in the previous chapter, PAP activity was dependent on the surface concentration of PA, with a maximum activity seen at 20mol%. At this surface concentration, the phospholipid-Triton X-100 mixed micelles are not homogenous in size (Robson and Dennis, 1983; Lichtenberg et al., 1983), thus making a kinetic analysis at this PA mole fraction imprecise. Consequently Triton X-100/PA mixed micelles with a PA mole fraction of 11.1mol% and lower were used. Both the 'surface binding' (i.e. PAP binds non-specifically to the mixed micelle) and the 'dual phospholipid' (i.e. PAP binds directly to PA and not to Triton X-100) models were examined in the Surface Dilution Kinetic analysis of PAP towards dioleoyl PA (Carman *et al.*, 1995).

7.2.1 The activity of PAP according to the surface binding model.

The Surface binding model was applied to PAP by measuring the activity as a function of the sum of the molar concentrations of Triton X-100 and dioleoyl-PA (**A**) at a series of set PA mole fractions (**B**). PAP activity increased with bulk concentration of substrate and showed typical saturation kinetics (Figure 7.1). As the surface concentration of PA was diluted within the mixed micelle, a decrease in V_{max} was observed, demonstrating the phenomenon of surface dilution. Below 5mM substrate (PA + Triton) PAP activity was dependent on the bulk and surface

concentration of substrate. Above this level, the activity was predominantly dependent on the surface concentration of the substrate.

A double-reciprocal plot of the data from Figure 7.1 was constructed (Figure 7.2) and the pattern of lines was indicative of an equilibrium-ordered step as predicted by the model. This confirmed that PAP exhibited saturation kinetics with the bulk substrate concentration at each fixed surface concentration of PA.

The 1/V intercepts and the slopes from Figure 7.2 were plotted *versus* 1/PA mole fraction (Figures 7.3 and 7.4). The resulting lines were linear, and used for the calculation of the various catalytic constants (Deems *et al.*, 1975). The intercept of 1/Vintercept axis in Figure 7.4 is $1/V_{max}$, whilst the intercept of 1/(PA mol fraction) axis is $-1/K_m^B$ (interfacial Michaelis constant). From the data in Figure 7.3, the V_{max} and the K_m^B were calculated as being 47Units/mg protein and 0.015 mole fraction (1.5 mol%), respectively. The dissociation constant for the mixed micelle binding site (K_s^A) was calculated on the basis that the slope of Figure 7.4 is equal to $K_m^B K_s^A/V_{max}$ and was calculated as 4.73mM. The line in Figure 7.4 passes through the origin, as predicted by the surface binding model. This suggests that the surface binding model is applicable to avocado PAP.

These data were calculated with the following assumptions (Deems *et al.*, 1975): (i) the size and aggregation number of the Triton X-100/PA mixed micelles remained constant within the range of bulk substrate concentration tested; (ii) the average Triton X-100 or PA molecule surface area was constant as the bulk and surface concentration was varied; (iii) the micellar surface area to which an enzyme binds remains constant under all experimental conditions.

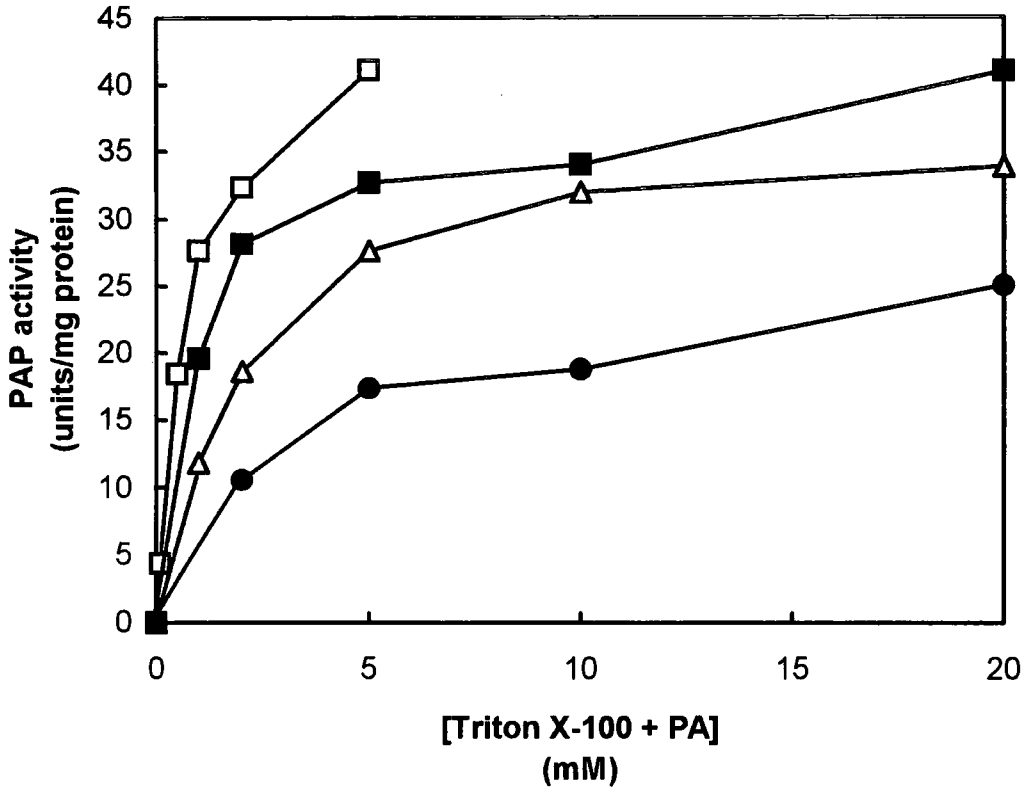

Figure 7.1: Activity of PAP towards dioleoyl-PA in mixed micelles with Triton X-100 according to the surface binding model. PAP activity was measured as a function of the sum of the molar concentrations of Triton X-100 plus dioleoyl-PA at the following set mole fractions of PA: (□)0.111; (■) 0.0588; (△) 0.0303; (●) 0.0154. All assays were conducted in duplicate in the otherwise standard assay conditions, with the mean data shown (with a variance of ≤ ±5%). One unit of PAP activity was defined as the amount of enzyme required to catalyse the formation of 1μmol Pi/min.

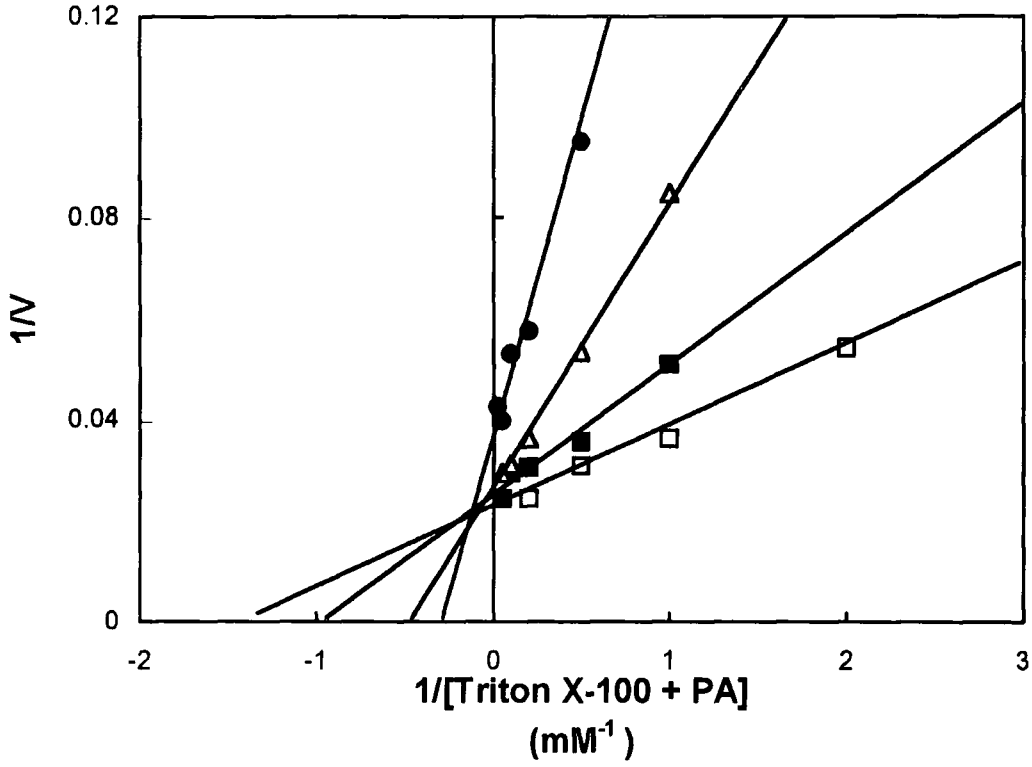

Figure 7.2: Demonstration of PAP saturation kinetics with varying bulk substrate concentration at fixed surface concentration of PA. A double reciprocal plot of the results from Figure 7.1 was constructed for each surface concentration (mole fraction) of PA: (□)0.111; (■) 0.0588; (△) 0.0303; (●) 0.0154. The lines drawn are the results of a least-squares analysis of the data.

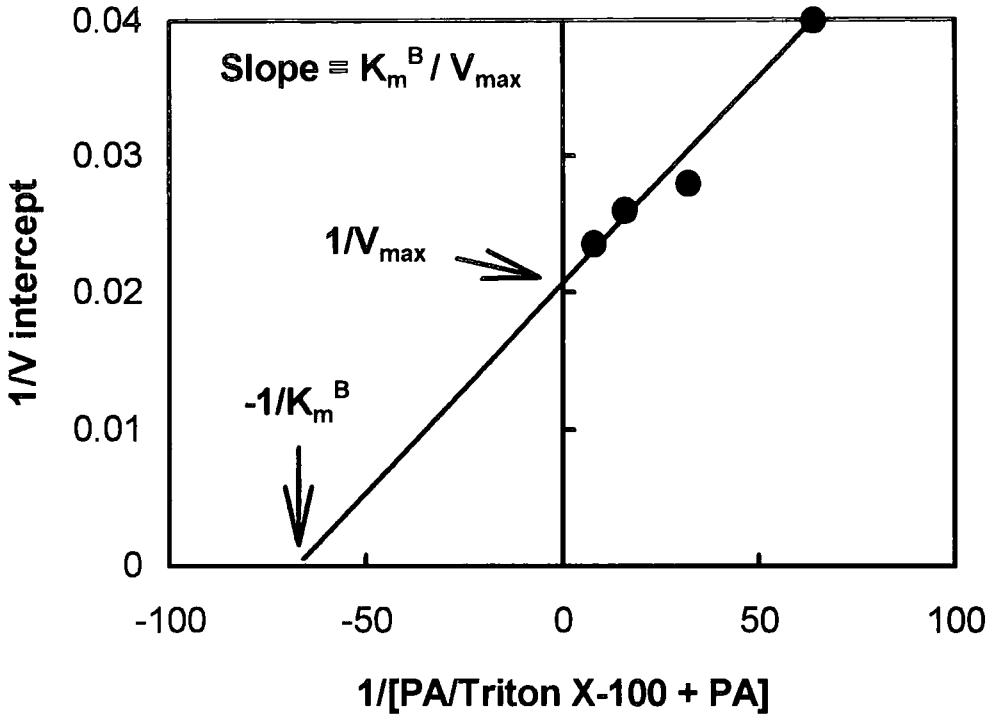

Figure 7.3: The derivation of V_{max} and interfacial Michaelis Constant for PAP. A replot of the 1/V intercepts from Figure 7.2 *versus* the reciprocal of the PA mole fraction was constructed. The kinetic values of V_{max} and K_m^B were calculated from the axes intercepts, using the equations as indicated. Values for V_{max} and K_m^B for dioleoyl-PA were calculated as 47Units/mg protein and 0.0149mole fraction, respectively. The line is the result of a least-squares analysis of the data.

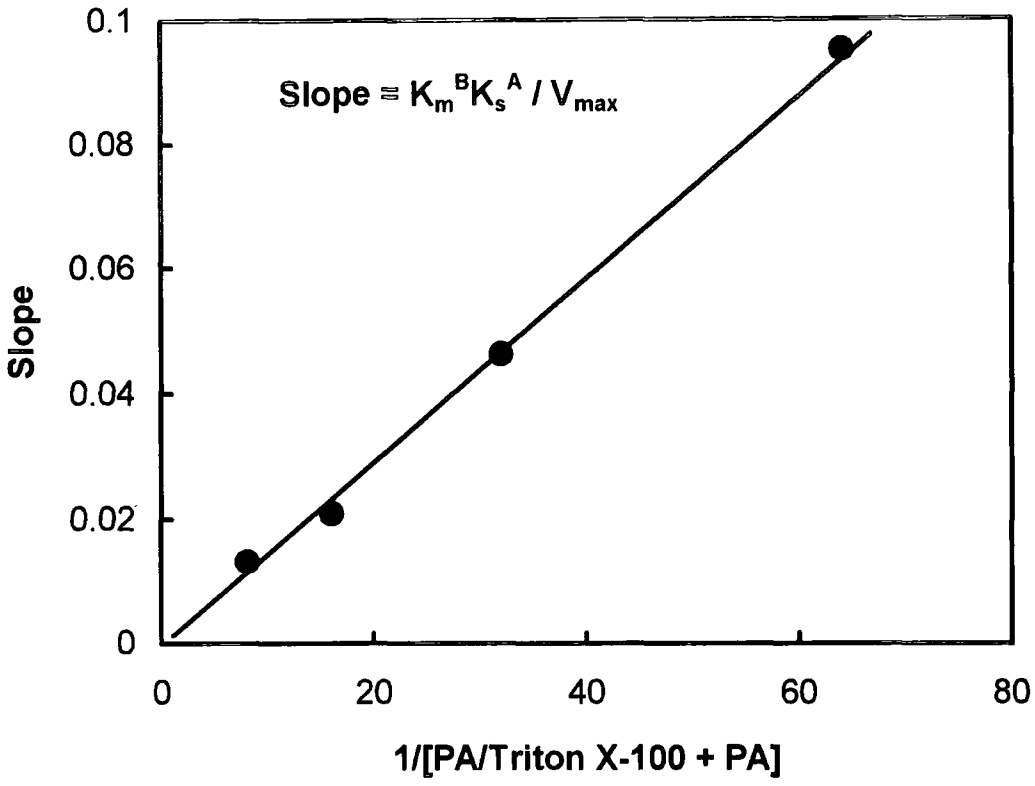

Figure 7.4: The derivation of the dissociation constant, K_s^A. A replot of the slopes obtained from Figure 7.2 *versus* the reciprocal of the PA mole fraction was constructed. K_s^A was calculated using the equation, as indicated, with the V_{max} and K_m^B previously derived (see Figure 7.3) and was 4.73mM. The line was drawn using a least-squares analysis of the data.

7.2.2 The activity of PAP according to the Dual Phospholipid model.

The data from the surface binding analysis was used to test the fit of the dual-phospholipid model (Hendrickson and Dennis, 1984; Carman *et al.*, 1995). In this way the analysis was investigating the ability of PAP to bind specifically and directly to the PA moiety and not the Triton X-100 components of the mixed micelles. The same data from Figure 7.1 was used but were plotted as PAP activity *versus* the bulk concentration of PA alone (Figure 7.5). PAP exhibited typical saturation kinetics with respect to the bulk concentration of PA. The decrease in the PA mole fraction caused a decrease in the apparent V_{max}. However, the difference of each PA surface dilution on PAP activity was not as noticeable as in the surface binding analysis (as was shown in Figure 7.1). Above PA concentrations of 0.2mM and below 5mol%, PAP activity was independent of the bulk substrate concentration and became solely dependent on the surface concentration of PA.

A double reciprocal plot of the data was constructed of activity *versus* the molar concentration of PA at each set mole fraction of PA with the generation of straight lines (Figure 7.6). However these lines did not display an equilibrium-ordered pattern, as expected. Subsequent replots of the data to determine kinetic values of PAP was futile as the derivation of kinetic values of PAP would be erroneous. Therefore the dual phospholipid model was found to be inappropriate for PAP under these conditions, as it was difficult to derive meaningful secondary plots. PAP activity did not fit the dual phospholipid model and instead indiscriminately bound to the micelle surface (surface binding model). This same phenomenon has been reported in the surface dilution kinetic analysis of PA Kinase from *Catharanthus roseus* (Madagascan periwinkle) towards Triton X-100/PA mixed micelles (Wissing *et al.*, 1994).

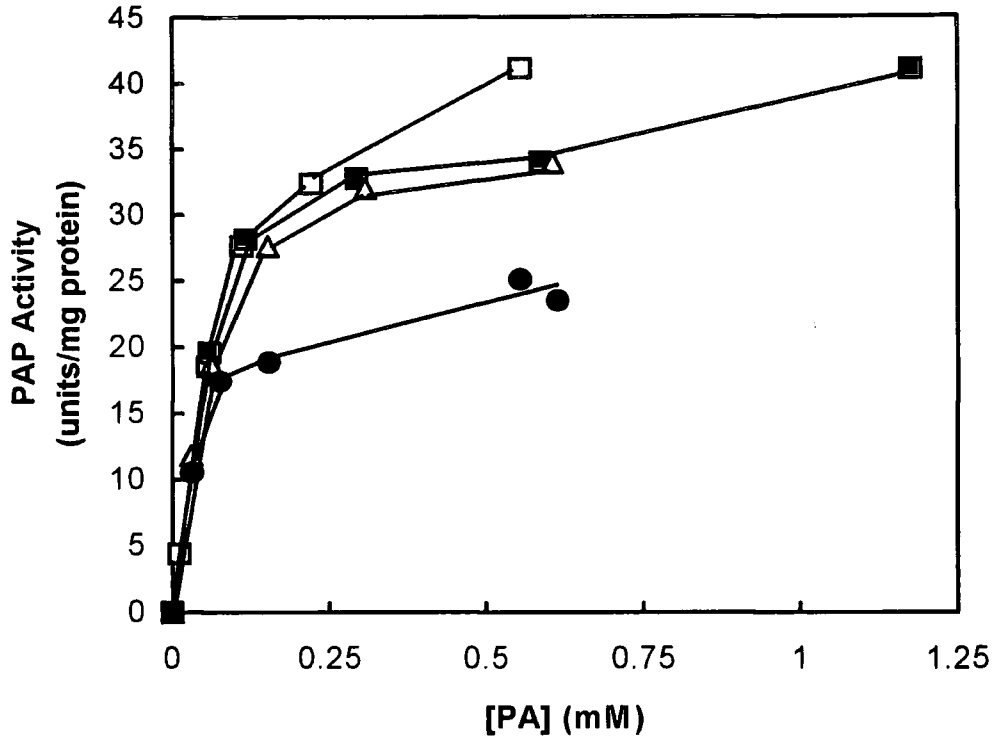

Figure 7.5: Activity of PAP towards dioleoyl-PA in Triton X-100 mixed micelles according to the 'phospholipid binding model.' The data from Figure 7.1 was analysed with the dual phospholipid model. PAP activity was measured as a function of the molar concentration of PA at the following set PA mole fractions: (□)0.111; (■) 0.0588; (△) 0.0303; (●) 0.0154.

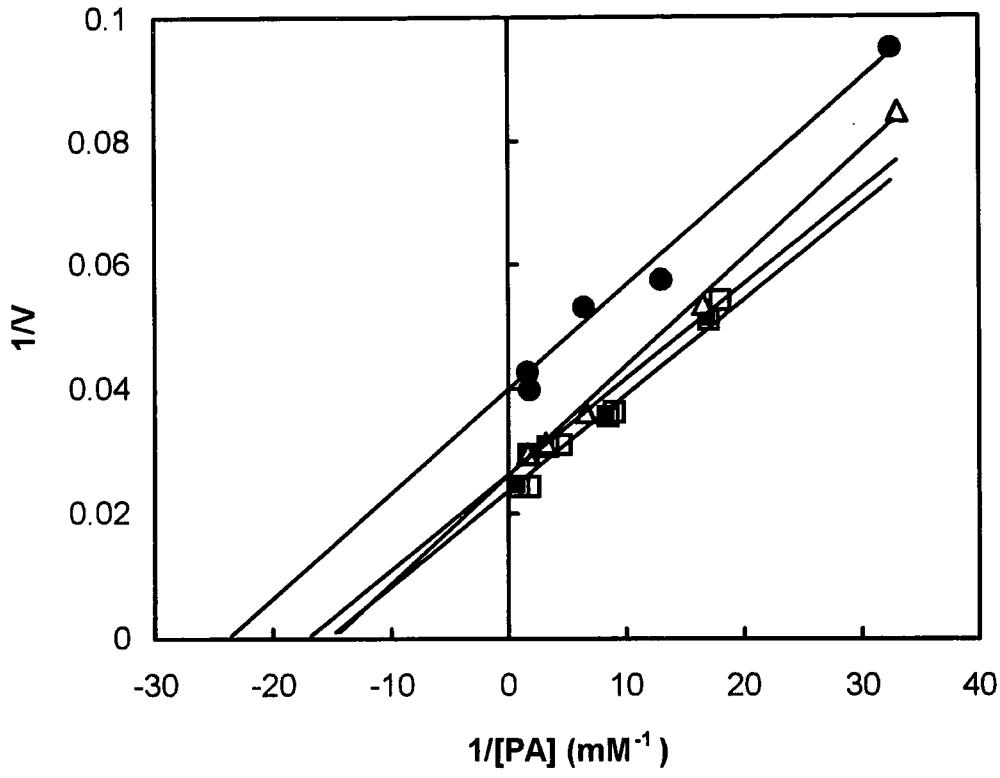

Figure 7.6: The double-reciprocal plot of the data from Figure 7.5. The reciprocal plot of PAP activity *versus* the bulk concentration of PA was constructed. The pattern of the lines, although linear, was not indicative of an equilibrium-ordered reaction, eliminating the suitability of the dual phospholipid model for PAP catalysis.

It was therefore assumed that PAP fits the surface binding model, where the enzyme associates with the mixed micelle in a non-specific manner, prior to the specific association to PA.

7.3 The kinetic analysis of homogenous PAP towards oleoyl-LPA in Triton X-100 mixed micelles.

In order to understand the relative substrate specificity of PAP towards PA and LPA, the surface dilution kinetic model was applied with *sn*-1-oleoylglycerol-3-phosphate (oleoyl-LPA) in mixed micelles of Triton X-100. Both the surface binding and the dual phospholipid models were investigated, using the identical conditions as for PA before. In this way the kinetic values for LPAP activity could be measured under the identical physical conditions that were used in the analysis of PAP activity.

7.3.1 The activity of LPAP according to the surface binding model.

LPAP activity was measured as a function of the sum of the molar concentrations of Triton X-100 and oleoyl-LPA at a series of fixed LPA surface dilution's. LPAP activity increased with bulk concentration of substrate and showed typical saturation kinetics (Figure 7.7). As seen with PAP activity, if the LPA mol% was decreased, a decrease in V_{max} was observed, indicating surface dilution of the substrate.

A double-reciprocal plot of the data from Figure 7.7 was constructed (Figure 7.8) and the pattern of lines was indicative of an equilibrium-ordered step. The 1/V intercepts and the slopes from Figure 7.8 were plotted *versus* 1/LPA mole fraction

(Figures 7.9 and 7.10). The resulting lines were linear, and used for the calculation of the various kinetic constants, as before. From the data in Figure 7.9, the V_{max} and the K_m^B were calculated as being 100Units/mg protein and 0.0106 mole fraction (1.06 mol%), respectively. The dissociation constant for the mixed micelle binding site (K_s^A) was calculated as before as 26.3mM, from the slope of Figure 7.10. The line in Figure 7.10 passes through the origin, as predicted by the surface binding model. As for PAP activity, LPAP fits the bulk binding model of the Surface Dilution Kinetic scheme.

The same assumptions as used for the analysis of LPA as were applied for PA, regarding the size and aggregation number of the mixed micelles, area of each micelle, the surface area of Triton X-100 was analogous to LPA and remained constant throughout the experiment, and the enzyme binding site remained constant. One additional assumption is made: LPA is sparingly soluble in water and it is assumed that this amount of soluble LPA is negligible in the presence of Triton X-100 mixed micelles. This assumption was considered valid because the addition of detergent caused a reduction in the activity and thus shows that LPA is surface active. If the concentration of soluble LPA was high, the phenomenon of surface dilution would not occur. It was therefore assumed that the measured LPA hydrolysis was at the micelle-water interface.

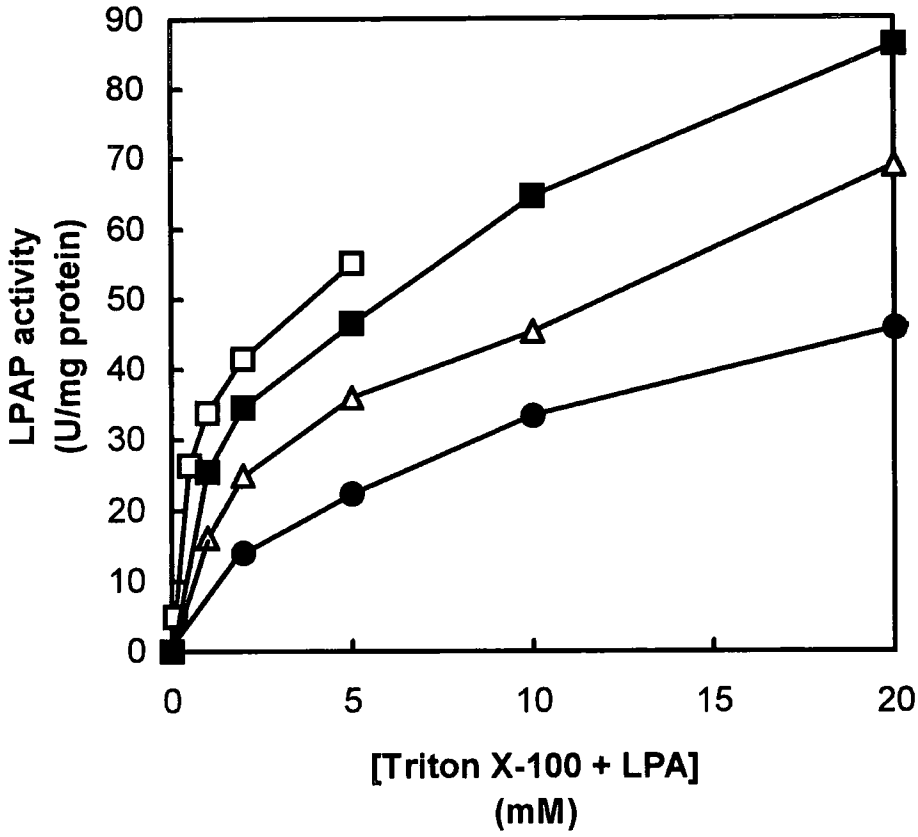

Figure 7.7: Activity of LPAP towards oleoyl-LPA in mixed micelles with Triton X-100 according to the surface binding model. LPAP activity was measured as a function of the sum of the molar concentrations of Triton X-100 plus LPA at the following set mole fractions of LPA: (□)0.111; (■) 0.0588; (△) 0.0303; (●) 0.0154. All assays were conducted in duplicate in the otherwise standard assay conditions, with the mean data shown (with an experimental variance of ≤ ±5%). One unit of LPAP activity was defined as the amount of enzyme required to catalyse the formation of 1μmol Pi/min.

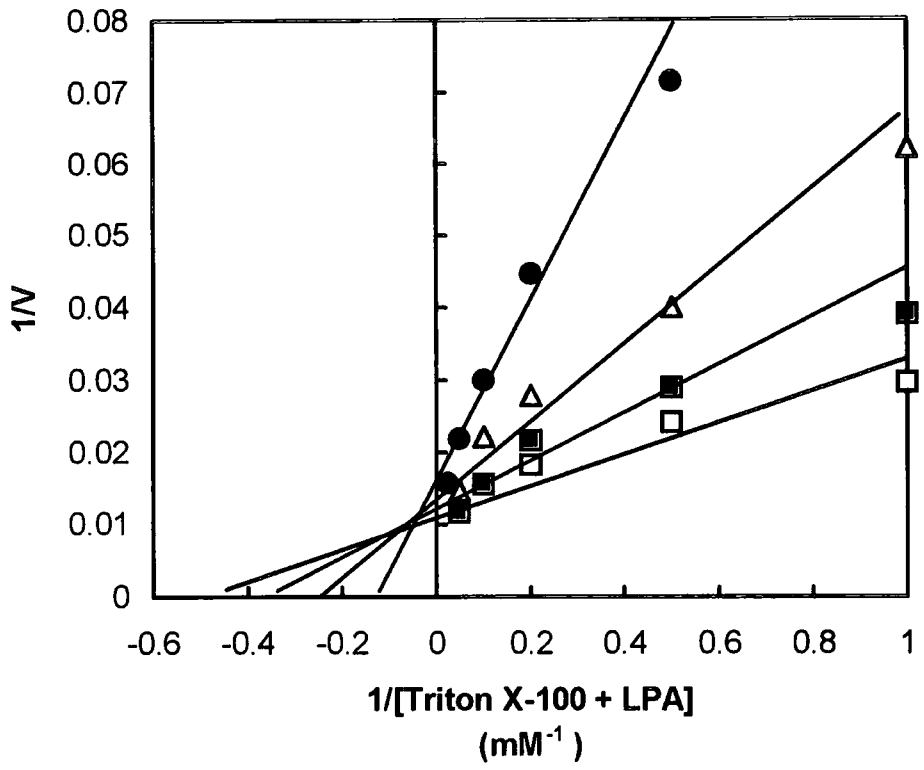

Figure 7.8: Demonstration of LPAP saturation kinetics with varying bulk substrate concentration at fixed surface concentration of LPA. A double reciprocal plot of the results from Figure 7.7 was constructed for each surface concentration (mole fraction) of LPA: (□)0.111; (■) 0.0588; (△) 0.0303; (●) 0.0154. The lines drawn are the results of a least-squares analysis of the data.

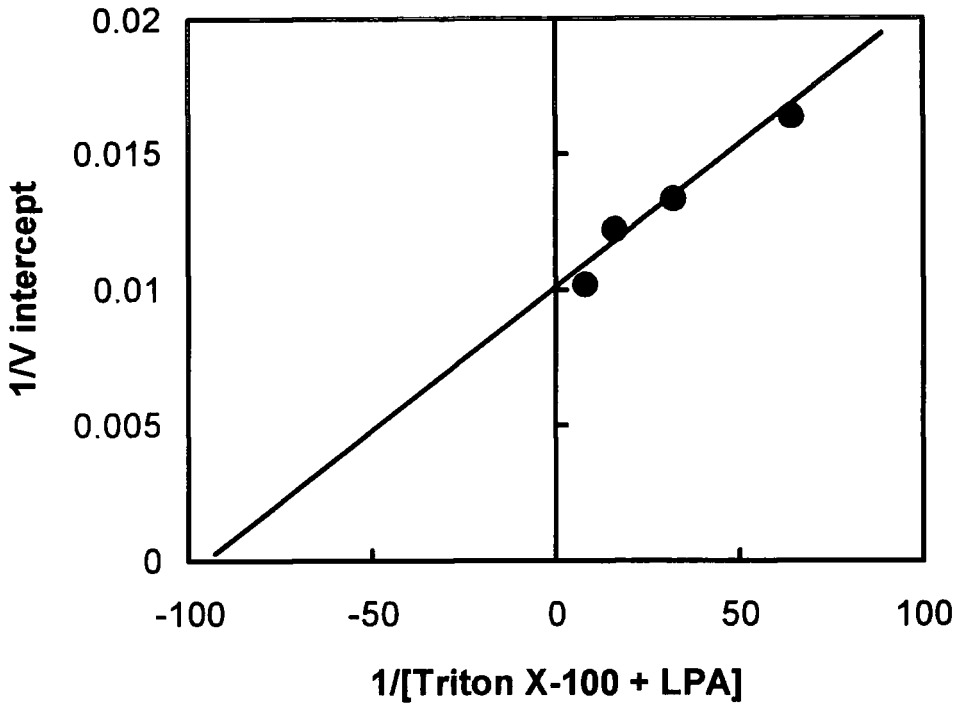

Figure 7.9: The derivation of V_{max} and interfacial Michaelis Constant for LPAP activity. A replot of the 1/V intercepts from Figure 7.8 *versus* the reciprocal of the LPA mole fraction was constructed. The kinetic values of V_{max} and K_m^B were calculated from the axes intercepts, using the equations as indicated previously. Values for V_{max} and K_m^B for oleoyl-LPA were calculated as 100μmol/min/mg protein and 0.0106 mole fraction, respectively. The line is the result of a least-squares analysis of the data.

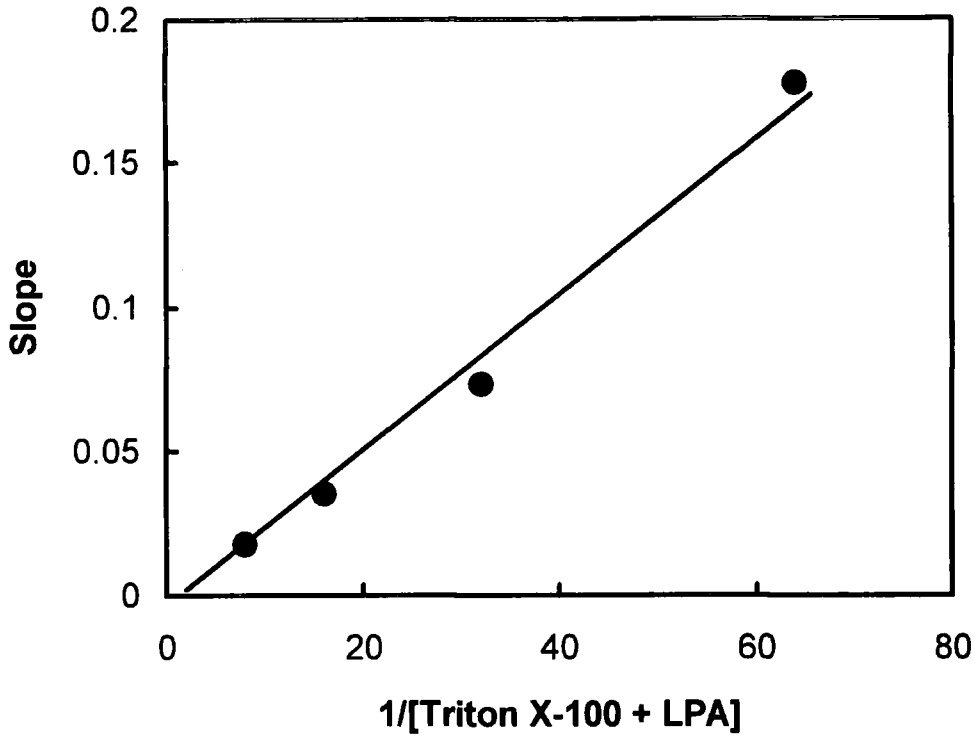

Figure 7.10: The derivation of the dissociation constant, K_s^A for LPAP activity. A replot of the slopes obtained from Figure 7.8 *versus* the reciprocal of the LPA mole fraction was constructed. The line was drawn using a least-squares analysis of the data. Using the gradient of the line and the V_{max} and K_m^B values, the dissociation constant (K_s^A) was calculated as 26.3mM using the equation:

slope = $K_m^B K_s^A / V_{max}$.

7.3.2 The activity of LPAP according to the Dual Phospholipid model.

As in the kinetic analysis PAP activity, the ability of LPAP activity to fit the dual phospholipid model was investigated, using the data from Figure 7.7. LPAP activity was plotted *versus* the bulk concentration of LPA (Figure 7.11). LPAP exhibited typical saturation kinetics with respect to the bulk concentration of LPA. The decrease in the LPA mole fraction appeared to have no significant effect on LPAP activity, with no change in the V_{max} observed, within the bulk LPA concentration tested.

A double reciprocal plot of the data was constructed of activity *versus* the molar concentration of LPA at each set mole fraction of LPA with the generation of straight lines (Figure 7.12). However these lines did not significantly display an equilibrium-ordered pattern. Therefore the dual phospholipid model was found to be inappropriate for LPAP under these conditions, as it would be difficult to derive secondary plots.

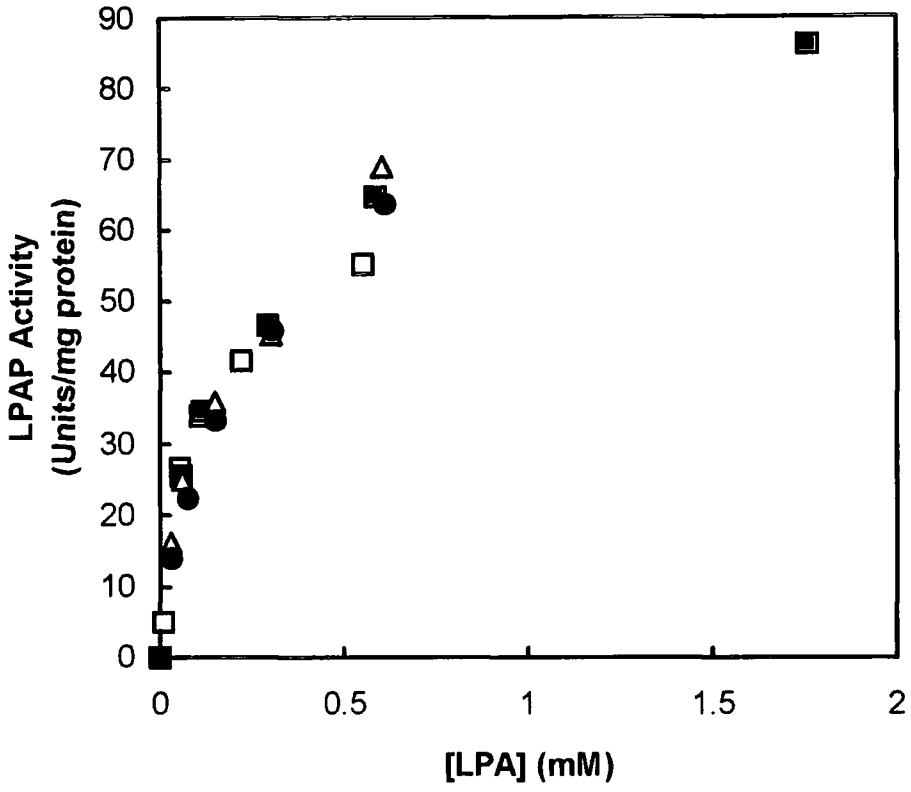

Figure 7.11: Activity of LPAP towards oleoyl-LPA in Triton X-100 mixed micelles according to the 'phospholipid binding model.' The data from Figure 7.7 was analysed with the dual phospholipid model. LPAP activity was measured as a function of the molar concentration of LPA at the following set LPA mole fractions: (□)0.111; (■) 0.0588; (△) 0.0303; (●) 0.0154. Lines were not added to the plot as they were considered both unnecessary and interfering.

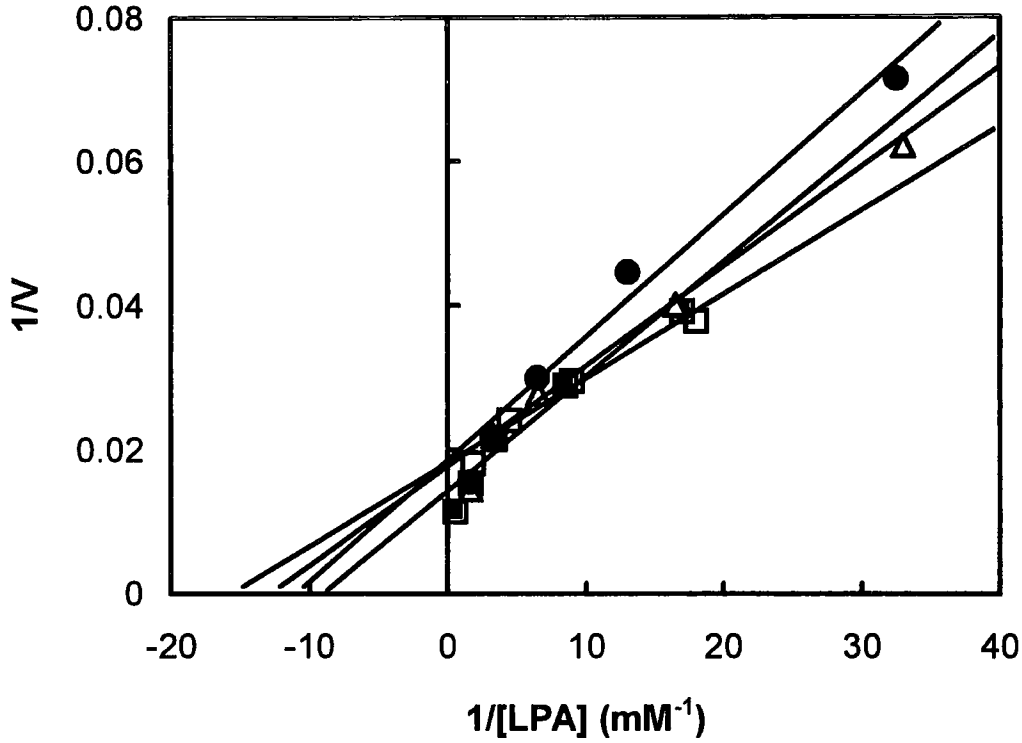

Figure 7.12: The double-reciprocal plot of the data from Figure 7.11. The reciprocal plot of LPAP activity *versus* the bulk concentration of LPA was constructed. The pattern of the lines, although linear, was not significantly indicative of an equilibrium-ordered reaction, eliminating the suitability of the dual phospholipid model for PAP catalysis.

A summary of the catalytic constants obtained from the bulk surface model for PA and LPA hydrolysis is shown in Table 7.1.

Substrate	V_{max} Units/mg	K_s^A mM	K_m^B mole fraction	V_{max}/K_m^B	K_{cat} sec^{-1}
Dioleoyl-PA	47	4.73	0.0149	3154	38
1-Oleoyl-LPA	100	26.3	0.0106	9434	82

Table 7.1: Summary of the catalytic constants, derived from the Surface Dilution Kinetic model. Values of V_{max}, interfacial Michaelis constant (K_m^B), dissociation constant (K_s^A), specificity constant (V_{max}/K_m^B) were calculated from the kinetic plots. The turnover number (K_{cat}) was calculated using the V_{max} and the PAP molecular mass of 49kDa. One unit of enzymatic activity was defined as the amount of enzyme required to catalyse the formation of 1μmol Pi/min.

7.4 The study of LPA inhibition of PAP activity with the surface dilution kinetic model.

The surface dilution kinetic model has been found effective in the study of activation and inhibition of immobilised enzymes with surface active compounds and aqueous soluble ions and co-factors (Walsh and Bell, 1986; Bae-Lee and Carman, 1990; Buxeda *et al.*, 1991; Yu and Dennis, 1992; Wu *et al.*, 1993; Carman *et al.*, 1995). The general method for analysing interfacial inhibition by surface active compounds in mixed micellar systems was originally proposed by Yu and Dennis (1992).

The kinetics of PA hydrolysis of avocado homogenous PAP was examined in the presence of various fixed surface concentrations of LPA. The bulk concentration

of PA in all assays was maintained at 0.2mM, with the activity measured as a function of PA surface concentration in Triton X-100 mixed micelles. At this concentration (in up to a 4mol% surface concentration), PAP activity was only dependent on the surface concentration of PA (as was shown in Figure 7.5). As the K_m value for PA was 1.49 mol%, the surface concentration of PA was used in the range of 0.4-4 mol%. This enabled a larger change in activity to be observed with the addition of LPA, throughout the analysis (Bae-Lee and Carman, 1990), because at substrate concentrations approximating the K_m value, the catalysis is responsive to changes in the concentration of substrate (Engel, 1977).

[^{32}P]PA (20 nmoles, 15 000DPM/nmole, 0.2mM final concentration) in $CHCl_3$ was added to each assay tube and the $CHCl_3$ removed under a stream of N_2 gas. Stock solutions of Triton X-100/LPA were prepared as 100mM (Triton X-100 + LPA), at various surface concentrations of LPA. Increasing amounts (5-50µl) of Triton X-100/LPA was added to the assay tubes. The other constituents of the standard assay mixture were added to 100µl, and each tube vigorously mixed, prior to reaction initiation with the addition of homogenous PAP (6.1ng/reaction). In this way, PAP was measured as a function of the surface concentration of PA (i.e. PA dilution in Triton X-100/LPA micelles) at various fixed surface concentrations of LPA. The effect of LPA on the kinetics of PA hydrolysis is shown in Figure 7.13. In the absence and presence of LPA, PAP activity showed typical saturation kinetics as expected. With increased surface concentrations of LPA, an increase in the apparent K_m of the reaction was observed. A double reciprocal plot of the data was constructed (Figure 7.14). LPA did not effect the V_{max} value but did cause an increase in the apparent K_m for PA. The pattern of lines was consistent with LPA being a competitive inhibitor of PA hydrolysis. PAP was inhibited by LPA in a dose-dependent manner. The addition of LPA increased the slope of each double-reciprocal plot. A replot of the slopes from Figure 7.14 was constructed *versus* the LPA mol% (Figure 7.15). The LPA mol% axis intercept was used to calculate the K_i value for LPA of 1.4mol%.

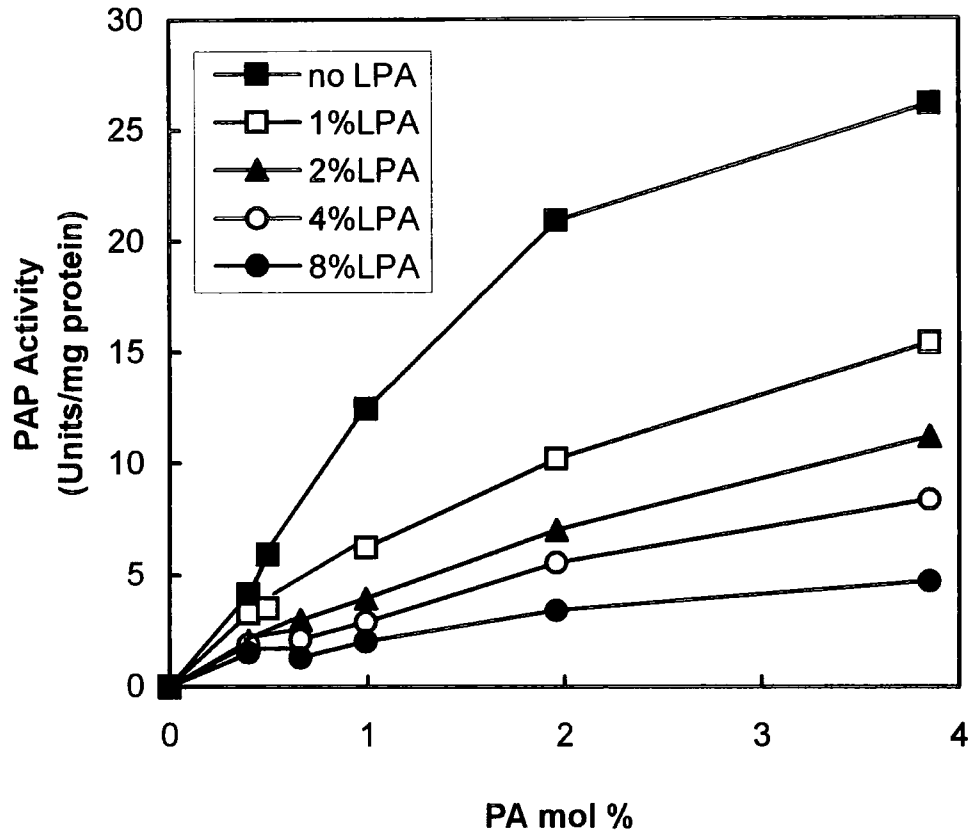

Figure 5.13: The effect of LPA on the kinetics of PA hydrolysis. PAP activity was measured as a function of the surface concentration (mol%) of PA at the following set surface concentrations (mol%) of LPA: (■) 0; (□) 1; (▲) 2; (○) 4; (●) 8. In all assays, the bulk concentration of PA was 0.2mM. The assays were conducted in duplicate, with the mean data shown (with a variance of ≤ 5%). One unit of PAP activity was defined as the amount of enzyme required to catalyse the formation of 1μmol Pi/min.

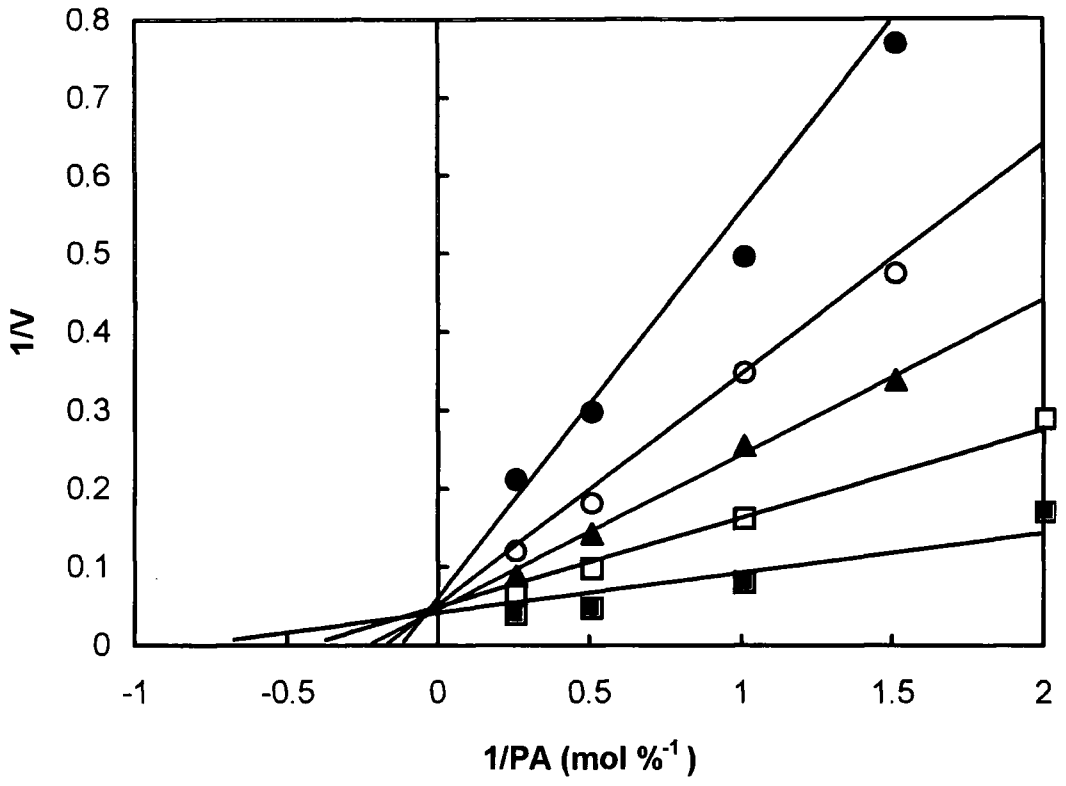

Figure 7.14: Demonstration competitive inhibition of PA hydrolysis by LPA. A double -reciprocal plot was constructed using the data from Figure 7.13 for each LPA surface concentration (mol%): (■) 0; (□) 1; (▲) 2; (○) 4; (●) 8. The *lines* drawn are a result of a least squares analysis of the data.

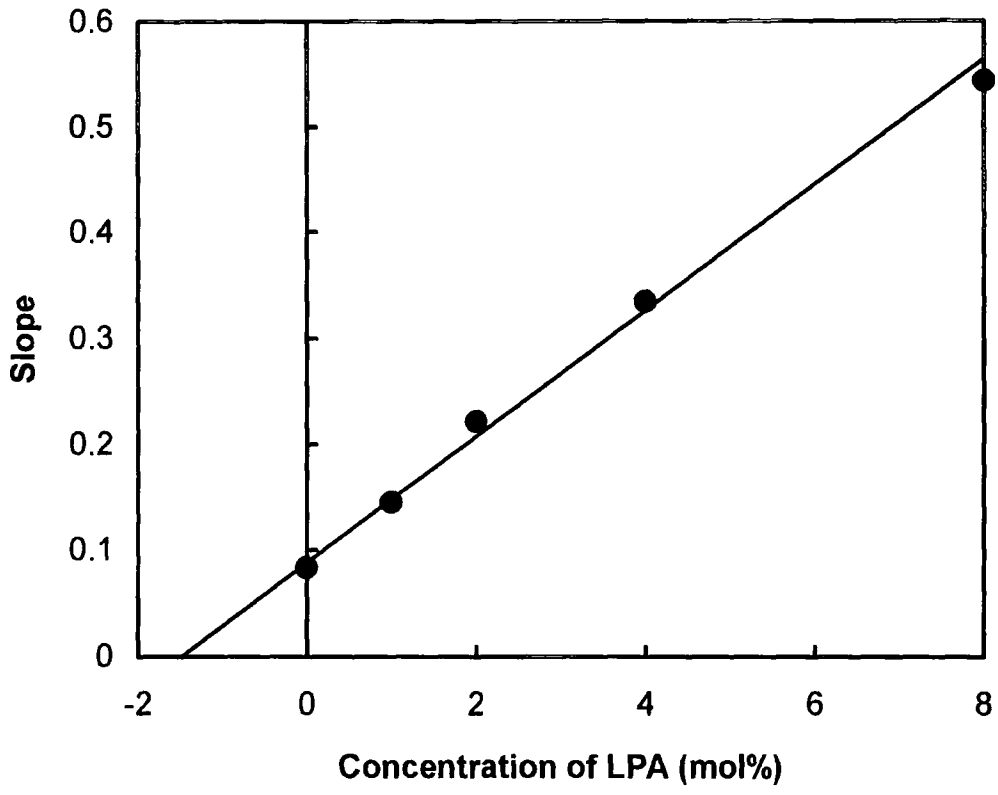

Figure 7.15: The determination of the K_i value for LPA competitive inhibition of PAP activity. A replot of the slopes obtained in Figure 7.14 *versus* the LPA surface concentration (mol%) was constructed. The line drawn is a result of a least squares analysis of the data. The K_i value for LPA was derived from the -LPA mol% axis intercept, and calculated as 1.4mol% LPA.

As discussed by Yu and Dennis (1992), this inhibition model assumes that the enzyme has equal access to both PA and LPA, with a negligible concentration of monomeric LPA. In this experiment, the LPA and PA would be evenly dispersed throughout the mixed-micelles (Robson and Dennis, 1983), and every lipid molecule was present at the interface and theoretically able to interact with the PAP protein (Verger, 1980). In this case the inhibition would only occur at the interface (site of reaction). It was also assumed that the addition of LPA to the Triton X-100/PA mixed micelles would not disrupt the micelle structure. During the experiment a maximum of 12mol% LPA + PA was used. It was therefore concluded that the micelles were uniform in structure throughout all mole fractions of PA and LPA tested.

7.5 The hydrolysis of *sn*-2-oleoyl-LPA and ceramide-1-phosphate

As shown earlier in this chapter, PAP hydrolysed *sn*-1-oleoyl-LPA. This indicated that PAP activity was independent of the presence of an acyl moiety in position *sn*-2 for catalytic activity, and had little substrate specificity. The ability for PAP to hydrolyse *sn*-2-oleoyl-LPA was examined in an attempt to determine the acyl-positional preference (if any) of PAP. *sn*-2-Oleoyl-LPA has the acyl moiety attached to the *sn*-2 position of the glycerol back bone, with no acyl group attached at position *sn*-1.

Ceramide-1-phosphate has a conformational resemblance to PA (Figure 7.16). The ability for PAP to hydrolyse ceramide-1-phosphate was also investigated in order to determine the specificity of PAP. It has recently been reported that an NEM-insensitive, Mg^{2+} independent 51kDa isoform of PAP from rat liver plasma membranes, can hydrolyse PA, LPA, ceramide 1-phosphate and sphingosine 1-phosphate (Waggoner *et al.*, 1996; Brindley and Waggoner, 1996). It was concluded that the enzyme in this system was more accurately described as a multifunctional lipid

phosphomonoesterase, and was believed to be involved in the regulation of lipid second messengers in cell activation and signal transduction. Considering the broad substrate specificity, a similar molecular mass, and the same NEM/Mg^{2+} catalytic profile it was possible that the PAP isoform identified in this study was the equivalent isozyme in plants. Ceramide-1-phosphate and *sn*-2-oleoyl-LPA were used in order to assess the discriminatory nature of homogenous PAP, and to test the hypothesis that the PAP activity described here is a multifunctional lipid phosphomonoesterase, as found in rat liver plasma membrane (Waggoner *et al.*, 1995; Brindley and Waggoner, 1996).

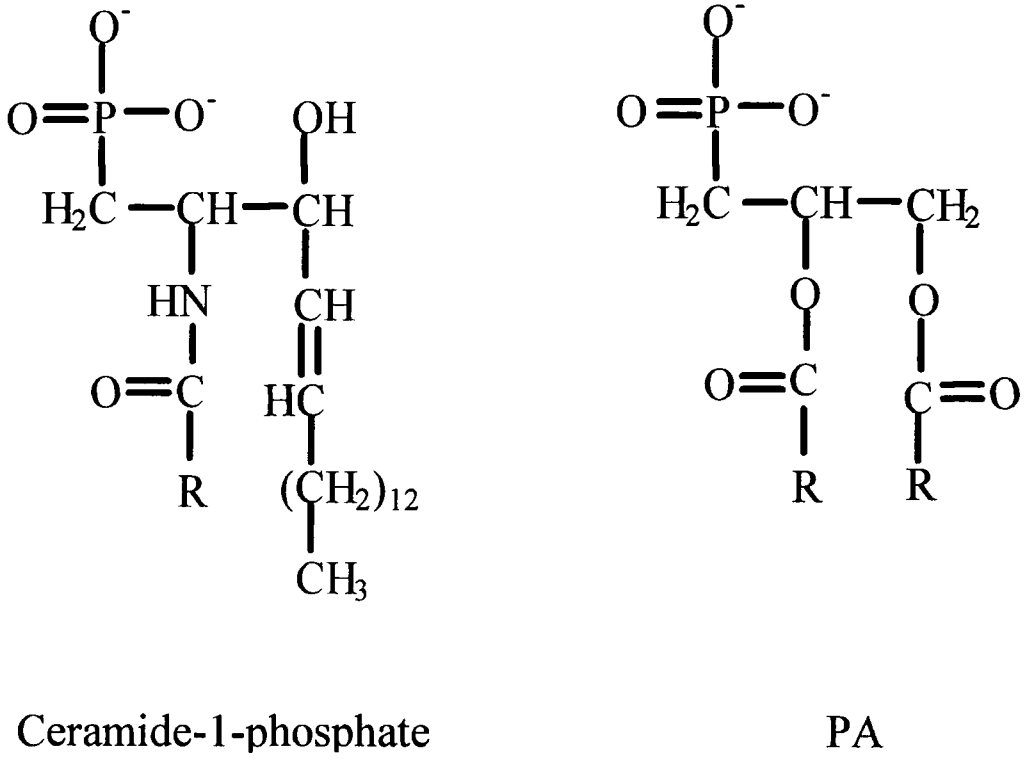

Figure 7.16: The structural similarity of ceramide-1-phosphate to PA.

Ceramide-1-[^{32}P]phosphate and *sn*-2-oleoylglycerol-3-[^{32}P]phosphate were synthesised from [γ-^{32}P]ATP and ceramide or *sn*-2-oleoylglycerol, respectively with DAG kinase, following the procedure of Waggoner *et al.* (1996) as described under *Materials and Methods*, Chapter 2.2.4. The final specific activities of each freshly

synthesised substrate was 11 000 CPM/nmol.. As was shown earlier in this chapter, PAP activity is dependent on both the surface and bulk substrate concentration. The aim of this experiment was to measure the PAP-catalysed hydrolysis of ceramide-1-phosphate and *sn*-2-LPA. PAP activity was assayed with increasing amounts of bulk substrate/Triton X-100 with the surface concentration of the substrate maintained at 20mol%. In this way, PAP activity was measured as a function of the bulk substrate concentration alone. This was because an activity profile relative to *sn*-1-LPA and PA and not a detailed kinetic analysis of each substrate was desired.

Assays were prepared in duplicate with various bulk concentrations of dioleoyl-PA, *sn*-1-oleoyl-LPA, *sn*-2-oleoyl-LPA and ceramide-1-phosphate in Triton X-100 mixed micelles (11.1mol% substrate), using the otherwise identical the standard avocado assay procedure (as described under *Materials and Methods*, Chapter 2.3.2). As shown in Figure 7.17, PAP hydrolysed all four substrates. However, in comparison to PA and *sn*-1-LPA, ceramide-1-phosphate and *sn*-2-LPA were very poorly hydrolysed. PAP activity with 500μM ceramide-1-phosphate and *sn*-2-LPA was about 4.5-fold lower than for either PA or *sn*-1-LPA.

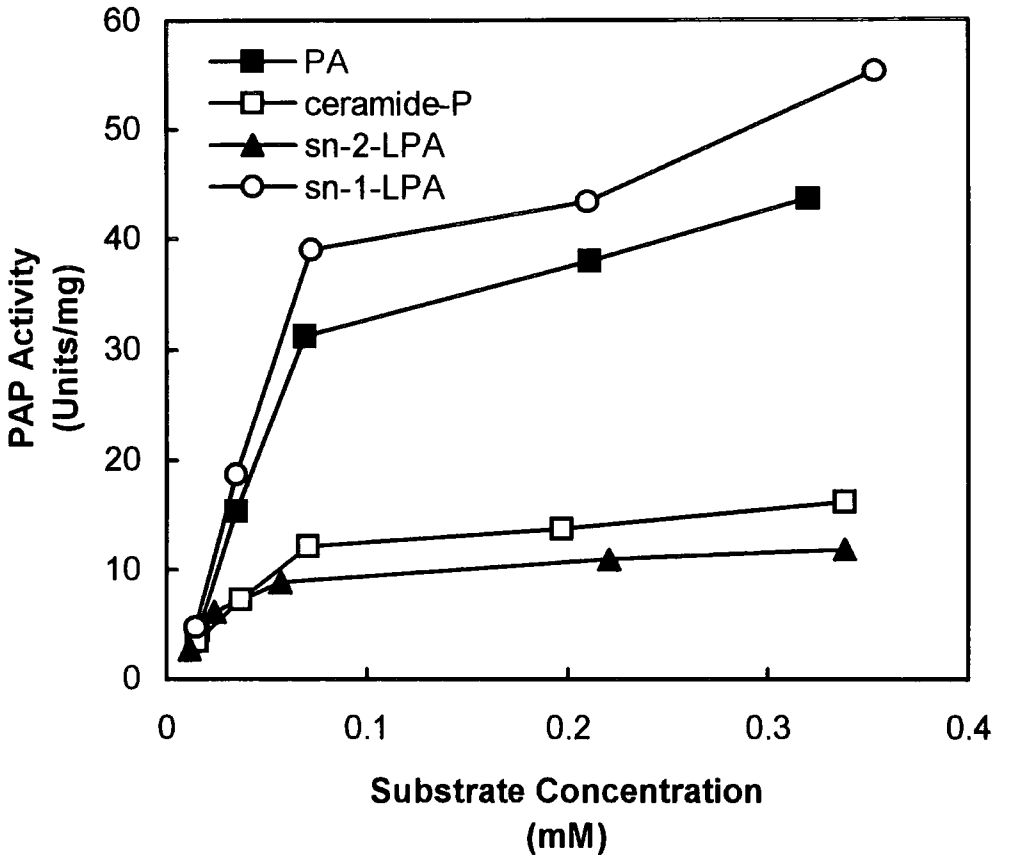

Figure 7.17: The substrate specificity of PAP. PAP activity was measured by following the release of [^{32}P]Pi from various concentrations of PA, *sn*-1-LPA, *sn*-2-LPA and ceramide-1-phosphate in mixed micelles of Triton X-100 using the otherwise standard avocado assay procedure described in Chapter 2.3.2. The surface concentration of all substrates was maintained at 11.1mol% throughout. The data are the mean results of duplicate experiments (variance $\leq$5%). One unit of enzymatic activity was defined as the amount of enzyme required to catalyse the formation of 1μmol Pi/min.

7.6 Discussion

As was demonstrated earlier in this study, the PAP-catalysed hydrolyses of PA and LPA occur at a lipid-water interface. The substrates are insoluble in water and buried within the membrane. It has been shown that the microsomal PAP isoform is membrane-associated. It is therefore clear that a kinetic model designed for aqueous soluble enzymes and it's substrates would therefore be inappropriate in the study of microsomal PAP. In enzymes that follow Michaelis-Menten kinetics, in which the substrates are aqueous soluble, the substrate concentration is 3-dimensional in character and is expressed in terms of molarity. In reactions that contain surface active substrates (i.e. insoluble or partially soluble), the reaction occurs at the interface where the substrate concentration has a 2-dimensional character, the 'quality of the interface' is crucial to the success of catalysis. The definition and measurement of the concentration of insoluble substrates presents the first obstacle and difference in interfacial enzyme kinetic studies (Verger, 1980). For this reason a detailed kinetic analysis of the enzyme was conducted using the Surface Dilution Kinetic model, which was designed for the action of phospholipase on immobilised substrates.

There are several physical considerations that need to be addressed experimentally, before the kinetic analysis can be conducted (Carman *et al.*, 1995). As the catalysis is measured as a function of the surface dilution of substrate, the other interfacial components (Triton X-100 in this case) should be neutral dilutors that do not interact with the catalytic sites of the enzyme. The mixed micelles should be homogenous in shape and form at all surface concentrations of substrate. In this study, these experiments were unnecessary because the structure and physical characteristics of Triton X-100/PA mixed-micelles (Lin and Carman, 1990) and Triton X-100/Lysophospholipid mixed micelles (Bhat *et al.*, 1994) have already been examined. Like most phospholipids, the addition of up to 15mol% PA/LPA had little

effect on the micelle size and the mixed micelles were analogous in structure to pure Triton X-100 micelles (Robson and Dennis, 1983).

The surface dilution model was applied to homogenous avocado microsomal PAP with PA and LPA as individual substrates, and the data analysed according to the bulk surface and dual-phospholipid binding models of the scheme. For both PA and LPA, enzyme activity fitted the bulk surface model, allowing the derivation of catalytic values for V_{max}, interfacial Michaelis constant, dissociation constant and specificity constant for each substrate.

As reflected in the dissociation constants (K_s^A, or equilibrium constants for non-specific binding) of the two micellar substrates, the PAP protein had a higher affinity for Triton X-100 mixed micelles containing PA. The affinity for Triton X-100/LPA mixed micelles was nearly 6-fold lower than for Triton X-100 mixed micelles. This suggests that the PAP protein requires two acyl moieties for tight association to the micelle surface, most likely through hydrophobic interaction. If PAP was an integral membrane protein, it would be assumed that that the concentration of 'free' enzyme would be very low (Wissing *et al.*, 1994). The dissociation constants for both substrates were relatively high, which is indicative of membrane-association. The dissociation constant value for dioleoyl-PA was similar (2.4mM) to that obtained by Lin and Carman (1990) for PAP from *Saccharomyces cerevisiae*, which was also a membrane associated protein.

The interfacial Michaelis constant (K_m^B) of oleoyl-LPA was 0.0106mole fraction, which was equivalent to a ratio of LPA:Triton X-100 of 1:93. The K_m^B of dioleoyl-PA was higher and was equivalent to a ratio of PA:Triton X-100 of 1:66. The surface concentration required for LPA catalysis to reach half maximal rate was 1.4-fold lower than for PA. The V_{max} values for LPA hydrolysis was over 2-fold higher than for PA. This meant that the specificity constant of LPA was 3-fold higher

than for PA. The K_{cat} for LPA was 2-fold higher than for PA, showing that LPA is hydrolysed twice as fast as PA. These data clearly show that LPA was a better substrate than PA.

Had the kinetic analysis been conducted using the standard Michaelis-Menten model, this data would have been grossly inaccurate. It was shown in the previous chapter that at 20mol% LPA and PA catalysis was similar. A Michaelis-Menten analysis conducted with variable bulk substrate concentrations at this constant surface dilution, would have yielded identical values of V_{max} and K_m. This clearly demonstrates the limiting effectiveness of the Michaelis-Menten model for interfacial enzyme reactions.

The K_{cat} for the 91kDa PAP from *S.cerevisiae* was calculated as $100sec^{-1}$ using the V_{max} value (65μmol/min/mg) reported by Lin and Carman (1990). This shows that the potential speed for PA hydrolysis in yeast is faster than in avocado. The K_m value for dioleoyl-PA was 10-fold lower than the value reported for homogenous PAP from *S.cerevisiae*, whilst the V_{max} was similar (Lin and Carman, 1990). Many enzymes possess K_m values that approximate the *in vivo* concentration of the substrate (Engel, 1977). Avocado is an extremely rich source of glycerolipid and as such would be expected to have a large pool of the intermediates such as PA, during TAG synthesis. The K_m value for PAP was found to be low, possibly reflecting a low *in vivo* PA concentration. This suggests that PA does not accumulate within the membranes of avocado, implying that PAP is not the rate limiting step in TAG biosynthesis. There is no data available concerning the *in vivo* concentrations of PA in avocado microsomes. Wissing *et al.* (1994) reported that PA consisted of 1.5% of the total phospholipid pool in *Catharanthus roseus*. Assuming that this is not too dissimilar to avocado under normal 'housekeeping' conditions, the K_m value of PAP for PA (1.4mol%) is explained. The low K_m and K_{cat} values however do not agree with the possible high PA concentration and turnover during TAG biosynthesis. The K_m and K_{cat} values for

PAP are most likely not be the main factors governing the extent of PA dephosphorylation and the overall metabolic flux of TAG biosynthesis. As demonstrated by Ichihara *et al.* (1990), PAP undergoes translocation between the cytosol and microsomal fractions in safflower. The cytosol forms a physiologically inactive reservoir of PAP protein because in this compartment, the enzyme has no access to the membrane integrated substrate. In this case the low K_m and K_{cat} for PA reflect the steady-state concentrations of PA under normal 'housekeeping' conditions. Upon the generation of a larger pool of PA or a greater demand for PA hydrolysis (i.e. during TAG biosynthesis), the enzyme's active sites would become rapidly saturated causing the rate limitation of the pathway. The translocation would generate more active sites, consequently alleviating the substrate saturation and rectifying the metabolic flux bottleneck. The low K_m and K_{cat} therefore could serve to make the translocation an effective means of controlling the metabolic flux of TAG biosynthesis. As was shown in chapter 5, the identification of high levels of PAP protein in the cytosolic compartment further demonstrates translocation to be a highly efficient regulatory mechanism in the control of PA hydrolysis. The presence of high levels of PAP protein in the physiologically inactive compartment allows the rapid alleviation of PA during increased glycerolipid metabolism.

LPA was found to be a more effective catalytic substrate than PA. This indicates that the enzyme is unspecific with regard to the presence of an acyl group in the *sn*-2 position of the glycerol back bone. The observation of this dual substrate specificity raises a fundamental problem in TAG biosynthesis. If the enzyme can use both LPA and PA as the substrate, with a preference for LPA (even in saturating PA concentrations), the Kennedy pathway could never be completed. This is clearly not the case *in vivo*. Various explanations can be found to rationalise these experimental results to the situation *in vivo*. There could be substantial structural differences between the purified and microsomal enzyme. The closest possible way to simulate the *in vivo* situation was to test fresh microsomal preparations for the ability to hydrolyse

both substrates (as shown in Chapter 6). The same ratio of product release from both substrates was seen, as with the homogenous enzyme, indicating that LPA hydrolysis can not be attributed to PAP solubilisation. This also eliminates the possibility of the emergence of an otherwise undetected activity upon detergent solubilisation, as seen in the solubilisation of spinach microsomal glycerol-3-phosphate acyltransferase (Frentzen, 1990). In this case, Tween-40/NaCl solubilisation induces a latent enzymatic activity with a different positional specificity and causes the production of *sn*-2-acylglycerol-3-phosphate.

The difference of the two substrates catalysis may lie in the accessibility of the two substrates at the mixed micelle interface. The dissociation constants for LPA and PA were high, indicating PAP-association but not integration into the mixed micelles. LPA has only one acyl chain and as such may not be as highly incorporated within the micelle as PA, and could therefore be more accessible to the active site that may not be buried within the detergent micelle. Thus the hydrophobicity of the substrates at the interface may be the reason for the differing catalytic rates.

Monoacylglycerol, one of the products of LPA dephosphorylation has strong detergent properties and could theoretically perturb membrane integrity if in sufficient quantities. These findings show that *in vitro* rates of LPA dephosphorylation are higher than for PA. A mechanism for preventing LPA dephosphorylation would therefore be required for the biosynthesis of triacylglycerol and the preserved integrity of the membrane. The concentration of LPA is believed to be low in plant microsomes, due to activities of glycerol-3-phosphate and lysophosphatidate acyltransferases (Frentzen, 1993). Sun *et al.* (1988) showed that microsomes prepared from the developing seeds of palm, maize and rape were able to synthesise TAG from glycerol-3-phosphate and oleoyl-CoA *in vitro*. Labelling studies revealed that the steady state concentration of LPA was consistently low in all samples throughout the time course. This was in direct contrast to the other TAG

intermediates; PA levels increased sharply and then decreased in maize and rape samples; whilst DAG increased in all samples.

LPA was also found to competitively inhibit PA hydrolysis. The K_i value (1.4mol%) for LPA was near to the K_m for PA (1.5mol%), suggesting an *in vivo* requirement of LPA and PAP segregation. Discreet metabolic channelling between the enzymes of the Kennedy pathway would prevent this premature dephosphorylation or inhibition during the synthesis of triacylglycerol. As shown in the model presented in Figure 7.18, the spatial organisation of the Kennedy pathway enzymes into an ordered metabolon would eliminate LPA contact with the PAP protein. Recently experimentation using gentle lysis of plastids implicated that all enzymes of fatty acid biosynthesis are assembled as a metabolon (Roughan and Ohlrogge, 1996). The dual specificity of PAP may well indicate that there is metabolic channelling for TAG biosynthesis, thus ensuring LPA and PAP segregation. The *in vivo* importance of these findings will be answered with the cloning and over-expression of PAP, and subsequent transgenic studies may provide answers to these important questions regarding the involvement of PAP in the metabolic flux of glycerolipids.

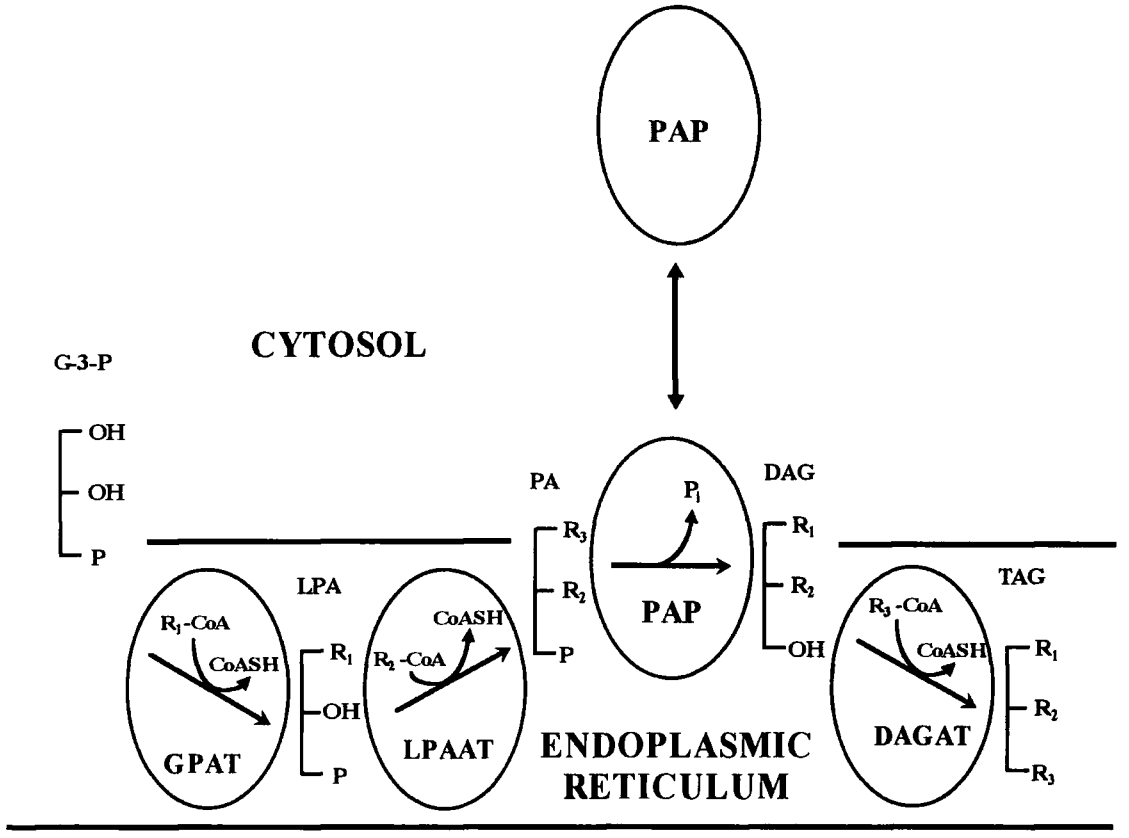

Figure 7.18: Proposed model for the Kennedy pathway metabolon. The enzymes of the Kennedy pathway are spatially arranged, so that the glycerolipid product from each reaction is channelled directly into the next step of the pathway. PAP translocation into the cytosol, allows the pathway to be controlled. **GPAT**, glycerol-3-phosphate acyltransferase; **LPAAT**, lysophosphatidate acyltransferase; **PAP**, phosphatidate phosphatase; **DAGAT**, diacylglycerol acyltransferase; **G-3-P**, glycerol-3-phosphate; **LPA** lysophosphatidate; **PA**, phosphatidate; **DAG**, diacylglycerol; **TAG**, triacylglycerol.

The hydrolysis of *sn*-2-LPA and ceramide-1-phosphate was investigated and compared to that of *sn*-1-LPA and PA. Hydrolysis of *sn*-2-LPA and ceramide-1-phosphate was very low. The inability to utilise *sn*-2-LPA as a catalytic substrate eliminated the possibility that PAP was a non-specific lipid phosphatase. The enzyme required an acyl group in position *sn*-1 for catalysis, and indicated that the hydrolysis may not be an *in vitro* experimental artefact. This raises the possibility that the hydrolysis of *sn*-1-LPA may have a function *in vivo*. LPA has been reported to act as a lipid mediator in the induction of cell proliferation in animals (English *et al.*, 1996). This has not been demonstrated in plants, but the dephosphorylation of LPA would allow the removal of the signal.

Ceramide-1-phosphate was found to be an equally poor catalytic substrate. Ceramide-1-phosphate is structurally similar to PA, and is involved in signal transduction in animals (Waggoner *et al.*, 1996; Brindley and Waggoner, 1996). The difference in catalytic activity towards both substrates revealed that PAP could differentiate between the two compounds. This indicated that PAP shows catalytic specificity.

A surface dilution kinetic analysis of *sn*-2-LPA and ceramide-1-phosphate hydrolyses is required for the provision of kinetic data and the detailed evaluation of these compounds as substrates for avocado PAP. However it is unlikely that the apparent V_{max} value for these substrates would be larger than that already observed. Further increases in Triton X-100 (i.e. an increase in surface dilution) would reduce the apparent V_{max} and increase the apparent K_m for each substrate, thus reducing catalytic efficiency. A low level of hydrolysis of ceramide-1-phosphate and *sn*-2-LPA was observed when the surface concentration of 20mol% was used. This surface concentration is far higher than the expected physiological concentration of the sphingolipid. The concentration of ceramide-1-phosphate *in vivo* is believed to be low in plants. This means that the surface concentration of the compound is very low *in*

vivo, causing the V_{max} to decrease and the K_m to increase substantially. This indicates that under physiological conditions, PAP would not hydrolyse ceramide-1-phosphate.

Waggoner *et al.* (1996) demonstrated that the apparent V_{max} for ceramide-1-phosphate hydrolysis was 2-fold lower than for PA at a surface concentration of 0.2mol%. At this concentration the K_m for ceramide-1-phosphate was 2-fold lower than for PA. The catalytic efficiency (V_{max}/K_m) of PA and ceramide-1-phosphate were the same. This is clearly different to the kinetic profile of avocado PAP. It is therefore concluded that the isoform of PAP identified by Waggoner *et al.* (1995; 1996) in rat liver plasma membranes is not the same enzyme as the avocado microsomal isoform described in this thesis. The rat liver enzyme is believed to be involved in signal transduction. As only one PAP activity was identified in the microsomal fraction it was concluded that this enzyme is involved in glycerolipid metabolism. The NEM/Mg^{2+} classification (Jamal *et al.*, 1991; Gomez-Muñoz *et al.*, 1992a) of PAP isoforms used in mammalian systems for the identification of glycerolipid synthesising and signal transduction related activities is therefore inappropriate to avocado PAP. Plants, like yeast, appear to have a unique isoform of PAP.

Chapter 8

Achievements of this research and suggestions for future work

The rationale behind the research in this thesis was to identify, characterise and purify phosphatidic acid phosphatase from an oleaginous plant source, in order to elucidate the enzyme's role in the metabolic partitioning of different glycerolipid species. Avocado (*Persea americana*) mesocarp was chosen as the source of the enzyme because it is extremely rich in glycerolipid and as such would be expected to contain high levels of PAP activity. No detailed kinetic or biochemical analyses have been reported on the microsomal plant enzyme and the enzyme has not been purified to homogeneity.

Arguably the most influential biochemical research on this enzyme has been conducted by Carman and co-workers with PAP from *S.cerevisiae* (Lin and Carman, 1989; Lin and Carman, 1990; Morlock *et al.*, 1991; Quinlan *et al.*, 1992; Wu *et al.*, 1993; Wu and Carman, 1996). In order to conduct the investigation successfully in plants, a sensitive assay was designed that was based on the proven assay system of yeast PAP. The assay was based on the release of aqueous soluble [^{32}P]Pi from chloroform soluble [^{32}P]PA in Triton X-100 mixed micelles. [^{32}P]PA is not available commercially and was synthesised by DAG kinase. To enable the routine analysis of PAP activity throughout the course of this study, the synthesis of [^{32}P]PA was optimised from the method originally described by Walsh and Bell (1986).

The purification of PAP from the microsomal fraction of avocado mesocarp was conducted, employing several purification strategies. The purification of PAP first required enzyme solubilisation with detergent, and was assisted with the estimation of native molecular mass for the protein. Those strategies incorporating Phenyl Superose were extremely successful in the fractionation of PAP. PAP was purified 7000-fold to homogeneity from the microsomal fraction, with a highly reproducible procedure that

utilised detergent solubilisation with CHAPS, anion exchange and Affi-Gel Blue chromatography, ammonium sulphate precipitation and Phenyl Superose. The homogenous protein had a molecular mass of 49kDa as determined by SDS-PAGE, and was found to be monomeric by gel filtration and Native PAGE analyses. Problems did arise, however, in respect to the protein stability during fractionation and particularly with the final protein concentration of the homogenous protein. All attempts to concentrate the homogenous protein for N-terminal amino acid sequencing resulted in loss of the protein.

The partially purified and homogenous protein was used for the biochemical characterisation of the enzyme. PAP was found to be Mg^{2+} and NEM independent and had a pH optimum of 6.0. However, the addition of Mg^{2+} ions to the assay reaction caused a 2-fold increase in PAP activity. The enzyme appeared to be more akin to the PAP2 isoform as reported from various mammalian tissues (see Kocsis and Weselake, 1996). In this system, the enzyme is believed to be involved in signal transduction. A 51kDa PAP2 isoform has been purified from rat liver (Waggoner *et al.*, 1995). Upon further characterisation of the enzyme, it became apparent that PAP could catalyse LPA at higher catalytic rates than PA. This was corroborated with the homogenous enzyme. The hydrolysis of LPA by 51kDa PAP2 has recently been reported (Waggoner *et al.*, 1996), indicating that the isoform identified in this thesis could be the plant equivalent to the mammalian 51kDa PAP2 isoform. However, the inability to hydrolyse ceramide-1-phosphate and *sn*-2-LPA at the equivalent rates as PA (or sn-1-LPA) raises the question that the two enzymes are functionally different. The PAP isoform identified here had a high specificity for glycerolipids with an acyl moiety esterified at position *sn*-1 of the glycerol backbone. The structural analogue of PA, ceramide-1-phosphate was found to be a very poor catalytic substrate, in terms of apparent V_{max} and K_m under the same conditions as for PA, where the substrate concentration was very high. This was in direct contrast to PAP2 from rat liver in which the hydrolysis of ceramide-1-phosphate was significantly greater at low

substrate surface concentrations. The phospholipase D signal transduction pathway has not been identified in plants. Only one isoform of microsomal PAP was identified. As avocado produces a major TAG pool, this isoform would be expected to be involved in glycerolipid biosynthesis. The preliminary identification of the cytosolic isozyme further confirmed that the enzyme described here was the glycerolipid synthesising enzyme.

PAP is microsomally associated and PA is a surface active compound. This made the traditional Michaelis-Menten kinetic model inadequate for the kinetic study of this enzyme. The surface dilution kinetic model was proposed for the study of lipolytic interfacial enzyme catalysis (Deems *et al.*, 1975). PAP activity was measured according to the model with LPA and PA as substrates. LPA was found to be a more effective substrate than PA. The kinetic model was used to study the effect of LPA on PAP kinetics. LPA was shown to competitively inhibit PAP activity. This explained the earlier observation that PAP preferentially hydrolysed LPA when presented with equimolar substrates. The kinetic model allowed the two enzyme activities to be individually evaluated under conditions that would otherwise be inaccurate in a traditional Michaelis-Menten kinetic analysis. The use of the model in this study allowed an insight into the bioassembly of TAG in avocado, and pointed to the necessity of a Kennedy pathway metabolon.

In order to elucidate the role of PAP in glycerolipid partitioning, an investigation into the effect of different glycerolipids on PAP kinetics, using the surface dilution kinetic model would be advantageous. Such biochemical analyses have already furthered the current understanding of glycerolipid partitioning and lipid-dependent enzyme regulation in yeast (Bae-Lee and Carman, 1990; Wu and Carman, 1996). The detailed biochemical analyses of how different glycerolipids affect PAP activity (using a kinetic evaluation with each lipid) may unveil the mechanisms by which an oil rich tissue regulates glycerolipid metabolism.

Central to the future success of these investigations, is the ability to obtain homogenous enzyme. The successful purification of PAP to homogeneity will allow subsequent studies to be undertaken. The problems encountered during protein purification might be overcome with further investigations. The use of Phenyl Superose chromatography proved to be an extremely effective way in which to fractionate PAP protein. With the benefit of hindsight, PAP protein could be identified on an SDS-PAGE gel after phenyl Superose chromatography of a crude CHAPS extract (as shown in Figure 5.12). The purification to homogeneity was essential for the initial identification of the PAP protein. For the purposes of amino-acid sequencing, a sample such as this, would be sufficient, provided the PAP protein could be identified.

With amino-acid sequence data, the cDNA encoding the PAP protein could be isolated from an avocado cDNA library, cloned and PAP protein overexpressed. The generation of antibodies against the PAP protein would greatly assist in the purification of the protein and in the understanding of PAP translocation. It may be that monoclonal antibody generation offers the most promise in the elucidation of PAP translocation and isozyme/isoform identification. The research presented in this thesis therefore represents a foundation for subsequent studies of this key enzyme in plant glycerolipid metabolism.

References

Alban, C., Joyard, J. and Douce, R. (1989) Comparison of glycerolipid biosynthesis in non-green plastids from sycamore (*Acer pseudoplatanus*) cells and cauliflower (*Brassica oleracea*) buds. Biochem. J. **259**: 775-783

Andrews, J., Ohlrogge, J.B. and Keegstra, K. (1985) Final step of phosphatidic acid synthesis in pea chloroplasts occurs in the inner envelope membrane. Plant Physiol. **78**: 459-465

Arakawa, T. and Timasheff, S.N. (1985) Theory of protein solubility. Methods Enzymol. **114**: 49-77

Asiedu, D., Skorve, J., Demoz, A., Willumsen, N. and Berge, R.K. (1992) Relationship between translocation of long-chain acyl-CoA hydrolase, phosphatidate phosphohydrolase and CDP:phosphocholine cytidyltransferase and the synthesis of triglycerides and phosphatidylchloline in rat liver. Lipids **27**: 241-247

Bae-Lee, M. and Carman, G.M. (1990) Regulation of yeast phosphatidylserine synthase and phosphatidylinositol synthase activities by phospholipids in Triton X-100/phospholipid mixed micelles. J. Biol. Chem. **265**: 7221-7226

Barron, E.J., Squires, C. and Stumpf, P.K. (1961) Fat metabolism in higher plants. J. Biol. Chem. 236: 2610-2614

Barron, E.J. and Stumpf, P.K. (1962) The biosynthesis of triglycerides by avocado-mesocarp enzymes. Biochem. Biophys. Acta **60**: 329-337

Battey, J.F. and Ohlrogge, J.B. (1989) A comparison of the metabolic fate of fatty acids of different chain lengths in developing oilseeds. Plant Physiol. **90**: 835-840

Bernerth, R. and Frentzen, M. (1990) Utilisation of erucoyl-CoA by acyltransferases from developing seeds of *Brassica napus* involved in triacylglycerol biosynthesis. Plant Science **67**: 21-28

Bhat, B.G., Wang, P. and Coleman, R.A. (1994) Hepatic monoacylglycerol acyltransferase is regulated by *sn*-1,2-diacylglycerol and by specific lipids in Triton X-100/phospholipid-mixed micelles. J. Biol. Chem. **269**: 13172-13178

Billah, M.M. and Anthes J.C. (1990) The regulation and cellular functions of phosphatidylcholine hydrolysis. Biochem. J. **269**: 281-291

Blank, M.L. and Snyder, F. (1970) Specificities of alkaline and acid phosphatases in the dephosphorylation of phospholipids. Biochemistry **9**: 5034-5036

Bligh, E.G. and Dyer, W.J. (1959) A rapid method of total lipid extraction and purification. Can. J. Biochem. Physiol. **37**: 911-917

Block, M.A., Forne, A.J., Joyard, J. and Douce, R. (1983) The phosphatidic acid phosphatase of the chloroplast envelope is located on the inner envelope membrane. FEBS Lett. **164**: 111-115

Bollag, D.M. and Edelstein, S.J. (1991) Protein methods. Wiley-Liss Inc., New York, USA.

Brindley, D.N. and Waggoner, D.W. (1996) Phosphatidate phosphohydrolase and signal transduction. Chem. Phys. Lipids **80**: 45-57

Brown, A.P., Coleman, C., Tommey, A.M., Watson, M.D. and Slabas, A.R. (1994) Isolation and characterisation of a maize cDNA that complements a 1-acyl-sn-glycerol-3-phosphate acyltransferase mutant of *Escherichia coli* and encodes a protein which as similarities to other acyltransferases. Plant Mol. Biol. **26**: 211-223

Brown, A.P., Brough, C.L., Kroon, J.T.M. and Slabas, A.R. (1995) Identification of a cDNA that encodes a 1-acyl-*sn*-glycerol-3-phosphate acyltransferase from *Limnanthes douglasii*. Plant Mol. Biol. **29**: 267-278

Browse, J. and Somerville, C. (1991) Glycerolipid synthesis: biochemistry and regulation. Annu. Rev. Plant Physiol. Plant Mol. Biol. **42**: 467-506

Butterwith, S.C., Martin, A., Cascales, C., Mangiapane, E.H. and Brindley, D.N. (1985) Regulation of triacylglycerol synthesis by translocation of phosphatidate phosphohydrolase from the cytosol to the membrane-associated compartment. Biochem. Soc. Trans. **13**: 158-159

Buxeda, R.J., Nickels, J.T., Belunis, C.J. and Carman, G.M. (1991) Phosphatidylinositol 4-kinase from *Saccharomyces cerevisiae*. J. Biol. Chem. **266**: 13859-13865

Cabacungan, E.A., Gustow, E. and Pieringer, R.A. (1988) *In vivo* studies on stereospecificity of the monoglyceride kinase, lysophosphatidic acid acyltransferase phosphatidic acid phosphatase and CDP-DAG synthase of *Streptococcus mutans* BHT using the stereoisomers of the ether lipid, dodecylglycerol. Biochim. Biophys. Acta **962**: 241-247

Cao, Y.-Z., Oo, K.-C. and Huang, A.H.C. (1990) Lysophosphatidate acyltransferase in the microsomes from maturing seeds of meadowfoam (*limnanthes alba*). Plant Physiol. **94**: 1199-1206

Carman, G.M. and Lin, Y.-P. (1991) Phosphatidate phosphatase from yeast. Methods Enzymol. **197**: 548-553

Carman, G.M. and Quinlan, J.J. (1992) Phosphatidate phosphatase from yeast mitochondria. Methods Enzymol. **209**: 219-224

Carman, G.M., Deems, R.A. and Dennis, E.A. (1995) Lipid signalling enzymes and surface dilution kinetics. J. Biol. Chem. **270**: 18711-18714

Chen, P.S., Toribara, T.Y. and Warner, H. (1956) Microdetermination of phosphorus. Anal. Chem. **28**: 1756-1758

Cornish-Brown, A. (1995) Fundamentals of enzyme kinetics. Portland Press, London, UK.

Davies, H.M., Kridl, J.C., Thompson G.A. and Voelker, T.A. (1993) Genetic engineering of altered fatty acid saturation and chain lengths in rapeseed. Plant Physiol. **102**: 1

Deems, R.A., Eaton, B.R., Dennis, E.A. (1975) Kinetic analysis of phospholipase A_2 activity toward mixed micelles and its implications for the study of lipolytic enzymes. J. Biol. Chem. **250**: 9013-9020

Duff, S.M.G., Sarath, G and Plaxton, W.C. (1994) The role of acid phosphatases in plant phosphorus metabolism. Physiol. Plant. **90**: 791-800

Dutta, P.C., Appelqvist, L.-Å. and Stymne, S. (1992) Utilization of petroselinate ($C18:0^{\Delta 6}$) by glycerol acylation enzymes in microsomal preparations of developing embryos of carrot (*Daucus carota* L.), safflower (*Carthamus tinctorius* L.) and oil seed rape (*Brassica napus* L.). Plant Sci. **81**: 57-64

Ecclestone, V. and Harwood, J.L. (1995) Solubilisation, partial purification and properties of acyl-CoA:glycerol-3-phosphate acyltransferase from avocado (*Persea americana*) fruit mesocarp. Biochim. Biophys. Acta **1257**: 1-10

Engel, P.C. (1977) Enzyme Kinetics - the steady state approach. Chapman and Hall, London, UK.

English, D., Cui, Y. and Siddiqui, R.A. (1996) Messenger functions of phosphatidic acid. Chemistry and Physics of Lipids **80**: 117-132

Fleming, I.N. and Yeaman, S.J. (1995) Purification and characterisation of *N*-ethylmaleimide-insensitive phosphatidic acid phosphohydrolase (PAP2) from rat liver. Biochem. J. **308**: 983-989

Frentzen, M. (1990) Comparison of certain properties of membrane bound and solubilised acyltransferase activities of plant microsomes. Plant Sci. **69**: 39-48

Frentzen, M. (1993) Acyltransferases and triacylglycerols. In Lipid Metabolism in Plants, Ed. Moore, T.S., CRC Press Inc, Boca Raton.

Frentzen, M., Heinz, E., McKeon, T.A. and Stumpf, P.K. (1983) Specificities and selectivities of glycerol-3-phosphate acyltransferase and monoacylglycerol-3-phosphate acyltransferase from pea and spinach chloroplasts. Eur. J. Biochem. **129**: 629-636

Gee, R.W., Byerrum, R.U., Gerber, D.W. and Tolbert, N.E. (1988) Dihydroxyacetone phosphate reductase in plants. Plant Physiol. **86**: 98-103

Gomez-Muñoz, A., Hatch, G.M., Martin, A., Jamal, Z., Vance, D.E. and Brindley, D.N (1992a) Effects of okadaic acid on the activities of two distinct phosphatidate phosphohydrolases in rat hepatocytes. FEBS Lett. **301**: 103-106

Gomez-Muñoz, A., Hamza, E.H. and Brindley, D.N (1992b) Effects of sphingosine, albumin and unsaturated fatty acids on the activation and translocation of phosphatidate phosphohydrolases in rat hepatocytes. Biochim. Biophys. Acta **1127**: 49-56

Griffiths, G., Stobart, A.K. and Stymne, S. (1985) The acylation of *sn*-glycerol-3-phosphate and the metabolism of phosphatidate in microsomal preparations from the developing cotyledons of safflower (*Carthamus tinctorius* L.) seed. Biochem. J. **230**: 379-388

Griffiths, G., Stymne, S. and Stobart, A.K.(1987) The utilisation of fatty-acid substrates in triacylglycerol biosynthesis by tissue-slices of developing safflower (*Carthamus tinctorius* L.) and sunflower (*Helianthus annuus* L.) cotyledons. Planta **173**: 309-316

Griffiths, G., Stymne, S. and Stobart, A.K.(1988) Phosphatidylcholine and its relationship to triacylglycerol biosynthesis in oil-tissues. Phytochemistry **27**: 2089-2093

Gulliver, B.S. and Slabas, A.R. (1994) Acetoacetyl-acyl carrier protein synthase from avocado: its purification, characterisation and clear resolution from acetyl-CoA:ACP transacylase. Plant Mol. Biol. **25**: 179-191

Gunstone, F.G., Harwood, J.L. and Padley, F.B. (Eds.) (1994) The lipid handbook, 2nd ed., Chapman and Hall, London, UK.

Helenius, A. and Simons, K. (1975) Solubilization of membranes by detergents. Biochim. Biophys. Acta **415**: 29-79

Hendrickson, H.S. and Dennis, E.A. (1984) Kinetic analysis of the dual phospholipid model for phospholipase A_2 action. J. Biol. Chem. **259**: 5734-5739

Herman, E.M. and Chrispeels, M.J. (1980) Characteristics and subcellular localisation of phospholipase D and phosphatidic acid phosphatase in mung bean cotyledons. Plant Physiol. **66**: 1001-1007

Hjelmeland, L.M., Nebert, D.W. and Osborne, J.C. (1983) Sulfobetaine derivatives of bile acids: nondenaturing surfactants for membrane biochemistry. Anal. Biochem. **130**: 72-82

Hjelmeland, L.M. and Chrambach, A. (1984) Solubilisation of functional membrane proteins. Methods Enzymol. **104**: 305-318

Hjelmestad, R.H. and Bell, R.M. (1991) Molecular insights into enzymes of membrane bilayer assembly. Biochemistry **30**: 1731-1740

Hopewell, R., Martin-Sanz, P., Martin, A., Saxton, J. and Brindley, D.N. (1985) Regulation of the translocation of phosphatidate phosphohydrolase between the cytosol and the endoplasmic reticulum of rat liver. Biochem. J. **232**: 485-491

Hosaka, H. and Yamashita, S. (1984a) Partial purification and properties of phosphatidate phosphatase in *Saccharomyces cerevisiae*. Biochim. Biophys. Acta **796**: 102-109

Hosaka, H. and Yamashita, S. (1984b) Regulatory role of phosphatidate phosphatase in triacylglycerol synthesis of *Saccharomyces cerevisiae*. Biochim. Biophys. Acta **796**: 110-117

Ichihara, K., Asahi, T. and Fujii, S. (1987) 1-acyl-*sn*-glycerol-3-phosphate acyltransferase in maturing safflower seeds and its contribution to the non-random fatty acid distribution of triacylglycerol. Eur. J. Biochem. **167**: 339-347

Ichihara, K., Norikura, S. and Fujii, S. (1989) Microsomal phosphatidate phosphatase in maturing safflower seeds. Plant Physiol. **90**: 413-419

Ichihara, K., Murota, N. and Fujii, S. (1990) Intracellular translocation of phosphatidate phosphatase in maturing safflower seeds: a possible mechanism of feedforward control of triacylglycerol synthesis by fatty acids. Biochim. Biophys. Acta **1043**: 227-234

Ichihara, K. (1991) The action of phosphatidate phosphatase on the fatty acid composition of safflower triacylglycerol and spinach glycerolipids. Planta **183**: 353-358

Icho, T. (1988a) Membrane-bound phosphatases in *Escherichia coli*: sequence of the *pgpA* gene. J. Bacteriol. **170**: 5110-5116

Icho, T. (1988b) Membrane-bound phosphatases in *Escherichia coli*: sequence of the *pgpB* gene and dual sub-cellular localisation of the *pgp B* product. J. Bacteriol. **170**: 5117-5124

Ide, H. and Nakazawa, Y. (1989) Rapid hydrolysis of diacylglycerol formed during phosphatidate phosphatase assay by lipase activities in rat liver cytosol and microsomes. Arch. Biochem. Biophys. **271**: 177-187

Jakoby, W.B. (Ed.) (1984) Enzyme purification and related techniques. Methods Enzymol. **104**

Jamal, Z., Martin, A., Gomez-Muñoz, A. and Brindley, D.N. (1991) Plasma membrane fractions from rat liver contain a phosphatidate phosphohydrolase distinct from that in the endoplasmic reticulum and cytosol. J. Biol. Chem **266**: 2988-2996

Joyard, J. and Douce, R. (1977) Site of synthesis of phosphatidic acid and diacylglycerol in spinach chloroplasts. Biochim. Biophys. Acta **486**: 273-285

Joyard, J. and Douce, R. (1979) Characterisation of phosphatidate phosphohydrolase activity associated with chloroplast envelope membranes. FEBS Lett. **102**: 147-150

Kai, M., Wada, I., Imai, S.-I., Sakane, F. and Kanoh, H. (1996) Identification and cDNA cloning of 35kDa phosphatidic acid phosphatase (Type 2) bound to plasma membranes. J. Biol. Chem. **271**: 18931-18938

Kamenan, A. and Diapoh, J. (1983) Properties of two membrane-bound acid phosphatases compared with those of a cytoplasmic acid phosphatase from *Dioscorea cayenensis rotundata*. Plant Sci. Lett. **32**: 305-312

Kanoh, H., Kondoh, H. and Ono, T. (1983) Diacylglycerol Kinase from pig brain. J. Biol. Chem. **258**: 1767-1774

Kanoh, H., Imai, S., Yamada, K. and Sakane, F. (1992) Purification and properties of phosphatidic acid phosphatase from porcine thymus membranes. J. Biol. Chem. **267**: 25309-25314

Kanoh, H., Sakane, F., Imai, S.-I. and Wada, I. (1993) Diacylglycerol kinase and phosphatidic acid phosphatase - enzymes metabolising lipid second messengers. Cellular signalling **5**: 495-503

Kates, M. (1955) Hydrolysis of lecithin by plant plastid enzymes. Can. J. Biochem. Physiol. **33**: 575-589

Kocsis, M.G., Weselake, R.J., Eng, J.A., Furukawa-Stoffer, T.L. and Pomeroy, M.K. (1995) Phosphatidate phosphatase from developing seeds and microspore-derived cultures of *Brassica napus*. Phytochemistry **41**: 353-363

Kocsis M.G. and Weselake, R.J. (1996) Phosphatidate phosphatase of mammals, yeast and higher plants. Lipids, **31**: 785-802

Königs, B. and Heinz, E. (1974) Investigation of some enzymatic activities contributing to the biosynthesis of galactolipid precursors in *Vicia faba*. Planta **118**: 159-169

Lacey, D.J. and Hills, M.J. (1996) Heterogeneity of the endoplasmic reticulum with respect to lipid synthesis in developing seeds of *Brassica napus* L. Planta **199**: 545-551

Laemmli, U. K. (1970) Cleavage of structural proteins during the assembly of the head of bacteriophage T4. Nature **227**: 680-685.

Lassner, M.W., Levering, C.K., Davies, H.M. and Knutzen, D.S. (1995) Lysophosphatidic acid acyltransferase from meadowfoam mediates insertion of erucic acid at the *sn*-2 position of triacylglycerol in transgenic rapeseed oil. Plant Physiol. **109**: 1389-1394

Laurent, P. and Huang, A.H.C. (1992) Organ- and development- specific acyl-Coenzyme A lysophosphatidate acyltransferases in palm and meadowfoam. Plant Physiol. **99**: 1711-1715

Lerouge, P., Roche, P., Faucher, C., Maillet, F., Truchet, G., Promé, J.C. and Dénarié, J. (1991) Symbiotic host-specificity of *Rhyzobium meliloti* is determined by a sulphated and acylated glucosamine oligosaccharide signal. Nature **344**: 781-784

Lichtenberg, D., Robson, R.J. and Dennis, E.A. (1983) Solubilisation of phospholipids by detergents - structural and kinetic aspects. Biochim. Biophys. Acta **737**: 285-304

Lin, Y.-P. and Carman, G.M. (1989) Purification and characterisation of phosphatidate phosphatase from *Saccharomyces cerevisiae*. J. Biol. Chem. **264**: 8641-8645

Lin, Y.-P. and Carman, G.M. (1990) Kinetic analysis of yeast phosphatidate phosphatase toward Triton X-100/phosphatidate mixed micelles. J. Biol. Chem. **265**: 166-170

Long, C., Odavic, R. and Sargent, E.J. (1967) The chemical nature of the products obtained by the action of cabbage-leaf phospholipase D on lysolecithin: the structure of lysolecithin. Biochem. J. **102**: 221-229

Loomis, C.R., Walsh, J.P. and Bell, R.M. (1985) *sn*-1,2-Diacylglycerol kinase of *Escherichia coli* - purification, reconstitution and partial amino-and carboxyl-terminal analysis. J. Biol. Chem. **260**: 4091-4097

Low, M.G. (1989) The glycosyl-phosphatidylinositol anchor of membrane proteins. Biochim. Biophys. Acta **988**: 427-454

Low, M.G. and Saltiel A.R. (1988) Structural and functional roles of glycosyl-phosphatidylinositol in membranes. Science **239**: 268-275

Lowry, O.H., Rosebrough, N.J., Farr, A.L. and Randall, R.J. (1951) Protein measurement with the folin phenol reagent. J. Biol. Chem. **193**: 265-275

Malherbe, A., Block, M.A., Joyard, J. and Douce, R.(1992) Feedback inhibition of phosphatidate phosphatase from spinach chloroplast envelope membranes by diacylglycerol. J. Biol. Chem. **267**: 23546-23553

Malherbe, A., Block, M.A., Douce, R. and Joyard, J. (1995) Solubilisation and biochemical properties of phosphatidate phosphatase from spinach chloroplast envelope membranes. Plant Physiol. Biochem. **33**: 149-161

Martin, A., Hopewell, R., Martin-Sanz, P., Morgan, J.E. and Brindley, D.N. (1986) Relationship between the displacement of phosphatidate phosphohydrolase from the membrane-associated compartment by chlorpromazine and the inhibition of the synthesis of triacylglycerol and phosphatidylcholine in rat hepatocytes. Biochim. Biophys. Acta **876**: 581-591

Martin, A., Gomez-Muñoz, A., Jamal, Z. and Brindley, D.N. (1991) Characterisation and assay of phosphatidate phosphatase. Methods Enzymol. **197**: 553-563

Martin-Sanz, P., Hopewell, R. and Brindley, D.N. (1984) Long-chain fatty acids and their acyl-CoA esters cause the translocation of phosphatidate phosphohydrolase from the cytosolic to the microsomal fraction of rat liver. FEBS Lett. **175**: 284-288

Mazliac, P., (1997) Lipids in cell signalling: a review. In Physiology, Biochemistry and Molecular Biology of Plant Lipids, Ed. Williams, J.P., Khan, M.U. and Lem, N.W., Kluwer Academic Publishers.

Moore, T.S. and Sexton, J.C. (1978) Phosphatidate phosphatase of castor bean endosperm. Plant physiol. **61** (Suppl.): 69

Morlock, K.R., Lin, Y.P. and Carman, G.M. (1988) Regulation of phosphatidate phosphatase activity by inositol in *Saccharomyces cerevisiae*. J. Bacteriol. **170**: 3561-3566

Morlock, K.R., Mc Laughlin, J.J., Lin, Y.P. and Carman, G.M. (1991) Phosphatidate phosphatase from *Saccharomyces cerevisiae*: isolation of 45- and 104-kDa forms of the enzyme that are differentially regulated by inositol. J. Biol. Chem. **266**: 3586-3593

Murata, N. (1983) Molecular species composition of phosphatidylglycerols from chilling sensitive and chilling-resistant plants. Plant Cell. Physiol. **24**: 81-86

Neugebauer, J. (1990) Detergents: an overview. Methods Enzymol. **182**: 239-253

Neugebauer, J. (1994) A guide to the properties and uses of detergents in biology and biochemistry. Calbiochem-Novabiochem International, La Jolla, CA, USA

Nishida, I., Tasaka, Y., Shirashi, H. and Murata, N. (1993) The gene and the RNA for the precursor to the plastid located glycerol-3-phosphate acyltransferase of Arabidopsis thaliana. Plant Mol. Biol. **21**: 267-277

Nishijima, M. and Raetz, C.R.H. (1979) Membrane lipid biogenesis in *Escherichia coli*: identification of genetic loci for phosphatidylglycerophosphate synthetase and construction of mutants lacking phosphatidylglycerol. J. Biol. Chem. **254**: 7837-7844

Ochs, D. (1983) Protein contaminants of sodium dodecyl sulfate- polyacrylamide gels. Anal. Biochem. **135**: 470-474

Oo, K.-C. and Huang, A.H.C. (1989) Lysophosphatidate acyltransferase activities from palm endosperm, maize scutellum and rapeseed cotyledon of maturing seeds. Plant Physiol. **91**: 1288-1295

Packard Instrument Company Technical Bulletin (1992) 'Back to Basics' information leaflet - quench. Packard Instrument Company, One State Street, Meriden, CT 06450, USA.

Peterson, G.L. (1983) Determination of total protein. Methods Enzymol. **91**: 95-119

Pharmacia LKB Biotechology Technical Bulletin (1991) Ion exchange chromatography - principles and methods. 3rd ed. Pharmacia LKB Biotechology, Uppsala, Sweden.

Pharmacia LKB Biotechology Technical Bulletin (1993) Gel Filtration - principles and methods. 6th ed. Pharmacia LKB Biotechology, Uppsala, Sweden.

Pharmacia LKB Biotechology Technical Bulletin (1993) Hydrophobic interaction chromatography - principles and methods. 6th ed. Pharmacia LKB Biotechology, Uppsala, Sweden.

Pieringer, R.A. and Kunnes, R.S. (1965) The biosynthesis of phosphatidic acid and lysophosphatidic acid by glyceride phosphokinase pathways in *Escherichia coli*. J. Biol. Chem. **240**: 2833-2838

Pittner, R.A., Bracken, P., Fears, R. and Brindley, D.N. (1986a) Insulin antagonises the growth hormone-mediated increase in the activity of phosphatidate phosphohydrolase in isolated rat hepatocytes. FEBS Lett. **202**: 133-136

Pittner, R.A., Fears, R. and Brindley, D.N. (1986b) Effects of Insulin, glucagon, demethasone cyclic GMP and spermine on the stability of phosphatidate phosphohydrolase activity in cultured rat hepatocytes. Biochem. J. **240**: 253-257

Post-Beittenmiller, D. (1996) Biochemistry and molecular biology of wax production in plants. Annu. Rev. Plant Physiol. Plant Mol. Biol. **47**: 405-430

Privett, O.S., Dougherty, K.A., Erdahl, W.L. and Stolyhow, A. (1973) Studies on the lipid composition of developing soybeans. J. Am. Chem. Soc. **50**: 516-520

Quinlan, J.J., Nickels J.T. Jr., Wu, W.-I., Lin, Y.-P. and Carman, G.M.(1992) The 45- and 104-kDa forms of phosphatidate phosphatase from *Saccharomyces cerevisiae* are regulated differentially by phosphorylation via cAMP-dependent kinase. J. Biol. Chem. **267**: 18013-18020

Rajasekharan, R., Ray, T.K. and Cronan, J.E. (1988) A direct nonchromatographic assay for 1-acyl-*sn*-glycerol-3-phosphate acyltransferase. Anal. Biochem. **173**: 376-382

Roberts, M.F., Deems, R.A. and Dennis, E.A. (1977) Interfacial phospholipid in phospholipase A_2 catalysis. Proc. Natl. Acad. Sci. USA **74**: 1950-1954

Robinson, N.C., Wiginton, D. and Talbert, L. (1984) Phenyl-Sepharose mediated detergent-exchange chromatography: its application to exchange of detergents bound to membrane proteins. Biochemistry **23**: 6121-6126

Robson, R.J. and Dennis, E.A. (1977) The size, shape and hydration of non-ionic surfactant micelles - Triton X-100. J. Phys. Chem. **81**: 1075-1078

Robson, R.J. and Dennis, E.A. (1983) Micelles of nonionic detergents and mixed micelles with phospholipids. Acc. Chem. Res. **16**: 251-258

Rock, C.O., Cronan, J.E. and Armitage, I.M. (1981) Molecular properties of acyl carrier protein derivatives. J. Biol. Chem. **256**: 2669-2674

Rotering, H. and Raetz, C.R.H. (1983) Appearance of monoglyceride and triglyceride in the cell envelope of *Escherichia coli* mutants defective in diglyceride kinase. J. Biol. Chem. **258**: 8068-8073

Roughan, G. (1987) Long chain fatty-acid synthesis and utilisation by isolated chloroplasts. Methods Enzymol. **148**: 327-337

Roughan, P.G. and Ohlrogge, J.B. (1996) Evidence that isolated chloroplasts contain an integrated lipid-synthesising asembly that channels acetate into long-chain fatty acids. Plant Physiol. **110**: 1239-1247

Roughan, P.G. and Slack, C.R. (1982) Cellular organisation of glycerolipid metabolism. Annu. Rev. Plant Physiol. **33**: 97-132

Roughan, G. and Slack, R. (1984) Glycerolipid synthesis in leaves. T.I.B.S. **9**: 383-386

Schägger, H. (1994) A practical guide to membrane protein purification. Ed. Von Jagow, G. and Schägger, H. Academic Press Inc., San Diego, CA, USA.

Schmidt, G. (1955) Acid prostatic phosphatase. Methods Enzymol. **2**: 523-530

Seiss, E.A. and Hofstetter, M.M. (1996) Identification of phosphatidate phosphohydrolase purified from rat liver membranes on SDS-polyacrylamide gel electrophoresis. FEBS Lett. **381**: 169-173

Sheldon, P.S., Kekwick, R.G.O., Sidebottom, C., Smith, C.G. and Slabas, A.R. (1990) 3-Oxoacyl-(acyl-carrier protein) reductase from avocado (*Persia americana*) fruit mesocarp. Biochem. J. **271**: 713-720

Slabas, A.R., Simon, J.W. and Elborough, K.M. (1995) Information needed to create new oil crops. INFORM **6**: 159-166

Slabas, A.R. and Fawcett, T. (1992) The biochemistry and molecular biology of plant lipid biosynthesis. Plant Mol. Biol. **19**: 169-191

Slack, C.R., Roughan, P.G., Browse, J.A. and Gardiner, S.E. (1985) Some properties of cholinephosphotransferase from developing safflower cotyledons. Biochim. Biophys. Acta **833**: 438-448

Somerville, C. and Browse, J. (1991) Plant lipids: metabolism, mutants and membranes. Science **252**: 80-87

Stark, R.E, Leff, P.D., Milheim, S.G. and Kropf, A. (1894) Physical studies of CHAPS, a new detergent for the study of visual pigments. J. Phys. Chem. **88**: 6063-6067

Staswick, P.E., Papa, C., Huang, J.-F. and Rhee, Y. (1994) Purification of the major soybean leaf acid phosphatase that is increased be seed-pod removal. Plant Physiol. **104**: 49-57

Steponkus, P.L., Uemura, M., Balsamo, R.A., Arvinte, T. and Lynch, D.V. (1988) Transformation of the cryobehaviour of rye protoplasts by modification of the plasma membrane composition. Pro. Natl. Acad. Sci. USA **85**: 9026-9030

Stobart, A.K. and Stymne, S. (1985a) The interconversion of diacylglycerol and phosphatidylcholine during triacylglycerol production in microsomal preparations of developing cotyledons of safflower (*Carthamus tinctorius* L.). Biochem. J. **232**: 217-221

Stobart, A.K. and Stymne, S. (1985b) The regulation of the fatty-acid composition of the triacylglycerols in microsomal preparations from avocado mesocarp and the developing cotyledons of safflower. Planta **163**: 119-125

Sturton, R.G. and Brindley, D.N. (1978) Problems encountered in measuring the activity of phosphatidate phosphohydrolase. Biochem. J. **171**: 263-266

Stymne, S. and Stobart, A.K. (1984) Evidence for the reversibility of the acyl-CoA:lysophosphatidylcholine acyltransferase in microsomal preparations from developing safflower (Carthamus tinctorius) cotyledons and rat liver. Biochem. J. **223**: 305-314

Stymne, S. and Stobart, A.K. (1987) Triacylglycerol biosynthesis. In, The Biochemistry of Plants, Volume 9, Ed. Stumpf, P.K. Academic Press, New York, USA.

Stymne, S., Ståhl, U., Tillberg, E. and Wiberg, E. (1993) Biosynthesis of vegetable oils with unusual fatty acids. Plant Physiol. **102**: 2

Sukumar, V. and Sastry, P.S. (1987) Triacylglycerol synthesis in developing seeds of groundnut (*Arachis hypogaea*): studies on phosphatidic acid phosphatase and diacylglycerol acyltransferase during seed maturation. Biochem. Int. **14**: 1153-1158

Sun, C., Cao, Y.-Z. and Huang A.H.C. (1988) Acyl Coenzyme A preference of the glycerol phosphate pathway in the microsomes from the maturing seeds of palm, maize, and rapeseed. Plant Physiol. **88**: 56-60

Taylor, S.J. and Saggerson, E.D. (1986) Adipose tissue Mg^{2+}-dependent phosphatidate phosphohydrolase: control of activity and sub-cellular distribution *in vitro* and *in vivo*. Biochem. J. **239**: 275-284

Thomas, T.C. and McNamee, M.G. (1990) Purification of membrane proteins. Methods Enzymol. **182**: 499-520

Tzen, J.T.C. and Huang, A.H.C. (1992) Surface structure and properties of plant seed oil bodies. J. Cell Biol. **117**: 327-335

Tzur, R. and Shapiro, B. (1976) Phosphatidic acid metabolism in rat liver microsomes. Eur. J. Biochem. **64**: 301-305

Verger, R. (1980) Enzyme kinetics of lipolysis. Methods Enzymol. **64**: 340-392

Vogel, G. and Browse, J. (1996) Cholinephosphotransferase and diacylglycerol acyltransferase. Plant Physiol. **110**: 923-931

Waggoner, D.W., Martin, A., Dewald, J., Gomez-Muñoz, A. and Brindley, D.N. (1995) Purification and characterisation of a novel plasma membrane phosphatidate phosphohydrolase from rat liver. J. Biol. Chem. **270**: 19422-19429

Waggoner, D.W., Gomez-Muñoz, A., Dewald, J. and Brindley, D.N. (1996) Phosphatidate phosphohydrolase catalyses the hydrolysis of ceramide 1-phosphate, lysophosphatidate, and sphingosine 1-phosphate. J. Biol. Chem. **271**: 16506-16509

Walsh, J.P. and Bell, R.M. (1986) *sn*-1,2-diacylglycerol kinase of *Escherichia coli*. J. Biol. Chem. **261**: 6239-6247

Walsh, J.P., Loomis, C.R. and Bell, R.M. (1986) Regulation of diacylglycerol kinase biosynthesis in *Escherichia coli*. J. Biol. Chem. **261**: 11021-11027

Walsh, J.P. and Bell, R.M. (1992) Diacylglycerol kinase of *Escherichia coli*. Methods Enzymol. 209: 153-162

Weaire, P.J. and Kekwick, R.G.O. (1975) The fractionation of the fatty acid synthetase activities of avocado mesocarp plastids. Biochem. J. **146**: 439-445

and Jain, J.G. (1992) Strategies in the purification of plant proteins. Physiol. Plant. **84**: 301-309

Weselake, R.J., Pomeroy, M.K., Furukawa, T.L., Golden, J.L., Little, D.B. and Laroche, A. (1993) Developmental profile of diacylglycerol acyltransferase in maturing seeds of oilseed rape and safflower and microspore-derived cultures of oilseed rape. Plant Physiol. **102**: 565-571

Wessel, D. and Flugge, I.U. (1984) A method for the quantitative recovery of protein in dilute solution in the presence of detergents and lipids. Anal. Biochem. **138**: 141-143

Wissing, J.B., Kornak, B., Funke, A. and Reidel, B. (1994) Phosphatidate kinase, a novel enzyme in phospholipid metabolism. Plant Physiol. **105**: 903-909

Wu, W.-I, Lin, Y.-P., Wang, E., Merrill, A.H. and Carman, G.M. (1993) Regulation of phosphatidate phosphatase activity from the yeast *Saccharomyces cerevisiae* by sphingoid bases. J. Biol. Chem. **268**: 13830-13837

Wu, W.-I, and Carman, G.M. (1996) Regulation of phosphatidate phosphatase activity from the yeast *Saccharomyces cerevisiae* by phospholipids. Biochemistry **35**: 3790-3796

Yu, L. and Dennis, E.A. (1992) Kinetic analysis of the competitive inhibition of phospholipase A_2 in Triton X-100 mixed micelles. Bioorg. Med. Chem. Lett. **2**: 1343-1348